UNIVERSITÀ
DEGLI STUDI
DI PADOVA

Sede Amministrativa: Università degli Studi di Padova

Dipartimento di Biologia

CORSO DI DOTTORATO DI RICERCA IN  BIOSCIENZE E BIOTECNOLOGIE
CURRICULUM: BIOTECNOLOGIE
CICLO XXIX

# Exosomes as a vehicle for α-Synuclein toxic species propagation in α-synucleinopathies

**Coordinatore:** Ch.mo Prof. Paolo Bernardi
**Supervisore**: Ch.mo Prof. Luigi Bubacco
**Co-Supervisore**: Ch.mo Prof. Emanuele Papini

**Dottorando** : Giulia Berti

# Table of contents

# Abstract

α-synucleinopathies are a group of neurodegenerative disorders characterized by the presence of abnormally aggregated aS. Recent evidence suggests that the early site of aS aggregation is synapses, where aS seems to play its physiological role. Moreover, aggregated aS is reported to be secreted by cells, suggesting its potential involvement in disease initiation and progression. Considering the nature of neurodegenerative disorders as well as the defined, step-wise spreading of Lewy body pathology in α-synucleinopathies, the idea of extracellular aS as a pathogenic 'prion-like' agent is extremely appealing.

This research project developed in this frame and it is focused on the propagation of aS toxic species mediated by a particular type of extracellular vesicles, exosomes.

To this aim, aS containing exosomes were first purified from aS-EGFP transfected HEK293T cells. Moreover, since in PD dopaminergic neurons are primary affected, we focused on the connection between aS aggregation process and dopamine metabolism. Therefore, we purified exosomes also from 3,4 Dihydroxyphenylacetaldehyde (DOPAL)-treated cells, a toxic dopamine metabolite, which induce the formation of toxic DOPAL/aS oligomers.

The purified vesicles exhibited the typical hallmarks of exosomes. They contained aS oligomeric species and, upon DOPAL incubation, DOPAL modified aS and aS/DOPAL oligomers. Interestingly the latter were able to interact with exosomal membranes and, likely through a pore formation mechanisms alter exosomal microenvironment.

Once purified exosomes containing aS and DOPAL modified aS oligomers, we focused on the effect of these vesicles on different cell types. After secretion in fact, aS can influence neighboring cells in a paracrine manner. In particular, we analyzed neurons and microglia cells.

In neurons, exosomes appear to be secreted in a spatially and regulated manner through synapses, where aS exert its physiological role. Hence, we first investigate the effect of exosomes on synapses of primary neuronal culture. Upon incubation, aS containing exosomes and, more significantly, DOPAL-modified aS containing

exosomes reduced the amount of synaptophysin and PSD-95, two synaptic proteins of the pre- and post-synapses respectively. Moreover, TEM images of the synapses of treated neurons, revealed not only an impaired vesicle pools distribution (vesicles were more distant from the active zone), but also a reduced number of vesicles/synapses. The observed synaptic dysfunction likely cause also the neurite retraction, as measured by Sholl Analysis upon aS containing exosomes incubation. Lastly, we checked also for neuronal survival, analyzing the activation of caspase 3 and PARP1, but, under our experimental conditions, no significant effect was measured.

Therefore, exosomal aS toxicity is at least delivered to synapses, where they alter proteins amounts, function and neuronal morphology. We did not investigate the mechanism of internalization and toxicity, but, considering recent evidence, we propose two possible mechanisms. aS oligomers enter synapses and impact their physiology either (i) through a pore mechanism formation as suggest by the membrane localization of DOPAL-modified aS oligomers at membranes and their capacity to alter exosomal environment or/and (ii) seeding neuronal endogenous aS, hindering its physiological function.

In the second part of this thesis, we also investigated another way of impacting neuronal physiology: neuroinflammation induced by microglia activation.

Microglia cells, in fact, upon chronic and excessive aS exposure, are reported to became active and secret toxic substances, including the pro-inflammatory cytokines IL-1β, that are reported to impact neuronal survival.

When we applied aS containing exosomes to primary microglia cells, an increased release of IL-1 β was measured by Western Blot analysis, suggesting an induced inflammation.

In conclusion, our results demonstrate an exosomes-driven toxicity of aS not only to neuronal synapses, but also to microglia, inducing the secretion of IL-1 β. Therefore, aS containing exosomes appear as a vehicle of aS toxicity, which might be interesting not only as a future therapeutic target, but also as a potential biomarker for α-synucleinopathies.

# Riassunto

Le α-sinucleinopatie sono un gruppo di malattie neurodegenerative caratterizzate dall'anormale aggregazione della proteina α-Sinucleina (aS). La localizzazione dell'aS è prevalentemente pre-sinaptica, ove sembra non solo svolgere la propria funzione fisiologica, ma anche iniziare l'alterazione patologica della sua struttura. Nonostante i meccanismi alla base di questo evento non siano noti, una delle ipotesi proposte è l'internalizzazione di specie tossiche di aS rilasciate da altre cellule. Queste forme di aS, infatti, al pari di quello che avviene nelle malattie prioniche, indurrebbero l'aggregazione dell'aS endogena.

Tali premesse hanno indotto uno studio principalmente focalizzato sull'impatto a livello sinaptico di specie tossiche di aS. Tra i vari meccanismi di secrezione riportati per l'aS, si è scelto quello esosomiale, perché queste vescicole sono rilasciate in maniera controllata a livello sinaptico, proteggono l'aS dalle proteasi extracellulari e ne inducono l'aggregazione, suggerendo l'ipotesi di un loro ruolo principale nella propagazione delle α-sinucleinopatie.

Gli esosomi sono stati purificati da cellule HEK293T trasfettate con aS-EGFP e trattate o meno con il DOPAL, un metabolita tossico della dopamina che è in grado di indurre l'aggregazione dell'aS. Una volta verificato che le vescicole contenessero specie aggregate di aS, queste sono state poi incubate con culture neuronali primarie. Per valutare il loro effetto a livello sinaptico sono stati presi in considerazione vari fattori. Per primo è stata dimostrata una riduzione dei livelli di sinaptofisina e PSD-95, due proteine marker rispettivamente della pre- e della post-sinapsi. Queste alterazioni sono anche accompagnate da una disfunzione a livello sinaptico, caratterizzata non solo da una diminuzione del numero di vescicole per sinapsi, ma anche da una loro maggiore distanza dalla zona attiva. Anche la morfologia neuronale è stata alterata mentre non si è registrato alcun aumento di marker necrotici o apoptotici.

Gli esosomi contenenti aS e aS modificata da DOPAL sono stati poi incubati con cellule di microglia primaria al fine di valutare se erano in grado di indurre una risposta infiammatoria. L'attivazione cronica della microglia è una componente importante nelle malattie neurodegenerative che può danneggiare le sinapsi e

portare a morte neuronale. Come readout è stato misurato il rilascio di una citochina pro-infiammatoria IL-1β e il trattamento con gli esosomi ne ha aumentato la concentrazione nel medium, facendo ipotizzare un loro coinvolgimento anche nella neuro-infiammazione.

In conclusione questi dati suggeriscono che gli esosomi rilasciati dalle cellule e contenenti specie aggregate di aS propaghino la tossicità a livello neuronale e stimolino nella microglia la produzione di fattori pro-infiammatori, creando una sorta di circolo vizioso che ne aumenta l'effetto patologico. Gli esosomi contenenti specie aggregate di aS potrebbero quindi non solo diventare nuovi target terapeutici, ma anche potenziali biomarker per la diagnosi delle α-sinucleinopatie.

# CHAPTER I:
# Introduction

## 1.1 α-synucleinopathies

The term α-synucleinopathies is used to name a group of neurodegenerative disorders characterized by fibrillary aggregates, called Lewy Bodies (LB), in the cytoplasm of selected populations of neurons and glia cells. LB are spherical cytosolic inclusions of 5-25 μm in diameter, with a dense eosinophilic core and a clearer surrounding halo [1]. The main constituents of LB are β-sheet-rich amyloid fibrils of α-Synuclein (aS), a small presynaptic protein, together with other proteins, including ubiquitin, parkin and neurofilaments [1]. Apart from some rarer disorders such as neurodegeneration with brain iron accumulation type 1 [2] and other neuroaxonal dystrophies, there are three main types of α-synucleinopathies: Parkinson's disease (PD), dementia with Lewy bodies (DLB), and multiple system atrophy (MSA) [3] (**Figure 1**).

### 1.1.1 Parkinson Disease

The most common subtype of α-synucleinopathies is PD with a prevalence of 1.6% of incidence in people over the age of 65 [4,5].

The pathophysiology of PD is characterized by a progressive misfolding of aS, amyloid and tau protein deposition and a widespread brain and peripheral LB pathology [6]. Multiple transmitter pathways are affected such as the dopaminergic, cholinergic, noradrenergic, and serotonergic systems, resulting in a highly heterogeneous Parkinson syndrome [6]. Coherently, PD is characterized both by the presence of motor signs (bradykinesia, rigidity, resting tremor, gait instability) that are responsive to levodopa therapy [7], but also a variety of non-motor symptoms and cognitive deficits including olfactory dysfunction, cognitive impairment, psychiatric symptoms, sleep disorders, autonomic dysfunction, pain, and fatigue [8]. Even if current diagnostic criteria for PD are largely based on motor

symptomatology, the Movement Disorder Society has recently proposed a revised set of clinical and research criteria for the diagnosis of PD, including the non-motor signs as part of the core parameters [8-10].

PD is a multifactorial pathology and most of the cases are classified as idiopathic with an undefined aetiology. Aging, gender, ethnicity, neurotoxin exposure, genetic predisposition, protein misfolding and accumulation, oxidative stress, neuroinflammation, mitochondrial and proteasome dysfunction are all reported contributors to the development of PD [4]. However, a fraction of patients, approximately 5-10%, have a clear monogenic inheritance of the disease (**Table I**) [11]. At least, 24 loci have been associated with disease risk [4].

| | Protein | Pathogenic mutation(s) |
|---|---|---|
| **Autosomal dominant** | | |
| SNCA | α-synuclein | Missense mutations (Ala18Thr, Ala29Ser, Ala30Pro, Glu46Lys, His50Gln, Gly51Asp, Ala53Glu, Ala53Thr); multiplications (duplications, triplications) |
| LRRK2 | Leucine-rich repeat kinase 2 | Missense mutations (Ile1371Val, Asn1437His, Arg1441Cys, Arg1441Gly, Arg1441His, Tyr1699Cys, Gly2019Ser [most common], Ile2020Thr) |
| VPS35 | Vacuolar protein sorting 35 | Missense mutation (Asp620Asn) |
| EIF4G1 | Eukaryotic translation initiation factor 4-γ 1 | Missense mutations (Arg1205His, Ala502Val) |
| DNAJC13 | Receptor-mediated endocytosis 8 (REM-8) | Missense mutation (Asn855Ser) |
| CHCHD2 | Coiled-coil-helix-coiled-coil-helix domain containing 2 | Missense mutations (Thr61Ile, Arg145Gln); splice-site alteration |
| **Autosomal recessive** | | |
| Parkin | Parkin | Exon rearrangements, including exon deletions or multiplications (most common); missense mutations, nonsense mutations, small deletions or insertions; splice-site alterations |
| PINK1 | PTEN-induced putative kinase 1 | Missense or nonsense mutations (most common); exon rearrangements, including exon deletions or duplications |
| DJ-1 | DJ-1 | Missense mutations or exon rearrangements (most common); splice-site alterations |

**Table 1. Monogenic forms of Parkinson's disease** [4].

In this frame, mutations in Leucine-rich repeat kinase 2 (*LRRK2* – PARK8), encoding a serine-threonine kinase involved in membrane trafficking processes,

are the most frequent cause of genetic PD, with an autosomal dominant transmission (among all mutations, G2019S has been identified in up to 42% of familial cases [12]). *SNCA* encodes aS and it was the first gene associated with autosomal dominant PD (PARK1 and 4). Both point mutations as well as multiplication of the gene, lead to an early onset and aggressive disease. Autosomal recessive forms of PD are caused by mutations in genes encoding parkin (PARK2), PINK1 (PARK6) and DJ-1 (PARK7) involved in the ubiquitin-proteasomal system, mitochondrial functions and protection mechanisms from oxidative stress. In addition to these monogenic forms of PD, genetic variations in *SNCA*, *LRRK2* and β-glucocerebrisidase (*GBA*) increase the risk of developing PD. Of note, homozygous mutations in GBA cause Gaucher's disease, a lysosomal storage disorder whereas heterozygous mutations increase the risk of PD, suggesting that impaired lysosomal function may underlie PD pathogenesis. Aside from genetic causes and susceptibility, environmental factors and exposure to neurotoxins are considered an important aspect for PD onset. Exposure to 1-methyl-4-phenyl-1,2,3,6-tetrahydropyridine (MPTP) which interferes with Complex-I of the mitochondrial electron transport chain, results in nigral loss and parkinsonism. Also, the exposure to pesticides is associated with the development of PD, i.e. rotenone and paraquat that are mitochondrial Complex-I inhibitors or dieldrin that interferes with DA storage and depletion [5].

Whatever factor is responsible for triggering neurodegeneration, the main pathological pathways involved are protein misfolding, aggregation and impaired protein degradation; on the other hand, mitochondrial dysfunction and alteration of dopamine metabolism with consequent oxidative stress and activation of programmed cell death are processes impaired in PD. Finally, another important aspect is neuroinflammation, due to activation of microglial cells that surround diseased neurons. Chronic exposure to aberrant aggregates of proteins like aS, which can be released in the extra-cellular space, promotes activation of the innate immune response of glial cells. Secretion of pro-inflammatory mediators from activated microglia leads to increased neuronal death and progression of the disease [13].

### 1.1.2 Dementia with Lewy Bodies

DLB has a lower prevalence than PD [14], but it is the most frequently occurring type of dementia aside from Alzheimer disease, accounting for approximately 4.2% of all dementia cases [15]

It is characterized by fluctuating cognition, parkinsonism, and visual hallucinations in the presence of global cognitive decline [15]. It is differentiated from PD with Dementia for the presence of striatal β amyloid deposition [16] There is little difference in the distribution or severity of LB between PD with Dementia and DLB [17], but many patients with DLB have intracytoplasmic aggregates of the aS in the midbrain, limbic, and neocortical regions [15].

### 1.1.3 Multiple System Atrophy

Multiple System Atrophy (MSA) is a rare neurological disorder, considered an orphan disease with prevalence just under 0.01% in persons older than 40 years of age [18]. It differs significantly in clinical and pathological characteristics with PD and DLB. MSA is diagnosed at a similar age as PD (at about 60 years), but have significantly shortened mean survival (6–9 years). According to the second consensus statement on the diagnosis of MSA [19], patients who present predominantly parkinsonian symptoms (i.e. bradykinesia, rigidity, tremor and postural instability) are designated as MSA with parkinsonism (MSA-P) [20]. Patients who present predominantly with a cerebellar syndrome are classified as MSA with cerebellar signs (MSA-C). In MSA-C the most common symptom is gait ataxia and uncoordinated, unbalanced movement. [20]. MSA-P and MSA-C have the same disease duration. Autonomic manifestations are common to both variants and affect urogenital (bladder and erectile dysfunction have been identified as some of the earlier clinical signs), gastrointestinal and cardiovascular systems. Additional symptoms include dysphagia, bowel dysfunction and orthostatic hypotension [20].

Even if cognitive impairment was previously considered as an exclusion criterion for diagnosis, it has been recently recognized as a typical hallmark of MSA[20]. In 14–18% of cases, in fact, patients display some degree of cognitive disability [21] , more severe and widespread in patients with the MSA-P variant. The diagnosis of MSA is commonly confused with PD, due to the overlap of symptoms between the two

diseases. Remarkably, levodopa is poorly efficient, if at all, to treat MSA symptoms [22] (**Figure 1**).

MSA is pathologically characterized by aS-positive cytoplasmic inclusions in glial cells (GCIs), widespread distributed throughout the brain. In addition to GCIs, MSA patients display aS-positive inclusions also in the cytoplasm and nucleus of neurons [23].
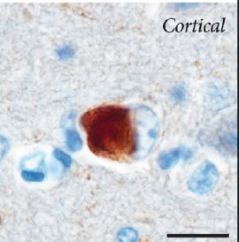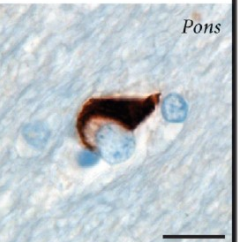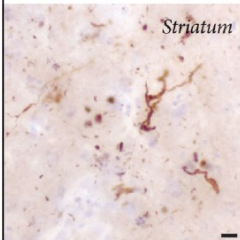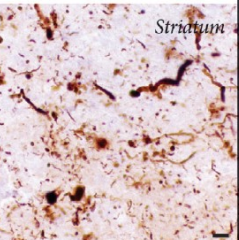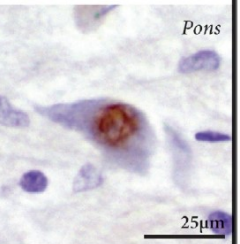
| Clinical | Parkinson's disease (PD) | Dementia with Lewy bodies (DLB) | Multiple System Atrophy (MSA) |
|---|---|---|---|
| Age of Onset (years) | ~60 | ~70 | ~60 |
| Duration (years) | ~12 | ~5 | 6-9 |
| Motor signs | All | Some | All |
| L-dopa responsive | Yes | Variable | No |
| Non-motor signs | | | |
| Autonomic | Late | Late | Early |
| Hallucinations | Late | Early | No |
| Olfactory dysfunction | Early | Early | No |
| Dementia | Late | Early | No |
| Main synucleinopathies | NCIs | NCIs | GCIs |



**Figure 1. Differences among the three main α-synucleinopathies, Parkinson's disease (PD), dementia with Lewy bodies (DLB) and multiple system atrophy (MSA).** [McCann, Parkinsonism Relat Disord (McCann)][3].

The clinical symptoms of MSA-P and MSA-C, generally reflect the pathological change in the brain regions mainly affected: in MSA-P, the striatonigral regions, while in MSA-C the olivopontocerebellar regions [23]. Concerning the inclusions localization, the glial one are mainly found in the putamen, pons, motor cortices

and underlying white matter, as well as the cerebellar matter; while neuronal inclusions have been observed in the putamen, SNpc, pons and cerebellar Purkinje cells.

To summarize, both patients medical history and physician evaluation are required to identify α-synucleinopathies, but the diagnosis of this group of neurodegenerative disorders remains very difficult, especially in the early stages of the pathologies, characterized by unspecific symptoms such as olfactory dysfunction [24] or sleep disorder [25].

Therefore, an increasing number of studies are searching for novel biomarkers, to improve the early clinical diagnosis of PD and DLB in addition to other α-synucleinopathies such as MSA [26].

## 1.2 α-Synuclein

α-Synuclein (aS) is a small, 140 aminoacids protein, encoded by a gene (SNCA) located on chromosome 4 encompassing seven exons. First described by Maroteaux in 1988, aS is mainly localized in the presynaptic nerve terminals and in the nucleus of neurons. Since, in 1997, a point mutation on aS gene was linked to early-onset familial PD, the discovery of other genetic alterations of SNCA gene together with the presence of aS as the main component of LBs in surviving neurons of PD patients, point out the study of this protein fundamental in understanding the pathophysiology of both familial and sporadic PD.

As reviewed by Breydo and Lashuel [27,28], aS is a natively unfolded protein thought to exist in equilibrium between a soluble cytosolic conformation and a membrane bound, alpha-helix conformation. Although the biological function of aS is not fully understood, it has been suggested to be involved in synaptic vesicles trafficking, neurotransmitter release and SNARE complex assembly [28].

### 1.2.1 Structure and folding pathways

aS 140 amino acids can be divided into three domains that confer unique properties to the protein.

The N-terminal region (residues 1–60) contains several imperfect repeats of a consensus motif (KTKEGV). This repeated motif, also present in Apolipoprotein A–I, is essential to the formation of a structural amphipathic alpha-helices upon aS membrane binding [29]. Interestingly, all reported six PD-related mutations (A53T, A30P, E46K, E50Q, E51D) are located in this domain [11,30-34]. The central region is commonly known as the non-Aβ component of plaque (NAC) domain and consists of residues 61 to 95. This highly hydrophobic region contains 12 amino acids (71–82) essential for aS to polymerize into amyloid filaments, which are the major components of aS pathological inclusions [35]. The last 44 amino acids of aS confer a negative charge to the protein due to the abundance of glutamates and aspartates. These negative residues appear to have an important effect in modulating aS aggregation [36]. This domain is essential for the formation of calcium-mediated annular oligomers via direct binding [37]. In addition, the C-terminus of aS has been suggested to contribute to a chaperone-like activity [38] (**Figure 2**).
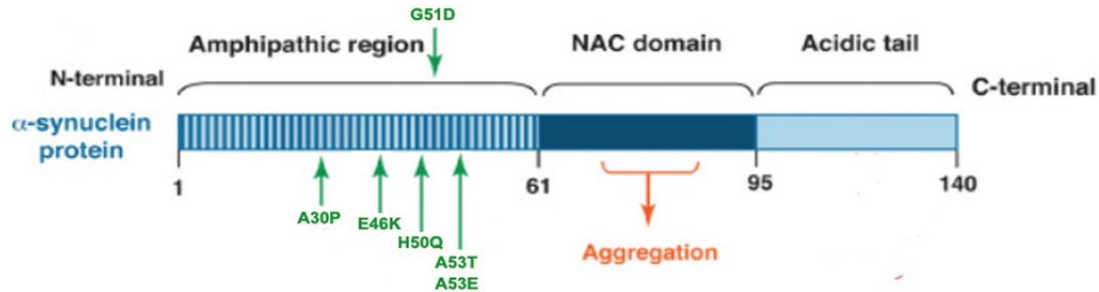


**Figure 2. aS protein domains structure.** The sequence can be divided into three regions with distinct structural characteristics: the amphipathic N-terminal, the NAC domain and the acidic C-terminal. The figure also illustrates the six missense mutations that segregate with PD, lied in the N-terminal region of the protein [Shengli and Chan, Biomolecules (2015)][39].

Cytosolic aS is soluble and considered to be natively unfolded with little secondary structure [40]. A debate has recently ignited around the true physiologically relevant conformation of aS, due to a proposed metastable tetrameric form [41,42]. In contrast, different studies do not find this cytosolic tetramer in the central nervous system, in erythrocytes, mammalian cells, and in *E. coli* [43-46]. The hypothesis is that the binding to cellular factors, such as lipids or membranes, can induce and stabilize

higher-order multimers like octamers [47], while endogenous multimers become unstable due to the protein purification protocols [48].
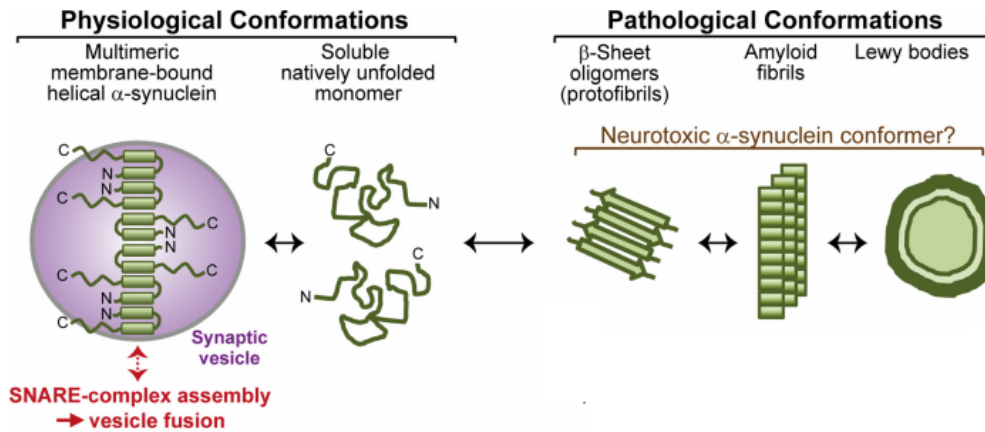


**Figure 3. Schematic representation of aS conformations associated with its physiological function and pathological activities** [Adapted from Burrè et al., J Neurosci (2015)][49].

Under pathological conditions, a number of factors, such as oxidative stress, post-translational modifications, proteolysis, glucose deprivation and altered concentrations of fatty acids, phospholipids and metal ions, have been linked to aS misfolding and aggregation into distinct soluble oligomeric species and eventually insoluble amorphous or fibrillar amyloid-like assembles, similar to aS found in LBs (**Figure 3**) [50].

### 1.2.2 α-Synuclein and membranes

In vivo, aS is in an apparently strictly regulated equilibrium between cytosolic and membrane-associated forms [51]. The interaction between aS and lipid surfaces is believed not only to mediate its cellular function [52], but also to modulate its propensity to self-assemble into amyloid fibrils [53,54](**Figure 4**) .

Despite the fact that two independent groups provided evidence for a tetrameric nature of aS, the widely accepted model is that aS exists as an intrinsically disordered protein in its physiological cytosolic form [55] and that, upon membrane binding, specific regions of the protein acquire a significant level of α-helical structure [56,57]. The first 90 residues of the aS, characterized by 11 residue repeats

encoding for amphipathic class A2 lipid-binding α-helical segments are considered to favour this transition [58].

aS binding to membranes involved both electrostatic and hydrophobic interactions [59]. The acidic head groups, such as phosphatidylethanolamine, phosphatidylserine or phosphatidylinositol, are essential in N-terminal domain [60-64], suggesting that the membrane head groups interact with lysine residues placed at opposites sides of the aS helix [52].
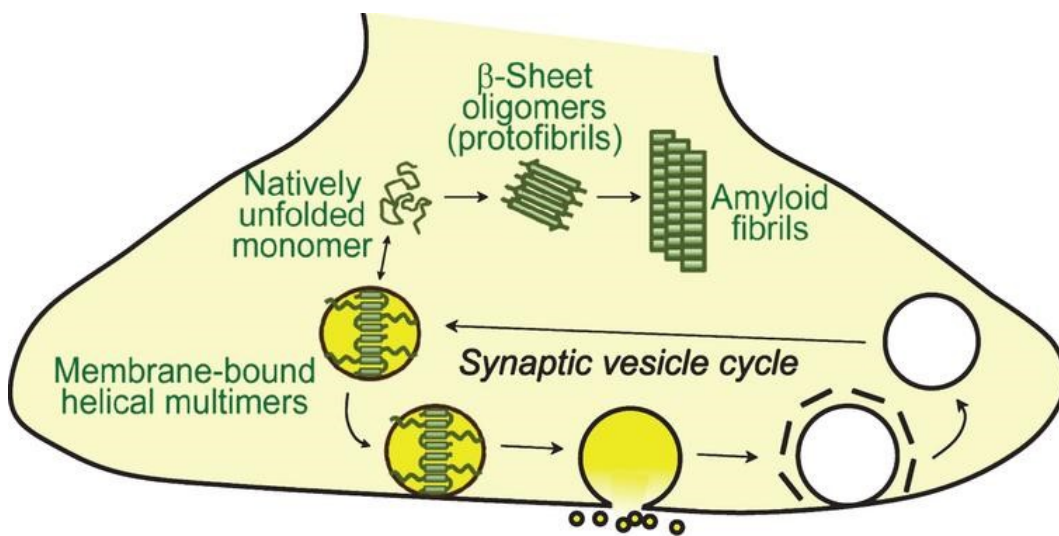


**Figure 4. Physiological and pathological conformations of aS at the synapse.** [Burrè, J Parkinsons Dis. (2015)] [52].

Indeed, increasing negative charge density of the membrane enhances the electrostatic interactions with positively charged aS residues (in particular the numerous lysines). Remarkably, synaptic vesicles, which are highly curved, and negatively charged on the membrane surface, appear as optimal target for aS binding [59].

Another key element, that is reported to enhance the binding of aS to lipids is membrane curvature [65-68]. Increasing curvature, in fact, raised the size and number of so-called packing defects in more highly curved membranes [69,70]. Packing defects are defined as membrane regions that transiently expose their interior hydrophobic acyl chain, acting as effective protein binding sites [59].

aS's preference for more highly curved membranes has led to its classification as a "curvature sensing" protein [67,69,71]. In addition to sensing membrane curvature, aS is also able to actively alter membrane shape/curvature [72-75]. Such direct effect on membranes could be involved in synaptic vesicle homeostasis and/or exocytosis.

Moreover, aS is susceptible to numerous post-translational modifications, such as serine/threonine and tyrosine phosphorylation [76-80], N-terminal acetylation [76], tyrosine nitration [81], ubiquitination [82], sumoylation [83], trans-glutamination [84] and methionine oxidation [85], which can induce changes in protein charge and structure. This may lead to altered binding affinities with other proteins and lipids. As an example, Anderson and coworkers reported that aS is N-terminally acetylated [76], by binding of an acetyl group to the alpha amino group of the first amino acid of aS [44]. N-terminal acetylation of aS has been detected both in healthy and Parkinson's disease individuals, and increases its helical folding propensity, its affinity for membranes and its resistance to aggregation, suggesting that N-terminal acetylation of aS might be implicated in both the native and pathological structures and functions of aS [52]. In addition, also phosphorylation regulates aS structure, lipid binding, protein interactions, but also its oligomerization, fibril formation, and neurotoxicity [52]. The main phosphorylation sites are Ser87, Tyr125 and Ser129, which is the best characterized. It occurs constitutively only in a small fraction (>4%) of aS in the brain, whereas in proteinaceous, pathological inclusions there is a dramatic accumulation ($\cong$90%) of aS phosphorylated at this site [86]. Phosphorylation of aS has been associated to many kinds of kinases, i.e. casein kinases, G protein-coupled receptor kinases (GRKs), LRRK2 and Polo-like kinases (PLKs). As Oueslati recently reviewed, however, whether P-Ser129 suppresses or enhances aS aggregation and toxicity remain controversial. So far, evidence supports the hypothesis that P-Ser129 may occur after LBs formation and could represent a late event in disease progression [86].

Under certain circumstances, the tight binding of aS N-terminal domain to the surface of lipid membranes can also have detrimental effects. It is, in fact, reported that it favours the population of conformational states in which the NAC aS region, which has been involved in aS aggregation [87,88], is exposed to the solvent by partial detachment from the membrane surface. Consequently, the interaction between aS

and lipid is potentially not only implicated in its functional state but also in the initial step for the aggregation of aS at the surface of vesicles membranes [53], a process strictly associated with α-synucleinopathies onset and progression. Indeed, the NAC domain, rather than actively contributes to aS fibril amyloidogenic core formation, may be involved in the aggregation at the surface of lipid vesicles due to its anchoring role to the membrane surface, permitting to the aS amyloidogenic region to be in equilibrium between membrane-associated and membrane-dissociated states [57]. The aS NAC region detachment from the membrane surface and the consequent reduction of aS freedom degrees in the membrane-associated state may promote aS fibrils formation via primary nucleation [53]. Coherently, Rientra and co-workers recently analysed several aS fibril forms by solid-state NMR (SSNMR) spectroscopy and they reported that the N-terminal region is not part of the amyloid core [89].

However, others hypothesized that aS aggregates derived from the less stable, natively unfolded forms of cytosolic aS [52].

### 1.2.3 α-Synuclein toxicity

aS synthesis, clearance and aggregation regulate its concentration in the central nervous system. Once the equilibrium among these processes is impaired, aS accumulation results in increasing amount of toxic aggregated species (**Figure 5**).

α-synucleinopathies are mainly sporadic disorder, characterized by aS misfolding and aberrant accumulation. aS toxic species may affect different cellular pathways. In particular, oligomers and intermediate fibrils are reported to impair protein degradation, mitochondrial functions, endoplasmic reticulum-Golgi trafficking, neurotransmitters release and synaptic transmission. One proposed toxicity mechanism is that aS monomers self-assembly in oligomers that can form pores in membranes, altering their permeability. As a result, these alterations may induce neuronal death through a direct effect on synaptic function (synaptic vesicles disruption and alter neurotransmitter release in the cytosol) or an increased calcium influx from the extracellular space [28].

Regarding aS toxicity, it should also be considered its genetic multifold contribution to α-synucleinopathies. As an example, aS gene multiplication, i.e.

duplication and triplication, cause an early onset, autosomal dominant form of PD with aggressive disease progression, by enhancing protein expression and aggregates formation. Moreover, different point mutations in the SNCA gene have been associated with familial forms of PD: A30P, E46K, H50Q, G51D and A53T-E.
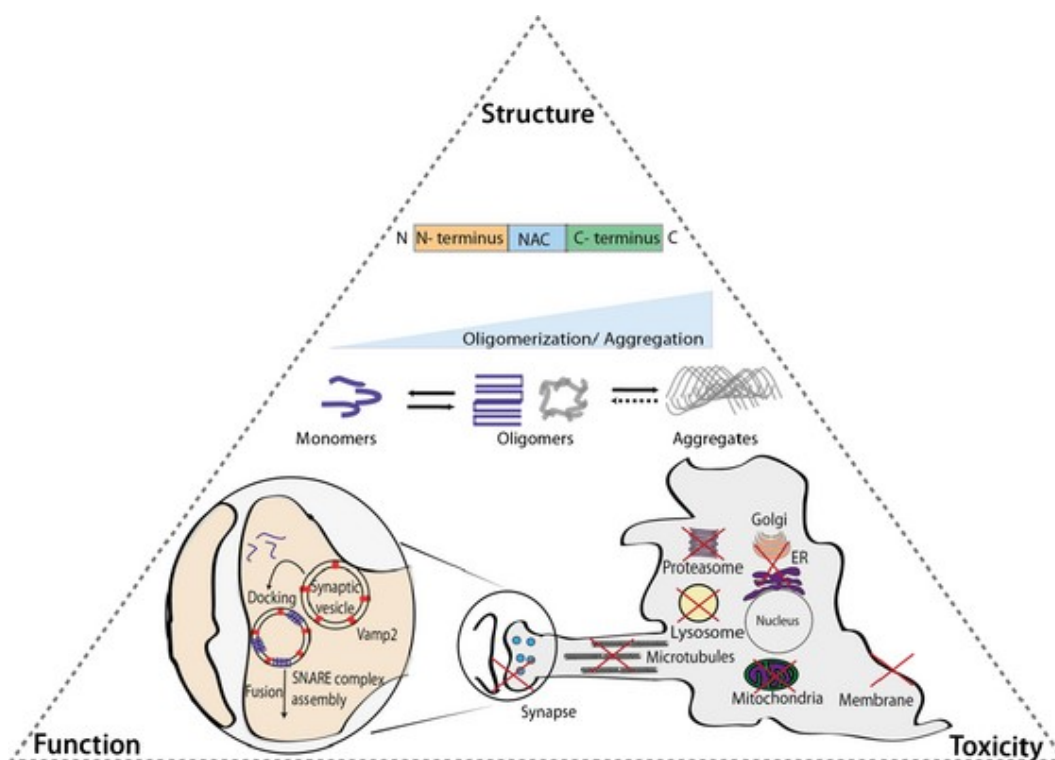


**Figure 5. aS as the proposed cornerstone of α-Synucleinopathies.** [Villar-Piqué J Neurochem. (2016)][90].

All these mutations have been implicated in aS oligomerization or enhanced fibrillization in numbers of both *in vivo* and *in vitro* studies [28].

## 1.3 The Catechol Hypothesis

Starting from the observation that dopaminergic neurons of SNpc are preferentially susceptible to aS toxicity in PD, over the last years, researchers tried to figure out a connection between aS aggregation process and dopamine metabolism. Increasing evidence supports the idea that altered dopamine metabolism is directly involved in the pathogenesis of PD. In this frame, the concept of "autotoxicity" of catecholamines and their metabolites led to the formulation of the "Catechol Hypothesis" [91].

**1.3.1 Dopamine metabolism**

The neurons of SNpc release Dopamine (DA). DA is a neurotransmitter endogenously synthesized in the body, from the dietary amino acid L-tyrosine (L-Tyr). As represented in **Figure 6**, two reactions produce DA from tyrosine: the enzyme tyrosine hydroxylase (TH) produces the intermediate 3,4-dihydroxyphenylalanine (L-DOPA) from L-Tyr and L-DOPA is then converted into DA by the L-aromatic amino acid decarboxylase (AADC) with the release of $CO_2$. In non-dopaminergic cells, DA can be further processed into norepinephrine and epinephrine by the dopamine-β-hydroxylase (DβH) and N-methyltransferase (NMT).
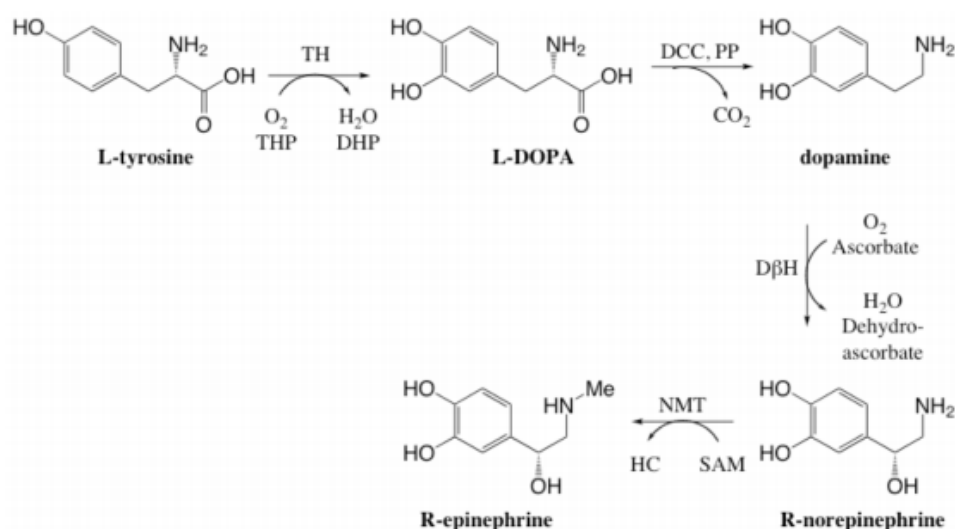


**Figure 6. Biosynthesis of catecholamines.** [Meiser J, Cell Commun Signal. (2013)] [92].

DA concentration in the cytoplasm of the terminal axon of neurons depends on the equilibrium between DA catabolism and its sequestration into storage vesicles. The latter is mediated by the vesicular monoamine transporter 2 (VMAT2), a vesicular antiporter that exchanges two protons for one DA molecule. An ATP-dependent proton pump located in the vesicular membrane assures the proton gradient and allows DA storage in vesicles at high concentrations (up to 1M). Moreover, pH inside storage vesicles is acidic (pH 5) to minimize DA spontaneous oxidation.

As vesicles fuse with the plasma membrane in response to neuron depolarization, DA is released in the synaptic cleft where it diffuses and interacts with post-synaptic receptors. Extracellular DA is then removed by metabolism or re-uptaken by microglia and neurons, through the DA-transporter (DAT). This is a symporter pump that co-transports DA and sodium. Once DA is back into neurons, it can be either stored in vesicles or be metabolized (**Figure 7**).
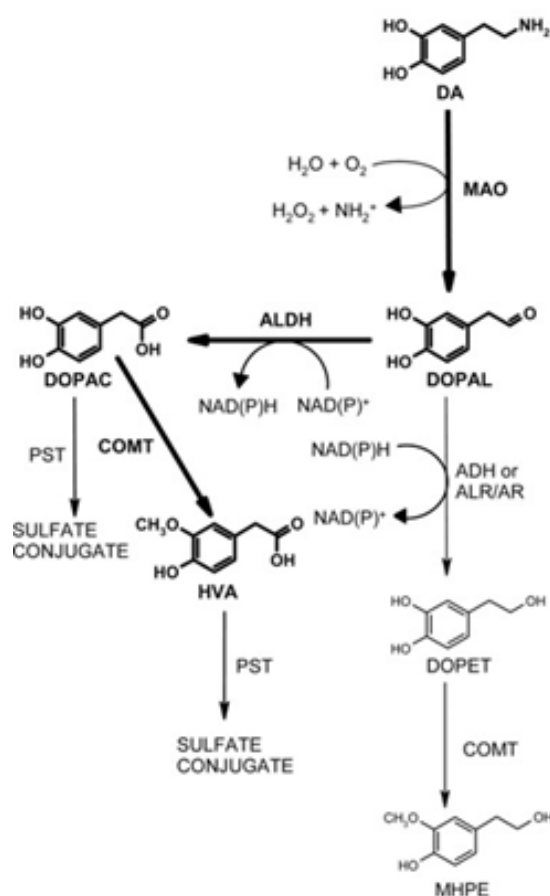


**Figure 7. Dopamine metabolism** [Adapted from Marchitti et al., *Pharmacol Rev* (2007)][93].

DA catabolism primary involves oxidative deamination mediated by the mitochondrial monoamine oxidase (MAO) with the release of $H_2O_2$ and ammonia. The product 3,4-dihydroxyphenilacetaldehyde (DOPAL) is then metabolized by two alternative pathways.

The prevalent one involves the enzymes aldehyde dehydrogenase (ALDH). In dopaminergic neurons of SNpc, there are two ALDH isoforms, the cytoplasmic

isoform ALDH1A1 and the mitochondrial one ALDH2. ALDHs reduce a NAD(P)$^+$ molecule to NAD(P)H and convert DOPAL into the acetate form 3,4-dihydroxyphenylacetic acid (DOPAC), which is further degraded by the catechol-O-methyl transferase (COMT) and removed from dopaminergic neurons. A minor pathway of DOPAL metabolism involves cytosolic aldehyde or aldose reductase (AR) [94] which convert NAD(P)H molecule to NAD(P) $^+$ and reduce DOPAL to hydroxytyrosol or 3,4-dihydroxyphenylethanol (DOPET). DA, DOPAL, DOPAC and DOPET can be metabolized by COMT, whose products can undergo biotransformations i.e. sulfation and glucuronidation [93].

## 1.3.2 DOPAL reactivity

In the past years, many studies addressed the potential neurotoxic effect of DA, due to its tendency to oxidize and generate reactive species such as radicals and quinones. These species can damage macromolecules such as DNA and proteins, but also deplete cellular oxidative defences, enhance ROS production and induce lipid peroxidation. However, in recent years, researchers focus their attention to DOPAL, the monoamino oxidase dopamine metabolite and its potential correlation to the pathogenesis of PD. In fact, DOPAL is several orders of magnitude more toxic than other catecholamines [95].
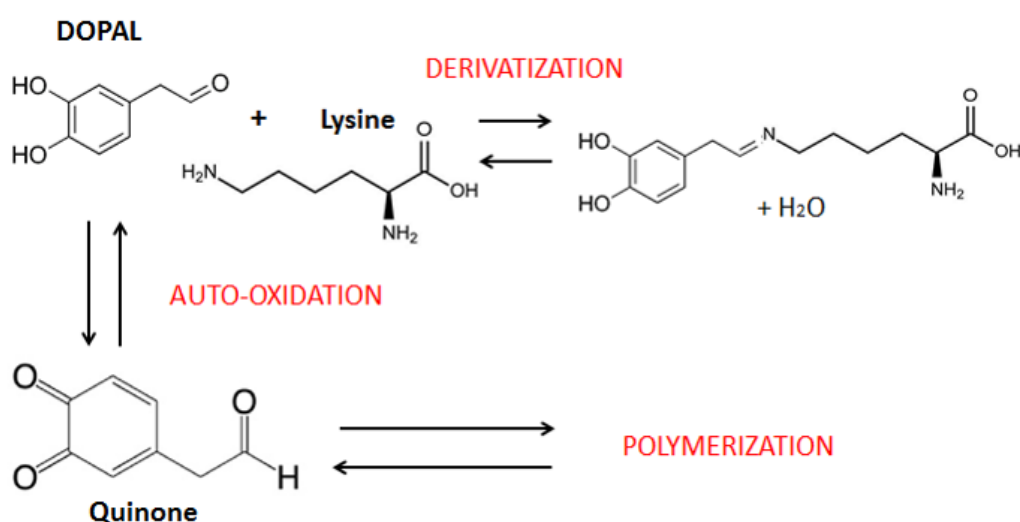


**Figure 8. DOPAL reactivity depends on both the catechol and the aldehyde moieties** [96].

DOPAL has two highly reactive functional groups, a catechol and an aldehyde. The first one has a similar tendency as DA to auto-oxidase, with the consequences described above. Auto-oxidation also leads to DOPAL polymerization and production of catechol adducts. On the other hand, the aldehyde moiety is highly reactive against amino groups such as the ones of lysine residues within proteins, through a Schiff base mechanism (**Figure 8**) [97].
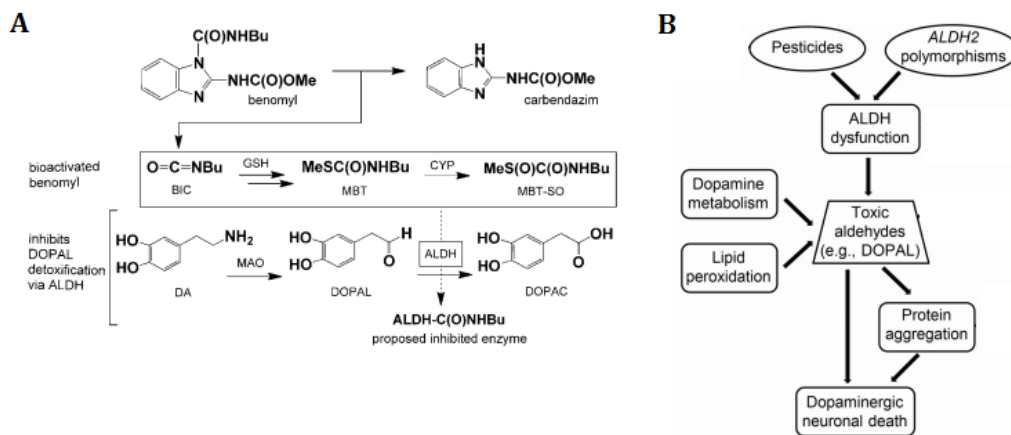


**Figure 9. Inhibition of ALDH as a possible mechanism for PD pathogenesis.** (A) Benomyl metabolites and ALDH inhibition [Fitzmaurice et al., *PNAS* (2014)]. (B) Parkinson development from ALDH inhibition via gene-environment interactions [Adapted from Fitzmaurice et al., *Neurobiology* (2014)][98].

Physiologically, DOPAL concentration in neurons is reported to be around 2-3 μM. In pathological condition, DOPAL levels may increase up to 6 μM, leading to cellular toxic effects, such as aberrant DA trafficking, protein cross-linking, proteasome impairment, ROS production and mitochondrial dysfunction [97].

Coherently, brains of PD patients present high levels of DOPAL in comparison with controls [99]. To date, the mechanism(s) that lead *in vivo* to increased DOPAL levels in dopaminergic neurons are still unknown. However, one of the proposed mechanisms is the ALDH inhibition, the enzymes implicated in DOPAL detoxification. The human ALDH belongs to a gene superfamily, which consists of 19 genes, putatively functional, with different chromosomal locations. Among the 19 isoforms, ALDH1A1 and ALDH2 are reported to be the most involved in DOPAL

metabolism, with a $k_m$ of 0.4-1.0 μM [93]. Supportively, Liu and co-workers recently demonstrated that the lack of ALDH1A1 expression in a SNpc dopaminergic neuron subpopulation increased cell vulnerability and neurodegeneration, together with the finding that PD brains display a significant reduction of ALDH1A1 expression [100]. Moreover, null mice for both the cytosolic ALDH1A1 and mitochondrial ALDH2 isoforms exhibits a parkinsonian-like motor phenotype, characterized by increased dopaminergic neurons degeneration and DOPAL accumulation [96,101].

*In vivo*, ALDHs may be inhibited by age-related dysfunction or inactivation, genetic deletion, pharmaceutical agents and environmental toxins, metabolic and oxidative stress (i.e. 4-Hydroxynonenal, a product of lipid peroxidation) [93]. As an example, benomyl, an environmental toxicant, after bioactivation to S-methyl N-butylthiocarbamate sulfoxide (MBT-SO), is able to irreversible inhibit ALDH (**Figure 9A**) [102].

Benomyl was largely used for more than 30 years as a fungicide in agriculture, until studies on animals attested its involvement in carcinogenesis, teratogenesis and neurotoxicity. As reported by Fitzmaurice in 2014, benomyl inhibits ALDH in primary mesencephalic neurons, leading to altered dopamine homeostasis. Supportively, epidemiological studies reported that high exposure to benomyl increased the risk to develop PD and ALDH variants enhances the effects of pesticides associated with PD pathogenesis [98]. The link between genetic alteration and environmental inhibition of ALDH could provide an explanation for sporadic forms of PD (**Figure 9B**). This can be truth for many other ALDH inhibitors, commonly used in the clinical practice, like hypoglycemic agents, the hypnotic agent chloral and disulfiram for the treatment of chronic alcoholism [103].

### 1.3.3 DOPAL induced aS aggregation

Being lysine residues in proteins among the most reactive moieties toward DOPAL, aS is predicted to be a preferential target for three reasons. (i) aS is highly abundant in presynaptic terminals, (ii) it possesses a high ratio of lysine residues in its sequence (15 lysines out of 140 amino acids) and (iii) finally, being an unfolded protein, these residues are relatively accessible to aldehyde reactivity [104].

To date, it has been widely demonstrated that DOPAL can covalently modify aS, inducing its aggregation both *in vitro* and *in vivo* systems. Burke and co-workers demonstrate that the over-expression of aS in SH-SY5Y cells leads to the formation of SDS-resistant aS oligomers upon exogenous DOPAL treatment. Moreover, DOPAL injection into rats SN induced neurodegeneration and aS high molecular weight species accumulation [105].

However, DOPAL may induce charge reduction and increased hydrophobicity in modified proteins, leading also to the formation in solution of large non-covalent aggregates of aS-DOPAL covalent oligomers[106]. Supportively, SDS treatment on *in vitro* produced aS-DOPAL oligomers, diminished the quantity of aS high molecular weight species, suggesting the presence of both covalent and non-covalent aS aggregates upon DOPAL treatment [107]. The formation of aS high molecular weight species was also detected *in vivo* upon DOPAL injection into the SN of rats [105]. Moreover, genetically inhibition of ALDHA1 leads to the formation of aS aggregates in transgenic mice expressing A53T, the mutant form of aS [100]. The over-expression of ALDH1A1 in ALDH1A1 knockout mice results in increased resistance to aS cytotoxicity in dopaminergic neurons, suggesting that ALDH absence increases cellular DOPAL levels and leads to the formation of aS oligomers.

The aS lysine residues, that seem to be preferentially modified by DOPAL, have been identified by mass spectrometry analysis both *in vitro* [108] and in cells [106]. Since, DOPAL-aS adducts appear to be off-pathway oligomers, preventing aS fibril formation [106,108], the toxicity mechanism may derive from their effect on aS physiologic function. As recently demonstrated by Follmer and co-workers, DOPAL modified aS monomers have a diminished affinity for membranes. This may lead *in vivo* to an increased level of cytoplasmic aS and to its aggregation. Alteration in aS membrane binding may hinder aS physiological function, i.e SNARE complex assembly and synaptic vesicles pools localization. As a consequence, a reduced amount of dopamine is released by neurons, contributing to PD pathogenesis/development. Moreover, DOPAL-modified aS oligomers are able to permeabilize synaptic vesicles, leading to dopamine release in cellular cytoplasm, where MAO catalyses its degradation into DOPAL. In that way, neurodegeneration can be induced faster due to the formation of always more DOPAL[104].

## 1.4 Prion-Like Spreading of α-Synuclein  Pathology

To date, increasing evidence supports the idea that proteins involved in neurodegeneration, such as aS, can transmit cell to cell their misfolded structures to native proteins, contributing to disease propagation in a so-called prion-like mechanism.

### 1.4.1 Pathological Studies

The hypothesis of a prion-like mechanism of α-synucleinopathies progression mainly derived from the Braak's hypothesis.  (**Figure 10**) [109].

It was 2003, when a German anatomist, Braak, and his co-workers reported that LB pathology evolved in a temporal, stereotypic pattern from the lower brainstem through susceptible regions of the midbrain and forebrain into the cerebral cortex, in a caudo-rostrally manner [110].
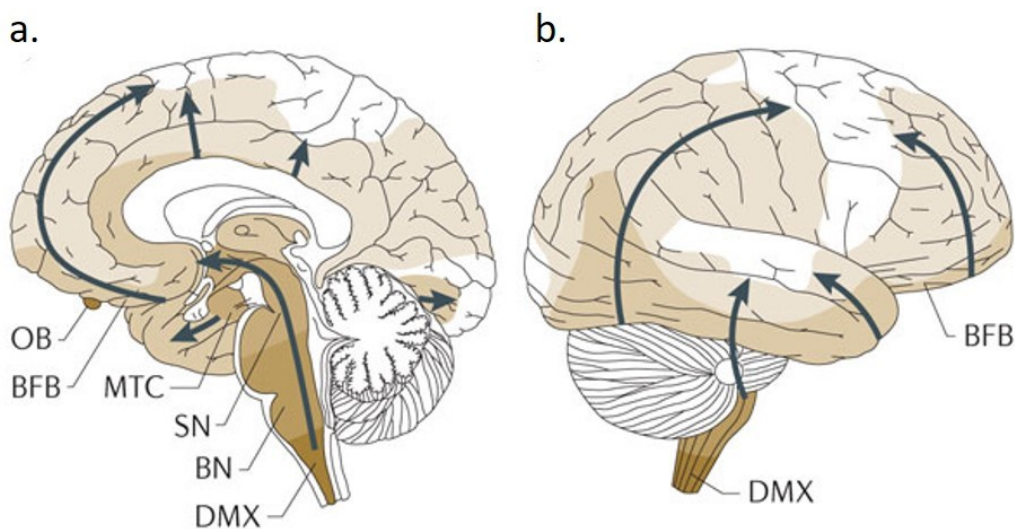


**Figure 10.  The spreading of aS-pathology in PD.** PD involves first darker areas and subsequently regions identified in lighter colors. **a**. cross section of the brain; **b.** lateral view of the human brain. Olfactory bulb (OB), dorsal motor nucleus of the *vagus* nerve (DMX), BFB, basal forebrain; BN, brainstem nuclei; MTC, mesiotemporal cortex; SN, *substantia nigra* [Adapted from Brettschneider et al., Nat Rev Neurosci (2015)][111].

This evidences could merely exist due to a different vulnerability among distinct brain region, but the topological evolution of the affected areas in each stage of the pathology suggest a spatial-temporal propagation, which correlates with disease severity [112].

*In vivo* confirmation of Braak's hypothesis came also from the observation that LB pathology could be transmitted to embryonic dopamine neurons transplanted into the putamen of human PD patients [113,114]. Kordower and co-worker reported that even after only 10 years from transplantation the grafted neurons in PD patients displayed LB pathology, a time not sufficient to normally have evidence of such aS-positive aggregates [114,115].

Cell-to-cell transmission of aS-aggregates was also reported by Hansen and co-workers in 2011. They demonstrated that aS could transfer between host cells and grafted dopaminergic neurons, inducing aS aggregation in the recipient cells [116]. Therefore, aS has been suggested to be the prion-like agents, transmitted from cell to cell and responsible for α-synucleinopathies propagation [112].

Supportively, aS was detected in many human body fluids, such as cerebrospinal fluid (CSF), saliva and blood plasma [117-119], but no significantly differences were found in the body fluids of PD patients in comparison with healthy controls, suggesting that aS was physiologically secreted [112]. On the contrary, increased levels of aggregated aS species have been detected in the CSF, saliva and skin of α-synucleinopathies patients [119-122], supporting evidence that extracellular aS concentration and aggregation state might reflect pathological conditions.

Moreover, aS positive inclusions have been also found in the gastrointestinal tract, mainly in the submandibular gland, esophagus and rectum [122]. Coherently, an increasing number of studies focus on the potential use of aS as a biomarker for α-synucleinopathies diagnosis [123].

## 1.4.2 aS propagation from cell to cell

To date, even if increasing evidence suggests a spatiotemporal regulated progression of α-synucleinopathies, the implicated molecular mechanism(s) is still largely unknown.

As reviewed by Costanzo [124] there are various possible mechanisms of aS propagation (**Figure 11**), probably dependent on the type of cell, its condition, and the aS propagated species [112].

To permit cell-to-cell transmission of aS pathology, at least three events are needed: (i) aS should be released by cells in the extracellular space; (ii) aS uptake by a recipient cell; and (iii) the induction of aS aggregation in the recipient cell probably due to misfolding of the endogenous aS [112].

In addition, α-synucleinopathies development might cause cell injury or death, inducing the passive release of aS. However, this mechanism does not appear as the main process of released, since aS levels are not significantly different between diseased and control cases [112].

Considering aS affinity for membranes, it might be secreted through an unconventional ER/Golgi-independent secretion pathway [125], or exosome-mediated pathway [126,127]. Indeed, the role of exosomes in the spreading of aS pathology is gaining attention.
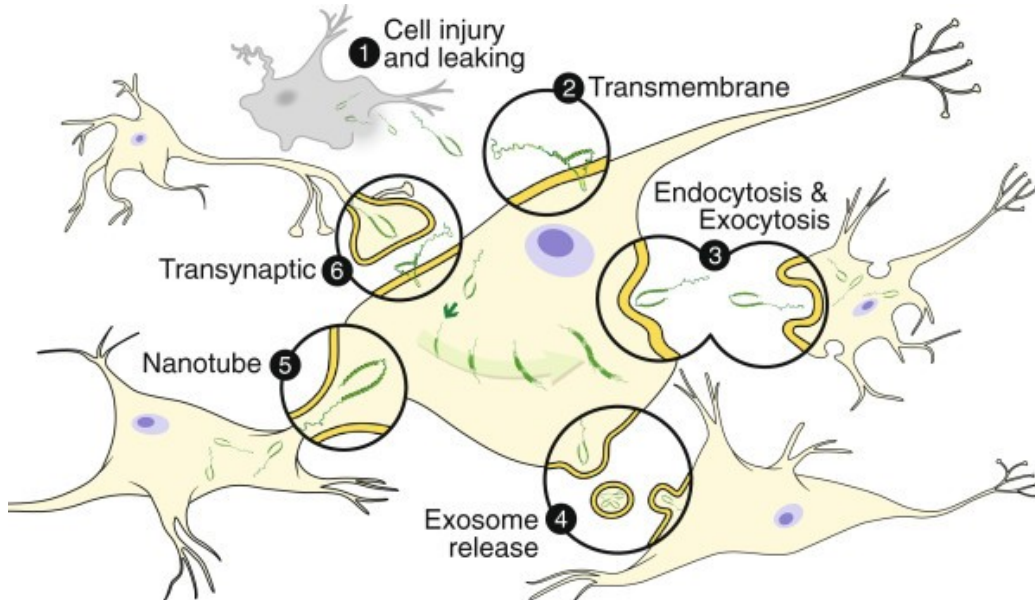


**Figure 11. Potential mechanisms of neuron-to-neuron transmission of aS.** [from Visanji et al., Acta Neuropathol Commun. (2013)][110].

Other putative mechanisms involved in a cell-to-cell transfer of aS include endocytosis. This was confirmed in experiments using dynasore, a potent endocytosis inhibitor that dramatically reduces aS uptake [128]. Coherently, Dawson

and co-workers have recently proposed the neuronal receptor LAG3 (lymphocyte-activation gene 3), as responsible for binding and endocytosis of pre-formed fibrillar aS species [129].

Alternative intercellular propagation pathways, such as transmission through axonal transport [130], which is both anterograde and retrograde [131], or via a trans-synaptic mechanism [132], have been proposed. Moreover, it was also found that aS fibrils can be transferred from donor to acceptor cells through tunneling nanotubes (TNTs) inside lysosomal vesicles, seeding soluble aS aggregation in the cytosol of acceptor cells [133].

It is important to mention that the identification of a specific receptor [129] or a specific propagation pathway for aggregated aS species could pave the way for the developing of novel drugs designed to slow the progression of α-synucleinopathies.

The other way around, cell stress, lysosome impairment, proteasomal dysfunction, and protein misfolding, are associated with an increase of aS release from cells [112]. Several factors are reported to enhance aS secretion. Among these, dopamine, which promotes secretion of aS aggregates and have no effects on monomers, suggesting that neurotransmitters could play a significant role in aS secretion [134]. Coherently, in the mice striata, GABA release controls aS release from the glutamatergic terminals through activation of the presynaptic GABAB receptors [135]. Moreover, the PD-associated Leucine-rich repeat kinase 2 (LRRK2) not only promote aS release but also the cell-to-cell transmission process [136]. Also, ATP13A2 (PARK9), a gene linked to Kufor-Rakeb syndrome (KRS), characterized by juvenile-onset parkinsonism, increased aS secretion. The same effect is obtained with the mutation in the SNCA gene associated with familial forms of PD, which are reported to induce the release of aS in the medium of SH-SY5Y cells [137,138].

Together this evidence suggests a role for aS secretion in the contribution to the α-synucleinopatheis pathogenesis.

## 1.5 Exosomes

As mentioned before one of the pathways of aS secretion is through exosomes [126,127]. These extracellular vesicles (EVs) are gaining more and more attention by scientific community due to the functions and potential applications that they have been ascribed, namely: (i) their capacity to act as mediators of cell–cell communication in many different contexts and pathologies [139]; (ii) their composition in terms of biomolecules, with biomarker potential for disease diagnosis and prognosis [140]; (iii) the possibility of engineering their content for numerous biomedical applications, including drug delivery [141].

### 1.5.1 Biogenesis of exosomes

Exosomes derive from the inward budding of endosomal multivesicular bodies (MVBs). The intraluminal vesicles contained in the MVBs can be either targeted to the lysosome or secreted as exosomes into the extracellular space. Accordingly, lysosome inhibition correlates with an increased release of aS from SH-SY5Y cells [142]. The activation of either of these pathways is linked to the coordinated activity of the different mechanisms that have been involved in the specific sorting of proteins into exosomes: (A) Endosomal Sorting Complexes Required for Transport (ESCRT) and (B) lipid-dependent mechanisms and tetraspanins (compare **Figure 12**). (A) ESCRT is necessary to ubiquitinate proteins and directs them to the MVBs. It has been reported that silencing of early components of the ESCRT machinery decreases exosome production and alters their content [143]. (B) Compelling evidence also supports the enzyme sphingomyelinase and the production of ceramide from raft-based microdomains rich in sphingolipids as important components of the vesicle budding process. Ceramide can self-associate through hydrogen bonding, thereby inducing the coalescence of microscopic rafts into a large membrane microdomain and facilitating exosome formation and release [144,145]. Tetraspanins are integral membrane proteins highly enriched in exosomes [146].

Through their interaction with other transmembrane proteins, cytosolic proteins and lipids, tetraspanins organize membranes into tetraspanin-enriched domains

(TEMs) [147]. Tetraspanin CD81 plays a key role in exosome composition, not only through the physical organization of membranes in microdomains, but also through the interactome of its cytoplasmic domain [148]. Similarly, the loading of metalloproteinase CD10 in exosomes is dependent on its interaction with the CD9 cytoplasmic domain [149].

Moreover, elevated expression of the of the P-type ATPase ion pump PARK9/ATP13A2 reduced intracellular aS levels and increased aS externalization in exosomes >3-fold [150].
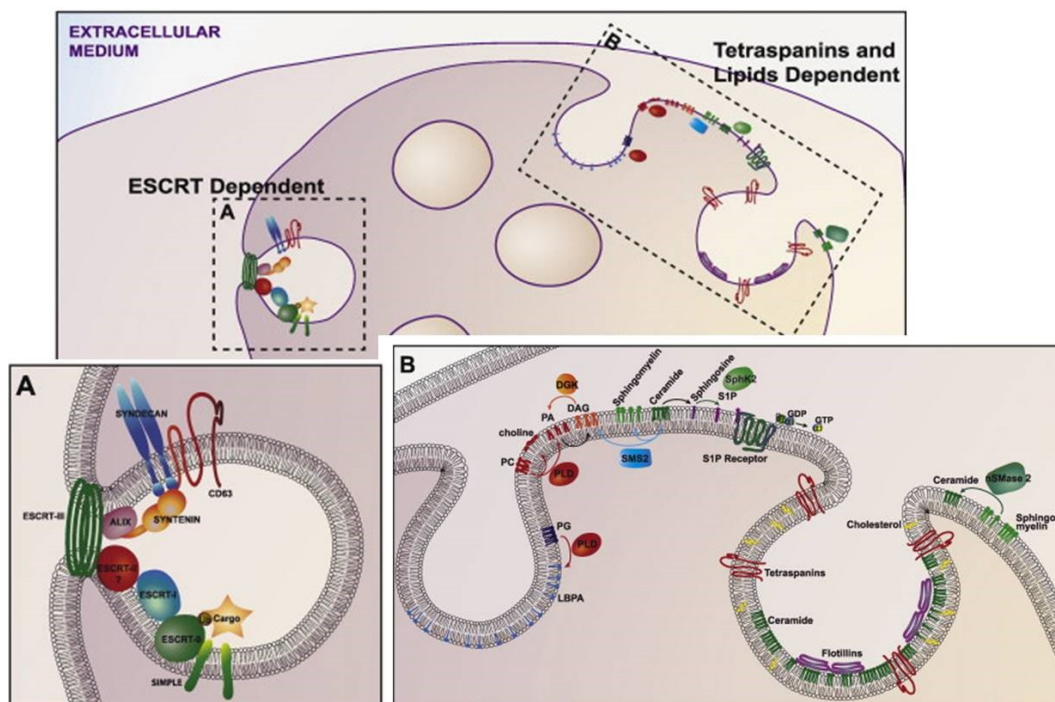


**Figure 12. Mechanisms that control the sorting of cargo into exosomes. (A)** [Adapted from Villarroya-Beltri et al, Seminars in Cancer Biology (2014)][151].

Upon movement of MVBs to the plasma membrane and subsequent fusion, the internal vesicles are released into the extracellular space as exosomes. Other molecules that facilitate fusion of the MBV to the cell membrane are small GTPases such as RAB27A, RAB11, and RAB35 [152]. This is not surprising considering that Rab GTPase proteins are important regulators of intracellular trafficking in secretory pathways such as cargo selection in vesicle formation, vesicle transport, tethering, and docking [153]. The mechanisms regulated by Rab GTPases are cell-specific, depending on the differential expression and function of particular effectors. The

first GTPase associated with exosomes release was Rab11 [154]. Moreover, Chutna and co-workers reported that Rab11 co-localizes with aS in intracellular inclusions and modulates its aggregation, secretion and toxicity in SH-SY5Y cells [155].

The subcellular location of MVBs is dependent on their interaction with the actin and microtubule cytoskeleton, which is also regulated by Rab proteins and their effectors. Rab effectors include motor proteins that facilitate the movement of the Rab-tethered vesicle along both the actin and/or microtubule cytoskeleton [139,156]. A good example of this is again Rab11, which can separately recruit myosin Vb via its effector FIP2 (Rab11 family-interacting protein 2) and cytoplasmic dynein via FIP3 [157]. The involvement of the actin cytoskeleton in exosome release has been studied in cancer, immune cells [158] and in the kidney, for the trafficking of Acquaporin-2 [159]. Regarding the role of the microtubule network, maturation of MVBs are governed by their movement along microtubules toward the cell center in a dynein-dependent fashion, whereas their localization to the plasma membrane requires kinesin-dependent movement toward microtubule plus ends. The movement of MVBs along microtubules is in part controlled by the cholesterol content of the cells [151].

Once MVBs are docked to the plasma membrane, Rabs are also implicated in the fusion of the limiting membrane of MVBs with the plasma membrane. This is mediated by direct or indirect regulation of SNARE proteins (soluble N-ethylmaleimide-sensitive fusion protein-attachment protein receptor) [160], through the pairing of a SNARE on a transport vesicle (v-SNARE) with its cognate SNARE-binding partner (t-SNARE) on the appropriate target membrane [161,162]. As demonstrated in K562 erythroleukemic cells [163] and in *Caenorhabditis elegans* [151,164].

### 1.5.2 Exosomes composition

Exosomes are lipid-bilayer enclosed vesicles with a floating density of 1.13–1.19 g/mL on sucrose density gradient separations. They displayed a cup-shaped morphology upon fixation for transmission electron microscopy (TEM) and a mean diameter between 30 and 100 nm [165]. Considering that exosomes formation is an active process, there are several membrane proteins that are unique to these

vesicles compared to the cell surface, providing additional markers for exosomal identity [166]. Most exosomes do not contain proteins of mitochondrial, nuclear, ER or Golgi origin [167]. They harbored instead in tetraspanins (CD9, CD63, CD81 and CD82), proteins required for membrane transport and fusion (flotillin, annexins; Rab proteins), proteins associated with MVB biogenesis (Alix, Tsg101), heat shock proteins (Hsp 70 and Hsp 90). These vesicles also carry a variety of cytoskeletal proteins (actin, tubulin, profiling, cofilin) and metabolic enzymes (GAPDH and pyruvate kinase) [168]. Additionally, the exosomal membrane is highly enriched in phospholipases raft-associated lipids such as cholesterol, sphingolipids, ceramide and glycerophospholipids. In recent years, exosomes are found to contain not only proteins and lipids, but also a rich repertoire of RNA transcripts [169]. These transcripts are enclosed in exosomes and can be translated to proteins by the cell receiving the exosomes [170]. Valadi et al. were the first to demonstrate the shuttle of exosomal RNA transcripts from mouse cells that could be translated into murine proteins by human mast cells. The successful transfer of transcripts indicated their role in establishing an exosome-medicated pathway, suggested a novel mechanism of genetic exchange between cells, either in microenvironment or over a distance. The study also revealed that the RNA transcripts enclosed in exosomes were different to the cells from which they were derived, and these exosomes were enriched with a distinctive set of RNAs [171]. The majority of these transcripts were highly enriched in the 3′-UTRs, which indicated that transcripts in exosomes were associated with more of a regulatory role than a functional role [170].

Moreover, exosomal composition is widely affected by cellular state and can reflect changes in the cell microenvironment. Stress situations such as hypoxia, starvation or oxidative stress can alter exosome content, and thus the message they carry [151]. For example, Fruhbeis and co-workers demonstrate that during neuronal development, oligodendrocytes secrete exosomes are taken up by neurons and induce neuronal viability under conditions of oxidative stress or starvation [151,172].

### 1.5.3 Exosomes uptake

The elucidation of the mechanisms of exosome targeting and uptake remains an important challenge. The binding of exosomes to the surface of recipient cells is

mediated by the classical adhesion molecules involved in cell–cell interactions, such as integrins and ICAMs. However, other molecular pairs more specific to the exosome membrane, such as TIM-binding phosphatidylserines, carbohydrate/lectin receptors and heparan sulfate proteoglycans (HSPGs), could be involved as well. ICAM-1-LFA-1 interactions are involved in exosome uptake by immune cells [172,173], and tetraspanins also contribute to exosome binding to target cells. For example, the integrin CD49d and Tspan8 contribute to exosome adhesion to endothelial cells [174]. MHC-TCR interactions can also facilitate the binding of exosomes derived from T cells to dendritic cells and viceversa [175]. Additionally, cells can use Tim4 and Tim1 as phosphatidylserine receptors for the engulfment of exosomes [176]. Exosomes are enriched in specific mannose- and sialic acid-containing glycoproteins; for example, $\alpha2,3$-linked sialic acid is enriched on B cell-derived exosomes, and allows their capture by CD169+ macrophages in both spleen and lymphonode. Exosome access to the lymphoid system is thus dysregulated in CD169 knock-out mice, resulting in aberrant trafficking of exosomes into the splenic red pulp or lymph node cortex [177]. In contrast, sialic acid removal causes a small but non-significant increase in uptake. The uptake of exosomes by macrophages is also mediated by a C-type lectin expressed in macrophages and by galectin-5 exposed on exosomes [178]. Virus and lipoproteins are internalized via HSPGs. In a similar way, HSPGs function as a receptor for cancer-derived exosomes [179]. Experiments with exogenous HS, pan-PG deficient cells, and pharmacological inhibitors of HSPG have shown that cell-surface HS is required for efficient exosome uptake [179].

To deliver their content, exosomes attached to a recipient cell can either fuse with the cell membrane, directly releasing their cargo into the cytoplasm, or get internalized by endocytic pathways. Fusion of exosomes with another membrane is more likely to occur at the acidic pH of the endosome rather than at the neutral pH of the plasma membrane [180]. Depending on the phagocytic and endocytic capacity of the recipient cells, exosomes can be internalized by clathrin-dynamin-caveolae-dependent endocytosis, pinocytosis, or phagocytosis. Neurons and microglia internalize oligodendroglial exosomes effectively, whereas uptake by oligodendrocytes and astrocytes occurs only sporadically. Microglia take up

exosomes non-specifically by macropinocytosis [181], while internalization of oligodendroglial exosomes by neurons is mediated by selective clathrin- and dynamin-dependent endocytosis [182]. Exosomes released from EBV-infected B cells are internalized via caveola-dependent endocytosis [183]. Dynamin has been also involved in mediating the endocytosis of exosomes [178,184]. For example, exosomes containing anthrax toxin are taken up by a dynamin-dependent mechanism that transports them to the endocytic pathway. The anthrax toxin is then released into the recipient-cell cytoplasm by ILV back fusion in an Alix- and Tsg101-dependent manner [185]. Fusogenic lipids, such as LBPA, also seem to be required for fusion between exosomes and the recipient late endosome membrane [180].

## 1.5.4 Exosomes and nervous system

Most cells in the CNS, including neurons, astrocytes, oligodendrocytes and microglia released exosomes. These extracellular vesicles are secreted by neural cells under both normal and pathological conditions and have been isolated not just from the cerebrospinal fluid [186], but also from adult human brain [187]. Exosomes in the CNS appeared to be implicated in the removal of cellular materials and to cell-to-cell communication. These extracellular vesicles are reported to contribute not only to CNS development, but also in controlling synaptic function regeneration following traumatic brain injury. In that regard, it has been reported that neurons are able to regulate oligodendrocyte differentiation by exerting an effect on the release of oligodendrocyte-derived autoinhibitory exosomes [188]. In parallel, due to glutamate activation, oligodendrocytes released exosomes, that are able to release their cargo into neurons. In that way, they are suggested to influence neuronal metabolism and exert a cytoprotective function on recipient neurons [172].

As mentioned before, exosomes can also affect synaptic function, which is central to neuronal activity. Interestingly, a number of neuronal cells are reported to release exosomes, containing essential molecules for synaptic activities. Once internalized by recipient neurons, these extracellular vesicles can contribute to neurotransmission. For instance, under high neuronal activity or cell stress, glial-derived exosomes contain synapsin, a protein associated to vesicle and involved in

neural development [189]. Supportively, these extracellular vesicles stimulate neurite growth and are neuroprotective under stressful environmental conditions [189]. Also, microglial-derived exosomes are reported to influence synaptic function[190]. Antonucci and co-workers demonstrated that microglial-derived exosomes enhance sphingolipid metabolism, stimulating neurotransmission in the recipient neurons without showing any toxic effect [190].

Another evidence for exosomes-mediated neuroprotective effect come from studies on astrocytes, cells implicated in maintaining brain homeostasis, providing nutritive elements to neurons and controlling their development and synaptic activities. Under oxidative and thermal stress conditions, astrocytes increase the release of heat shock protein 70 (Hsp70) via exosomes [191], that are able to protect neurons during injury [192]. Moreover, also peripherally, cells-derived exosomes are reported to mediate neuroprotective effect. Schwann cells, the principal glia of the peripheric nervous system, release exosomes, that enhance axonal regeneration after nerve damage both *in vivo* and *in vitro*. The proposed mechanism is at least in part mediated by the decreased RhoA activity, a GTPase with an inhibitory effect on axonal regeneration activated in response to injury [193].

## 1.5.5 Exosomes and α-synucleinopathies

Patients suffering from PD typically exhibit higher levels of plasma exosomal aS compared to controls [140]. Importantly, cerebrospinal fluid exosomes derived from Parkinson's disease and dementia with Lewy bodies induce oligomerization of aS in human H4 neuroglioma cells, suggesting that they contain a pathogenic species of aS, which could initiate oligomerization and confer disease pathology [194]. The hypothesis of exosomes as information mediators to the brain was confirmed in the work of 2014 by Alvarez-Erviti and coworkers: injected exosomes containing aS small interfering RNA (siRNA) were able to decrease aS mRNA and protein levels throughout the mice brain in 7 days [195]. These extracellular vesicles, in fact, have been shown to be involved in transporting aS to the extracellular environment and spreading the toxic oligomers to naïve neurons [126]. Uptake of aS containing exosomes has been shown to induce cell death in healthy neurons [127] further highlighting the potential of exosomes in the pathogenesis of α-

synucleinopathies. Not only neurons internalize aS deposits released by pathologic neurons, but also other cell types such as astrocytes [196]. This process induced the aggregation of endogenous aS in the recipient cells, as demonstrated both *in vitro* and *in vivo* [196] as well as initiation of an inflammatory response. Supportively, microglia cells phagocytosed exosome-containing aS aggregated species and this mechanism induced an increased release of TNFα, a neurotoxic cytokine [197]. Inflammation, in fact, is a key aspect in α-synucleinopathies pathogenesis/progression, that will be better addressed in the paragraph 1.6. Another interesting connection between exosomes and α-synucleinopathies insurgence derives from genetical studies. Mutations in several genes related to the endocytic pathway such as vacuolar sorting protein 35 (VPS35) and leucine-rich receptor kinase 2 (LRRK2) have been linked to PD [198]. LRRK2, for instance, has been reported to influence synaptic activity and its overexpression induced trafficking defects in neuronal models [199]. In addition, a mutant form of LRRK2 exhibits an increased number of morphologically distinct MVBs [200]. This phenotype suggests a potential accumulation of exosomes containing aS aggregated species that, upon release, might be transmitted to neighboring cells.

In conclusion, increasing evidence suggests a role for exosomes in neuron-to-neuron propagation of α-synucleinopathies. In addition, aggregated extracellular aS can also induce an immune response in glial cells, causing the release of nitric oxide, ROS and pro-inflammatory cytokines, which are neurotoxic.

## 1.6 Neurotoxicity: α-Synuclein and synapses

To date, α-Synuclein and synapses appear strictly linked both in physiologic and pathologic conditions. Even if aS physiological function is still largely unknown, it appears to primarily localize in the presynaptic terminals of mature neurons, where it fulfils roles in synaptic function and plasticity. In addition, increasing evidence suggests that aS gain of toxic function starts at synapses, that, coherently, are the primary sites of aS aggregation, but also propagation in α-synucleinopathies.1.6.1 α-Synuclein localization

aS is highly abundant in presynaptic terminals of neurons, with a concentration of ~40μM [201] and it accounts for 0,5-1% of the total soluble brain proteins [27]. In addition, aS has been shown to colocalize with presynaptic proteins such as synapsin 1 [202], synapsin III [203], synaptotagmin [204] and synaptophysin[205-207] . It has a high affinity for membranes and, in particular, it appears to be associated with lipid rafts. This interaction is considered essential to its synaptic localization, since pharmacological disruption of lipid rafts in primary neuronal cultures diminished aS levels within synapses [208] [63]. However, aS has not been identified in all neuronal synapses and not all terminals display aS-positive aggregates in α-synucleinopathies [209], suggesting a selective level, localization, and susceptibility only in certain neuronal populations [52].

In the nervous system, aS protein levels increase during development and remain high throughout adulthood [210]. Both in rodents and in humans, aS moves from neuronal soma to presynaptic terminals during early weeks of development, where it interacts with synaptic vesicles [52]. Its targeting to presynaptic boutons seemed to be driven by its affinity for synaptic vesicle membranes and the vesicles-associated proteins synaptobrevin-2 (sybII), synapsin III, or rab3A. Although its high amount in presynaptic terminals, aS is among the last proteins to reach the synapse, suggesting that it has an activity required for a more complex cellular function that is not essential for basic neurotransmitter release or synapse development [52].

## 1.6.2 α-Synuclein function at the synapse

aS's localization at the presynaptic terminals (I), its affinity with highly curved, negative charged membranes (II) and its interaction with different synaptic proteins (III) strongly supports a physiologic function associated with synapses, such as synaptic activity and plasticity, learning, neurotransmitter release, dopamine metabolism, synaptic vesicle pool maintenance, and/or vesicle trafficking (**Figure 13**) [52].

Under physiological conditions, aS is thought to exist in equilibrium between a cytosolic conformation and a membrane-associated, alpha-helix multimeric conformation [211,212]. As shown by photo-bleaching experiments, aS is a highly

mobile protein and disperses rapidly from synaptic vesicles upon neural activity [213,214]. aS association with membranes is reported to contribute to aS physiologic function and prevent aggregation [50].
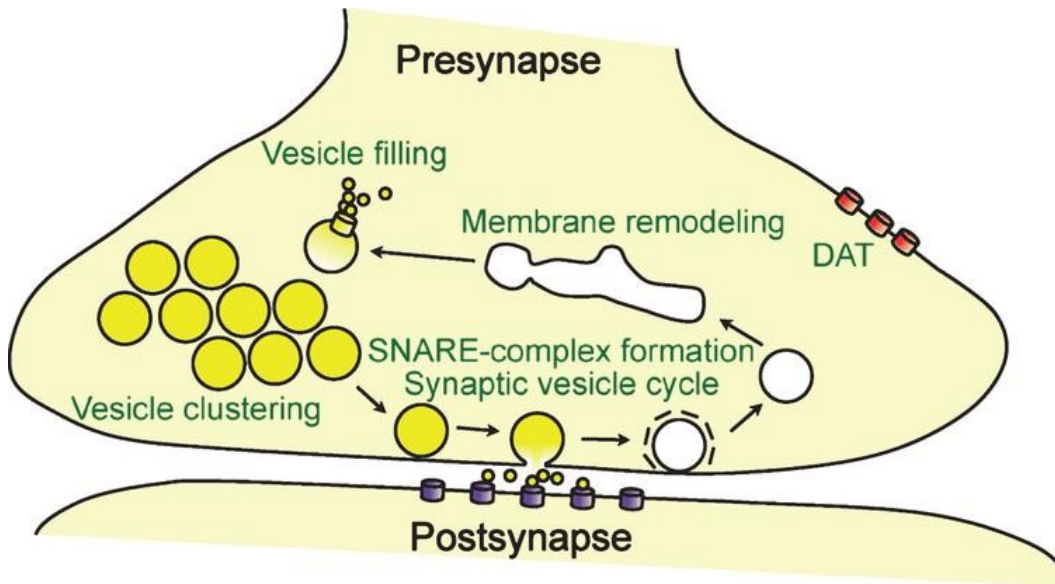


**Figure 13. aS Function at the synapse**. [Burrè, J Parkinsons Dis. (2015)] [52].

Probably the neural activity at synapses regulated the recruitment of aS to the membranes that are under high fusion activities. In this way, aS reduces the mobility of synaptic vesicle pools between presynaptic boutons and maintains the overall size of the recycling pools at individual synapses [52].

*In vitro*, aS inhibits docking of synaptic vesicle mimics without interfering with their fusion [215,216] . This effect results from clustering of synaptic vesicle mimics, a process strongly dependent on aS's ability to associate with acidic lipids [215] and synaptobrevin-2 (sybII) [216]. Experiments on mouse models confirm the interaction between the acidic C-terminal domain of aS and the N-terminal 28 amino acids of synaptobrevin-2 (sybII) [207] (**Figure 14**). Since SybII has a central role during synaptic exocytosis [217], aS appears to be implicated in vesicles fusion and clustering at the neural active zone.

Coherently, aS has been recently demonstrated to induce synaptic vesicles clustering in neurons. A function probably supported by the multimerization of aS on the vesicles membranes, which reduces synaptic vesicle motility, likely

conditioning neurotransmitter release [52]. According to this hypothesis, separation of different population of synaptic vesicles reveals that aS associates only with specific subpopulations [211,218], and cooperatively regulates synaptic function with synapsin III in dopaminergic neurons [219]. Moreover, when aS is knocked out, synapses reveal a selective reduction of undocked vesicles without any effects on docked vesicles [220] and knockdown of aS significantly diminished the distal pool of synaptic vesicles [206].

The clustering function of aS may increase the local concentration of synaptic vesicles and thereby of the SNARE protein sybII at the active zone, inducing the assembly of neuronal SNARE-complexes by blocking additional synaptic vesicles close to the active zone [52]. Supportively, the SNARE-complex assembly deficit in α/β/γ-aS triple knockout mice become more severe with increased synaptic activity [221].
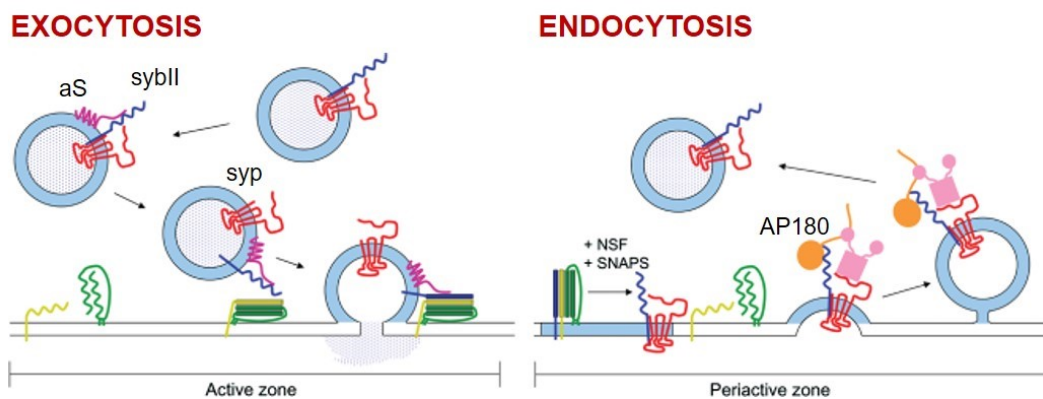


**Figure 14. The process of exo- and endocytosis are controlled by Synaptobrevin II (syb II), Synaptophysin (syp), aS and AP-180.** [Adapted from Gordon et al, Traffic. (2014)] **[222].**

To summarize, aS' s effect on neurotransmission does not appear mediated by directly acting on the release machinery, but by affecting the synaptic vesicle pools organization. This effect is likely supported by the formation of aS multimers, induced by membrane association and promotes SNARE-complex assembly. In this way, aS contributes to the long-term operations of the nervous system, suggesting that alterations in its physiological function could contribute to the pathogenesis and progression of α-synucleinopathies [52].

### 1.6.3 α-Synucleinopathies pathology at the synapse

As mentioned before, α-synucleinopathies are characterized by aS-positive intracytoplasmic inclusions in different type of cells of the nervous system[223-225]. Surprisingly, their small number relative to the total neuron count does not correlate with the extent of cognitive impairment [226]. Moreover, it was shown that the dysfunction of dopaminergic cells may precede the development of Lewy pathology, in PD [227].

Although LB are the most noticeable aS pathological species, some other forms of aS aggregates such as oligomers, small aggregates, or protofibrils may be involved in the pathogenesis of α-synucleinopathies [50]. This hypothesis received strong support from numerous experimental data showing that such intermediate species may be more toxic to the cells than LB [228,229].

In addition, considering the fact that presynaptic terminals are the physiologically most active compartments of neurons, it would seem to suggest that they could also become the sites of aS aggregation.

In contrast to juxta nuclear Lewy bodies, native aS is localized at presynaptic terminals [206,230], where it exerts its physiological function [52]. One possibility is that this process of aggregation alters the equilibrium between free and membrane-bound aS, leading to an increase in aS concentration in the cytoplasm, enhancing aggregation and altering aS physiologic function [231,232]. This hypothesis was supported by studies in patients and animal models. Oligomer-prone transgenic mice carrying the synthetic aS E57K mutation displayed synaptic and dendritic loss, reduced levels of synapsin I and synaptic vesicles, and behavioural deficits [233].

In post-mortem brain tissue from patients with PD, analysis of the distribution of aS oligomers shows significant differences with Lewy pathology [234]. Small aggregates are especially abundant in synapses, where they can be found in the early stage of the disease, often prior to the formation of LB.

A synaptic accumulation of aS was shown in DLB, thanks to a paraffin-embedded tissue blot. This technique allows visualization of small insoluble aggregates by removing non-aggregated, physiological aS by proteinase K (PK) digestion [235]. Similarly, immune-histochemical analysis after pretreatment with PK allowed for the identification of numerous presynaptic aS aggregates also in PD brains.

Moreover this pathological aS accumulation in synapses was progressive over the course of the disease, suggesting that synaptic α-synucleinopathy precedes Lewy pathology in cell bodies disease [236]. It has been proposed, in fact, that pathogenesis of several neurodegenerative diseases may feature a dying-back mechanism of cell degeneration and retrograde progression of pathology (**Figure 15**). LB could be formed by an aggresome-related process as a general cytoprotective measure in which smaller aS aggregates are sequestered from the neuronal periphery by active retrograde transport on microtubules [237,238].

Axonal α-synucleinopathy was also observed in the peripheral nervous system, where aS was shown to aggregate in the distal axons of the cardiac sympathetic nerve before it accumulated in the neuronal somata of their mother cells in the paravertebral sympathetic ganglia in PD patients [239].

## 1.6.4 Synaptic dysfunction in α-synucleinopathies

A feature of PD and other α-synucleinopathies is an impairment of neurotransmission, especially dopaminergic and cholinergic transmission, as shown by different clinical data [240-244]. These deficiencies are confirmed by overexpression of aS in different *in vitro* [245,246] and *in vivo* models [247-250]. Importantly, as synaptic aS aggregation precedes α-synucleinopathy in cell bodies, there are strong evidence suggesting that this synaptic deficit anticipates cell death in disease progression [50].

At the time of PD diagnosis, for example, the loss of nigral dopaminergic neurons is significantly minor than the impairment of striatal dopaminergic neurotransmission and neurite degeneration [251-253]. Moreover, experimental data show that alterations in striatal DA release may not be paralleled by changes in total DA content in striatal tissue, suggesting that the dopaminergic dysfunction in PD is not initially a direct effect of cell death and/or reduction of DA content, but is rather caused by functional impairment of neurotransmitter release at the synapse. In a transgenic model, aS(1-120) mice, in which truncated, aggregation-prone human aS is expressed under a tyrosine hydroxylase promoter in catecholaminergic cells, aS aggregates are present at striatal dopaminergic

terminals where, in the absence of nigral dopaminergic neuron loss, the release of DA from nigrostriatal synaptic terminals is progressively impaired [50].

At a molecular level, as reported in **Figure 15**, the abnormal interactions of aggregated aS with the components of the synaptic apparatus such as the protein members of the SNARE complex could represent the basis for functional deficits of synapses in α-synucleinopathies. Supportively, in primary neurons overexpressing aS as well as in brains of α-synucleinopathy animal models and in patients, changes in presynaptic proteins relevant to neurotransmitter release and axonal transport are observed [226,245]. The experimental data from aS 1-120 mice demonstrate that the impairment in DA release in the striatum displayed in this model is accompanied by redistribution of SNARE proteins in nigrostriatal terminals [249].
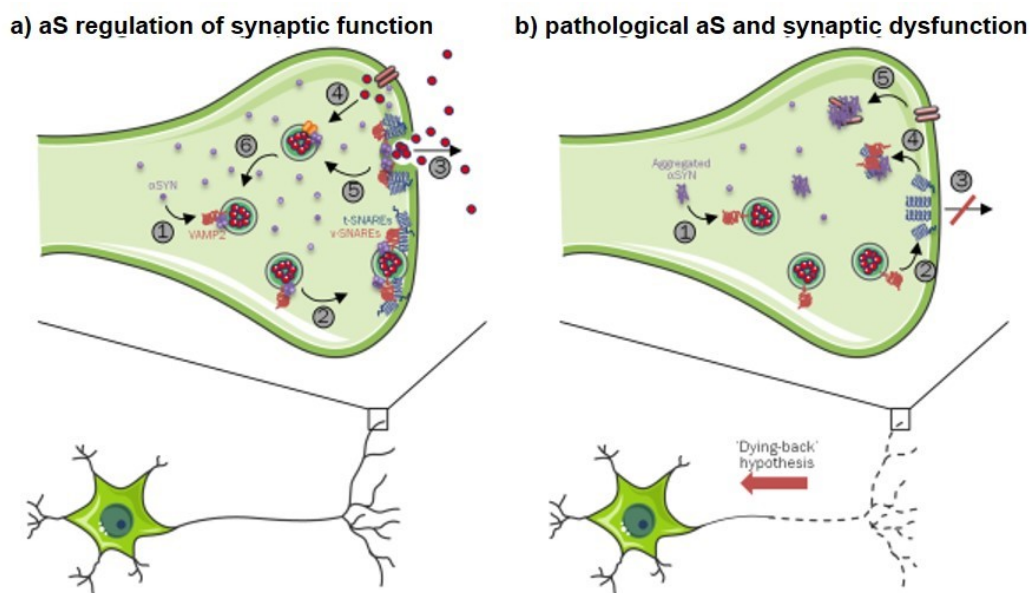


**Figure 15. Synaptic aS involvement in neurotransmitter release in physiological (a) and pathological (b) conditions.** [Adapted from Calo et al, Mov Disord. (2016)] [50].

Moreover, when primary neuronal cultures were exposed to preformed aS fibrils, a loss of SNARE proteins, i.e. sybII and SNAP25 as well as CSPα, were measured [254]-. Finally, alterations in SNARE complex proteins are also detected in patients — SNAP25 and syntaxin are accumulating in the striatum of PD patients [249]. Interestingly, opposite effect on syntaxin has been reported in DLB, in which loss of this protein is observed in the cortex [226,245]. These observations suggest a

mechanism whereby accumulation of aS in the presynaptic terminal might lead to impairment of its function and that of its binding partners such as sybII, which is sequestered into aS aggregates, thus hampering SNARE-mediated vesicle fusion. Furthermore, changes in membrane curvature by misfolded aS might account for impairment of the binding and function of other vesicle-bound SNARE co-chaperones, thus affecting vesicle cycle and neurotransmitter release [50]. Indeed, an in vitro mechanistic study with lipid mixing assay showed that large aS oligomers inhibit SNARE complex formation blocking vesicle docking, a process necessary for exocytosis [232].

## 1.6 Neuroinflammation in α-synucleinopathies

Findings from epidemiological studies and analysis of post-mortem brains and animal models have provided number of observations, suggesting a role for inflammation in the pathogenesis of α-synucleinopathies [255,256]. Increasing evidence supports, in fact, the hypothesis that the immune system plays a key active part in the initiation and development of these neurodegenerative diseases, mainly through the release of neurotoxic substances [257]. For instance, PD patients brains are characterized by an extensive microglial activation and infiltration of blood-derived mononuclear phagocytes and lymphocytes [258]. Moreover, several polymorphisms in inflammatory genes have been associated with PD. Examples include polymorphisms in the genes encoding TNF, TNF receptor 1 (TNFR1), IL-1β, IL-1 receptor antagonist and CD14 [259], TREM2 [260] and, more recently, HLA-DRB1 [261]. However, only a few cases of the disease are familiar and the risk of developing the pathology is only mildly increased in carriers of this haplotype. Neuroinflammation has been reported to active contribute to 1-methyl-4-phenyl-1,2,3,6-tetrahydropyridine (MPTP)-induced mouse models of PD. The suppression, in fact, of the Toll-like receptor 4 (TLR4), responsible for microglia activation, increases the dopaminergic neuronal survival [262]. This evidence has been also supporting by epidemiological studies, correlating  the use of non-aspirin NSAIDs to a reduced risk of developing PD [263].

## 1.6.1 The function of microglia cells in the brain

Microglia are the main immunocompetent cells within the CNS [264], involved in antigen presentation to lymphocytes [265] and rapid activation in response to pathological change in the CNS [266].

These cells are distributed within all brain, in close proximity to neurons and astrocytes, although their densities vary between different brain areas [267]. In the healthy brain, microglia form an almost evenly distributed lattice in a ramified phenotype. This is characterized by a high number of processes that are constantly moving and that facilitate the interaction of microglia with neighboring blood vessels, neurons and astrocytes. These interactions are important for cerebral tissue maintenance and neuronal plasticity [268,269, 270, 271].
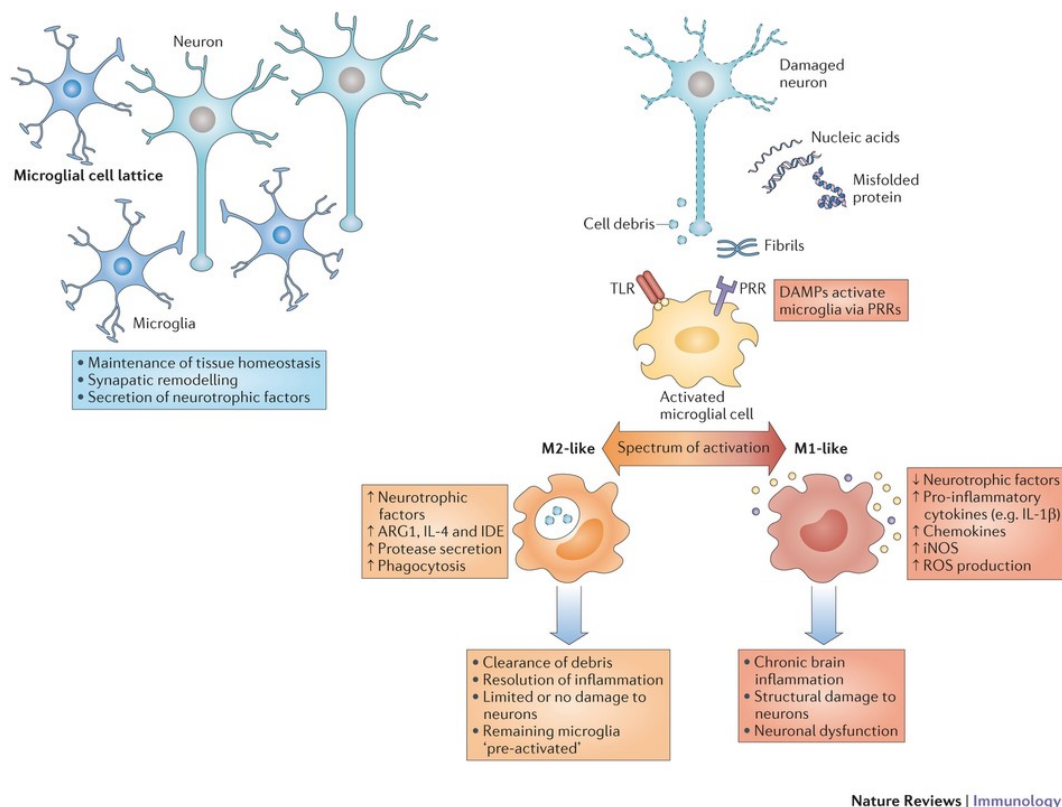


**Figure 16. Physiological and pathological functions of microglia in the brain.** [Heneka et al., Nature Reviews Immunology (2014)][13].

Microglia cells are implicated in synaptic remodeling (especially synaptic pruning) and neurotrophic factors secretion, such as brain-derived neurotrophic factor (BDNF , that maintain proper neuronal circuits [269]. Microglia is also involved in the

maintenance of tissue homeostasis, removing accumulating debris from the brain [267].

Microglial cells express specialized pattern recognition receptors (PRRs), which are implicated in the trigger of inflammatory responses. These receptors activate in the presence of microbial molecules, which accumulate in infected areas and are called pathogen-associated molecular patterns (PAMPs). Moreover, PPRs binds also to danger-associated molecular patterns (DAMPs), which are host-derived molecules, like misfolded proteins. Coherently, aggregated aS has been reported to bind to two specific PRRs, TLR2 and TLR4, inducing an inflammatory response through microglia activation. Different factors, such as the nature of the stimulus and the infection site, influence microglia response. These immunocompetent cells can, in fact, either remove the DAMPs or PAMPs or secrete inflammatory mediators.

As reported in **Figure 16**, activated microglia can assume two different phenotypes. Typically, the 'M2-like' is associated with a beneficial role and it is characterized by an increased secretion of proteases and neurotrophic factors, the production of interleukin-4 (IL-4), the expression of the enzymes arginase 1 (ARG1) and insulin-degrading enzyme (IDE) and augmented phagocytic activity. In contrast, the 'M1-like' is associated with detrimental effects and it is characterized by the expression of inducible nitric oxide synthase (iNOS), the production of reactive oxygen species (ROS) and pro-inflammatory mediators (such as IL-1β) and a diminished secretion of neurotrophic factors. These divergent responses may be responsible for a physiologic resolution of the inflammation or instead of the presence of a chronic inflammation state, which leads to neuronal death [13].

### 1.6.2 LPS stimulus and IL-1β secretion

Even if a lot of different signaling pathways are involved in microglia activation, neurodegenerative diseases are characterized by the deleterious increased of inflammatory cytokines release, such as IL-1β and IL-18. Both IL-1β and IL-18 are initially expressed as pro-enzymes, that are converted to the active forms by caspase 1 or caspase 8 cleavage. Caspase 1 itself is recruited and activated by the

inflammasomes, a multimeric protein complex, which acts as a signaling platforms [272].

Inflammasomes assembles in the cell cytosol in response of a DAMPs or a PAMPs. It is composed of one or two sensor molecule from the NOD-like receptor (NLR) family or the pyrin and HIN domain-containing protein (PYHIN) family, the adaptor protein, apoptosis-associated speck-like protein containing a CARD (ASC) and caspase 1 [273]. The NOD-, LRR- and pyrin domain-containing 3 (NLRP3) inflammasome appears to be particularly important in the maintaining of an acute and chronic inflammatory state, since it is extremely reactive against a wide range of aggregated molecules.
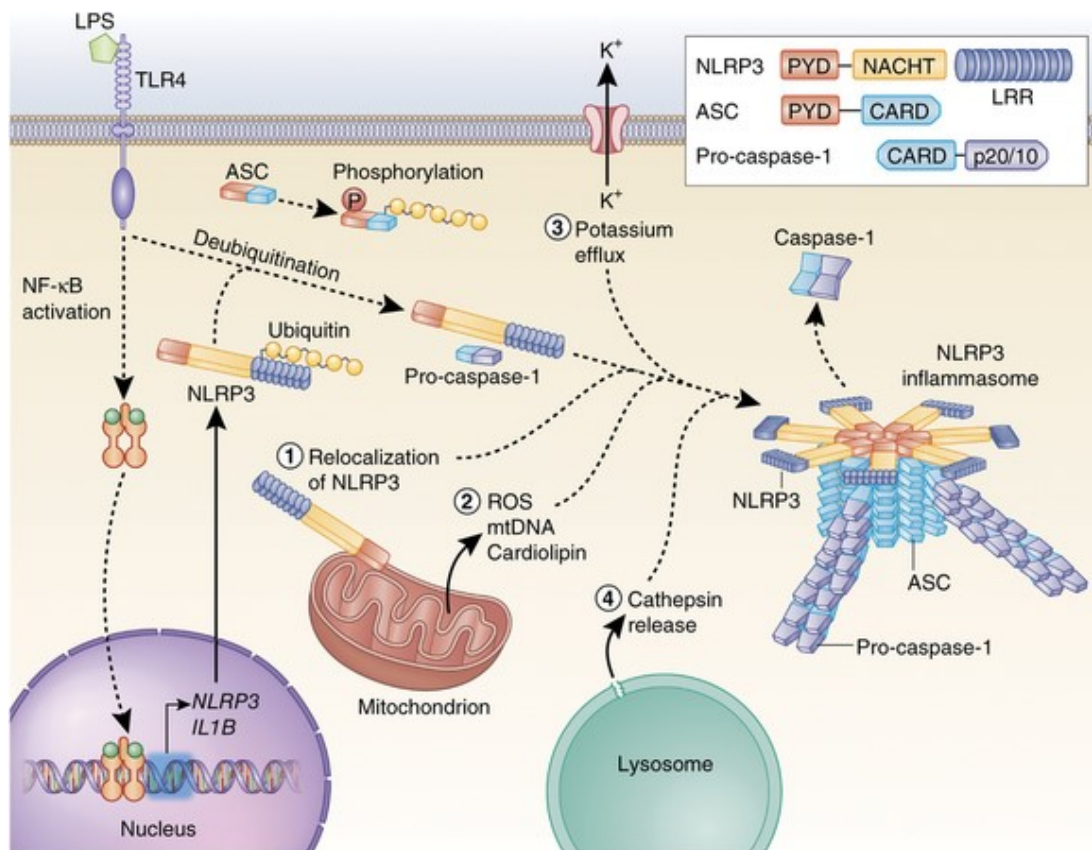


**Figure 17. Schematic representation of lipopolysaccharide (LPS)-induced NLRP3 inflammasome activation.** [Adapted from Guo et al., Nature Medicine (2015)][274].

The microglial activation effects on neighboring cells, especially on neurons, are divergent and they remain still completely unknown. However, the continuous release of pro-inflammatory molecules has been demonstrated to inhibit

neurogenesis [275]. Microglia's phenotype upon activation exhibit a more amoeboid-like form, with no processes, which may be involved in the loss of synaptic remodeling function. In this way, activated microglia, along with the toxic effects of released substances, may participate to synaptic damage, that characterized neurodegenerative diseases [13].

Moreover, a neuroinflammatory state reduces neurotrophic factors supply to glial cells [276] and likely impacts neuroprotective physiological processes, like autophagy [277]. This chronic inflammation may not only be toxic to neurons, but also on microglia itself. For instance, chronic exposure to PAMPs and DAMPs induces a reduced microglia phagocytosis activity, leading to the accumulation of misfolded and aggregated proteins [278].

A lot of different immunological stimuli have been used to directly induce glial activation and study neurodegeneration in α-synucleinopathies. Among these, the most extensively utilized has been Lipopolysaccharide (LPS) (**Figure 17**). It is an endotoxin, which is the major component of the outer membrane of gram-negative bacteria. In non-capsulated strains, LPS is exposed on the cell surface and is made up of three structural components: (I) a hydrophilic O-antigenic side chain with multiple repeating units of monosaccharides that is specific to the bacterial serotype; (II) a hydrophilic core polysaccharide chain with an unusual sugar (2-keto-3-deoxyoctonate), and (III) an hydrophobic lipid part, lipid A, responsible for the toxic properties of the molecule.

LPS associates with the soluble LPS binding protein (LBP) and CD14, localized in the outer leaflet of the plasma membrane. In this way, LPS-CD14 complex can interact with the transmembrane receptor TLR4 and its extracellular accessory protein MD2, leading to the activation of kinases, implicated in different intracellular pathways and to the gene transcription of a variety of pro-inflammatory mediators and free radical-generating enzymes. LPS stimulates the release of pro-inflammatory cytokines, free oxygen species and other lipid mediators both in peripheral, such as macrophages and monocytes, and central immune cells, microglia and astrocytes [279-282]. Moreover, LPS has been widely used in inflammation-mediated neurodegeneration studies, since its glia-specificity.

Neurons, in fact, do not express a functional TLR4 [283], making them LPS-insensitive [284].

### 1.6.3 aS induction of microglia activation

One of the critical questions concerning neuroinflammation in α-synucleinopathies is what induces microglia to move from a beneficial to a detrimental role. Increasing evidence support neuron-released aS as a central player: (I) microglia is the main cell type implicated in extracellular aS clearance [285]; (II) this process efficiency depend on the activation state and age [197] of microglia and on aS state [285,286] and (III) aS, especially if aggregated, trigger a pro-inflammatory activation state in microglia.

It is known, in fact, that aS can be secreted by exocytosis from neuronal cells [125] but it may also be released from dying cells [287]. In addition to direct toxic effects on neurons, aggregated aS activates microglia. This effect creates a vicious circle, that support aS neurotoxicity in vitro [288], providing a link between neuronal cell death and microglial cell activation. aS-triggered inflammatory responses have been demonstrated in rat primary microglia cultures [288], human microglia cultures and monocytic cell line THP-1 [287], when treated with exogenous aS. These studies demonstrate that, following aS activation, microglia release extracellular superoxide, increases intracellular ROS concentrations (iROS) and change morphology. Moreover, microglia exert also a phagocytic activity on aS and cytochalasin D inhibits ROS production upon aS incubation, suggesting that phagocytosis is a key process in aS-induced microglial activation [288]. Supportively, aS neurotoxicity is enhanced when dopaminergic neurons and glia are co-cultured [288]. These observations with the recombinant aS have recently been confirmed with neuron-derived aS. aS secreted from differentiated SH-SY5Y neuroblastoma cells triggers microglia activation, induces morphological changes, increases proliferation, iROS, and cytokine production and motility [289,290].The evidence of a cell-dependent mechanism of aS-triggered neurotoxic effects comes from a recent study of Kim and colleagues. They demonstrated that neurons released aS induces microglia secretion of substances, that in turn cause neurodegeneration [291]. Therefore, in addition to a direct aS effect on neurons, an indirect mechanism

through the inflammatory responses evoked in glial cells could account for aS-induced neurodegeneration. Concerning the microglia activation mechanism(s), recent studies suggest that Toll-like receptor 2 (TLR2) acts as the receptor for neuron-secreted aS. TLR2 mediates both the uptake of aS and the signaling leading to inflammation [290,292]. The interaction between aS and TLR2 has been shown on the surface of microglia, and these proteins co-localized in the intracellular compartments after internalization, but there might be other receptor molecules mediating the internalization of this protein [292].

TLR4 has also been suggested to be involved in aS-dependent activation of microglia and astrocytes [293]. Fellner and coworkers suggested that TLR4 acts as a modulator of proinflammatory responses in glia and the production of reactive oxygen species induced by aS. The same group also suggested that TLR4 plays an important role in aS clearance in a mouse model of MSA [294]. In addition, scavenger receptors and integrins might serve as receptors for aS [290,295]. The precise functions of these cell surface proteins in the inflammatory activation of microglia and in aS clearance remain to be determined. Each of the cell surface receptors mentioned above may interact with specific forms of aS. TLR2 is one of the PPRs, and is recognized by and responds only to certain types of aS oligomers and fibrils, but not monomers [292,296]. Independent of TLR2, neuron-secreted aS increases the motility of microglia through b1-integrin [290]. However, the integrin pathway is not required for the cytokine production in response to aS. Therefore, it appears that separate receptor/signaling systems are working together to trigger the full spectrum of microglial activation in exposure to neuron-secreted aS. The fact that separate signaling systems are responsible for different aspects of microglia activation opens up the possibility that microglia can be manipulated in such a way that beneficial clearance function is activated and detrimental inflammation is blocked.

In conclusion, the physiological functions of microglia are important for maintaining tissue homeostasis, neuronal integrity and network functioning in the brain (**Figure 16**). The loss, deviation or functional perturbation of microglia may

occur in response to neurodegeneration and may contribute to pathogenesis and disease progression.

# CHAPTER II:
# Materials and Methods

**2. 1 Cell cultures and trasfection**

## 2.1.1 Immortalized cell cultures

Human Embryonic Kidney 293T (HEK293T) cells were cultured in Dulbecco's modified Eagle's medium (DMEM, Life technologies), BE(2)-M17 and SH-SY5Y cells were cultured in DMEM/F12 Nutrient Mix (Life technologies) and BV2 cells were cultured in RPMI-40 medium (Sigma Aldrich) 2 mM Glutamine (Sigma Aldrich). All media cell lines were supplemented with 10% FBS (Life technologies), 100U/ml penicillin and 100µg/ml streptomycin (1% P/S, Life Technologies) and cells maintained at 37°C in a 5% $CO_2$ controlled atmosphere.

## 2.1.2 Primary neuronal cell cultures

All animal procedures were performed following the guidelines issued by the European Community Council Directive 2010/63/UE and approved by Ethics Committee of the University of Padua (Project ID: 46/2012). Neuronal cells were derived from postnatal mouse (P0-P1) brains (CD1 strain). Cerebral cortices were isolated and cells mechanically dissociated in EBSS (Sigma Aldrich). Cells were centrifuged, resuspended in Neurobasal media (Life Technologies) supplemented with 2% v/v of B27 supplement (Invitrogen), 0.5mM L-glutamine (Life Technologies), penicillin (100 Units/ml) streptomycin (100 µg/ml) and 2.5 µg/ml fungizone (Life Technologies). Cells were then plated at 2 x 106 cells/well on poly-L-lysine (0.1 mg/ml, Sigma Aldrich) coated wells of a 6-well plate and cultured at 37°C in 5% $CO_2$. After 7 days half medium was replaced and the neuronal culture was maintained until day 14. At 14 days neuronal cells were treated.

## 2.1.3 Primary microglia cell cultures

All animal procedures were performed following the guidelines issued by the European Community Council Directive 2010/63/UE and approved by Ethics Committee of the University of Padua (Project ID: 46/2012). Microglia cells were derived from postnatal days 1-4 (P1-P4) (CD1 strain). Cerebral cortices were mechanically dissociated in cold HBSS (Sigma Aldrich), then cellular suspension was allowed to settle for 5 min and the top fraction was collected, centrifuged for 5 min at 1000g and re-suspended in DMEM-F12, supplemented with 10% FBS, 2 mM Glutamine, 2mM Sodium Pyruvate (Sigma Aldrich), penicillin and streptomycin. Cell suspension obtained from three brains was plated on poly-L-lysine (0.1 mg/ml, Sigma Aldrich) coated T-75 flask. After 4 days the medium was replaced and the mixed glial culture was maintained until day 14. At 14 days microglia cells were isolated from the mixed culture by shaking 4 h at 160 rpm. The primary microglia yield was ~5x105 cells/flask.

## 2.2 Cellular Biology

### 2.2.1 Cell transfection and DNA plasmids

Cells were transfected with the plasmids aS-EGFP, aS-mCherry or their corresponding empty vector pEGFP-N1 or pmCherry-N1 (Novagen). HEK 293T were transfected with Polyethylenimine (PEI) in a 1:4 ratio with DNA (g), BE(2)-M17 and SH-SY5Y with lipofectamine (Lipofectamine 2000, Invitrogen) in a 1:2 ratio with DNA (g). DNA plasmids were obtained inducing their multiplication in *E. coli* DH5α bacteria and subsequently purified with NucleoBond® Xtra Midi / Maxi (Macherey- Nagel).

### 2.2.2 Cell lysis and Protein quantification

To extract protein contents of cells, cells were solubilized in Lysis Buffer (20mM Tris-HCl pH7.5, 150mM NaCl, 1mM EDTA, 2.5mM sodium pyrophosphate, 1mM β-glycerophosphate, 1mM sodium othovanadate) supplemented with Triton® X-100 (Sigma-Aldrich) and protease inhibitor (IP) cocktail (Sigma-Aldrich). The

resuspendend cells were incubated in ice for 30 minutes and then centrifuged at 20000g for 30 minutes at 4°C. Supernatants were transferred in new tubes whereas pellets were discarded. Protein concentration in cells lysates was determined thought the Pierce® BCA Protein Assay Kit (Thermo Scientific) following the manufacturer's instructions. Each measure was performed in duplicate. Protein contents were determined preparing a standard curve of bovine serum albumin (BSA) and measuring the absorbance of BSA samples of known concentration.

## 2.2.3 Exosomes purification

Exosomes purification method was adapted from Hoang et al [297] . $4x10^6$ HEK293T cells were plated in 150 mm dishes. After 24 hours they were transfected with 30 μg of DNA/dish in a 1:4 ratio DNA:PEI. 24 hours later cell medium was changed with Opti-MEM (Life Technologies) and keep at least 15 hours. For activation with $Ca^{2+}$ ionophore, cells were incubated for 30 min in the presence of 2 μM ionomycin (Sigma) at 37°C. EGTA (4 mM final concentration, Sigma) was added to stop the reaction and the remaining cells were pelleted by sequential centrifugations of the supernatants at 750 g for 15 min, directly followed by a centrifugation at 1,500 g at 4°C. Then centrifugation at 100,000 g for two hours (in 24 ml tubes, rotor 70Ti, XL90 Ultracentrifuge Beckman) allowed to pellet exosomes. After discarding the supernatants, PBS was added to the tubes, which were centrifuged again in the same condition. A small white pellet could be seen and was resuspended in appropriate volume of PBS (20-100 μL).

## 2.2.4 Cell viability assay

HEK 293T cells were plated in a 96-well plate with 100μl of culture medium added with 20μl of CellTiter 96Aqueous One Solution Reagent (Promega). Then the plate was incubated 1 hour at 37°C in a humidified, 5% $CO^2$ atmosphere. To measure the amount of soluble formazan produced by cellular reduction of MTS, absorbance was recorded at 490nm using a 96-well plate reader (VICTOR X3, Perkin Elmer).

## 2.2.5 Compounds and treatments

One day and a half after transfection, DOPAL treatments on cells were performed in growth medium without FBS, to avoid DOPAL interaction with proteins that are present in the serum. DOPAL was used at concentration of 100μM, overnight.

BV2 and primary microglia cells during treatment were cultured in medium containing 1% FBS. Inflammation was induced using lipopolysaccharide (LPS, Sigma Aldrich) at 100 ng/ml for 5 hours for BV2 cells or 90 minutes for primary microglia.

Exosomes were applied on microglia and neurons for 24 hours.

## 2.2.6 Detection of IL-1β in culture supernatants

The entire culture supernatants (1 mL) were collected, precipitated with 10% TCA overnight at 4°C; protein pellets were resuspended in 15 μl of Sample Buffer, Laemmli, boiled, and conserved at −80°C. Cell extracts and the total protein content of culture supernatants were loaded on a 4–12% SDS-PAGE (Mini-PROTEAN® TGX Stain-Free™ Precast Gels, Bio-Rad) and analyzed by immunoblotting.

## 2.3 Biochemical Techniques and in vitro assays

## 2.3.1 SDS-PAGE

Proteins were separated by Poly-Acrylamide Gel electrophoresis, in denaturing conditions through the presence of SDS. After quantification with the BCA assay, the desired amount of protein of each sample was denatured by adding Sample Buffer; Laemmli, (stock solution 4x: 200mM Tris-HCl pH6.8, 8% w/v SDS, 400mM DTT, 40% v/v glycerol and Bromophenol Blue) to a final concentration of 1X. After 10 minutes at at 90°C, samples were loaded into gels. Gels were prepared with the opportune percentage of acrylamide (between 7.5 and 13%) according to the size of the analysed proteins. Gels were run in a Tris-Glycine-SDS Running Buffer (25mM Tris, 250mM Glycine, 0.1% w/v SDS). As standards of proteins at different fixed molecular weight (Prestained Protein Ladder, BioRad -Prestained Protein SHARPMASS VII 6,5-270kDa, EuroClone) were used. After running, gel was stained

in agitation with Coumassie Brilliant Blue (0.25 % w/v Brilliant Blue R-250 Sigma Aldrich, 40% v/v ethanol, 10% v/v isopropanol, 10% v/v acetic acid and water) for 45 minutes and destained in agitation with a Destaining Solution (10% v/v isopropanol, 10% v/v acetic acid and water). In the end, gels were kept in a 10% v/v acetic acid solution in agitation.

## 2.3.2 Western blotting

After electrophoresis onto SDS-PAGE gels proteins were transferred onto Immobilon-P membrane with a Trans-Blot Turbo Transfer System (Bio-Rad). Membranes were incubated 1 hour at room temperature (RT) with the following antibodies: rabbit anti-alpha synuclein (1:1000 or 1:20000, Abcam, ab138501 for human cells and ab52168 for mouse neurons); Mouse anti-GFP (1:1000, Roche); mouse anti-GM130 (1:1000, BD Transduction Laboratories); rabbit anti-CD9 (1:500, BD Transduction Laboratories); mouse anti-Flotillin (1:500, BD Transduction Laboratories); mouse anti-SOD2 (1:5000, Sigma); rabbit anti-Cytochrome C (1:1000, Abcam); rabbit anti-Caspase-3 (1:1000, Abcam); mouse anti-Synaptophysin (1:1000, Dako); rabbit anti-IL1β (1:1000, R&D Systems); rabbit anti PARP-1 (1:1000, Cell Signaling); mouse anti-GAPDH, mouse anti-β-tubulin, mouse α-actin, mouse anti-Hsp90, mouse anti-Hsp70 (1:20000, OriGene Technologies). Subsequently, membranes were incubated 1 hour at RT with HRP-conjugated secondary antibodies (Sigma Aldrich) and finally incubated with ECL western blot substrate (Thermo Scientific).

## 2.3.3 Western blotting and ABPA resin

For ABPA resin (A8530 Sigma) pulldown, 50 μg total protein were incubated with 50 μl of the resin overnight at 4°C shaking. The resin was then pelleted, the supernatant removed and the resin was washed 2 times with PBS/acetronitrile and finally with water. Protein was collected from the resin by adding 20 μl Laemmli buffer, loaded into 10% or 4%-20% gradient SDS-PAGE and compared with the total lysate. Proteins were detected as previously reported (**paragraph 2.3.2**).

### 2.3.4 Proteinase K digestion

Proteinase K (Sigma) was serially diluted and added to samples to final concentrations of 0, 0.05, 0.25, and 1. 5 µg/ml. The samples were then incubated at 37°C for 30 min, and 5 mm PMSF was added before adding Laemmli sample buffer. For detergent treatment, Triton® X-100 (1%) was added to the vesicle preparations. The samples were then incubated on ice for 30 min before they were subjected to proteinase K digestion as described above.

### 2.3.5 Size Exclusion Chromatography (SEC) and Dot Blot Analysis

The Superdex 200 (10/300GL) column coupled to an Äkta Purifier (GE Healthcare) was equilibrated with PBS. Molecular mass was estimated according to manufacturer's instruction using following standard samples: ferritin (440 kDa), BSA (67 kDa), Citochrome C (13.6 kDa). aS-EGFP transfected HEK293T cells and derived exosomes treated and not-treated with DOPAL, were lysates as previously described and injected to the column and proteins were eluted with the equilibration buffer at a flow rate of 0.5 ml/min and the eluate was monitored at 280 nm. SEC fractions of 0.25 ml were collected and further analyzed for GFP fluorescence with a Plate Reader (VICTOR X3, Perkin Elmer). 2 µl of each fraction was also applied to a nitrocellulose membrane (pore size 0.22 µm; Protran; Whatman) and analyzed for Dot Blot. The membrane was blocked with 10% w/v skimmed milk in TBST (made on 20 mM Tris pH 7.4, 150 mM NaCl and 0.1% v/v Tween 20) at RT for 1 h and incubated with rabbit anti-alpha synuclein antibody (1:1000, Abcam, ab138501) overnight at 4 °C. Then membranes were then washed 3 times for 10 min with TBST, incubated HRP-conjugated secondary antibodies and ECL western blot substrate, as described in **paragraph 2.3.2**.

### 2.3.6 Atomic Absorbtion

Purified exosomes were diluted to 400 µl in 20% nitric acid (Suprapure, Merck) final concentration. The samples were transferred into glass tubes and wet-digested during 48 h at 70°C until the solution became clear.

Copper, iron and calcium concentrations were determined by flame atomic absorption spectroscopy using a Perkin-Elmer Analyst 100 spectrophotometer (Perkin-Elmer, Norwalk, CT, USA). Each metal was measured in digested sample solution compared to five points standard curve in 20% nitric acid. The assay was performed by average of 10 successive readings and error as the SD. The results were expressed as metal/ protein concentration ratio. Lowest detection limits: Cu=0.003 mg/l, Fe=0.006 mg/l, Ca=0.001 mg/l.

### 2.3.7 In vitro modifications of aS-EGFP and EGFP by DOPAL

1μg/ μL of recombinant aS-EGFP and EGFP were incubated with 100 μM DOPAL in a PBS solution, pH 7.4. Reaction mixtures were allowed to react at 37 °C for 15 hours, protected from light. Samples aliquots were collected, loaded onto a gradient 4%-20% SDS-PAGE and stained with Coumassie blue.

### 2.4 Recombinant protein purification

For expression of GFP and aS-EGFP with a poly-histidine (HIS) tag, pRSETB-EGFP and pET28a syn-GFP-his constructs were used, gently gifted by Mireille Claessens' lab. The constructs were expressed in in E. coli B121 (DE3) using a pT7 based expression system. Bacteria were grown at 37 °C to an OD of 0.4-0.6 then induced with 0.5 mM Isopropyl β-D-1-thiogalactopyranoside (IPTG) overnight at 20 °C. Cells were then harvested by centrifugation and  the bacterial pellet was resuspended in 5-10 mL of PBS pH 8.0, added with phenylmethylsulfonyl fluoride (PMSF) and a cocktail of protease inhibitor (Sigma Aldrich) 1:100. Cells were subsequently sonicated using a Sonic Dismembrator (Fisher Scientific) model 300 for 6 cycles (30 s sonication/30 s rest) at 60% power. The cell homogenate was centrifuged 30 min at 4 °C and the supernatant added to a Ni-NTA resin (Invitrogen) and incubated for at least one hour. After 2x PBS pH 8.0 washing, the proteins were eluted with 150mM imidazole. Imidazole was removed from the solution with a PD10 (HiTrap Desalting Columns, GE Healthcare Life Sciences) and proteins in PBS were stored at −80 °C in aliquots until further use. The protein concentration were quantified by UV absorbance, with an UV-Visible

spectrophotometer (Agilent 8453). EGFP and aS-EGFP have an absorption maximum between 275 and 280 nm and extinction coefficient of 21890 $M^{-1}$ $cm^{-1}$ and 27850 $M^{-1}$ $cm^{-1}$, respectively.

### 2.5 Fluorescence and Microscopic Techniques

#### 2.5.1 Immunofluorescence and confocal imaging

Cells were washed once with PBS and fixed using 4% paraformaldehyde for 20 minutes. Then, cells were permeabilized with 0,3% Triton-X in PBS for 5 minutes and saturated with blocking solution containing 5% FBS, 0,3% Triton X-100 in PBS for 30 minutes at RT. Primary antibodies anti-CD9 (1:200), rabbit anti-Na+/K+-ATPase α (1:100, Santa Cruz), rabbit anti-GFP (1:100, Cell Signalling), mouse anti PSD-95 (1:200, Abcam); mouse anti Anti-β-Tubulin III (1:200, Sigma); rabbit anti Anti-MAP-2 (1:200, Santa Cruz); Alexa Fluor 488 phalloidin (1:200, Life Technologies) diluted in blocking solution were incubated 1 hour at RT. After several washes, the cells were incubated 1 hour at RT with secondary antibodies Alexa-fluor 488 and Alexa-fluor 546 (1:200, Life Technologies), and after repeated washes were mounted using Mowiol reagent containing Hoechst (Roche). Images were acquired with a Leica TCS SP5 confocal microscope using Zeiss objectives. Quantifications were performed using ImageJ software. Enclosing radius, Centroid radius and Sum of intersections were quantified using the Sholl Analysis extension of ImageJ as described by Ferreira et al, 2010 [298].

#### 2.5.2 Fluorescence measurement

Fluorescence emission of purified vesicles from FM 1-43FX labelled HEK293T were recorded on a Cary Eclipse fluorescence spectrophotometer (Varian, Agilent Technologies, Santa Clara, CA) using the Cary Eclipse Program. Sample measurements were carried out using optical path length of 10 mm. Fluorescence spectra were obtained using an excitation wavelength of 530 nm with an excitation bandwith of 5 nm and slit width of 20 nm. Emission spectra were recorded between 550 and 800 nm at a scan rate of 10 nm/s.

## 2.5.3 Membrane labelling

FM 1-43FX dye (Thermo Fisher) was used for plasma membrane labelling of HEK293T cells. After at least 15 hours transfection with aS-Cherry, cells medium was replaced with Hanks' balanced salt solution (HBSS, Invitrogen) added with 5 µg/mL of FM 1-43FX for 5 minutes at 37℃. Cells were then stimulated with Ionomycin as reported in **paragraph 2.2.3** and visualized with at an inverted microscope (Leica DMI4000).

## 2.5.4 Transmission electron microscopy (TEM)

**TEM imaging on vesicle and analysis:** Control and DOPAL treated neurons were fixed with 2.5% glutaraldehyde in 0.1M sodium cacodylate buffer pH 7.4 for 1 hour at 4°C. Neurons were then postfixed with a mixture of 1% osmium tetroxide and 1% potassium ferrocyanide in 0.1M sodium cacodylate buffer for 1 hour at 4° and incubated overnight in 0.25% uranyl acetate at 4°C. After three water washes, cells were dehydrated in a graded ethanol series and embedded in an epoxy resin (Sigma-Aldrich). Ultrathin sections (60-70 nm) were obtained with an Ultrotome V (LKB) ultramicrotome, counterstained with uranyl acetate and lead citrate and viewed with a Tecnai G2 (FEI) transmission electron microscope operating at 100 kV. Images were captured with a Veleta (Olympus Soft Imaging System) digital cam-era. EM images have been processed on NIH ImageJ before performing the analysis on LoClust tool [299]. Single vesicle has been manually annotated and the distance to the active zone is expressed in nm.

**TEM imaging on exosomes:** Exosomes-resuspended in PBS were absorbed onto a carbon-coated copper grid and were then negative stained with 0.05% uranyl acetate solution. TEM micrographs were taken as reported above.

## 2.5.5 Fluorescence Microscopy of exosomes

Resuspended vesicles were spotted on glass microscope slides, covered with glass coverslips, sealed and observed with a fluorescence Leica 5000B microscope; images were acquired with a 60X objective (Leica) and analyzed using Image J

software. Staining for Na$^+$/K$^+$ ATPase (abcam), CD9 (abcam) were performed as follows: vesicles were fixed in 4% paraformaldehyde (Sigma) for 20 min at RT and washed in PBS for 12 h at 4°C. Primary antibodies were added in a 1:1 volume of PBS buffer containing 17% bovine serum, 0.3% Triton X-100, 0.45M NaCl and incubation was allowed for 1h at RT. Primary ab-conjugated vesicles were then washed with PBS and pelleted at 38900$g$ for 1,5 h, before incubation with fluorochrome-coniugated secondary Abs for 2h at RT and then wash in PBS. Re-pelletted labelled vesicles were then spotted on glass microscope slides and observed at fluorescence microscope (obj 63X or 40X). Adapted from *Bianco et al.*, 2009 [300].

## 2.5.6 Fluorescently-label exosome RNAs

50 µL of Exo-Red (System Biosciences) were added to 500 µL volume of resuspended exosome suspension in 1x PBS. The tube was then mixed by flicking/inversion and exosome solution were incubated at 37°C for 10 minutes. To stop labeling reaction, 100 µl of the ExoQuick-TC reagent were added to the labeled exosome sample suspension and mix by inverting. Labeled exosome were placed on ice for 30 minutes, and then centrifugated for 3 minutes at 14,000 rpm. After discarding supernatant with excess of label, exosome pellet were resuspended in the desired volume of 1x PBS and were ready to be monitored with a fluorescence microscope.

## 2.5.7 STED microscopy

Exosomes Exo-Red labelled (see **paragraph 2.5.6**) were deposited on a polylisinated glass coverslip. After 30-60 minutes incubation at RT, the sample was carefully washed and then analyzed by STED. The experiment was done in collaboration with Paolo Bianchini, IIT, Genoa. The setup used for the experiments is based on a conventional multiphoton, confocal, and super-resolution Leica TCS SP5 STED-CW gated microscope (Leica Micro- systems, Mannheim, Germany).

## 2.5.8 STED super-resolution techniques coupled with Atomic Force microscopy (AFM)

Exosomes were incubated 15 minutes in milliQ water and then the suspension was deposited on a deeply cleaned glass coverslip. After 30-60 minutes incubation at room temperature, the sample was carefully washed and analyzed. The experiment was done in collaboration with Paolo Bianchini and Claudio Canale, IIT, Genoa. AFM experiments were carried out using a NanoWizard II system (JPK Instruments,Berlin, Germany), working in buffer solution at room temperature and using V-shaped silicon nitride cantilevers with a nominal spring constant of 0.24 N/m (DNP-S, Veeco, Woodbury, NY; US) and typical tip radius of curvature of 10 nm. Images were collected working in tapping mode to minimize the lateral force applied to the sample during scanning. The drive amplitude was set between 0.6-1.5 V to induce a free amplitude oscillation of 0.7 V RMS. The tip resonance frequency was in the range between 15and 20 kHz. The AFM system is mounted on a multiphoton, confocal, and super-resolution Leica TCS SP5 STED-CW gated microscope (Leica Micro- systems, Mannheim, Germany).

## 2.5.9 TIRF imaging and analysis

Experiment performed in collaboration with C. Perego; University of Milan. Single-cell imaging under TIRF illumination was carried out on live cells at 1 frame per second for 40 seconds in the continuous presence of Krebs (KRH) solution, 125 mM NaCl, 5 mM KCl, 1.2 mM $MgSO_4$, 1.2 mM $KH_2PO_4$, 25 mM 4-(2-Hydroxyethyl)piperazine-1-ethanesulfonic acid (HEPES) (buffered to pH 7.4) and 2 mM $CaCl_2$ (Sigma Aldrich), at 37°C with or without DOPAL 100 μM at different time points. Up to eight cells were imaged on each coverslip in three independent experiments by means of an AxiObserver Z1 inverted microscope (Carl Zeiss Inc.) equipped with an Argon laser at 37°C using a 100× 1.45 numerical aperture (NA) oil immersion objective. Green fluorescence was excited using the 488-nm laser line and imaged through a band-pass filter (Zeiss) onto a Retiga SRV CCD camera. TIRF images were analysed using Image-Pro Plus Analyser Image Software (Media Cybernetics, Bethesda, MD, USA). A set of automated image processing macro/subroutines was developed on the basis of existing algorithms of the Image-Pro Plus Analyser software (nearest neighbouring deconvolution, High Gaussian filtering). The resulting corrected images were then analysed for

selection and quantification of fluorescent spots according to their shapes, size and intensity. For each recorded cell image, the total number of vesicles, the average vesicle mobility and fluorescence intensity, the ratio between fixed (vesicles visible in at least 30 out of the 40 frames) and mobile vesicles and its associated standard deviation in each frame were calculated.

## 2.6 Statistical analysis

All quantitative data are expressed as mean ± SEM. Statistical significance of differences between two groups was assessed by unpaired t-test, while for multiple comparisons by one-way ANOVA with Turkey's post-hoc test. Data were analyzed using using OriginPro 8.0 or GraphPad Prism 5.

# CHAPTER III:
# Results and Discussion

## I PART. 1. Characterization of exosomes containing aS and DOPAL modified aS produced by transfected HEK293T cell

Cells, as neurons [301], continuously secrete different types of vesicles to the extracellular space. In recent years, research on these vesicles has expanded considerably with a major focus on exosomes due to their emerging role in intercellular communication [302,303].

*In vitro* experiments suggest that exosomal secretion by neurons depends on synaptic activity and that released exosomes are taken up by other neurons [304]. Several studies have identified aS associated with these vesicles [126-127], suggesting that exosomes containing aS may contribute to the hierarchical propagation of α-synucleinopathies seen in patient brains [127]. Coherently, also aS prefibrillar species, like oligomers, considered harmful and fundamental to the diseases process, are reported to be released within exosomes by neurons [126,197, 49].

However, the details of aS transport via exosomes are not understood and whether exosomes play an important role in α-synucleinopathies spreading is still unclear.

To address this question, we purified aS containing exosomes from aS-EGFP transfected HEK293Tcells and analyzed several biochemical properties.

Since in PD dopaminergic neurons are primary affected, we focused on the interplay between aS aggregation process and dopamine metabolism. Increasing evidence supports the idea that altered dopamine metabolism is directly involved in the pathogenesis of PD. In particular, the levels of a toxic metabolite of dopamine, 3,4 Dihydroxyphenylacetaldehyde (DOPAL) has been found elevated in PD patient brains compared to controls [99]. DOPAL has been demonstrated to chemically react with aS, inducing its aggregation. These aggregated species are strictly linked to cellular toxicity [49], but the role of DOPAL-modified aS containing exosomes in disease propagation has not been investigated yet.

Hence we decided to treat cells with DOPAL to induce aS aggregation and subsequently study the role of these modified aS species in disease spreading.

In summary, in this part we will first illustrate the rationale in the choice of the experimental model and the strategies used to obtain purified vesicles. Then we will describe the characterization of aS and DOPAL-modified aS containing exosomes which have been used in the second part of this work to evaluate their effect when applied to neuronal and microglia cells.

### 3.1 Experimental model

One of the factors hindering the production of exosomes is the very low yield, therefore a high number of cells is needed to obtain an amount of exosomes suitable for their characterization and for their use as stimuli as described in the second part [305]. Human Embryonic Kidney (HEK293T) cells appeared to be the most fitting cell line, since they grow robustly and replicate fast [306].

In addition, the project aims to purify exosomes that contain aS. In literature, a number of studies reported a strong correlation between the concentration of cytoplasmic proteins and their secretion through exosomes [307]. Hence, we first quantified the amount of endogenous aS expressed by HEK293T cells. As reported in **Figure 18a**, HEK293T cells contain a modest amount of endogenous aS, about 40 pg/µg of total proteins.

The amount of aS in HEK293T cells was assessed by comparing HEK293T cell lysate with samples of recombinant aS monomer of known concentrations ranging from 0.125 ng to 1 ng. The detection of aS in the standard curve and in the cell lysates was performed by Western Blot using an antibody against human aS (the epitope was mapped to amino acids 118-123: VDPDNE). Two aliquots of total proteins of cell lysate were loaded for each cell line and the average of ng of aS/µg of total proteins between two samples was calculated (**Figure 18**).

To validate our experimental choice, HEK293T cells were compared with a neuronal model, which could be considered a better paradigm of dopaminergic neuron physiology. Two human neuroblastoma-derived cell lines were tested, BE(2)-M17 and SH-SY5Y cells, which are both catecholaminergic. The SH-SY5Y cell

line (ATCC CRL-2266) is frequently used as a PD model, for its neuronal origin from SK-N-SH cells.
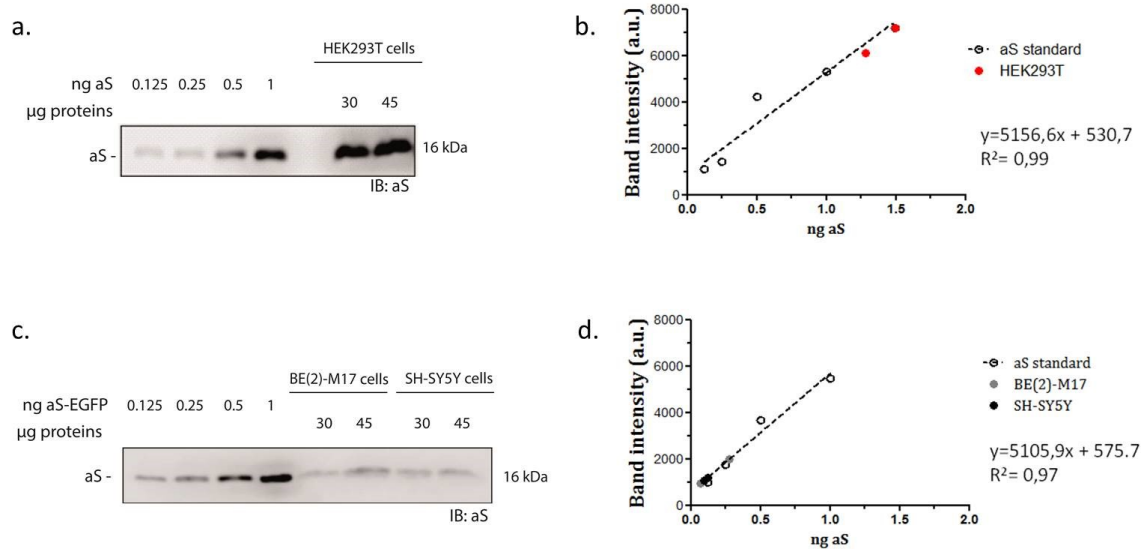


**Figure 188. Quantification of endogenous aS.** Cell lysates of BE(2)-M17, SH-SY5Y and HEK293T were analyzed by Western Blot. **a-c** Western blot analysis using anti aS antibody (ab138501) revealed comparable amount of endogenous aS between BE(2)-M17, SH-SY5Y and HEK293T cells compared with a calibration curve of recombinant aS; **b-d** Standard curve extracted from the densitometry analyses of Western Blot.

They express Tyrosine Hydroxylase and moderate levels of Dopamine βeta-Hydroxylase, typical of noradrenergic cells. On the other hand, BE(2)-M17 cells (ATCC CRL-2267) have been cloned from SK-N-BE(2) cells, but their use has been limited. Recently, our group published an analysis of the catecholaminergic phenotype in SH-SY5Y and BE(2)-M17 cell lines upon differentiation [308] . This study pointed out that both cell lines can be easily differentiated to assume a neuron-like morphology. In terms of catecholamines levels and expression pattern of the relevant enzymes, SH-SY5Y cells acquire a more prominent noradrenergic phenotype upon differentiation with staurosporine. BE(2)-M17 cells reveal a more dopaminergic profile after treatment with retinoic acid and the basal level of both DA and NA in undifferentiated cells is higher in BE(2)-M17 cells.

SH-SY5Y and BE(2)-M17 cells have a aS levels of 4,3 pg/μg and 3,5 pg/μg respectively (**Figure18 c-d**).

The differences in aS expression level become very evident when over-expression

levels of aS-EGFP upon transient transfection were compared in the three cell lines. While PEI were suitable for HEK293T transfection, in BE(2)-M17 and SH-SY5Y it causes nucleus fragmentation and cell death. In order to avoid toxicity, BE(2)-M17 and SH-SY5Y cells were transfected with Lipofectamine, a reagent optimized for efficiency and reproducibility across a broad range of cell types .
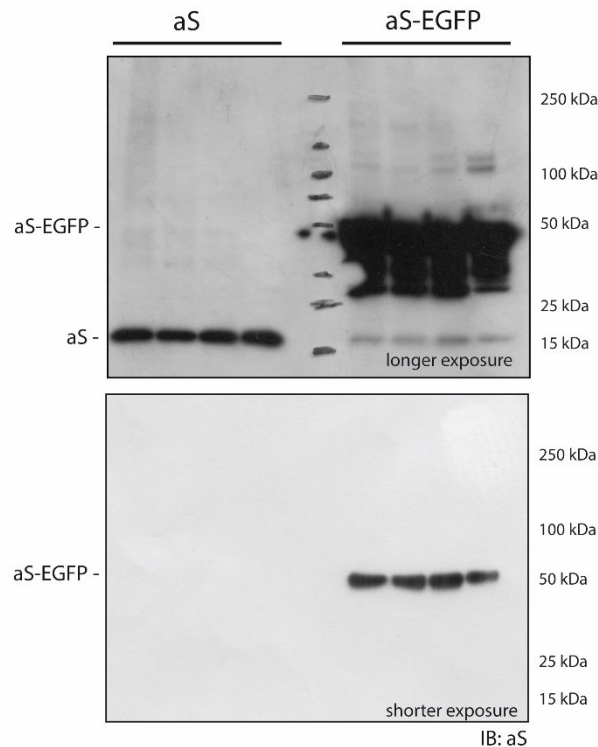


**Figure 19. aS-EGFP expression compared to WT aS in BE(2)-M17 cells.** Western Blot of BE(2)-M17 cells transfected with aS or aS-EGFP plasmids. Bands were visualized using an antibody against aS (ab138501) upon longer or shorter exposure (upper and lower panel, respectively).

The choice to transfect cells with aS-EGFP instead of wild-type aS has three reasons. First, EGFP permits to follow directly the protein in transfected cells and, as described in the second part, exosomes treated cells, thanks to the fluorescent tag. Second, an anti EGFP antibody allows discriminating between endogenous aS and overexpressed aS. Third, the transfection with the wild type form is by far less efficient than the EGFP tagged one. Once equal amounts of cell lysates were loaded, a much longer exposure (at least 5-fold more) was necessary to reveal aS bands of transfected wild-type protein than aS-EGFP (**Figure 19**).

aS expression in transfected cells was then quantified using a calibration curve of recombinant aS-EGFP sample in the concentration range from 7.8 ng to 62.5 ng of purified protein (**Figure 20a**). Once the standard curve of aS-EGFP was obtained (**Figure 20b**), transfection levels in the three cellular models were calculated: 2.7 ng/µg of total proteins for BE(2)-M17 cells, 15.1 ng/µg of total proteins for SH-SY5Y cells and 30.0 ng/µg of total proteins for HEK293T cells (**Figure 20c**). These data indicate that aS-EGFP over-expression is three orders of magnitude higher than the endogenous aS in the considered cell lines. Moreover, HEK293T cells possess a level of expression at least 2 times higher than the other cell lines.
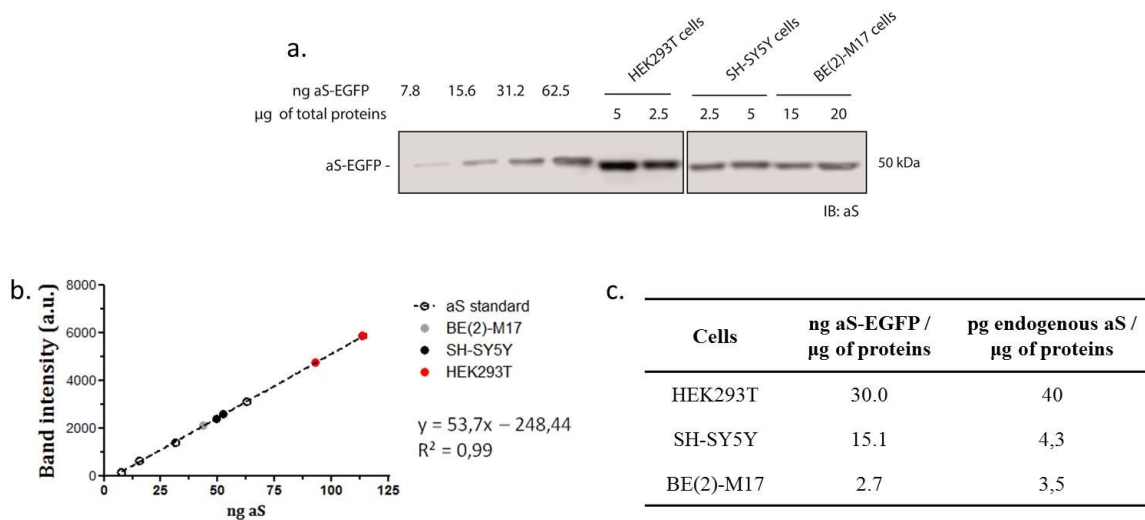


**Figure 20. Quantification of aS-EGFP expression.** BE(2)-M17, SH-SY5Y and HEK293T cells aS-EGFP transfected with Lipofectamine (LIPO) and aS-EGFP transfected HEK293T with PEI. **a.** Western blot analysis, using anti aS antibody (ab138501), of different amount of total proteins (µg) of cell lysates from BE(2)-M17, SH-SY5Y and HEK293T compared with a calibration curve of recombinant aS-EGFP; **b.** Standard curve extracted from the densitometry analyses of Blot a; **c.** Extracted values of ng of aS-EGFP and pg of endogenous aS per µg of total proteins present in the lysates of different cell types.

Vesicles were then purified from the supernatant of BE(2)-M17, SH-SY5Y and HEK293T cells and each purification step was analyzed by Western Blot for both aS and aS-EGFP. As revealed by the Western Blot in **Figure 21**, endogenous aS could not be revealed, suggesting that a high amount of intracellular protein is needed to detect aS in exosomes fraction. Coherently, in BE(2)-M17 cells, which express less aS-EGFP/µg of total proteins in comparison to SH-SY5Y cells, also aS-EGFP was not detectable in the exosomal fraction (**Figure 21a**).
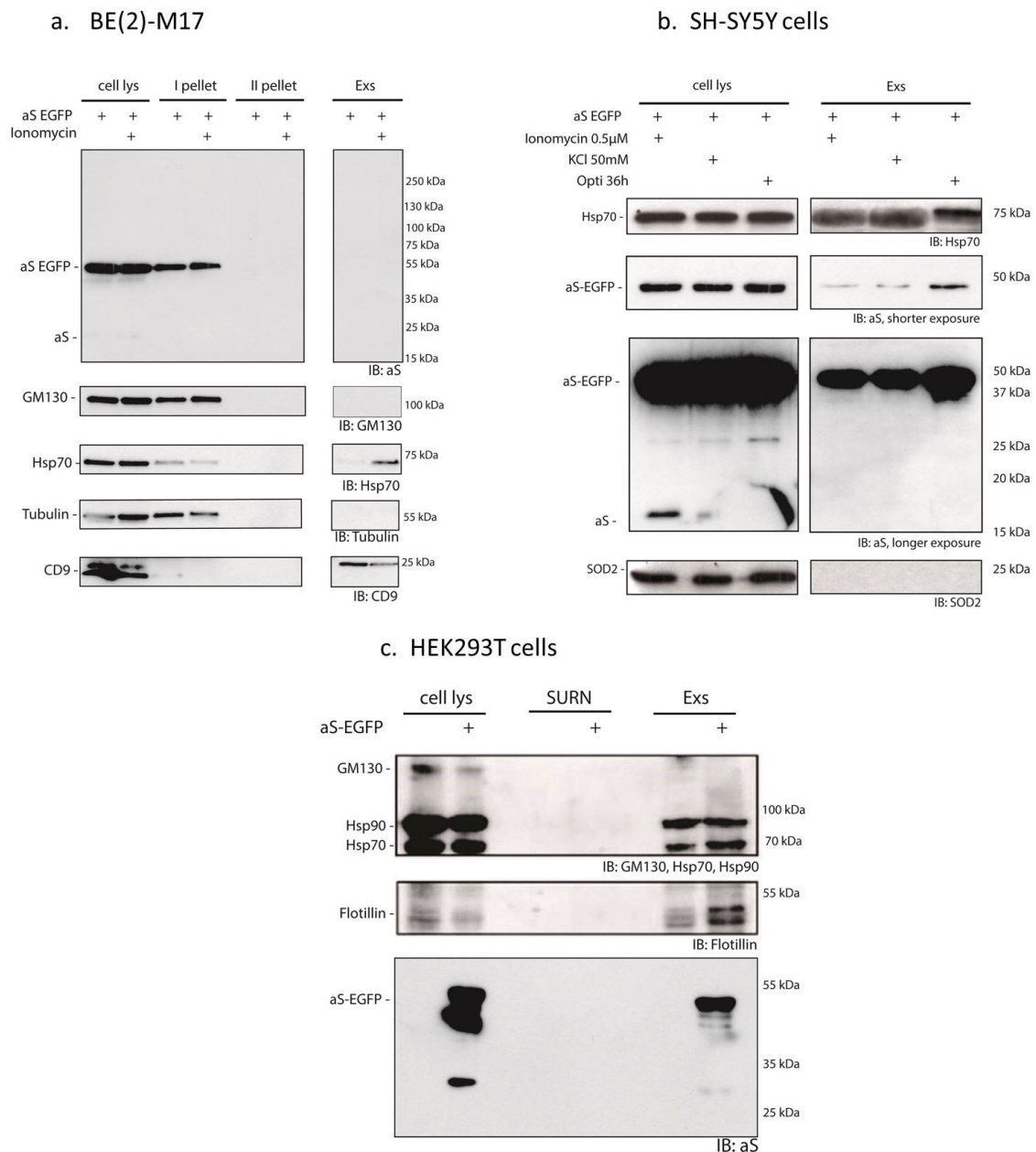
**Figure 21. aS is detectable in the SH-SY5Y and HEK293T derived exosomes.** Western Blot analysis of exosomes purification from a. BE(2)-M17; b. SH-SY5Y and c. HEK293T cells. **a.** Exosomes purification from BE(2)-M17 non-treated and stimulated with 2 μM Ionomycin were compared. **b.** Exosomes purification from SH-SY5Y non-treated (cells were maintained in Opti-mem for 36 hours) and stimulated (with 0.5 μM Ionomycin or 50 mM KCl) were compared. **c.** Exosomes purification from aS-EGFP transfected and non-trasfected HEK293T cells stimulated with 2 μM Ionomycin were compared. Antibodies against aS (ab138501), GM130 and SOD2 for exosomes purification contamination, Hsp90, Hsp70, Flotillin, Tubulin and CD9 as exosomal proteins were used. cell lys= cell lysates; I and II pellet=the two first step of purification; SURN=surnatants; Exs=exosomal pellet.

As reported in **Figure 21** however, typical exosomal proteins, i.e. Hsp70 and CD9 were present in our purification, while contaminants like a protein of the cis-Golgi, GM130, were absent. Instead, in SH-SY5Y and HEK293T cells, aS-EGFP was easily

detectable in the exosomes fraction. Also in this case the quality of the purification was confirmed by the presence of the exosomal proteins Hsp90, Hso79 and Flotillin, and by the absence of contaminants, i.e. SOD2 and GM130 (**Figure 21b-c**). Altogether these results suggest that aS can be detected in exosomal fractions, using the available tools, only when substantially overexpressed by the cells.

It is important to mention that even if SH-SY5Y derived exosomes were positive for aS-EGFP, these cells are very delicate to grow, to plate and to transfect in comparison with HEK293T cells, making exosomes purification more complicated and giving very low yields.

The aim of this part of the project was to define an effective protocol to obtain exosomes at high yield and purity. Furthermore, we were interested in identifying an effective protocol to obtain both aS and DOPAL-modified aS.

Although the detailed exosomes composition varies according to their origin and physiological conditions, most of the exosomes share a common set of lipids, proteins, and nucleic acids.

In this frame, HEK293T cells appeared the most suitable experimental model and they were chosen for all vesicles isolation, similar to other works focused on aS propagation studies [297,309].

### 3.2 Validation of Ionomycin as stimulus for exosomes purification

Emmanoulidou and coworkers reported that exosomes release is a calcium dependent process [127]. Hence, in order to increase exosomes purification yield, it was decided to stimulate cells with Ionomycin (**Figure 22c**)[297], an ionophore that raises the intracellular level of calcium [310].

To assess whether Ionomycin could be effectively used to increase exosomes release, different strategies were followed. First, HEK293T membranes were labeled with FM 1-43 (**Figure 22a,c**). This water-soluble dye, which is nontoxic to cells and non-fluorescent in aqueous medium, inserts into the outer leaflet of the cell membrane where it becomes intensely fluorescent with a maximum in emission at 598 nm.

Hence, HEK293T cells were FM 1-43 labeled, but transfected with aS-mCherry instead of aS-EGFP, to avoid overlay in the emission spectra of the two probes (**Figure 22a**). Then cells were treated with 2 µm Ionomycin and the labeled membrane fluorescence intensity of the purified vesicles was measured in bulk with a spectrofluorimeter (**Figure 22b**). The exosomes sample obtained from cells treated with Ionomycin (red line) show an increased fluorescence intensity (∼3-fold), confirming a higher volume of labeled membranes. We also tried to measure EGFP fluorescence ascribed to aS, but we detected no signal with the used quantity of sample.
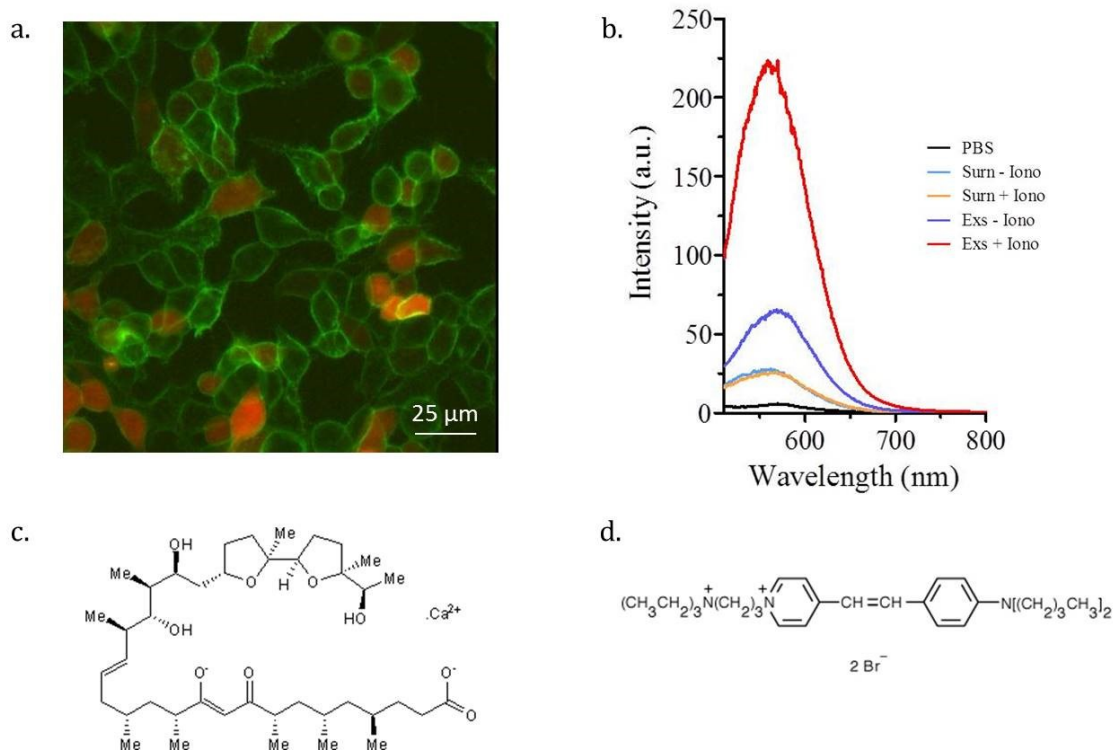


**Figure 22. HEK293T cells treated with Ionomycin. a.** HEK293T cells transfected with aSmCherry (red fluorescence) and labelled with the membrane dye FM 1-43 (green fluorescence). The image was acquired with an inverted microscope (Leica DMI4000), scale bar 25 µm; **b.** Fluorescence intensity graph of FM 1-43 shows an increased volume of labelled membranes in the presence of Ionomycin (Exs + iono) in comparison with the absence of the stimulus (Exs – Iono). As further control, the fluorescence intensity of the utilized buffer (PBS) and the supernatant of the last centrifuge (Surn) are reported; **c-d** Chemical formulae of Ionomycin calcium salt and FM 1-43 dye, respectively.

To validate the assignment of the increased fluorescence to an actual increased amount of exosomes, a Western Blot analysis was performed, using antibodies against proteins specifically enriched in exosomes, i.e. flotillin and the chaperon

proteins Hsp70 and Hsp90 [139.]

As detailed in materials and method (**paragraph 2.2.3**), exosomes were purified from the cell culture medium by differential steps of centrifugation with a final ultracentrifugation, which results in a pellet of small vesicles, among which exosomes.

HEK293T cell lysate, the supernatant resulting from the last ultracentrifugation step and the purified exosomes are compared in the Western Blot reported in **Figure 23**, to determine the effectiveness of the purification protocol. The absence of exosomal proteins in the supernatants, even in the presence of Ionomycin, indicates that the protocol was effective to pellet all suspended exosomes. Moreover, the results reported in **Figure 23** confirmed that, upon Ionomycin treatment, the amount of produced and consequentially purified exosomes was significantly higher, as demonstrated by the increased intensity of the bands relative to the exosomal proteins Hsp90, Hsp70 and Flotillin.
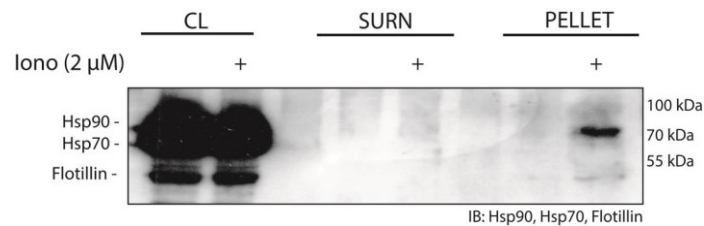


**Figure 23. Increased exosomes release upon Ionomycin stimulus.** Western Blot analyses of transfected aSmCherry HEK293T cells stimulated with 2 µM Ionomycin. Hsp90, Hsp70 and Flotillin proteins were analyzed in the cell lysates (CL), supernatants of the pelleted exosomes (SURN) and purified vesicles (PELLET) using specific antibodies.

A potential caveat in exosomes purification could be the presence of cell debris contaminations. Even if these extracellular vesicles are purified from the medium, cell debris in suspension, generated by occasional cell death, can co-precipitate with exosomes and spoil the purity of the pellet. Moreover, Ionomycin, that has been reported to induce apoptosis [311], can further contribute to cell death and exosome purification contamination. To define the toxicity threshold of the compound in our experimental model, an MTT test was performed to assess cell viability upon increasing Ionomycin concentration (from 0.2 µM to 10 µM) (**Figure 24a**). The working concentration chosen for Ionomycin (2 µM) does not induce a

significant cell death when compared to untreated cells.

a.



b.
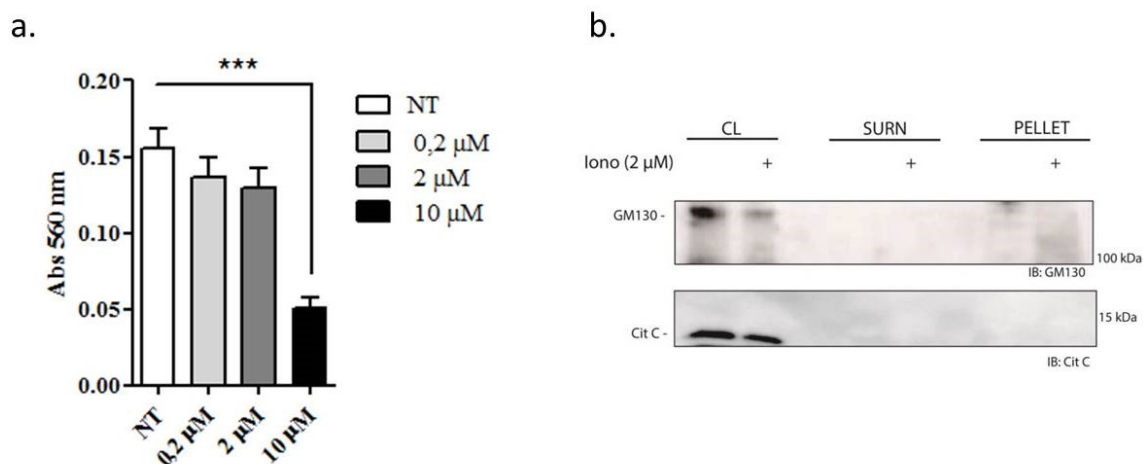


**Figure 24. Ionomycin does not contaminate HEK293T cells derived exosomes purification. a.** MTT test was performed on HEK293T non treated (NT) and incubated with increasing Ionomycin concentration: 0.2 µM, 2 µM (our working concentration) and 10 µM (toxic concentration). Data are expressed as mean ±SEM. Statistical significance was determined by one-way ANOVA with Tukey's test (***p<0.001). Three independent experiment were assessed per condition; **b.** Western Blot analyses of cell lysates (CL), supernatants of the pelleted exosomes (SURN) and purified vesicles (PELLET) of HEK293T cells were probed against GM130 and cytochrome c (Cit C) proteins.

However, this result was *per se* not sufficient to exclude a contamination in exosomes purification, being that it may still induce occasional cell death. To test this possibility, Western Blot analysis was performed, using antibodies against two proteins that should be present in the cell lysates, but not in exosomes: GM130, which is a cis-Golgi marker [312] and cytochrome C a mitochondrial membrane marker [313]. As shown in **Figure 24b**, both are present only in the two lanes relative to cell lysates (positive control), suggesting that within the detection threshold of the antibody the purified exosomes were not contaminated by cell debris.

### 3.3 Characterization of aS containing exosomes

Two of the features that differentiate exosomes from other circulating vesicles are size and shape [139]. To start the characterization of the purified exosomes we first analyzed their morphology by microscopy. In order to achieve a resolution compatible with expected exosomes size (30-100 nm), Transmission Electron Microscopy (TEM) was used (**Figure 25a**). This type of microscopy uses a beam of electron and their small de Broglie wavelength allows for imaging at a significantly

higher resolution than light microscopes (~5 nm).
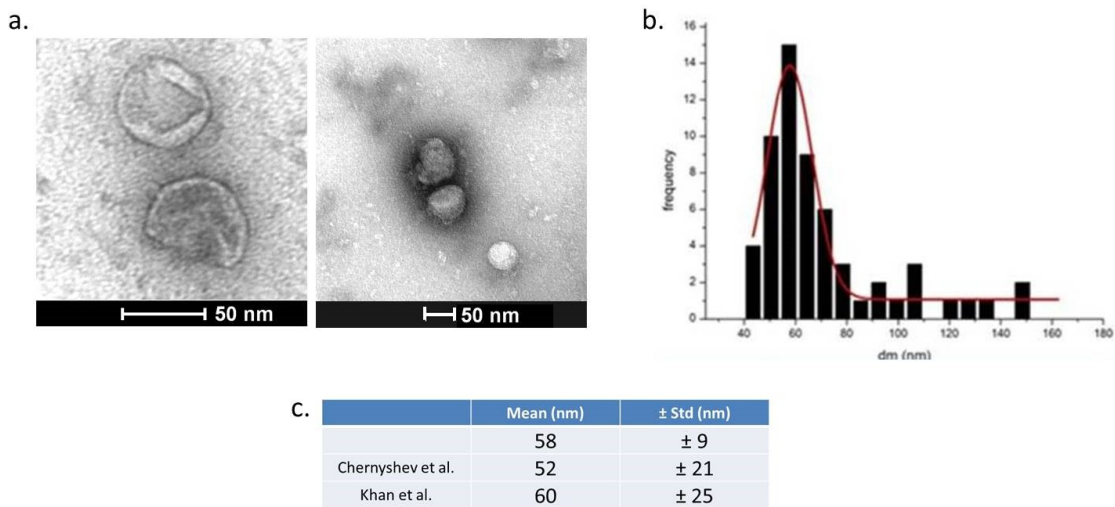


**Figure 25. Determination of exosomes size and shape by TEM. a.** TEM images of purified exosomes from HEK293T cells transfected with aSmCherry. Scale bar 50 nm; **b.** Distribution of exosomes diameter (nm), measured by ImageJ; **c.** The first row of the table indicates the mean size and the standard deviation of measured exosomes diameter (n=59), in the other two rows are reported the results of the paper [314] and [315].

The morphometric analysis of our exosomes preparation allowed to define a distribution of diameters for the vesicles purified from aS-EGFP or aS-mCherry transfected HEK293T cells, using the image processing program (ImageJ).

As reported in **Figure 25b**, purified exosomes comprised a homogenous population with an average particle diameter of about 60 nm, a value consistent with the range expected for exosomes, as reported by two others independent studies [314,315]. In terms of actual shape, considering that TEM images are generated by electrons transmitted through an ultra-thin specimen of staining agent (0.05% uranyl acetate solution) and give two-dimensional projections of three-dimensional exosomes, our results show that these projections are close to circular, as previously reported (see Table, **Figure 25c**) [314]. Especially in the first image in **Figure 25a** appears some shrinkage effect likely due to the preparation of the sample for TEM imaging.

The purified vesicles were also probed by Western Blot. As reported in **Figure 26a**, proteins previously described as associated to exosomes, i.e. flotillin, Hsp90 and Hsp70, were present in purified exosomes pellet. The presence of reporter

proteins associated to contaminations from cell debris, such as GM130 and cytochrome C [139] were below detection levels. Of relevance, aS was detected in the exosomes pellet using an antibody against aS (**Figure 26a**).

The following question we addressed was the localization of aS, that, consistently with its aS membrane-binding properties and its emerging role in vesicle trafficking [316], could be associated to vesicle both on the inside or outside of the exosome membrane.



**Figure 26. Western Blot characterization of aS containing exosomes. a.** Western Blot of exosomes purified from aS-EGFP trasfected HEK293T cells: GM130 (cis-Golgi Marker), Hsp90 (Heat Shock Protein 90), Hsp70 (Heat Shock Protein 90), Flotillin (exosomes marker) and aS (ab138501) antibodies were used; **b.** Proteinase K (PK) digestion of exosomes: exosomes were incubated with increased concentration of PK (0; 0,5 and 1.5 μg/mL) in the absence (-) and presence (+) of the detergent (1% Triton). Hsp90, CD9 (exosomes marker) and aS (ab138501) antibodies were used.

To this aim, purified exosomes were incubated with a nonspecific protease (Proteinase K, PK), which could act only on proteins exposed to the outer surface of vesicles.

As reported in **Figure 26b**, vesicles exposed to the proteolytic treatment were tested by Western Blot against Hsp90 (as negative control) which is a heat shock protein confined in exosomes and CD9, a tetraspanin commonly used to identify exosomes [139], which is present on their membrane with four hydrophobic transmembrane domains and two extracellular domains (as positive control).

Hsp90 and aS are not affected by PK digestion, indicating that both are confined

within the vesicles. At 1.5 µg/mL concentration of PK the band assigned to CD9 decrease in intensity, probably because PK has access to the protein extracellular domains. As expected, upon detergent treatment (+ Triton 1%), no bands were detected in the Western Blot, since Triton disrupts exosomes and these are not able to protect Hsp90 and aS from PK degradation.
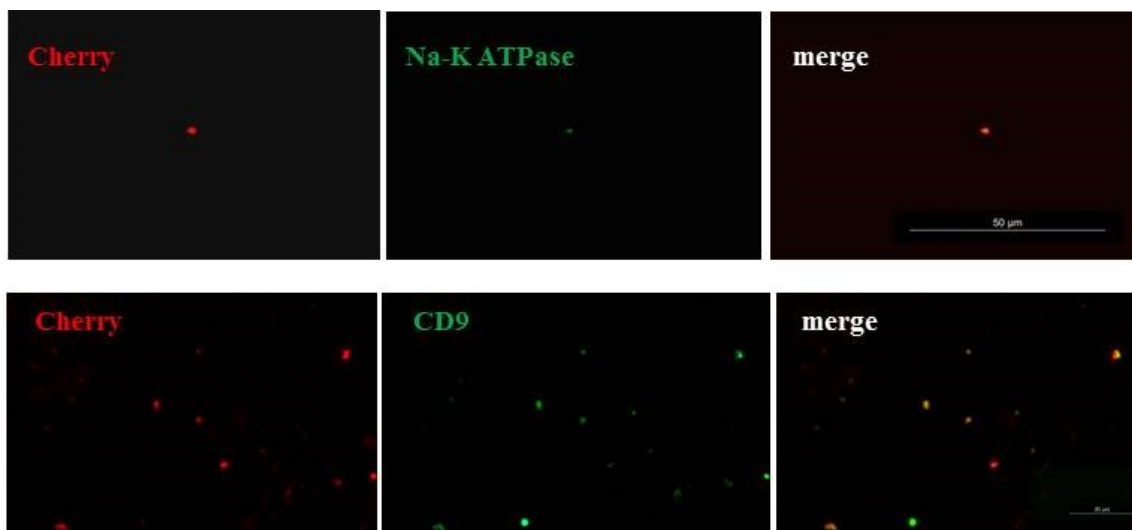


**Figure 27. Immunofluorescence characterization of aS containing exosomes.** Exosomes purified from aSmCherry trasfected HEK293T cells show colocalization between aSmCherry (Cherry, red fluorescence) and CD9 and Na+/K+-ATPase immunoreactivity (green fluorescence), as illustrated by yellow spots in the merge panel. Images were acquired using an epifluorescence microscopy (Leica 5000B). Scale bar 50 µM.

To further validate the presence of aS within purified vesicles, immunostained exosomes were spotted on a glass slide and analyzed by fluorescence microscopy. As reported in **Figure 27,** a significant colocalization was detected between aS and two exosomal marker proteins, CD9 and Na+/K+-ATPase [317], confirming their presence in the preparation.

It is important to mention that the size of the spots (about 0.8 µm in diameter) suggest that the visualized exosomes could be clustered, rather that single vesicles. As reported above, the mean exosomes diameter should be, in fact, in the 60 nm range. It follows that the resolution of the epifluorescence microscope, is simply not enough to distinguish single vesicles from vesicle clusters. A typical epifluorescence illumination compound microscope, in fact, cannot resolve or distinguish between two objects that are close than 200 nm. Additionally, because

the whole sample is illuminated at the same time, both in-focus and out-of-focus objects are detected.



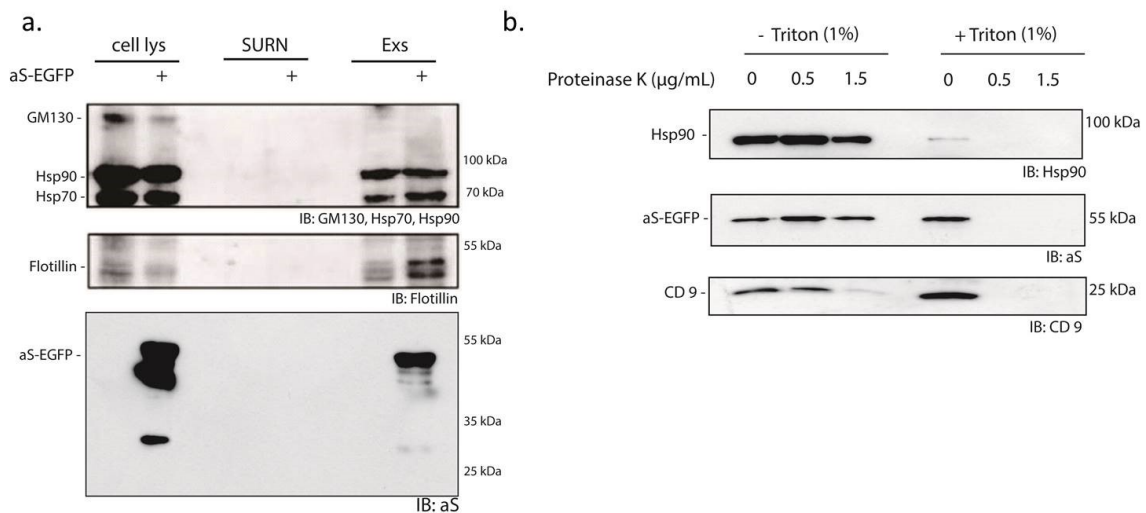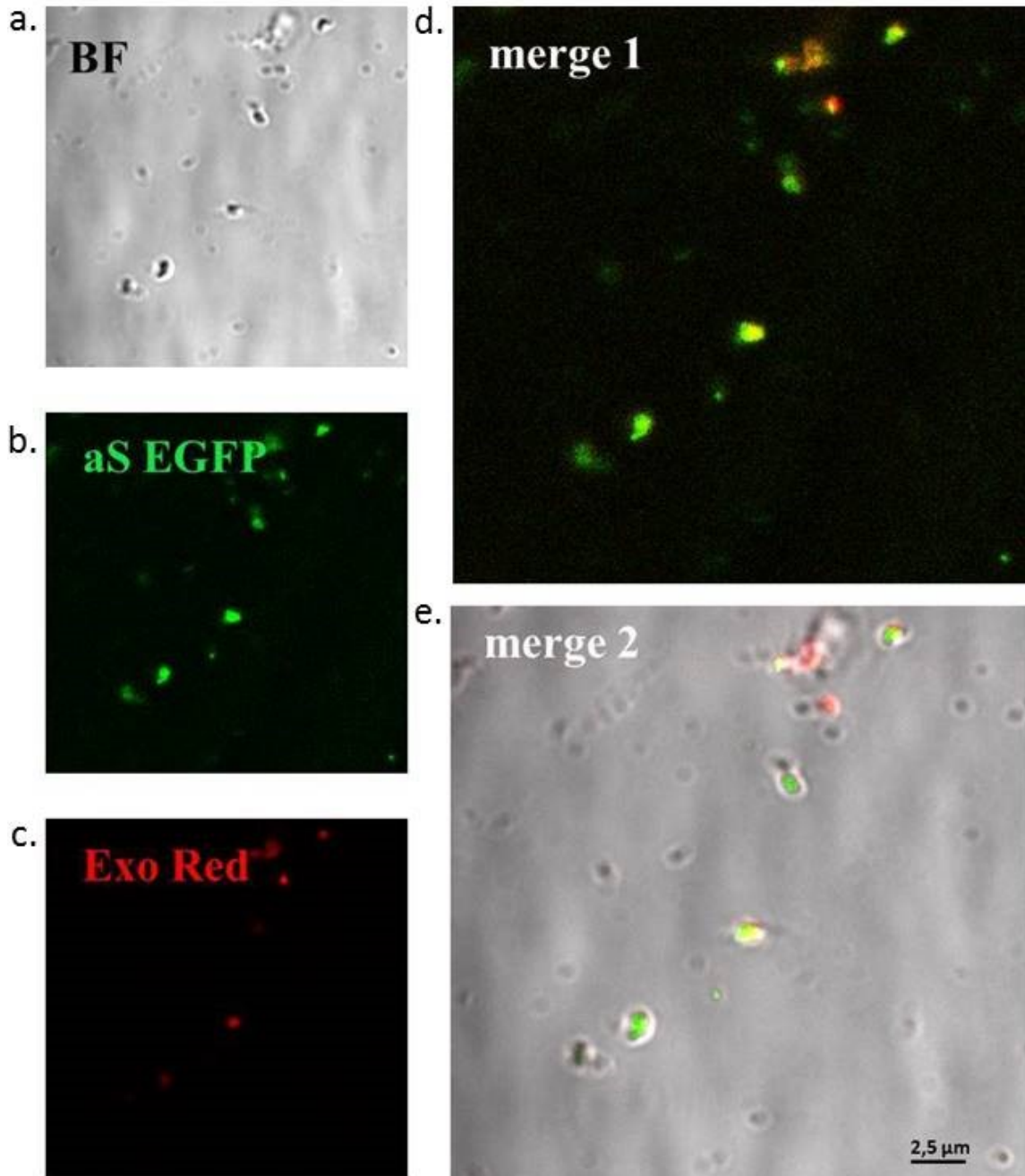**Figure 19. STED characterization of aS containing exosomes.** Exosomes purified from aS-EGFP trasfected HEK293T cells labelled with ExoRed. **a.** bright field image (BF); **b.** aS-EGFP (green fluorescence); **c.** exosomes RNA (red fluorescence); **d.** merge of aS-EGFP channel (green fluorescence) and exosomes RNA channel (red fluorescence) (merge 1); **e.** merge of BF, red and green channels (merge 2) . Images were acquired using a STED microscopy (Leica TCS Sp5 STED-CW gated). Objective 100x. Scale bar 2.5 μM.

These limitations mean that it is not possible to resolve the spatial relationship of two different-colored probes, such as aS and CD9 or Na+/K+-ATPase.

To overcome these problems, we moved to super-resolution microscopy using stimulated emission depletion (STED). STED microscopy operates by using two laser beams to illuminate the specimen. An excitation laser pulse (generally generated by a multiphoton laser) is closely followed by a doughnut-shaped red-shifted pulse that is termed the STED beam. Excited fluorophores exposed to the STED beam are instantaneously returned to the ground state by means of stimulated emission. The non-linear depletion of the fluorescent state by the STED beam is the basis for super-resolution. Even though both laser pulses are diffraction-limited, the STED pulse is modified to feature a zero-intensity point at the center of focus with strong intensity at the periphery. When the two laser pulses are superimposed, only molecules that reside in the center of the STED beam can emit fluorescence, thus significantly restricting emission. This action effectively narrows the point-spread function and increases resolution beyond the diffraction limit. STED microscopy is in fact capable to reach 20 nm of lateral resolution and 40 to 50 nm of axial resolution.

To identify exosomes by STED, a specific commercial dye (Exo-Red) was used. The Exo-Red stain is based on an Acridine Orange (AO). AO is membrane permeable and it fluorescently-labels single-stranded RNAs inside of exosomes, emitting at 650 nm (red).

As reported in **Figure 28,** STED microscopy allows to better visualize the purified exosomes, permitting to distinguish individual exosomes, thanks to the improved resolution. To both confirm the presence of aS inside exosomes and determine the fraction of aS positive vesicles, we also analyzed the overlapping between aS and the Exo Red signals.

Being that all the Exo Red labelled exosomes co-localize with the green fluorescence relative to aS-EGFP, it is confirmed that a homogeneous sample of aS containing exosomes were successfully purified. It should be mentioned that not all vesicles, which emitted in green (aS positive), were also Exo Red labelled. This observation can be explained in two ways: either they are not exosomes, but other types of extracellular aS loaded vesicles without internal RNA or, being Exo Red

labelling a post purification procedure, not all exosomes were effectively marked. Considering that contaminants in the purified fraction of exosomes were below detection limit of the Western Blot analysis (**Figure 26**), all of the presented results suggest that the used protocol allows the purification of aS-EGFP loaded exosome from aS-EGFP transfected HEK293T cells.

## 3.4 Characterization of exosomes containing DOPAL modified aS

As mentioned above, DOPAL is a highly toxic dopamine metabolite that accumulate in neurons of parkinsonian brains, where it can chemically modify aS, leading to its oligomerization [318]. Our hypothesis is that these misfolded aS species can be transmitted to other cells of the CNS. In this way, DOPAL-induced aS aggregates might exert deleterious effect, as impair synaptic vesicle function in recipient-neurons [106]. Moreover, DOPAL is also transmissible to glial cells and enhances intracellular oligomerization of aS, suggesting a possible mechanism for glial cytoplasmic inclusions formation in MSA [319]. With these premises, the purification of exosomes containing DOPAL-modified aS appears of a great interest to define an experimental model of exosomes based spreading not only for PD, but for all α-synucleinopathies, characterized by abnormal aS aggregation.

### 3.4.1 Exosomes containing DOPAL modified aS are released from DOPAL treated HEK293T cells

HEK293T cells were treated with exogenously administered DOPAL, that, being a neutral catechol is expected to easily cross membranes [319].

In line with previous works [105,319-321], DOPAL was added to the growth medium at the final concentration of 100 μM, for overnight treatments [97,318].

To verify whether DOPAL treatment leads to aS modifications in HEK293T cells, aS-EGFP overexpressing cells were incubated with 100 μM DOPAL. After 12 hours, cell lysates were subjected to the aminophenylboronic acid (APBA) resin (**Figure 29b**), which allow the pull-down of DOPAL-modified proteins by binding to the diphenyl moiety [322]. This is possible because the amino group links the

phenylboronate to the resin and the di-hydroxide on the Boron interacts with any molecule that contains a 1,2-cis-diol group, like DOPAL.
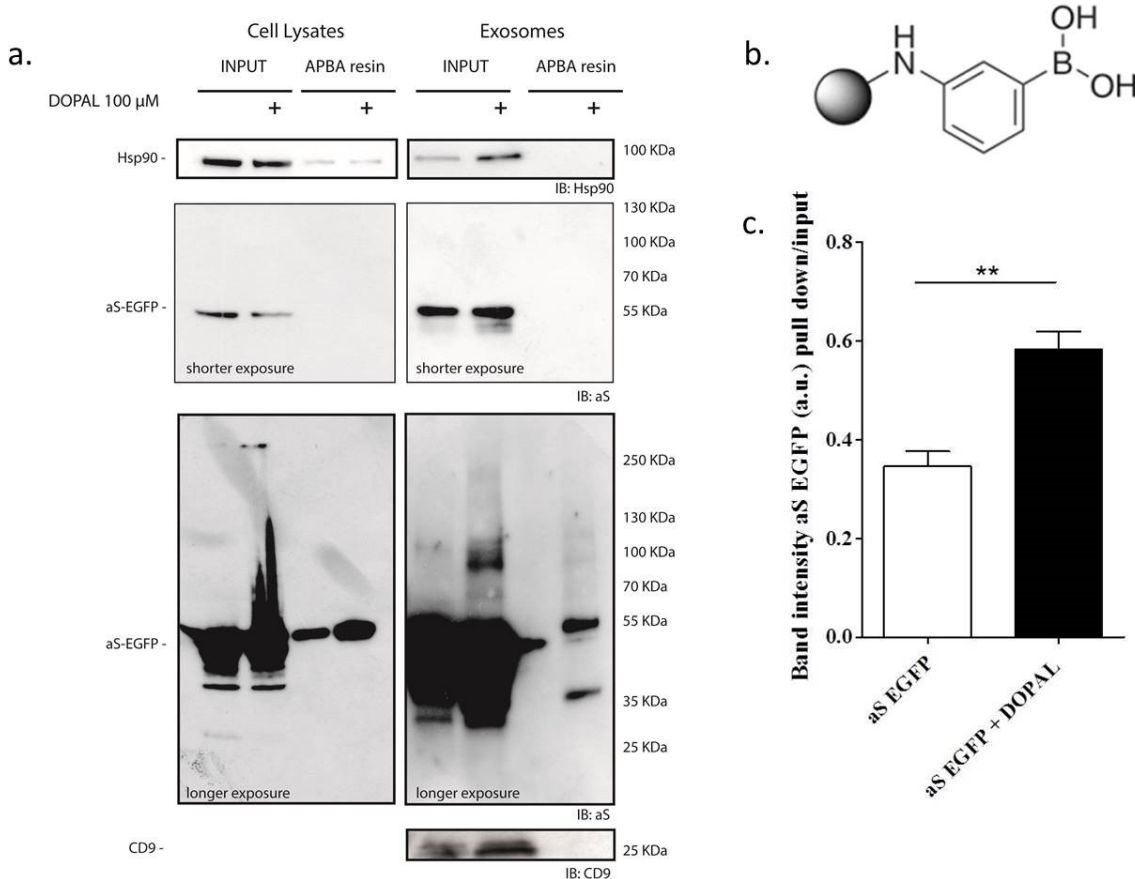


**Figure 20. aS is DOPAL modified in cell lysates and exosomes of HEK293Tcells. a.** Pull down of DOPAL treated HEK293T cell lysates and derived exosomes were analyzed by Western Blot against aS and the exosomal markers Hsp90 and CD9. aS antibody (ab138501) revealed SDS-resistant oligomers formation upon DOPAL treatment; **b.** Chemical formula of 3,4 Dihydroxyphenylacetaldehyde (DOPAL); **c.** The column graph represents aS EGFP band intensity in the pull down lines of cell lysates normalize to the relative inputs. Data are expressed as mean ±SEM. Statistical significance was determined by unpaired t test (**$p<0.01$). Three independent experiments were assessed per condition.

Considering that DOPAL mainly reacts with aS lysines at its N-term domain [97,108], both total cell lysates and the pull-down samples were analyzed by Western Blot using an antibody against the C-terminal domain of aS, and in particular to a no-lysines region (amino acids 118-123: VDPDNE). In this way both aS and DOPAL-modified aS are expected to be similarly recognized in our Western Blot analyses. Supportively, aS antibody recognized a smear and a more defined band corresponding to SDS-resistant aS oligomeric species at about 250 kDa only upon

DOPAL treatment (**Figure 29a**).

As depicted in the pull-down panel, the resin bound also to non-modified aS. APBA is reported to interact, in fact, with any molecule that contains a 1,2-cis-diol group, like DOPAL, but also, for example, glycosylated proteins, like aS and Hsp90 [323,324]. Upon DOPAL treatment the enrichment of aS band in the correspondent pull-down lane, suggested that aS is DOPAL-modified in our experimental condition.

In particular, in non-treated cell the pull-down aS relative to the inputs was 35% and increased up to 58% upon DOPAL treatment (**Figure 29c**).

These results suggest that aS monomers in the exosomes were covalently modified by DOPAL molecules and formed SDS-resistant oligomers upon DOPAL treatment. Hsp90, used as a control, was detected in the pull-down lines too, but in an equal amount, suggesting that Hsp90 is not DOPAL-modified or at least not as much as aS.

Once verified that in HEK293T aS-EGFP overexpressing system, DOPAL-modified aS and aS-DOPAL oligomers were formed upon DOPAL treatment, we next investigated whether aS-DOPAL oligomers were also present in the isolated exosomes.

Exosomes were purified from the supernatant of HEK293T cells overexpressing aS-EGFP treated overnight with 100 µM DOPAL. Purified vesicles were enriched in typical exosomal proteins, i.e. CD9 and Hsp90, which were not detectable in the pull-down lanes even upon longer exposures as demonstrated by Western Blot analysis (**Figure 29a**). The presence of aS and DOPAL modified aS in exosomes was assessed with the same method used for cell lysates. As reported in **Figure 29a,** exosomes present a band at about 55 kDa relative to aS-EGFP and the correspondent pull-down lane shows an increase in the detected aS. Moreover, only upon DOPAL treatment an aS positive band was detected at about 100 kDa, suggesting that these vesicles contain not only DOPAL-modified aS, but also DOPAL induced aS aggregated forms. Of note, not all the detected SDS-resistant aS-species in cell lysates have correspondent species in the lysates of exosomes obtained after DOPAL treatment. It is likely that the high level of transfection in HEK293T cells, which in fact are characterized by higher molecular weight aS species, can explain this difference.
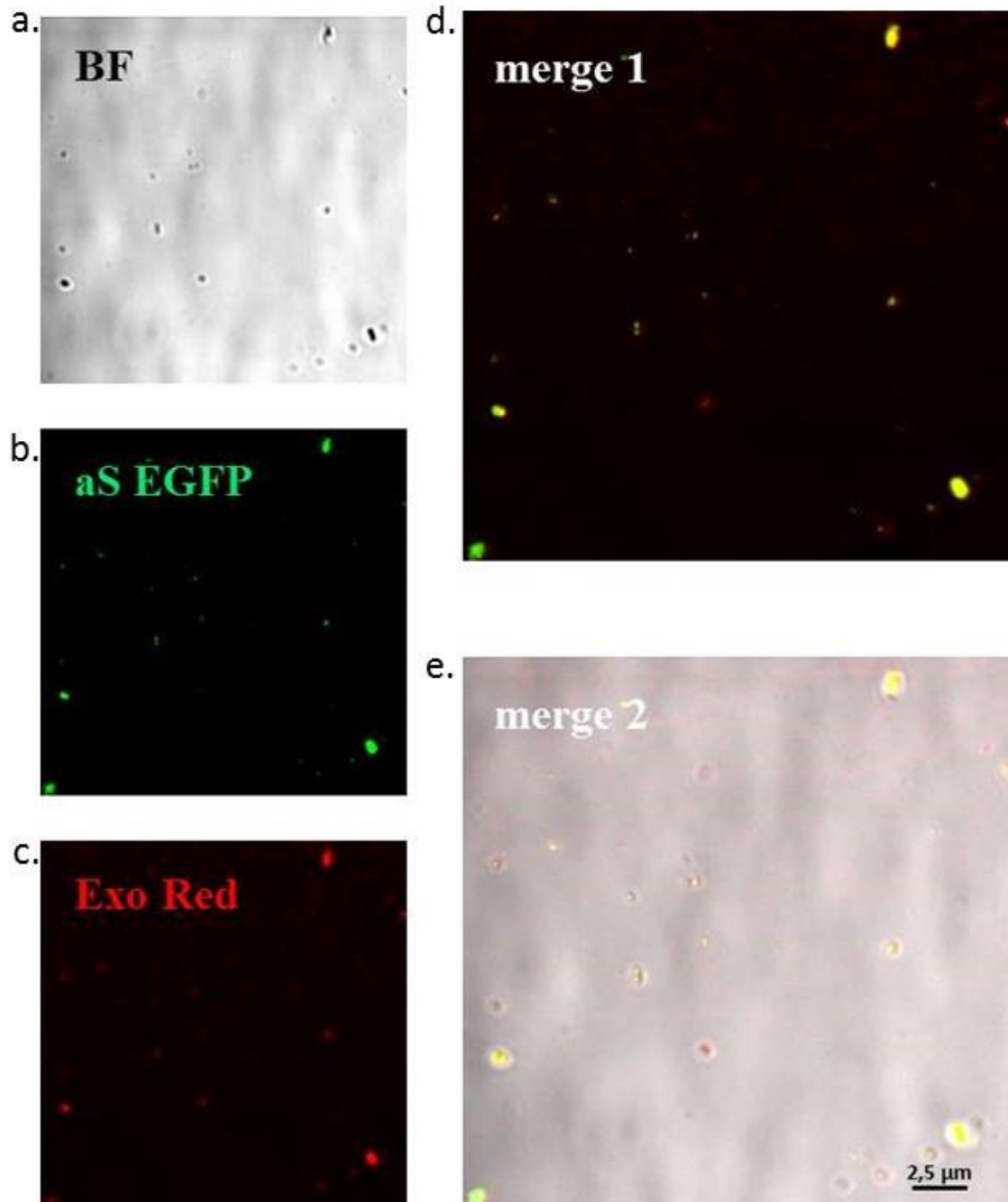
**Figure 30. STED characterization of DOPAL modified aS containing exosomes.** Exosomes purified from aS-EGFP trasfected HEK293T treated with DOPAL and labelled with ExoRed. **a.** bright field image (BF); **b.** aS-EGFP (green fluorescence); **c.** exosomes RNA (red fluorescence); **d.** merge of aS-EGFP channel (green fluorescence) and exosomes RNA channel (red fluorescence) (merge 1); **e.** merge of BF, red and green channels (merge 2) . Images were acquired using a STED microscopy (Leica TCS Sp5 STED-CW gated). Objective 100x. Scale bar 2.5 μM.

It is also important to mention, however, that exosomes are not only able to select their cargos, but also, in response of different stimuli, to enhance the concentration

of specific contained proteins [325]. Therefore, it is probable that upon DOPAL treatment exosomal pathway select specific aS aggregated species to be secreted out from cells.

These vesicles were further analyzed by STED microscopy (**Figure 30**). As for aS containing exosomes, they presented a good overlap between aS and the ExoRed signals, confirming the presence of aS inside exosomes.

All together these results indicate that overexpression of aS and treatment of HEK293T cells with DOPAL result in the production of exosomes containing DOPAL modified aS.

### 3.4.2 DOPAL induces aS aggregation in exosomes

What emerges from the Western Blot analysis reported in **Figure 29** is that, upon DOPAL treatment, both in HEK293T cells lysates and in the derived exosomes, aS forms SDS-resistant aggregates. To further characterize aS state, we have used size-exclusion chromatography (SEC) analysis, which permits to achieve additional information on non SDS-resistant aS forms.

SEC is, in fact, a separation technique based on the relative differences in size or hydrodynamic volume of macromolecules, which interact with a porous stationary phase. Being an indirect analysis, SEC required a column calibration in order to determine for each experimental condition a correlation curve between the elution profile and the apparent molecular weights [326]. Thus, as indicated by dash lines in **Figure 31,** Ferritin, BSA and cytochrome C were used as reference molecular weight for column calibration.

The purified exosomes and cells lysates were then analyzed. For each SEC fraction eluted a Dot Blot analysis was performed, using an antibody against aS to identify aS positive fractions. Moreover, thanks to the EGFP-tag, for each SEC fraction eluted EGFP fluorescence intensity was measured (green continuous line in **Figure 31**). The elution profiles of EGFP fluorescence intensity and aS Dot Blot intensities were then normalized to a corresponding total intensity for the area under the curves and then plotted as function of the elution volume (mL), to identify differences in terms of aS forms.
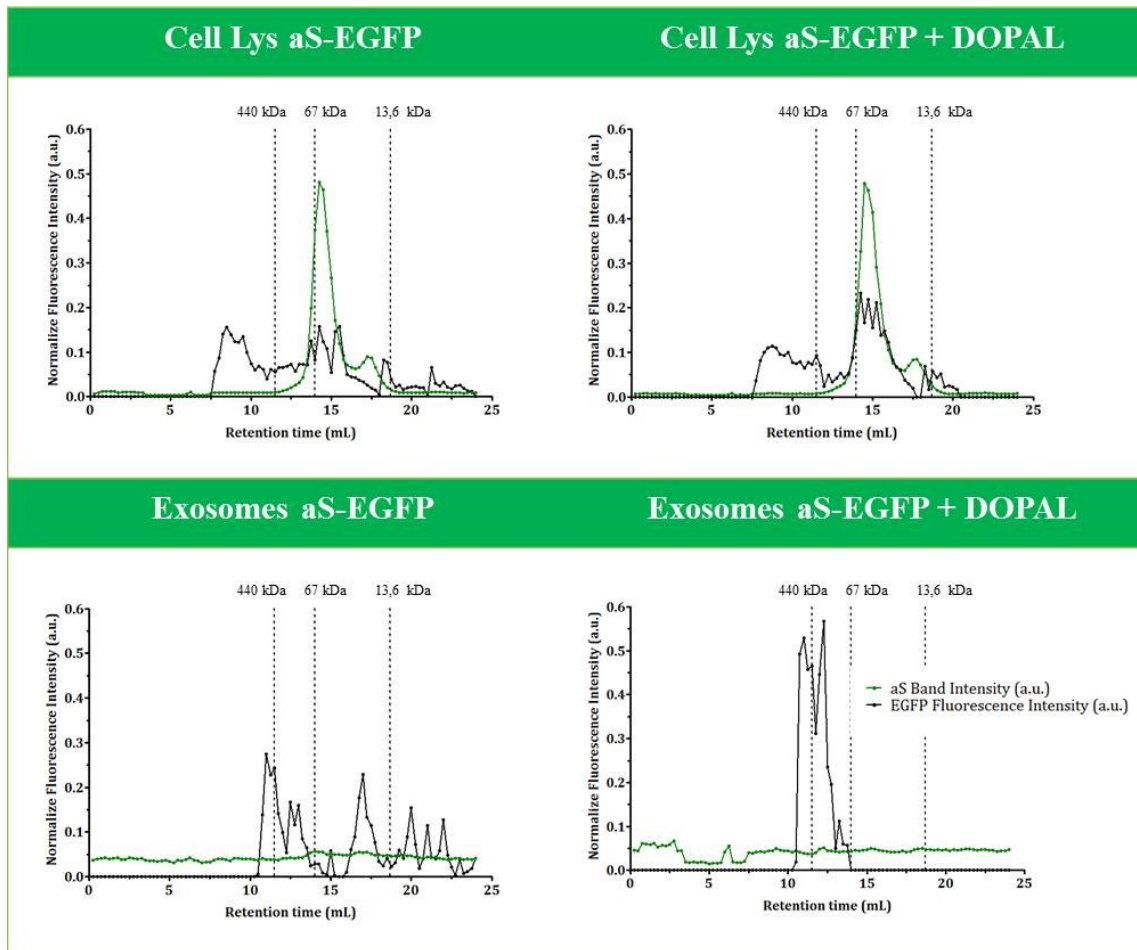
**Figure 31. EGFP fluorescence signal is not sensitive enough to distinguish different aS-EGFP population in SEC separation.** Quantification of the EGFP fluorescence (in green) and aS dot intensity (in black, antibody ab138501) in each SEC fraction normalized on total intensity area, except for exosomes EGFP fluorescence (n=1 for cell lysates, n=1 for three different exosomes purification). Dash line (--) indicated standards: Ferritin (440 kDa) at 11.5 mL, BSA (67 kDa) at 14 mL and Cytochrome C (13.6 kDa) at 18.7 mL.

Analyzing the profile of fluorescence intensity in cell lysates (green lines in the upper panel of **Figure 31**), a main peak at about 15 mL (57 kDa) is observed, which probably corresponds to aS-EGFP monomer. It appears bigger of its expected molecular weight (at about 55 kDa) likely because of its large hydrodynamic radius as monomeric aS [327]. Accordingly, the 15 mL peak corresponds to a peak in the Dot Blot profile. The longer retention time shoulder (at 17 mL) instead, may correspond to degradation product of EGFP and it is not recognized by aS antibody.

Interestingly aS band intensity profile appeared to have a higher resolution in comparison with EGFP signal. This is even more evident when the elution profiles

of exosome are compared: in the case of EGFP fluorescence almost no signal was detected, conversely the Dot Blot show different aS positive fractions (**Figure 31**). It would be also interesting to analyze in parallel EGFP positive fraction by Western Blot, in order to discriminate between endogenous and transfected aS, but EGFP antibody was not sensitive enough and endogenous aS was never detected in purified exosomes. Therefore, in the following experiments we chose to consider only aS Dot Blot intensity, even if a problem in this case is the narrow dynamic range of detection, that often result in signal saturation [328].

First, cell lysates were analyzed and they did not show differences upon DOPAL treatment (left panel, **Figure 32**).
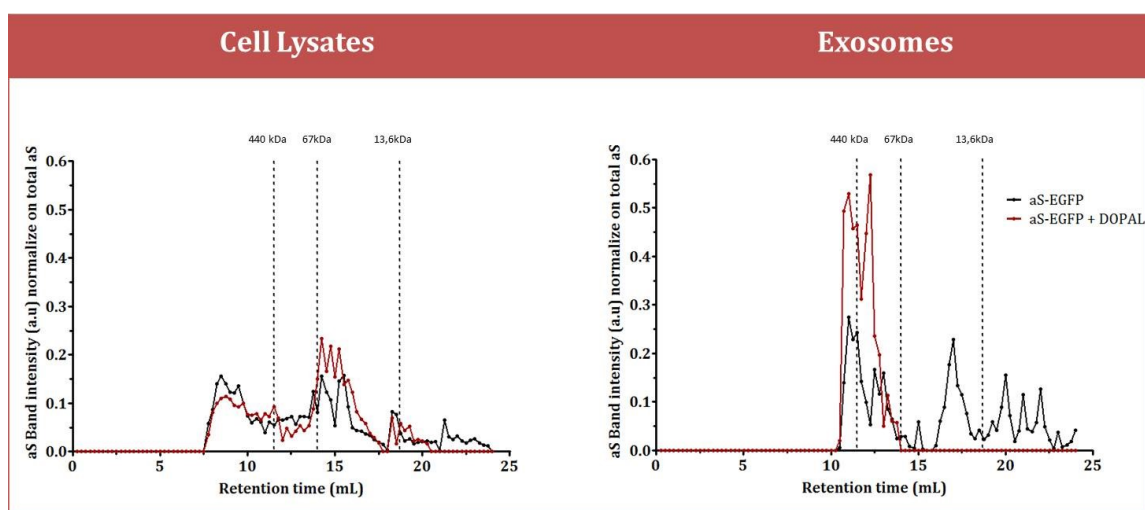


**Figure 32. DOPAL treatment induce aS-EGFP oligomerization in exosomes.** Quantification of aS band intensity not treated (in black) and upon DOPAL treatment (in red) in each SEC fraction normalized on total intensity area (n=1 for cell lysates, n=1 for three different exosomes purification). In the right panel cell lysates, in the left panel exosomes. Dash line (--) indicated standards: Ferritin (440 kDa) at 11.5 mL, BSA (67 kDa) at 14 mL and Cytochrome C (13.6 kDa) at 18.7 mL.

Under both conditions, the resulting chromatographic profile was very similar: a peak at about 15 mL, corresponding to aS-EGFP monomers, some degradation products at lower retention times and a big amount of aS positive aggregates after the void volume of the column (at 8 mL).

The fact that this high molecular weight aS species were present in the absence of DOPAL treatment, suggests that aS aggregates by itself probably as a consequence of the high level of its expression in HEK293T cells. aS concentration in cytoplasm

in fact depends on the equilibrium between synthesis, clearance and aggregation. Once the balance among these processes is impaired, accumulation of the protein may result in increasing amount of aggregated species. This link has been demonstrated in many cellular lines, frequently with transient transfection of aS gene to reproduce protein over-expression, as in this case [28,329,330]. Also in familial and sporadic PD cases, multiplication of aS gene, i.e. duplication and triplication, enhance protein expression and buildup of aggregates [331]. It is plausible to assume that the high amount of intracytoplasmic aS-EGFP led to its aggregation, hindering the aggregating effect induced by DOPAL. DOPAL-modified aS oligomers are better resolved by SDS-Page and Western Blot techniques [108,318], being them SDS resistant, as they result from the formation of covalent bounds. However, the reduced charge and increased hydrophobicity that is associated to the modification of aS lysines residues by DOPAL, might also cause the formation of intramolecular hydrophobic interactions leading to larger DOPAL induced aS-oligomers, not SDS-resistant [107], which probably elute in the large peak corresponding to the void volume. It is important to mention, however, that also physiologically functional multimers [211] are characterized by a large hydrodynamic radius and are disrupted by SDS, suggesting that they might also elute in the void volume of the column. To distinguish between these two possible explanations, we are planning to perform a SDS-Page of the different SEC fraction in treated and not-treated cells in order to achieve more information on SDS resistant and non-resistant aS species.

The SEC analysis was then applied to purified exosomes obtained from HEK263T cell naïve and exposed to DOPAL. As reported in the right panel of **Figure 32,** in this case the profiles present some differences upon DOPAL treatment. In vesicles derived from non-treated cells, the peak at 15 mL corresponding to the aS-EGFP monomer is still present, but in a small percentage relative to all detected aS (1.6 %). The main aS positive fractions in fact are at higher and lower retention time. Interestingly, upon DOPAL treatment, aS population is almost exclusively present at a high molecular weight, suggesting an enrichment in large aggregated species in comparison with the non-treated sample.

In **Figure 33**, HEK293T cells and corresponding exosomes are compared. It appeared evident that they present a different aS positive fraction patterns.

In the cell lysates, the most abundant aS fractions are the peak corresponding to aggregated species, which eluted between 7 and 10 mL and the monomer at 15 mL. In exosomes, instead aS eluted only after 10 mL, suggesting that these vesicles are able to load specific aS-EGFP populations. Coherently, cargo selection is finely regulated in exosomes [332], supporting their role as vehicle of information and toxicity.
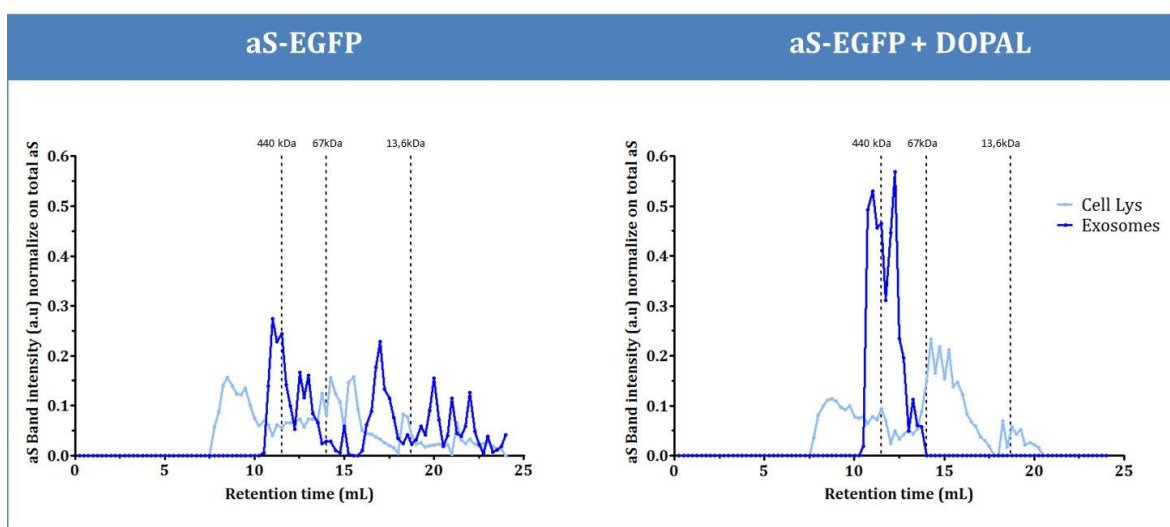


**Figure 33. Exosomes select a specific aS-EGFP population.** Quantification of aS band intensity in HEK293T cell lysates (light blue) and in exosomes (blue) in each SEC fraction normalized on total intensity area (n=1 for cell lysates, n=1 for three different exosomes purification). In the right not treated, in the left panel upon DOPAL treatment. Dash line (--) indicated standards: Ferritin (440 kDa) at 11.5 mL, BSA (67 kDa) at 14 mL and Cytochrome C (13.6 kDa) at 18.7 mL.

In conclusion purified exosomes contain SDS non-resistant oligomeric/multimeric aS, as reported by others [126,127]. Upon DOPAL cell treatment, they display also SDS-resistant DOPAL-modified aS oligomers and increased SDS non-resistant species. This has a particular relevance since oligomers are considered the most toxic aS species and exosomes can protect them against extracellular protein degradation mechanisms, enhancing α-synucleinopathies propagation [49].

### 3.4.3 DOPAL modified aS localizes at the membranes and alters exosome's microenvironment

Different mechanisms of cytotoxicity have been proposed for aS oligomers, in the several studies present in the literature on this subject [90, 333]. Among others, a widespread hypothesis is that cytotoxicity is caused by the interaction of oligomers with the lipid bilayer of the cell membranes. This interaction is however highly dependent on the nature of both the oligomers and the lipids. Anionic lipids are required for interaction of the positive charges associate to the several lysines residues of aS with the lipid membrane, while increased exposure of hydrophobic patches from highly dynamic protein oligomers have been proposed to be structural determinants of cytotoxicity of the oligomers [333]. The latter observation is particularly relevant for exosomes, in which lipids play a vital role in their biogenesis and are characteristic of the cell origin [166].

Therefore, once demonstrated the presence of aS oligomers inside purified exosomes, the following step was to explore their interaction with exosomes membrane.

To this aim, a correlative approach based on coupling STED super-resolution techniques with Atomic Force microscopy (AFM) was used. In this way it was possible to combine precise topological information, local stiffness measurements and specific fluorescence imaging [334].

AFM, in fact, has been largely used to reveal the oligomeric assemblies on lipid membrane due to its nanometer-scale resolution combines with the ability to image biomolecular interactions in liquid environment [335].

As reported in **Figure 34**, broken exosomes were firstly observed by STED microscopy, which permitted to identify aS in a crowded exosomes environment thanks to its EGFP tag. Then STED was combined with AFM in order to provide topological information on the very same frame of the analyzed sample.

Interestingly, only in DOPAL treated cells derived exosomes, aS-EGFP was identify on a surface, which was compatible in thickness with a lipid bilayer (3-4 nm). Moreover, the STED-identified green fluorescence region associated to aS-EGFP corresponded to a high rise of 3-4 nm, identified by AFM, confirming the perfect

overlap between the images generated by the two microscopies and suggesting the presence of one oligomer of aS-DOPAL placed on the membrane surface. The fact that aS containing exosomes did not present aS localized at the exosomal membrane can be explained by the different nature of their oligomers. DOPAL oligomers are, in fact, characterized by a reduced proteins charge and increased hydrophobicity, due to lysines modification [108].
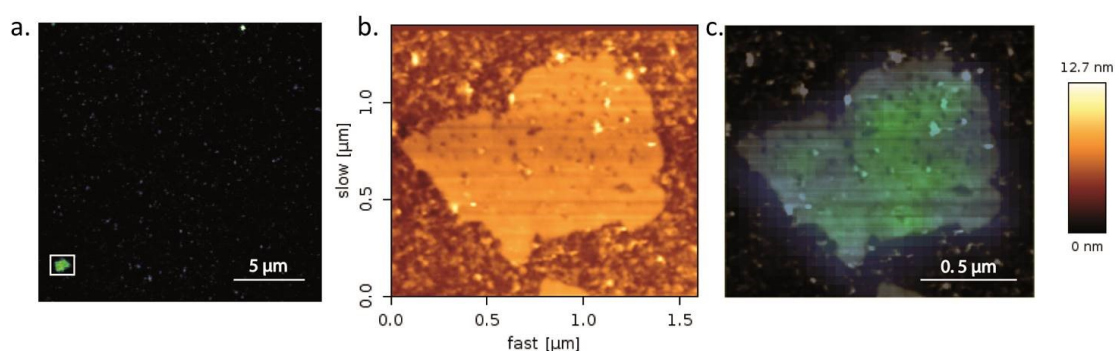


**Figure 34. aS DOPAL oligomers localize at the membranes.** Broken exosomes purified from aS-EGFP transfected cells and treated with DOPAL were analyzed by STED microscopy coupled with AFM. **a.** STED images of the green fluorescence associated with aS-EGFP inside exosomes. The image was acquired using a Leica TCS Sp5 STED-CW gated. Objective 100x c. Scale bar5 μm; **b.** AFM image corresponding to the area identified by the white square in (**a**). The image was acquired using a JPK Instruments, Berlin, Germany; **c.** Merge of the STED (a) and AFM (b) image underlining the presence of the aS-EGFP associated fluorescence on the lipid membrane. At least, three independent experiments were performed.

The interaction between oligomers and the lipid bilayer of the cell membranes are supposed to lead to membrane disruption or even pore formation. The formation of an actual ion channel could lead to membrane disruption, eventually resulting in depolarization, dysregulation of signal transduction and perturbations in ion homeostasis [333].

Since it was previously shown in our laboratory that DOPAL modified aS oligomers can permeabilize cholesterol-containing lipid membranes mimicking synaptic vesicles *in vitro* [107], we made the hypothesis that they were also able to alter exosomes microenvironment.

To investigate the capacity of aS-DOPAL oligomers to permeabilize exosomes, we used atomic absorption to quantify the ionic composition of exosomes.

Several studies reported the composition of the loaded cargo of exosomes,

indicating the presence of copper, iron and calcium-binding proteins like transferrin [336], SOD1 [337] and calmodulin [338]. Moreover, endolysosomes, exosomes biogenesis compartment, provide storage for intracellular $Ca^{2+}$ (approximately 0.5 mM of luminal $Ca^{2+}$ concentration [339,340]).

In this frame, purified vesicles were analyzed for the presence of $Ca^{2+}$, Cu and Fe. The quantity of ions (µg) were normalize on exosomes protein content.

As illustrated in **Table 2**, purified, $Ca^{2+}$ and Cu (µg) were at about 50 times less in vesicles derived from DOPAL treated in comparison to untreated aS transfected cells. Fe amount showed smaller differences between the two conditions.

| | Ca (µg)/ proteins (µg) | Fe (µg)/ proteins (µg) | Cu (µg)/ proteins (µg) |
|---|---|---|---|
| Exosomes | 1.86 | 0.60 | 4.35 |
| Exosomes + DOPAL | 0.035 | 0.18 | 0.085 |
| Ratio − / + DOPAL | 53 | 3 | 51 |

**Table 2. The table resume the µg of Ca, Fe and Cu per µg of proteins in purified exosomes from DOPAL treated and not treated HEK293T cells.** The ratio is calculated between treated and not treated samples.

These results suggest that DOPAL lead to the formation of DOPAL aS oligomers, which in turn alters exosomes microenvironment, possibly by permeabilizing their membrane, leading to $Ca^{2+}$ and Cu free diffusion. Conversely, Fe did not display the same trend and this observation can be partially explained by analyzing iron homeostasis.

Redox active metals ion such as iron (but also copper) are cofactors in multiple redox reactions, thus they are also involved in the production of potentially damaging radical species through Fenton or Haber–Weiss reactions[341]. Consequentially, all organisms have redundant mechanisms for controlling their concentrations. For this reasons, it is highly probable that in the exosomes there is almost no free iron, but it is mostly bound to proteins, like transferrin (80 kDa, Kd = 10-23 M at neutral pH). Coherently, transferrin, or any other iron protein, due to their size do not pass through permeabilizing DOPAL aS oligomers. The same argument should hold for copper ions; however we observe a significant decrease in exosomes from DOPAL treated derived cells. The hypothesis of

permeabilization is perfectly coherent with the observed decrease, instead, in the calcium content.

To summarize, these results suggest that the microenvironment of DOPAL modified aS containing exosomes is altered in comparison with exosomes containing unmodified aS, probably due to the alteration of exosomes membrane as confirmed by localization of DOPAL-modified aS oligomers on the lipid bilayer. This aspect might indicate in the permeabilization activity one of or the toxic mechanism(s) associated to DOPAL aS oligomers and contribute to the increased toxicity of DOPAL modified aS containing exosomes upon incubation with neuronal cells, as it will be illustrated in the following section.

## II PART: Effects of aS containing exosomes on cells

The second part of this thesis focuses on the consequences of DOPAL modified-aS free or within exosomes on microglia activation and neuronal function.

In recent years, extracellular aS received extensive scientific attention for its potential role in disease initiation and progression. Considering the nature of neurodegenerative disorders as well as the defined, step-wise spreading of Lewy body pathology in PD [109] the idea of extracellular aS as a pathogenic 'prion-like' agent is appealing.

Among different mechanisms of aS secretion reported in the literature, exosomes seem to be of relevance for several reasons: (i) aS containing exosomes are released and internalized by neurons and microglia [342]; (ii) exosomal encapsulation of aS confers protection against extracellular protein degradation mechanisms [343], enhancing exosomes probability to play a role in aS toxic species transmission; (iii) these vesicles provide a confined and controlled environments for aS nucleation, which may promote aggregation and lead to toxicity and neurodegeneration [127,344]; (iv) it was recently shown that exosomes isolated from plasma of PD patients contain higher levels of aS when compared to exosomes from control individuals [345].

However, the precise role of exosomes in the spreading of aS pathology needs to be further detailed and the aim of this second section is to explore the effect(s) of purified exosomes on neurons and microglia, which are for different aspects the two main cell players in α-synucleinopathies.

### 3.5 DOPAL modifies also EGFP in aS-EGFP protein

We initially characterized the DOPAL-modifying properties of aS-EGFP *in vitro,* to rule out any potential effect of DOPAL on the GFP tag. For this purpose, recombinant aS-GFP and the empty vector (with only the EGFP sequence) were expressed in *E. coli*.

As reported in **Figure 35**, the molecular weight of recombinant aS-EGFP and EGFP produced by *E. coli* were comparable to the proteins expressed in HEK293T cell

lysate. As indicated by the arrow (**Figure 35a**), in EGFP gel purification, a band of approximately 20 KDa was detected, which is probably due to a degradation products of EGFP protein.
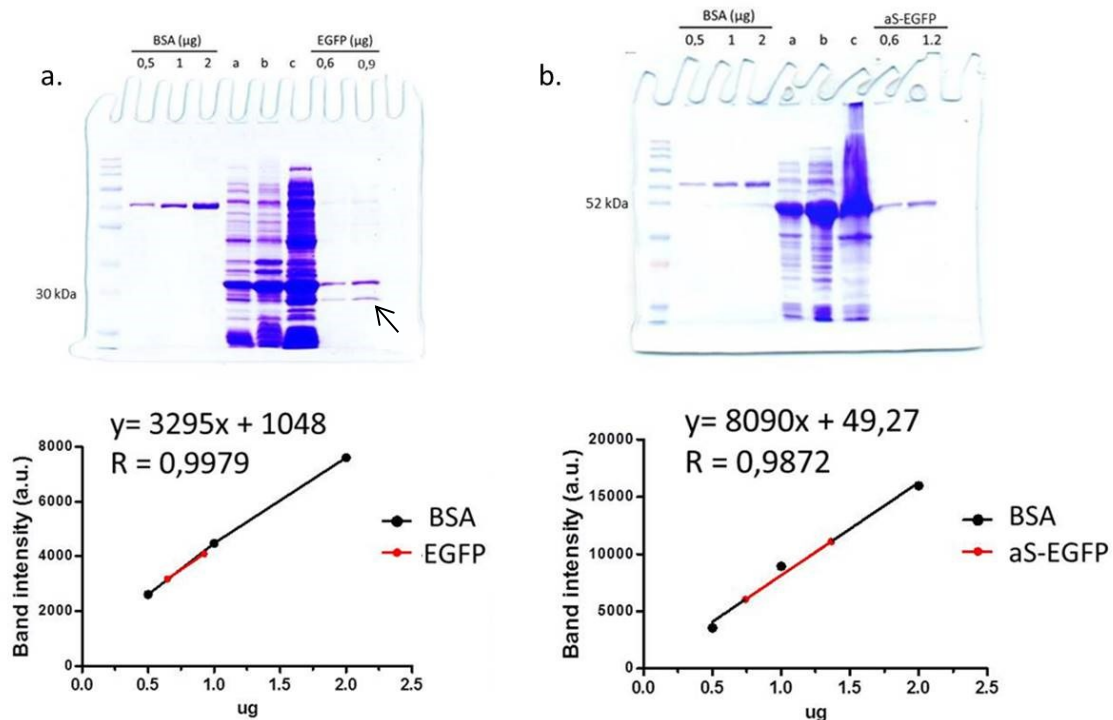


**Figure 35. Production of recombinant EGFP and aS-EGFP. a.** SDS-PAGE gel Coumassie stained with 0.5, 1 and 2 μg of BSA and 0.6 and 0.9 μg of EGFP; **b.** SDS gel Coumassie stained with 0.5, 1 and 2 μg of BSA and 0.6 and 1.2 μg of aS-EGFP. a, b, c are different steps of the purification. In the correspondent bottom panel, there are the standard curves extracted from the gel densitometry analysis.

Recombinant aS-EGFP and EGFP concentrations were assessed by comparison with BSA samples of known concentrations in the concentration range of 0.5 μg to 1 μg. Protein relative amounts were determined measuring band intensity. Once a standard curve was obtained, the EGFP and aS-EGFP contents were estimated (**Figure 35**). The quantification was confirmed by UV absorbance. As expected recombinant EGFP and aS-EGFP showed an absorption maximum between 275 and 280 nm, due to the presence of the aromatic amino acids tryptophan (Trp) and tyrosine (Tyr): EGFP has 1 Trp, 11 Tyr and no disulfide bonds (Ext. coefficient 21890 $M^{-1}$ $cm^{-1}$); aS-EGFP has 1 Trp, 15 Tyr and no disulfide bonds (Ext. coefficient 27850 $M^{-1}$ $cm^{-1}$) (**Figure 36**).
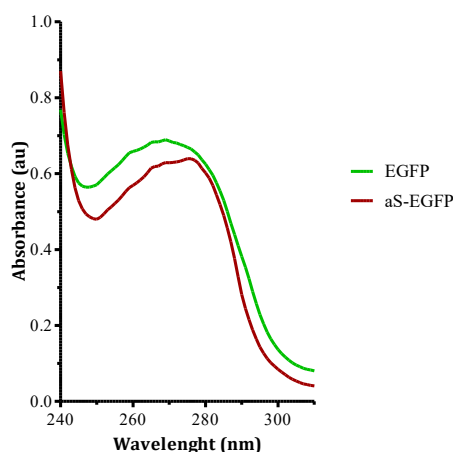
**Figure 36. UV-Vis spectra from 240 to 300 nm of recombinant aS-EGFP and EGFP.**

In order to operate within the relevant range of concentrations, before starting the study of the *in vitro* reaction between the recombinant proteins and DOPAL, the molarity of aS-EGFP and EGFP was estimated in transfected HEK293T cells. To this aim, EGFP expression level in transfected cells was assessed in relation to a calibration curve of recombinant aS-EGFP samples of known concentration in the range from 0.125 ng to 2 ng (**Figure 37a**). Once the standard curve of aS-EGFP was obtained (**Figure 37b**), the first part of the curve was fitted and the EGFP transfection levels were calculated: 55 ng of EGFP/µg of total proteins for HEK293T cells (**Figure 37c**). We also measured aS-EGFP transfection levels, confirming that was around 30 ng of aS-EGFP per µg of total proteins for HEK293T cells (compare **Figure 20c**). Considering the total volume of plated cells, these data provide the indication that aS-EGFP and EGFP are present in cells at about 1 µM concentration.

To maintain a similar concentration present in the cell model, the *in vitro* control reaction was conducted with 1 uM proteins and a EGFP or aS-EGFP: DOPAL ratio of 1:100, at 37°C overnight.

As reported in **Figure 38b**, DOPAL *per se* did not form any detectable high molecular weight aggregates. The presence of attached EGFP-tag did not prevent aS aggregation, as demonstrated by bands at 250 kDa and over. Interestingly, also EGFP aggregated. As mentioned before, DOPAL is a reactive aldehyde with no

particular specificity: the aldehyde moiety is highly reactive against amino groups such as lysine residues of proteins, through a Schiff base mechanism [97].
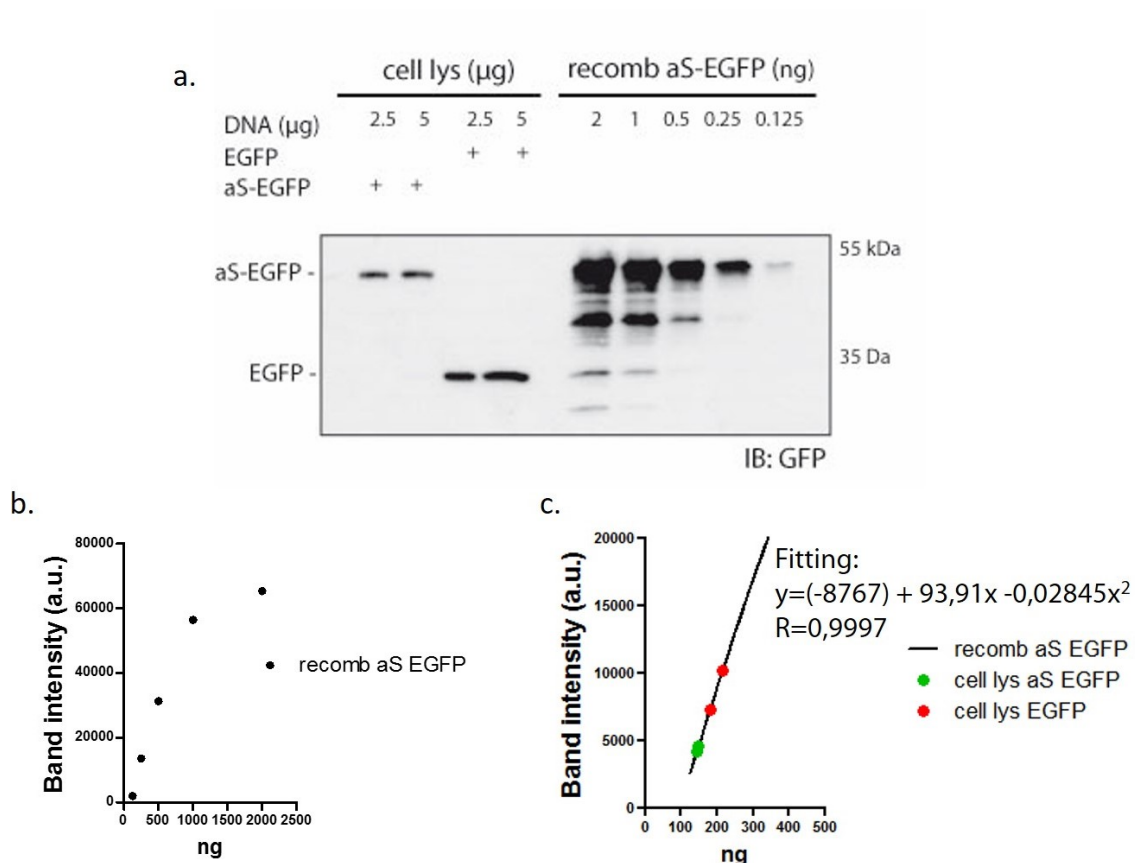


**Figure 37. Molarity calculation of EGFP and aS-EGFP expression in HEK293T cells.** HEK293T cells EGFP and aS-EGFP transfected with PEI. **a.** Western blot analysis using an anti-GFP antibody of different amount of total proteins (μg) of cell lysates from HEK293T compared with a calibration curve of recombinant aS-EGFP; **b.** Standard curve extracted from the densitometry analyses of Blot a; **c.** Extracted values of ng of EGFP and aS-EGFP per 2.5 and 5 μg of total proteins present in the lysates of HEK293T cells.

EGFP has 20 lysines almost all exposed to the solvent (**Figure 38a**) and, hence, it is easily modifiable by DOPAL.

In the light of these results, the subsequent experiments were carried out using as controls exosomes derived from HEK293T cells transfected with only EGFP in parallel with aS-EGFP containing exosomes.

In this way, it was possible to directly follow aS thanks to its fluorescent tag, but also discriminate potential EGFP's contribution.
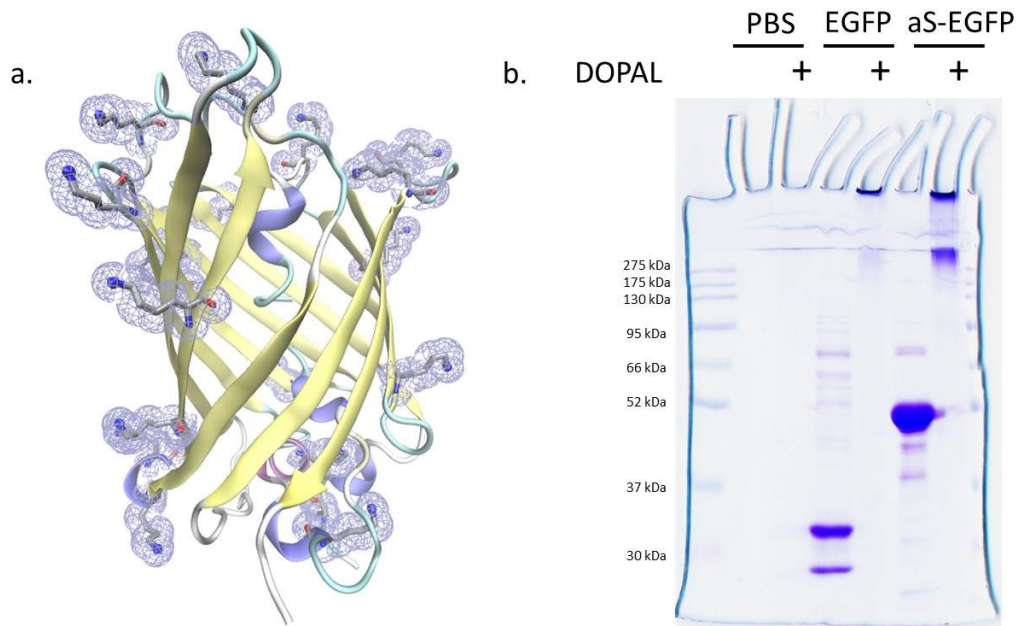
**Figure 38. DOPAL modifies also EGFP lysines. a.** PDB extracted structure of EGFP protein with depicted lysines residues, Reference: UniProtKB (P42212); **b.** Coumassie stained SDS-PAGE gel reporting, from left to right, molecular weight, buffer (PBS), PBS + DOPAL, recombinant EGFP, EGFP + DOPAL, aS-EGFP and aS-EGFP + DOPAL.

To better determine which are the DOPAL modified amino acids, mass spectrometry analysis is ongoing on cells -and exosomes-derived aS-EGFP and EGFP.

### 3.6 Quantification of exosomes cargo

The actual amount of purified exosomes depends on several variables, such as the quantity of cells seeded, transfection efficiency, DOPAL treatment and pellet resuspension leading to variable yields across preparations. As reported in **Figure 39a**, in fact, three different purifications led to different exosomes yields. The ratio between the analyzed cargos loaded into the exosomes and the housekeeping proteins (Hsp90) does not show statistically significant differences among the four conditions (**Figure 39b**), suggesting that in all cases exosomes were loaded with comparable amounts of aS-EGFP or EGFP even in the presence of DOPAL treatment.

Considering these results, prior to any further experiment in which exosomes are used as stimuli, it was decided to define a procedure to quantify exosomes in terms of diverse cargo amounts loading that correspond to the same number of

exosomes (in terms of Hsp90 amount, **Figure 39a**).
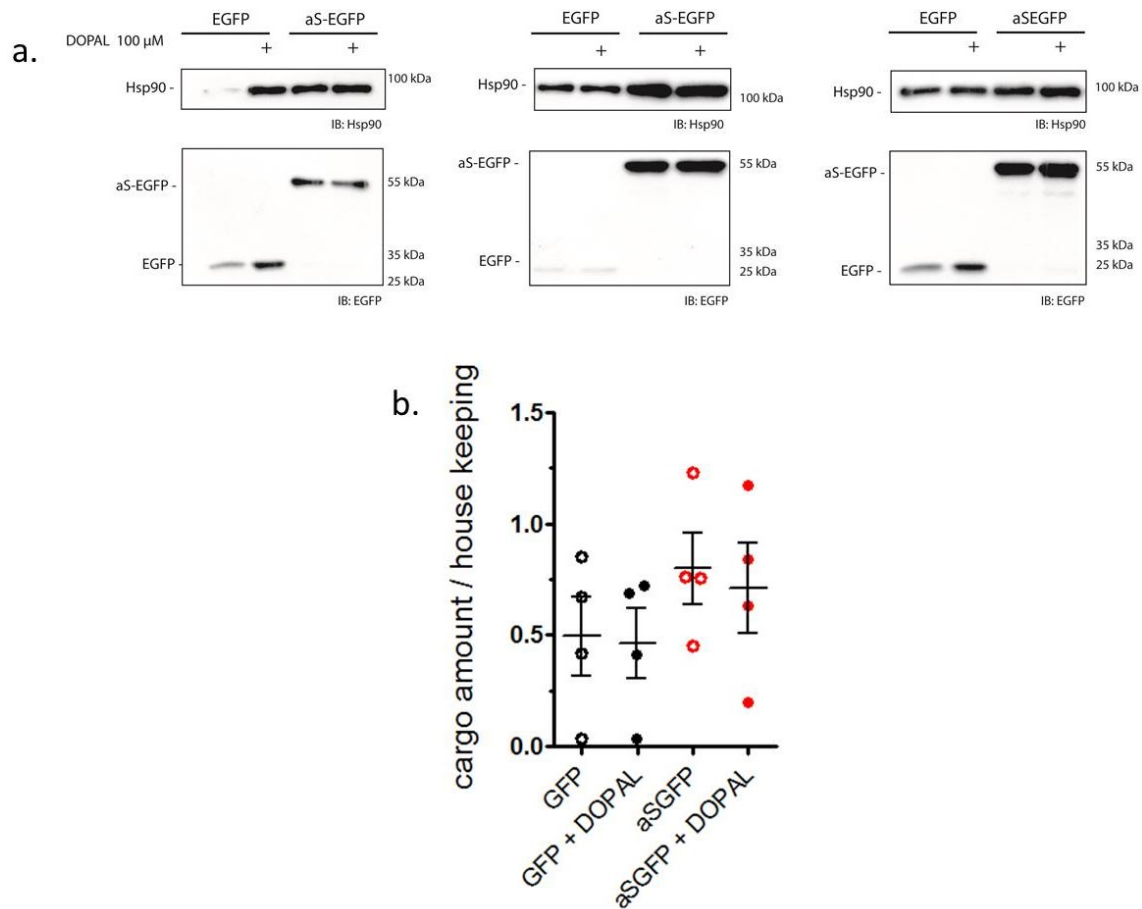


**Figure 39. Distinct exosomes purification leads to different exosomes amount. a.** Western Blot analysis of HEK293T cell derived exosomes containing EGFP and aS-EGFP, treated and non-treated with DOPAL (100 µM). Vesicle cargos were detected with an anti-GFP antibody, Hsp90 with an anti-Hsp90 antibody; **b.** Column graph of cargo amount (EGFP or aS-EGFP respectively) normalize on Hsp90. Data are expressed as mean ±SEM. No statistical significance was determined by one-way ANOVA with Tukey's test. Four independent experiments were assessed per condition.

To this aim, different exosomes purification was combined and the same volume of exosomes resuspension was loaded in a gel. An example is reported in **Figure 40a,** vesicles containing EGFP, DOPAL-modified EGFP, aS-EGFP and DOPAL-modified aS-EGFP were analyzed by Western Blot using an antibody against EGFP, and their quantification were evaluated by comparison with recombinant aS-EGFP samples of known concentration used to generate a calibration curve in the concentration range of 0.08 ng to 2.5 ng.
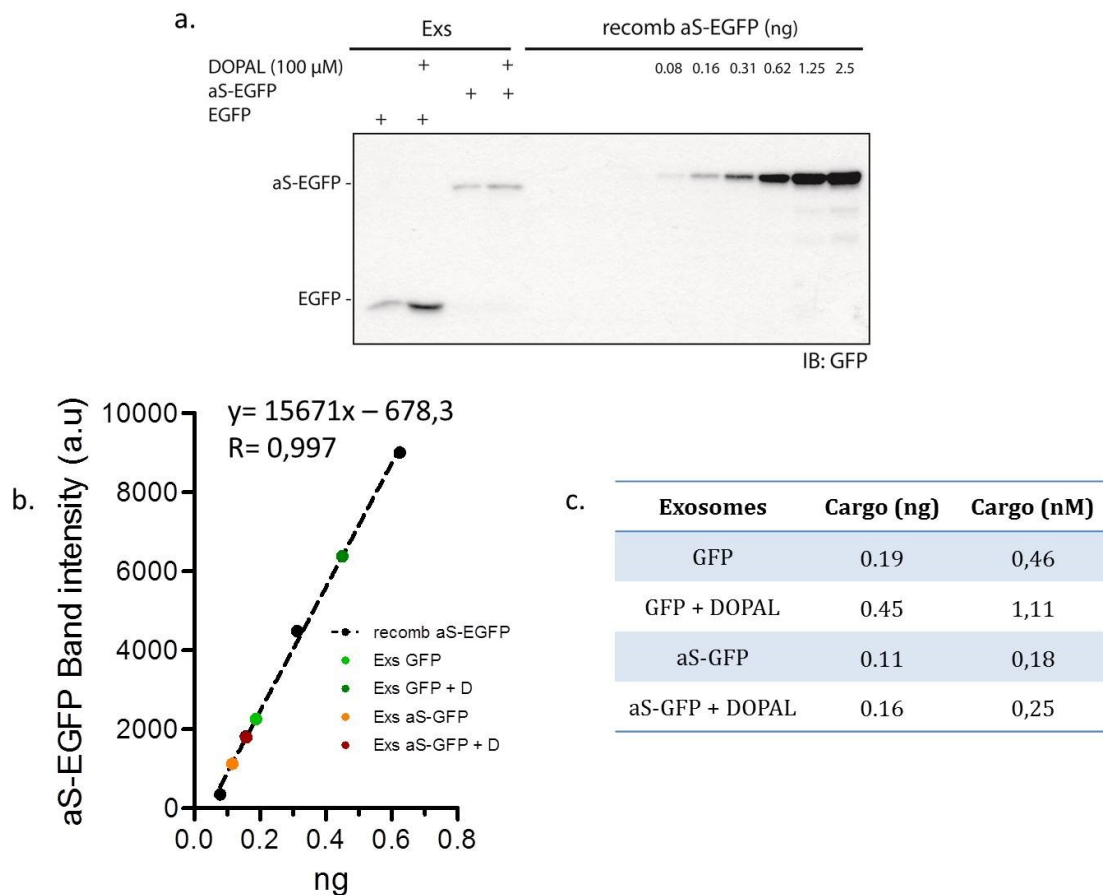
**Figure 40. Quantification of exosomes cargo. a.** Western Blot analysis of HEK293T cell derived exosomes containing EGFP and aS-EGFP, treated and non-treated with DOPAL (100 μM) compared with a calibration curve of recombinant aS-EGFP. Vesicle cargos and recombinant aS-EGFP were detected with an anti-GFP antibody; **b.** Standard curve extracted from the densitometry analyses of Blot a; **c.** Extracted values of ng and molarity (nM) of EGFP and aS-EGFP per 15 μl of purified exosomes suspension.

The relative amounts of proteins were determined by measuring band intensity. Once a standard curve was obtained (**Figure 40b**), the EGFP and aS-EGFP ng were established as reported in the table (**Figure 40c**). Then, the molarity of each sample was calculated in order to treat neurons and microglia with the same amounts of aS-EGFP and EGFP molecules.

## 3.7 Effects of aS containing exosomes on neurons

The pathophysiological role of aS containing exosomes on neurons remains essentially unknown [126,301], however, these vesicles have been proposed to be secreted in a spatially and temporally directed manner in neuronal synapses [346].

Under pathological condition, synapses appeared as the primary sites of aS aggregation and increasing evidence suggests the presence of these misfolded aS species inside exosomes [126]. Coherently, many synaptic boutons contain the sites of exosomes storage and formation (MVBs) in close contact with the presynaptic membrane [347,348] and exosomes secretion is modulated by synaptic activity in mature neurons [134,349,350].

On these bases, we investigated the hypothesis that exosomes are involved in both release of aS toxic species and their transmission among cells, probably through a trans-synaptic pathway.

To this aim, we planned to study the effect of both aS-EGFP and DOPAL-modified aS-EGFP loaded exosomes on synapses of primary cortical neurons.

As reported in **3.4 paragraph**, these exosomes carried oligomeric forms of the protein, that are strictly linked to cellular toxicity [107] and might mediate a role in α-synucleinopathies propagation.

### 3.7.1 aS containing exosomes alter synaptic proteins amount

Before treating neurons, purified exosomes were quantified by Western Blot analyses in terms of cargo amount, as reported in **paragraph 3.6**.

Then, primary cortical neurons were incubated 24 hours with the same amount of EGFP, DOPAL-modified EGFP, aS-EGFP and DOPAL-modified aS-EGFP containing exosomes.

To investigate our hypothesis of a synaptic effect upon exosomes treatment, we first choose to quantify synaptophisin. This protein, in fact, is commonly used as a synaptic marker [351], being one of most abundant pre-synaptic vesicles proteins [222]. Moreover, not only it plays a key role in the physiologic function of the sybII, a known binding partner of aS [222], but its levels have been correlated with synaptic function, memory and neuronal survival [352,353].

As reported in **Figure 41**, after 24 hours of incubation with DOPAL-modified aS-EGFP loaded exosomes, primary neurons displayed a reduced amount of synaptophysin in comparison with controls, as demonstrated by Western Blot

analysis of cell lysates. This result could be correlated with a decline in the number and quality of synapses in neuronal networks as occurs in dementia disease states [249,354,355].
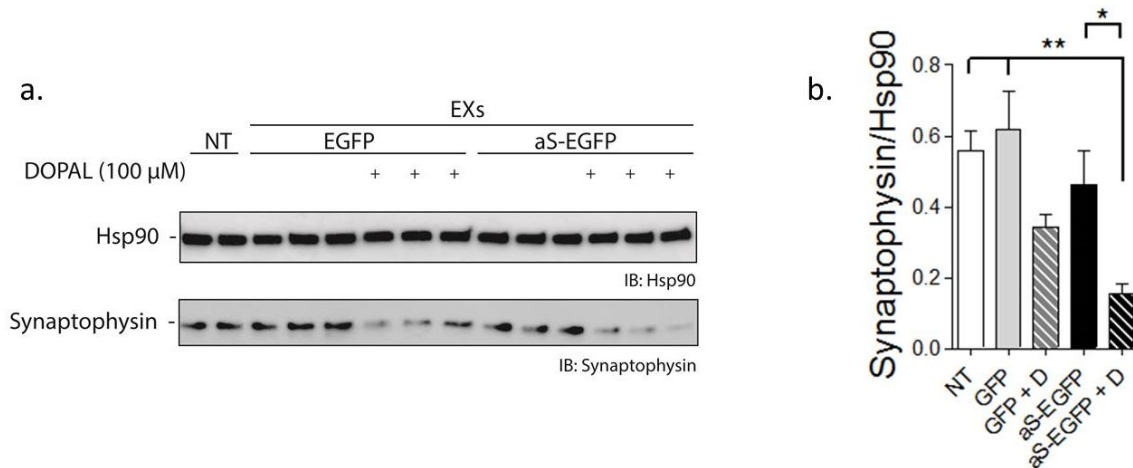


**Figure 41. Exosomes effect on synaptophysin amount.** Primary cortical neurons at DIV 14 were incubated with EGFP, DOPAL-modified EGFP, aS-EGFP and DOPAL-modified aS-EGFP containing exosomes. **a.** Western Blot analysis of non-treated (NT), and exosomes (Exs) treated neurons, antibodies against Hsp90, as loading control and synaptophysin were used; **b.** Column graph of synaptophysin band intensity normalize of Hsp90 in all conditions. Data are expressed as mean ±SEM. Statistical significance was determined by one-way ANOVA with Tukey's test * $p < 0.1$; ** $p < 0.001$. Three independent experiments were assessed for each condition.

However, an altered amount of synapses could also be associated with an impairment in the postsynaptic density (PSD) microdomains. The best studied marker of the post-synapses is PSD-95, a key multimeric scaffold for clustering receptors, ion channels, and signaling proteins in the PSD [356].

Hence, primary neurons at DIV 14 were incubated 24 hours with exosomes and immune fluorescence labeling of PSD-95 was performed. MAP2 positive neurons demonstrate punctate PSD-95 labeling co-localizing with dendritic spines (**Figure 42a**). However, cells incubated with aS containing exosomes displayed decreased dendritic PSD-95 immunoreactivity compared to control neurons (**Figure 42a-b**), suggesting reduced inputs between treated neurons [357]. Moreover, this effect was more significantly different upon incubation with DOPAL-modified aS-EGFP containing exosomes in comparison with controls, i.e. non-treated neurons and EGFP, DOPAL-modified EGFP containing exosomes treated neurons.

The measured PSD-95 reduction upon aS containing exosomes incubation is coherent with synaptophysin alteration and suggests that the treated neurons exhibited an altered level of synaptic proteins compared to non-treated cells. Coherently, reductions in PSD-95 have been observed in Alzheimer Disease (AD) [358], although not consistently [359], and associated to learning and memory deficits in mice [360]. Moreover, a study by Francis and co-workers demonstrate that DLB and PD post mortem brains were characterized by significant reductions of PSD-95 in prefrontal cortex compared with controls and AD [361].
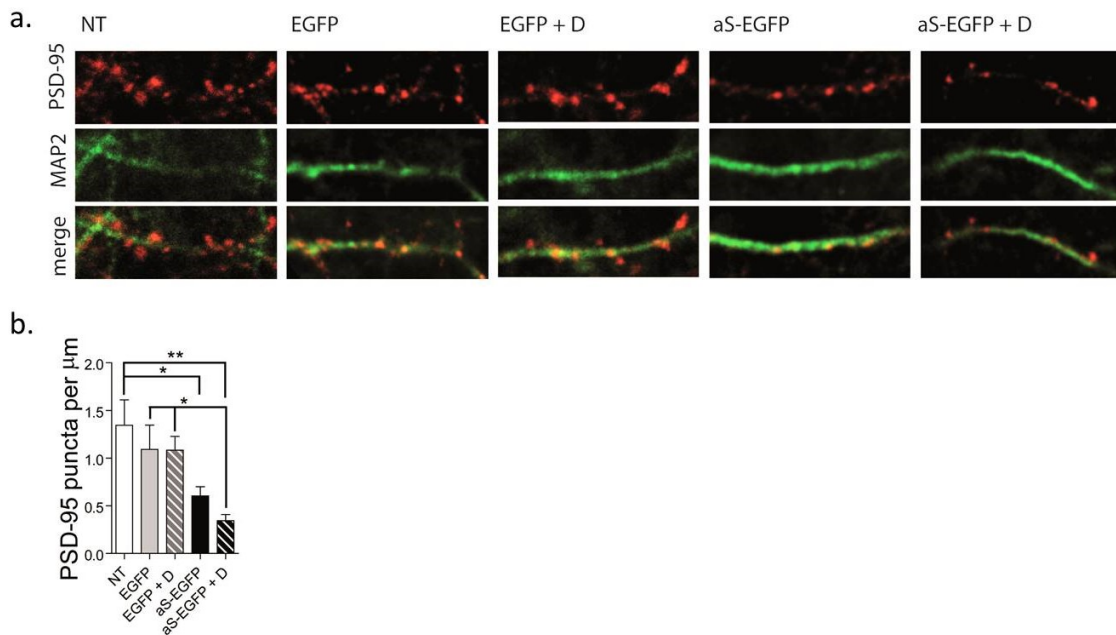


**Figure 42. aS containing exosomes reduced the amount of PSD-95.** Primary cortical neurons at DIV 14 were incubated with EGFP, DOPAL-modified EGFP (EGFP + D), aS-EGFP and DOPAL-modified aS-EGFP (aS-EGFP + D) containing exosomes for 24 hrs. **a.** Confocal images of non-treated (NT), and exosomes (EGFP, EGFP + D, aS-EGFP and aS-EGFP + D) treated neurons. Antibodies against the neuronal marker MAP2 (green) and PSD-95 (red) were used. Images were acquired using a Leica confocal microscopy (Leica TCS SP5) with a 63x objective. Scale bar 4 µM; **b.** Column graph of the number of PSD-95 puncta per µm of neurites. Data are expressed as mean ±SEM. Statistical significance was determined by unpaired t test (*p<0.001, **p<0.01 ). Three independent experiment were assessed per condition.

In conclusion, these results suggest that aS containing exosomes alter the normal amount of the synaptic proteins, i.e. synaptophysin and PSD-95. The effect was more evident in the presence of aS DOPAL-modified containing exosomes, likely due to the increased amount and different natures of their aS aggregated species. DOPAL aS oligomers have been, in fact, proposed to interact with lipid bilayer of

the cell membranes, leading to membrane disruption or pore formation [104,107]. This hypothesis is consistent with the fact that DOPAL aS oligomers localized at membranes and they can alter exosomes content, as previously assessed by AFM and atomic absorption experiments (**paragraph 3.4.3**.).

Another hypothesis is that DOPAL-modified aS contained in exosomes might seed the aggregation of neuronal endogenous aS (as reported in **Figure 53**) causing the alteration of its physiological function [50,52] and a redistribution of the synaptic proteins [249].

## 3.7.2 aS containing exosomes impact synaptic vesicle pools

A reduced amount of the synaptic proteins synaptophysin and PSD-95, however, could also be correlated with an altered synaptic function [362].
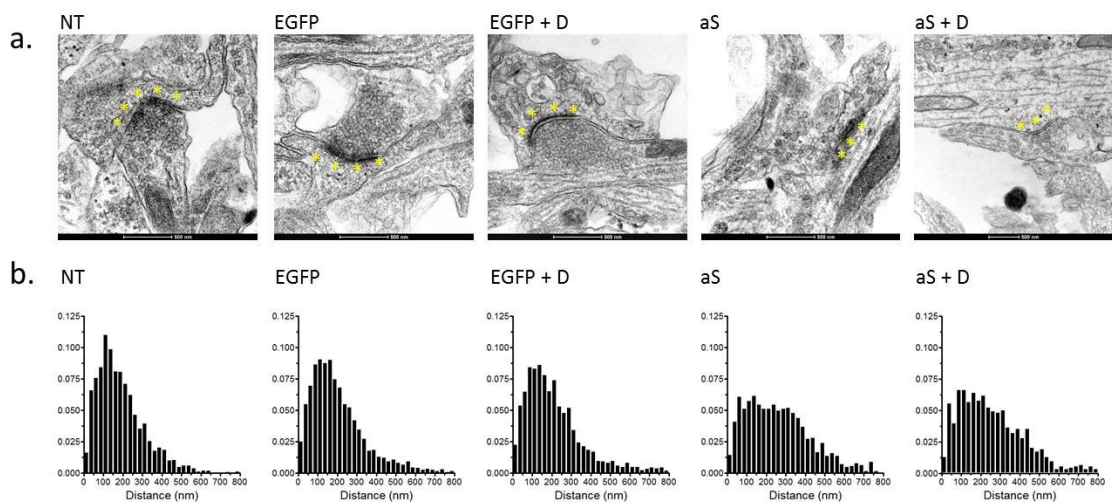


**Figure 43. aS containing exosomes alter synaptic vesicles pools in primary neurons. a.** TEM images of mice primary neurons synapses not treated (NT) and treated with EGFP, DOPAL-modified EGFP (EGFP + D), aS-EGFP, DOPAL-modified aS-EGFP (aS-EGFP + D) containing exosomes for 24 hours. Asterisks indicate the active zone. Scale bar 500 nm; **b.** Frequency distribution of vesicles distance from the active zone of primary neurons in NT and treated neurons (from left to right); n=20-25 synapses from at least three independent experiments were analyzed.

A clear readout for synaptic impairment is however, synaptic structure, since its alteration has profound effects on function [363]. This is substantiated by the fact that many neurological and psychiatric illnesses are associated with alterations in synapse structure. The presynaptic terminal has a complex architecture, with synaptic vesicles located at different distances from the active zone and

functionally organized in three main pools: reserve, recycling, and readily releasable pool [363]. Therefore, to evaluate synaptic structure, we measured the relative distributions of the distances between vesicles pools and the active zone of the synapses [364]. To this aim, primary neurons at DIV 14 were treated 24 hours with exosomes and synapses were imaged by TEM (**Figure 43a**). As it emerges from the relative distributions of the distances between vesicles and the active zone, aS-EGFP and DOPAL-modified aS-EGFP containing exosomes lead to an alteration of the synaptic vesicles pools (**Figure 43b**).

Upon aS-EGFP and DOPAL-modified aS-EGFP containing exosomes incubation, synaptic vesicles were not only more distant from the active zone, but also reduced in number, as depicted in **Figure 44.**
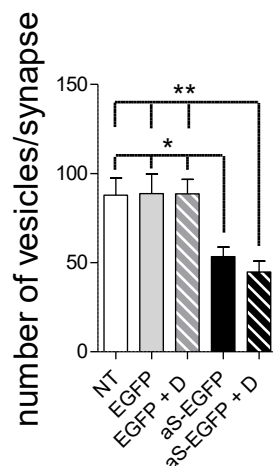


**Figure 44. aS containing exosomes affect vesicle number.** Column graph of the number of vesicles/synapse show a significant reduction after aS-EGFP and DOPAL-modified containing exosomes (aS-EGFP + D) treatment. Bars represent mean ±SEM from n=20-25 synapses from at least three independent experiments. Asterisks indicate statistical significance by two-way ANOVA (**p< 0.01, *p< 0.1).

This result correlate only in part with a reduced amount of the presynaptic vesicles marker synaptophysin, which was significantly different in comparison with controls only for DOPAL-modified aS containing exosomes (**Figure 41**). This apparent incongruence can be explained by the increased sensitivity of TEM analysis in comparison with Western Blot. On these basis, we proposed to increase the biological replications for the synaptophysin amount quantification, in order to likely underline a toxic effect ascribable also to aS containing exosomes.
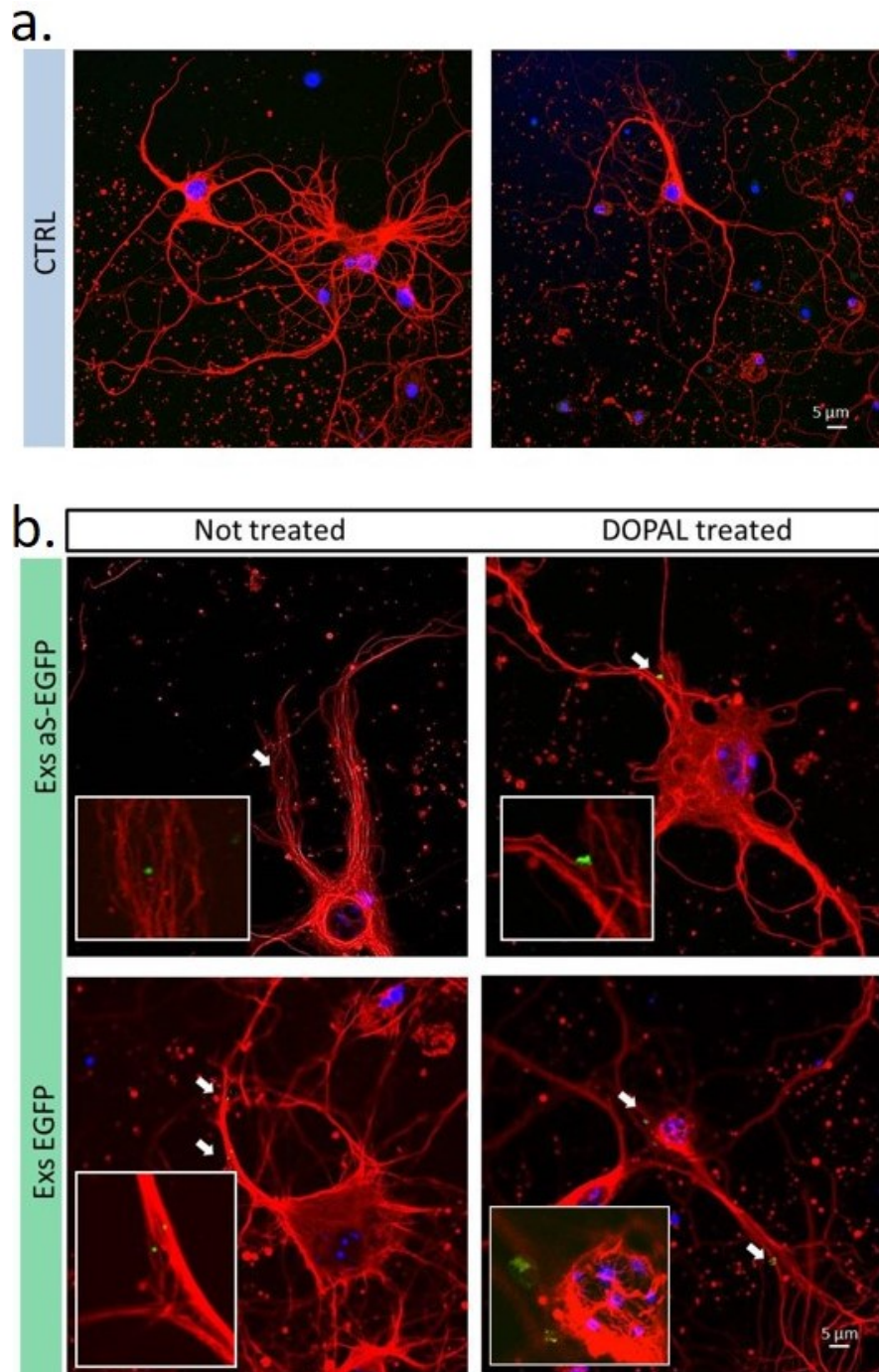
**Figure 45. Primary cortical neurons interact with exosomes.** Primary cortical neurons (DIV 14) were labeled with β-tubulin III (red), a neuronal marker; GFP antibody (green) and DAPI (blue). **a.** Confocal images of non treated neurons; **b.** confocal images of neurons incubated with EGFP containing exosomes (upper left panel); DOPAL modified EGFP containing exosomes (upper right panel), aS-EGFP containing exosomes (bottom left panel); DOPAL modified aS-EGFP containing exosomes (bottom right panel). White arrows indicated EGFP positive signals and in the bottom left of each image ROI are zoomed. Images were acquired using a Leica confocal microscopy (Leica TCS SP5) with a 40x objective. Scale bar 5 μM.

However, these results suggest that aS and DOPAL-modified aS containing exosomes exert a toxic effect at the synaptic level.

Therefore, we next investigate if these damages were effectively mediated by exosomes internalization.

To this aim, treated neurons, identified by the specific β-tubulin III protein (red, **Figure 45**), were washed, fixed and imaged by means of a confocal microscope. As reported in **Figure 45b** exosomal cargo associated fluorescence (green EGFP) is close to β-tubulin III, with no apparent differences among the diverse type of stimuli used.

This result suggests internalization, but was not sufficient to clearly assess it. Therefore, we are planning to correlate Cryo-electron microscopy (cryo-EM), to take advantage of the high-resolution technique and observe synapsis, and fluorescence microscopy, to detect specifically aS-EGFP. In this way, we would be able not only to detect exosomal cargos internalization, but also whether it occurs preferentially at synaptic sites.

## 3.7.3 aS containing exosomes alter neuronal morphology

Reduced synaptic proteins amount and functional impairment can also impact neurite length and neuronal morphology, as reported in primary neurons by induced-aS toxicity [353].

To verify if aS containing exosomes can exert a similar effect, we quantified the complexity of dendritic arbors by Sholl analysis [365,366], a widely used method in neurobiology [367].

In the basic procedure, the number of intersections of neuritic processes with circles of increasing radii centered in the cell soma are counted.

As reported in **Figure 46**, the chosen descriptors were (1) <u>enclosing radius</u> express in μm, which reflects the Feret length of the arbor, (2) <u>centroid radius</u> express in μm, which is the abscissa of the centroid (i.e., the geometric center or barycenter) of the linear profile, (3) <u>sum of intersection</u> express as power of ten, which is represents the degree of ramification of a neurite tree.

In comparison with the control, exosomes *per se* did not alter neuron arbors, as

demonstrated by non-significant differences between non-treated and EGFP containing exosomes treated neurons. Moreover, also DOPAL treatment does not cause any significant effect (negative control DOPAL-modified EGFP containing exosomes).
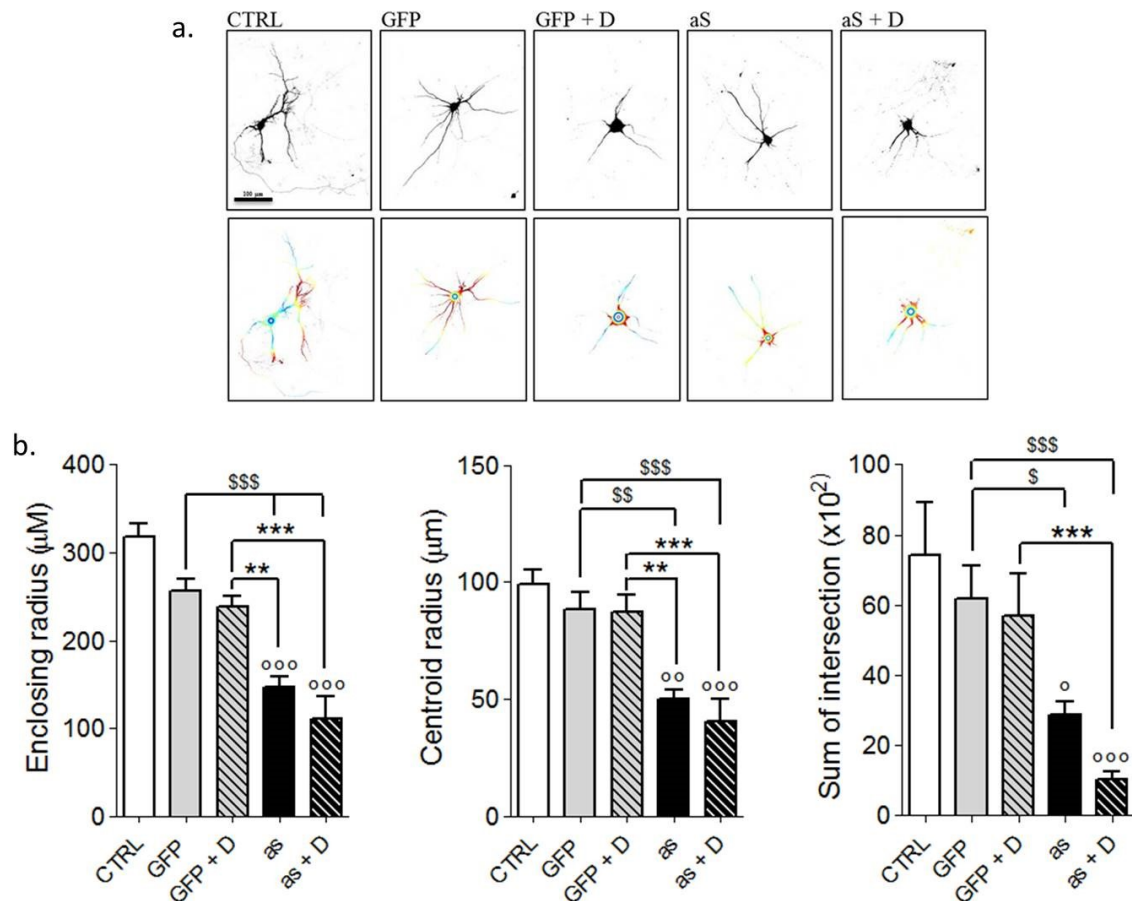


**Figure 46. Sholl analysis of exosomes treated primary cortical neurons.** GFP expressing neurons at DIV 14 were incubated 24 hours with the same amount, in terms of cargo, with exosomes containing GFP; DOPAL-modified EGFP, aS-GFP and DOPAL-modified aS-EGFP. **a.** Fluorescence images representative of the analyzed neurons for each condition (upper panel) and corresponded segmented images showing what will be sampled by Sholl Analysis (bottom panel). Images are taken with a Leica microscope 5000B with a 40x objective. Scale bar is 100 μm; **b.** Column graphs of, from left to right, Enclosing radius, Centroid radius and Sum of intersections. Data are expressed as mean ±SEM. Statistical significance was determined by one-way ANOVA with Tukey's test (* stands for significance to control, $ stands for significance to GFP containing exosomes and ° stands for significance to DOPAL modified GFP containing exosomes) *,$,° $p < 0.1$; **, $$, °° $p < 0.001$; ***,$$$,°°° $p < 0.0001$. Three independent experiments were assessed per condition. CTRL=control; GFP= upon GFP containing exosomes incubation; GFP+D= upon DOPAL-modified EGFP containing exosomes incubation; aS=upon aS-EGFP containing exosomes incubation and aS+D = upon DOPAL-modified aS-EGFP containing exosomes incubation.

Interestingly, neurons morphology was altered not only by DOPAL-modified aS, as

synaptophysin amount, but also by aS containing exosomes *per se*, confirming the reduced PSD-95 and impaired synaptic structure reported above and suggesting a possible role of aS aggregated species in inducing neuronal alteration.

It is important to mention that a significant toxicity of DOPAL oligomers was confirmed also in this experiment, as assessed by a significant reduction in terms of <u>centroid radius</u> and <u>sum of intersections</u> in comparison with control (**Figure 46b**).

In conclusion, aS containing exosomes seem to exert a specific toxic role at neuronal synapses, as demonstrated by reduction of synaptic proteins levels, alteration of the synaptic structure and neurites retraction.

### 3.7.4 Exosomes effect on neuronal viability

aS cannot only affects synaptic function and neuronal morphology, but also cell viability, as report by many groups [142,254,353]. For instance, conditioned media of aS expressing cells impact neuronal survival, inducing drastic morphological changes, characteristic of cellular degeneration such as process retraction and membrane blebbing [127].

Hence, we decided to investigate whether the same effect can be achieved if aS is vehiculated in exosomes [127,368].

Cell death has historically been classified according to morphological characteristics as either necrotic or apoptotic [369]. Apoptosis is a programmed cell death generally characterized by distinct morphological characteristics and energy-dependent biochemical mechanisms. The alternative to apoptotic cell death is necrosis, which is considered to be a toxicity process in which the cell is a passive victim and follows an energy-independent path to death.

As in the work by Emmanoulidou and coworkers [127], we analyzed the activation of caspase 3, which is a key enzyme in apoptosis activation and progression. In vertebrate cells, apoptosis typically proceeds through one of two signaling cascades termed the intrinsic and extrinsic pathways. Both of them converge on activating caspase 3 [370], which exists as an inactive proenzyme (ProCaspase 3 in **Figure 47a-c**). The proteolytic processing, leads to the assembly of the active

heterotetrameric enzyme (Caspase 3 in **Figure 47a, c**) [371]. The decreasing quantity of the pro enzyme and the increasing quantity of the active form relative to the inactive, are normally considered markers for apoptotic activation [370].

As reported in **Figure 47**, primary cortical neurons at DIV14 were incubated for 24 hours with EGFP, DOPAL-modified EGFP, aS-EGFP and DOPAL-modified aS-EGFP containing exosomes.
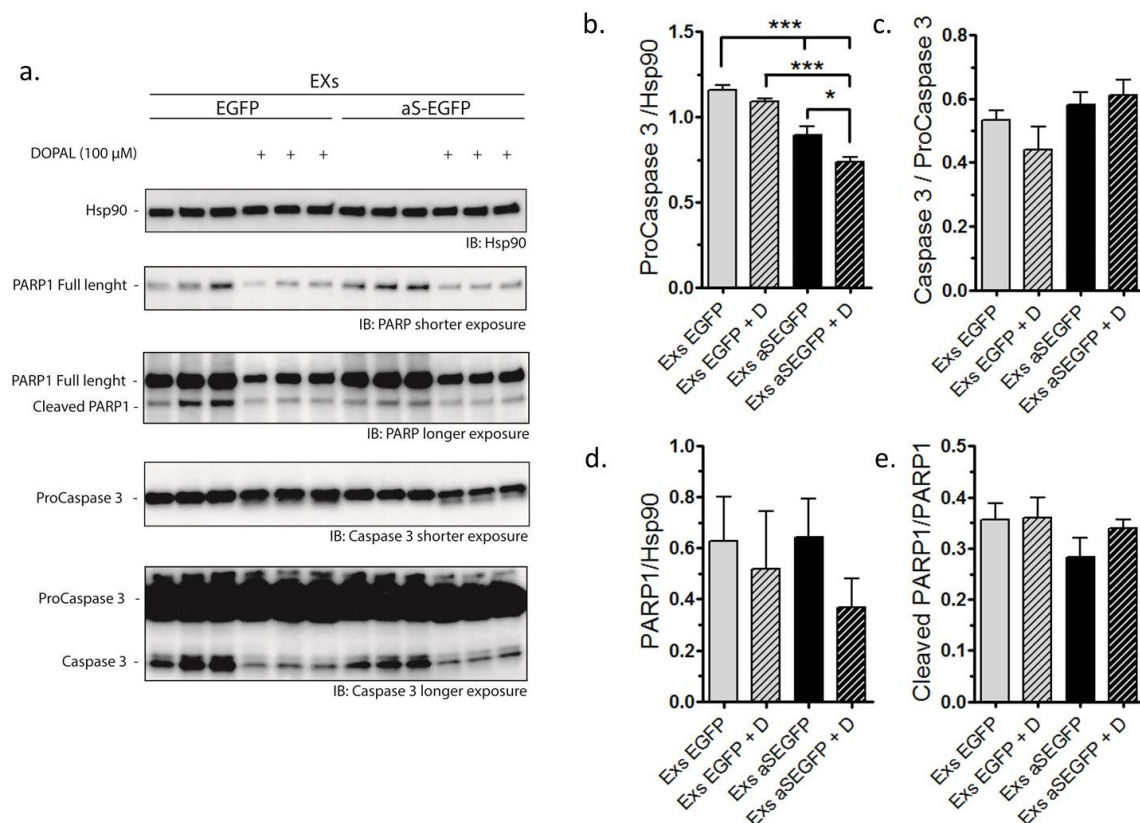


**Figure 47. Exosomes effect on neuronal activation of caspase 3 and PARP1.** Primary cortical neurons at DIV 14 were incubated with EGFP, DOPAL-modified EGFP, aS-EGFP and DOPAL-modified aS-EGFP containing exosomes for 24 hours. **a.** Western Blot analysis of exosomes (Exs) treated neurons was performed utilizing antibodies against Hsp90, as loading control PARP1 and caspase 3; **b-e** Column graph represents the amount of **b.** ProCaspase 3 normalize on Hsp90 as loading control; **c.** Caspase 3 on ProCaspase 3; **d.** PARP1 on Hsp90 as loading control and **e.** Cleaved PARP1 on PARP1.Data are expressed as mean ±SEM. Statistical significance was determined by one-way ANOVA with Tukey's test * $p < 0.1$; *** $p < 0.0001$. Three independent experiments were assessed for each condition.

Cell lysates were then analyzed by Western Blot using antibodies against Caspase 3. Hsp90 was used as loading control. Interestingly, aS-EGFP containing exosomes in comparison with control, i.e. the EGFP containing exosomes, presented a

significant decrease of ProCaspase 3 band intensity and partial increase in the amount of cleaved Caspase 3, suggesting an activation of the apoptotic cascade. Moreover, this effect seems to be more pronounced when aS-EGFP is DOPAL-modified.This hypothesis is not confirmed by Poly (ADP-ribose) polymerase-1 (PARP1) profile (**Figure 47**). PARP1 is a nuclear protein, which, under basal conditions, detects and repairs DNA damages. However, cleavage of PARP-1 by caspases 3 results in the formation of 2 specific fragments. The first is a catalytic fragment, which has reduced DNA binding capacity and is released from the nucleus into the cytosol (which corresponds to the band at 89 kDa named Cleaved PARP1 in **Figure 47a,e**) [372].

The second fragment is 24 kDa (not recognized by the anti-PARP1 used antibody), which is retained within the nucleus, where it irreversibly binds to nicked DNA and acts as a trans-dominant inhibitor of active PARP-1. Irreversible binding of the 24-kD PARP-1 fragment to DNA strand breaks inhibits DNA repair enzymes and compromises DNA [373]. If unchecked, this activity inevitably leads to passive necrotic cell death [374]. Rapid cleavage and inactivation of PARP-1 is achieved by the action of caspases (among all also caspase 3) [375]. However, insults which initiate necrosis cause PARP-1 overactivation that proceeds unchecked due to inadequate caspase activation [375], lower PARP-1 cleavage and less PARP-1 24-kD fragment formation. Exogenous administration of 24-kD PARP-1 fragments might attenuate PARP-1 overactivation and divert necrosis towards apoptotic cell death. Hence, a decrease of the 89 kDa fragment leads to ATP-depletion and subsequently to necrosis, instead an increase of the 89 kDa fragment is due to the inactivation of PARP-1 by caspase-3 cleavage, which is one of the key events of apoptosis.

If, as hypothesized, aS containing exosomes induce apoptosis and activate caspase 3, we should observe an increase intensity of the band corresponding to the PARP1 89 kDa fragment. As reported in **Figure 47**, no differences were registered in neuronal PARP1 upon aS containing exosomes incubation, either in terms of an overactivation (increase PARP1), considered a necrotic marker, or in terms of an inactivation (increase 89 kDa) as expected in apoptosis.

These results exclude that aS-EGFP containing exosomes induce necrosis but rather suggest some apoptotic features in the process, that might exacerbate with

increasing incubation time of the neurons with exosomes [376]. It is important also to mention that PARP1, caspase 3 and Hsp90 are not neuronal specific proteins. Therefore, by Western Blot analysis we are measuring their content not only in neurons, but also in the glial cells, that are normally present as contaminants in primary neuronal culture, likely hindering a specific neurotoxicity effect of aS containing exosomes.

In conclusion, these results suggest that after interaction with neuronal cells, aS-containing exosomes alter synaptic proteins as assessed by the reduced level of synaptophysin and PSD-95. The altered synaptic structure and neuronal morphology, measured by Scholl Analysis proposed also an impaired synaptic plasticity and function. These effects appeared to be mediated by the oligomeric species of aS inside exosomes. It is in fact hypothesized that oligomeric aS induces endogenous aS aggregation, compromising its capacity to be part of SNARE-complex assembly [221]. They are also reported to interact with lipid bilayers of cell membranes, leading to membrane disruption or even pore formation [107]. All mentioned hypothesized mechanisms are based on a toxic gain-of-function of the oligomeric species involved in the aggregation pathway. It is likely that the cytotoxicity does not arise from a single mechanism but that several of the proposed mechanisms are involved in the aS propagation mediated by exosomes in α-synucleinopathies. However, these data suggest a trans-synaptic exosomal transfer of aS from cell-to-cell as a key mechanism in the spread of aS aggregates between neurons in the brain and point out synapses as an early site of aS gaining of toxic function.

### 3.8 Effects of aS containing exosomes on microglia activation

To prevent aS damages to neurons, astrocytes and primary microglia remove extracellular aS through endocytosis [377,196]. However, aS exposure could induce in these cells the secretion of toxic substances, including reactive oxygen and pro-inflammatory cytokines (like TNF-α and IL-1β) that impact neuronal survival [295,378,379].

To investigate this hypothesis, we studied aS containing exosomes effect on

microglia cells following the release of IL-1β.

Considering that DOPAL is also transmissible to glial cells, where it enhances intracellular oligomerization of aS [319], we incubated microglia cells also with DOPAL-modified aS containing exosomes.

Microglia activation mechanism by exosomes is largely still unknown, but some works suggest that is mediated by exosomes macropinocytosis or phagocytosis [181,184]. Hence, we decided to first investigate whether aS-EGFP and DOPAL-modified aS-EGFP containing exosomes were internalized by microglia cells. To this aim, the BV2 cell line was chosen as experimental model for a set of scouting experiments: they derive from v-raf/myc-immortalised murine neonatal microglia and are the most frequently used substitute for primary microglia. It has to be mentioned that the proliferation capacity of primary microglia is limited and so they have to be isolated freshly for each experiment. For a typical preparation of rodent microglia, 15-30 brains are required to yield cells for a limited amount of experiments.
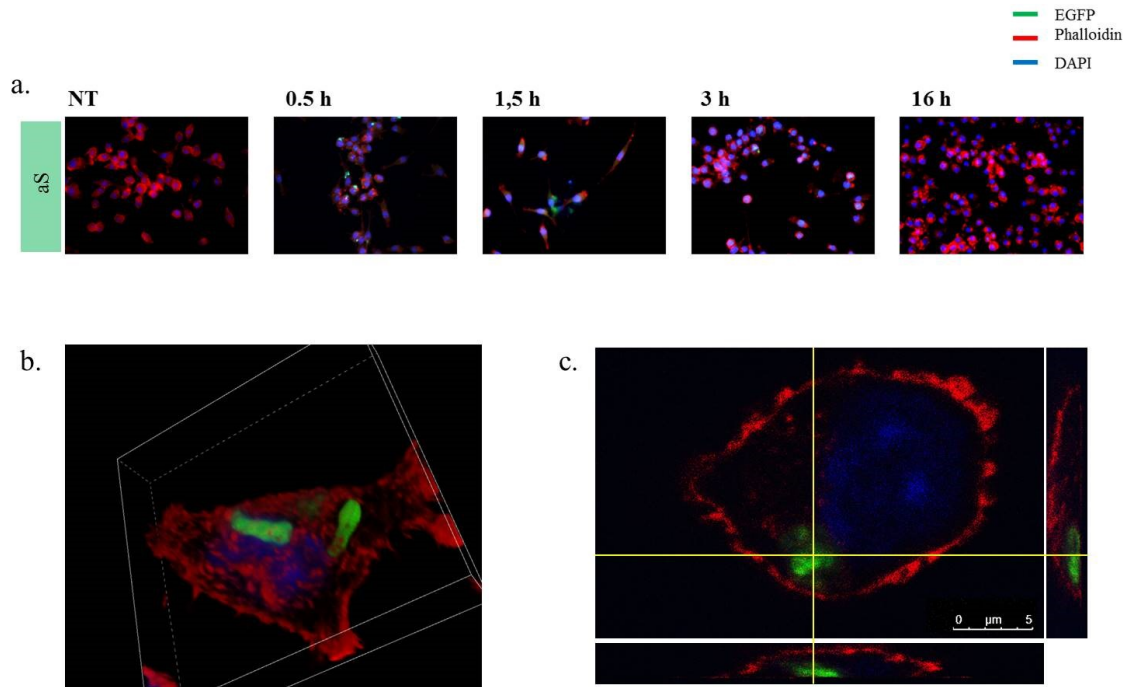


**Figure 48. BV2 cells internalized exosomes.** BV2 cells were labeled with antibodies against Phalloidin (red), GFP (green) and DAPI (blue). **a.** Fluorescence images of BV2 cells incubated with aS-EGFP containing exosomes for 0.5; 1.5, 3 and 16 hours. Images were acquired with a Leica microscope 5000B, using a 40x objective. Scale bar 25 μm; **b.** 3D image and **c.** Z-projection of Z-stack images of BV2 cells incubated with DOPAL-modified aS-EGFP containing exosomes for 0.5

hours. Images were acquired with a Leica confocal microscope (TCS sp5), using a 63x objective. Scale bar 5 μm.

Thus, we have chosen for the first experiments immortalized cell line in order to minimize the number animals, time and valuable consumables. As reported in **Figure 48**, BV2 cells were incubated with exosomes containing DOPAL-modified aS-EGFP and aS-EGFP, monitoring the process under fluorescence microscope. Thanks to the EGFP tag exosomes derived aS was easily discriminated from endogenous aS [380] and it was identified inside microglia cells already after 30 minutes of incubation. Sixteen hours later no more aS-EGFP associated fluorescence was detected, suggesting that probably it has been degraded [196,377].

Once proved the internalization of exosomes (or at least their content), we investigated whether aS containing exosomes can activate microglia cells, monitoring the secretion of interleukin-1beta (IL-1β). As previously described in fact, activated microglia is characterized by an increased production of key pro-inflammatory cytokines like IL-1β, which modulates neurodegeneration and likely disease progression [381]. Increased levels of IL-1β have been detected in *post mortem* tissue of cases of PD, DLB, and MSA[382,383].
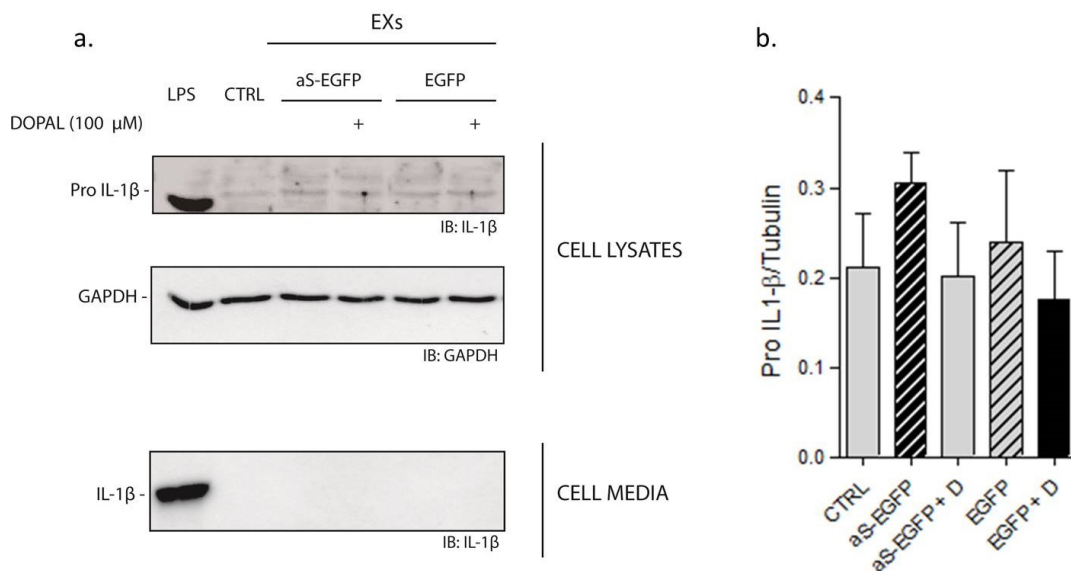


**Figure 49. aS containing exosomes did not activate BV2 cells.** BV2 cells were incubated 24 hours with EGFP, DOPAL-modified EGFP, aS-EGFP and DOPAL-modified aS-EGFP containing exosomes. LPS was used as positive control. **a.** Western Blot analysis of cell lysates and cell culture media were both tested with anti-IL-1β antibody. In cell lysates GAPDH was used as loading control; **b.** Column graphs reported the analyzed band intensity quantification. No statistical

significance was determined by one-way ANOVA with Tukey's test. Three independent experiments were assessed for each condition.

As for neurons, firstly exosomes were quantified in terms of cargo amount (**paragraph 3.6**) in order to treat microglia with the same amount of exosomal EGFP and aS-EGFP molecules.

Then, BV2 cells were treated for 24 hours with HEK293T purified exosomes containing DOPAL-modified aS-EGFP, aS-EGFP and the respective controls, i.e DOPAL-modified-EGFP and EGFP (**Figure 49**).

As readout for BV2 activation, we followed the level of Pro IL-1β expression in cell lysate and the secretion of the active form IL-1β in cell medium. The result of this experiment is reported in **Figure 49** and it is evident that, under these conditions, exosomes did not activate BV2 cells: with no increase in either Pro IL-1β or active IL-1β. LPS control confirmed that BV2 cells were active, as demonstrated by intense bands corresponding to the pro and active form of IL-1β (**Figure 49a**).

In considering the result of the experiment described above, we reconsider our choice of the BV2 cell line. It is important to mention that BV2 cells contain oncogenes that render them in some ways different from primary microglia, such as increased proliferation, adhesion and variance of morphologies [384]. Therefore, the validity of BV2 cells as substitute for primary microglia has been a subject of debate and a few studies comparing different microglia lines has emerged. The major idea that BV2 immortalized cells have similar functions as primary microglia, but not to the same extent, clearly emerged in the work by Henn et al.[385]. This group examined the BV2 cells as an appropriate alternative to the primary cultures. They found that in response to LPS stimulus 90% of genes induced by the BV2 cells were also induced by primary microglia; however, the up-regulation of genes in the BV2 was far less pronounced than in primary microglia [385].

For all these reasons, we decide to do the experiment in the same condition, but now on primary microglia. Hence, cells were treated 24 hours with the stimuli and active IL-1β in the cells supernatant was increased upon aS-EGFP containing exosomes treatment in comparison with the controls as reported in **Figure 50**. In the cell lysates, no differences were detected both in term of Pro IL-1β or active IL-

1β. This is probably due to the fact that after 24 hours the Pro IL-1β in the cells is all cleaved and secreted, leading to a detection in the supernatant, but not in the cell lysates.

In the medium, EGFP and DOPAL-modified EGFP containing exosomes lead to the release of IL-1β, even if at a lower level relative to aS-EGFP containing exosomes. This evidence can be explained with the fact that exosomes maintain some characteristic of the origin cell, i.e HEK293T cells, which are of different origin (human) than microglia (mouse), inducing an immune response [386].
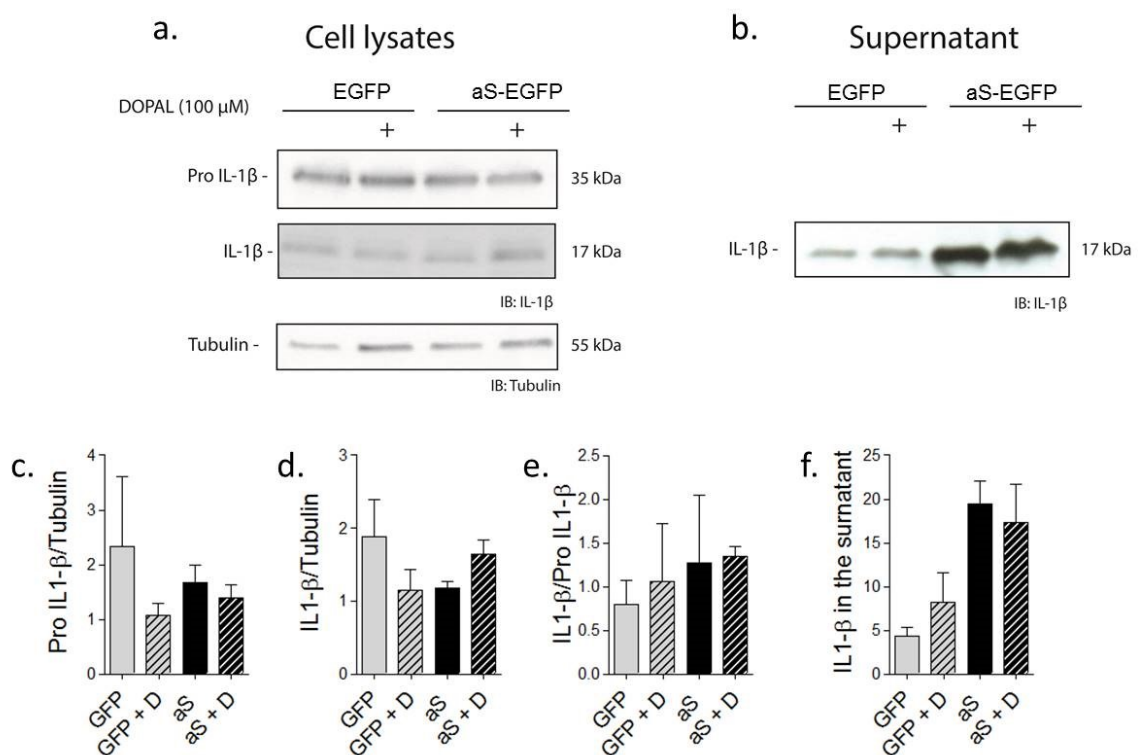


Figure 50. aS containing exosomes activate primary microglia cells. Primary microglia cells were incubated 24 hours with EGFP, DOPAL-modified EGFP, aS-EGFP and DOPAL-modified aS-EGFP containing exosomes. a-b Western Blot analysis of cell lysates (a.) and supernatants (b.)were tested with anti-IL-1β antibody. In cell lysates tubulin was used as loading control; c-f Column graphs reported the analyzed band intensity quantification of c. Pro IL-1β on Tubulin as loading control; d. IL-1β on Tubulin as loading control; e. IL-1β on Pro IL-1β and f. IL-1β in the cell media. **Only** two independent experiments were assessed for each condition, not suffiecient to make a statistical analysis.

Moreover, another reason can be LPS contamination in purified exosomes. To exclude this possibility, we plan to estimate the endotoxin levels of our exosome preparations, by limulous amoebocyte lysate test (LAL test) [387]. However, it is also

important to mention that these controls are more relevant when recombinant proteins are used as stimulus, since the latter are normally produced in gram negative bacteria, i.e. *E. Coli* [388].

In this case exosomes are cell-derived and purified under sterile conditions, suggesting that they do not contain LPS or, at least, not as abundant as the quantity needed to induce the secretion of IL-1β. In contrast to neurons, that appeared more sensible to oligomeric aS as demonstrated by a more pronounced effect on synaptic function upon DOPAL-modified aS containing vesicles; primary microglia activation is not influenced by DOPAL treatment, but rather by the presence of aS. Microglia, play a crucial role as specialized macrophages in safeguarding CNS against infections and injury. As resident phagocytes in the brain, microglia serve to clear cellular debris[389], suggesting a less sensitivity against dangerous molecule in comparison with neurons. Moreover, it is also possible that IL-1β production reached a *plateau*, not permitting to register more differences.

Lastly, it is also important to mention that we are planning to investigate whether exosomal cargos are phagocytosed by primary microglia, in order to determine if this process is essential to IL1β release

In conclusion, we demonstrated that primary microglia cells are activated by aS containing exosomes, causing the release of a pro-inflammatory factor such as IL-1β [390], as reported by others [197].

These data point out a role (to our knowledge, for the first time) for exosomes containing DOPAL-modified aS and aS-DOPAL oligomers in microglia activation, suggesting their contribution in neuroinflammation and in the progression of α-synucleinopathies.

Microglia is likely to be in constant contact with aS mainly because they express it and they sense it at synaptic terminals [391], but exosomes are vehicle of particular interest for aS transmission and propagation. They prevent, in fact, aS from degradation by extracellular enzyme [343] and catalyze its aggregation [344], enhancing its transmissibility and toxicity.

In this contest, it will be also interesting to assess the toxicity effect of the substances released by microglia upon aS containing exosomes incubation, in

order to demonstrate the instauration of the proposed "positive loop": neurons release aS toxic species inside exosomes, that are toxic to other neurons and activate microglia, which in turn secretes neurotoxic substances.

Moreover, being inflammatory status believed to contribute to the progression of α-synucleinopathies, the exosome secretion pathway may become an interesting therapeutic target to block this vicious circle. This observation is particularly relevant if we considered that microgliosis is considered an early event, as it occurs in the absence of cell death [391]. Hence, target the immune system and, in particular, microglia, is considered a promising strategy for treating α-synucleinopathies, due to its involvement in disease progression and its potential as a tool to modulate neuroinflammation.

## III PART: DOPAL impacts synaptic vesicle pools

In parallel to the study of exosomes effects on neurons and glia, we have investigated the effect of DOPAL on synaptic function as part of a recently published project [106].

To this aim, we used two different strategies and cell models in the presence of aS-DOPAL oligomers formed upon DOPAL treatment.


### 3.9 DOPAL impairs vesicle trafficking in aS overexpressing cells

We first studied the DOPAL effect on aS-EGFP transfected neuroblastoma-derived cell line BE(2)-M17.

To assess the formation of aS-DOPAL oligomers upon exogenous DOPAL treatment, aS-EGFP overexpressing BE(2)-M17 cells were treated with 100 µM DOPAL for 1, 18 and 24 hours.
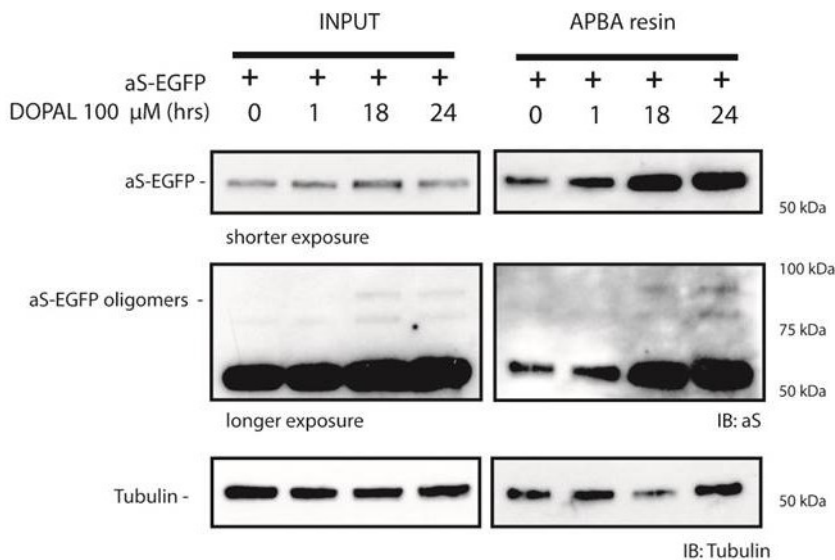


**Figure 51. DOPAL induced aS aggregation in BE(2)-M17 cells overexpressing aS-EGFP.** Cell lysates of aS-EGFP overexpressing BE(2)-M17 cells treated with 100 µM DOPAL for 0, 1, 18 and 24 hrs were pulled down with APBA resin and analyzed by Western Blot against aS and the housekeeping protein Tubulin. aS antibody (ab138501) revealed SDS-resistant oligomers formation upon DOPAL treatment.


Cell lysates were subsequently subjected to the APBA resin, that, as previously described (**Paragraph 3.4.1**), allows the pull-down of DOPAL-modified proteins. As reported in **Figure 51**, both total cell lysates and the pull-down samples were

analyzed by Western Blot using an antibody against aS. Upon increasing incubation time with DOPAL, high molecular weight aS-positive bands were detected and pull-down lanes show an increase in aS, suggesting the formation of SDS-resistant aS-DOPAL oligomers.

Once demonstrated the formation of aS-DOPAL oligomers upon DOPAL treatment in BE(2)-M17 cells, synaptic vesicle trafficking was studied with a Total Internal Fluorescence (TIRF) experiment. TIRF microscopy (TIRFM) can be used in a wide range of cell biological applications, and is particularly well suited to analyze the localization and dynamics of molecules and events near the plasma membrane, as neurotransmitter release. The TIRF excitation field decreases exponentially with distance from the cover slip on which cells are grown. This means that fluorophores close to the cover slip (e.g. within ~100 nm) are selectively illuminated, highlighting events that occur within this region. The advantages of using TIRF include the ability to obtain high-contrast images of fluorophores near the plasma membrane, very low background from the bulk of the cell, reduced cellular photodamage and rapid exposure times [392].

To perform TIRFM, BE(2)-M17 were transfected with aSmCherry or the empty vector mCherry to avoid overlap signal with a green pH-sensitive fluorescent protein directly targeted to synaptic vesicles, i.e synaptobrevin2-pHluorin (Syb2pHluorin) (**Figure 52a**) [364,393]. Syb2pHluorin is a fusion construct of the vesicle protein syb II with a pH-sensitive GFP, normally used in neurotransmitter release studies [394], since its fluorescence intensity increases if pH becomes basic, i.e. if vesicles fusion and/or permeabilisation occurs.

Upon 100 μM DOPAL treatment BE(2)-M17 cells were then analyzed by TIRFM. Normally, vesicles continue fusing with the plasma membrane, becoming fluorescent and then, after endocytosis, they are immediately switched off [107]. DOPAL, instead, increased the intensity and the persistence of the fluorescent signal of Syb2pHluorin as reported in **Figure 52c**, likely due to a vesicles permeability action. Moreover, after 24 hours of DOPAL treatment, the inflexion point of the curve reporting the cumulative distribution moves toward higher intensities values compared to time 0 in the aS-mCherry overexpressing cells, but not in control, i.e. mCherry (**Figure 52b**).
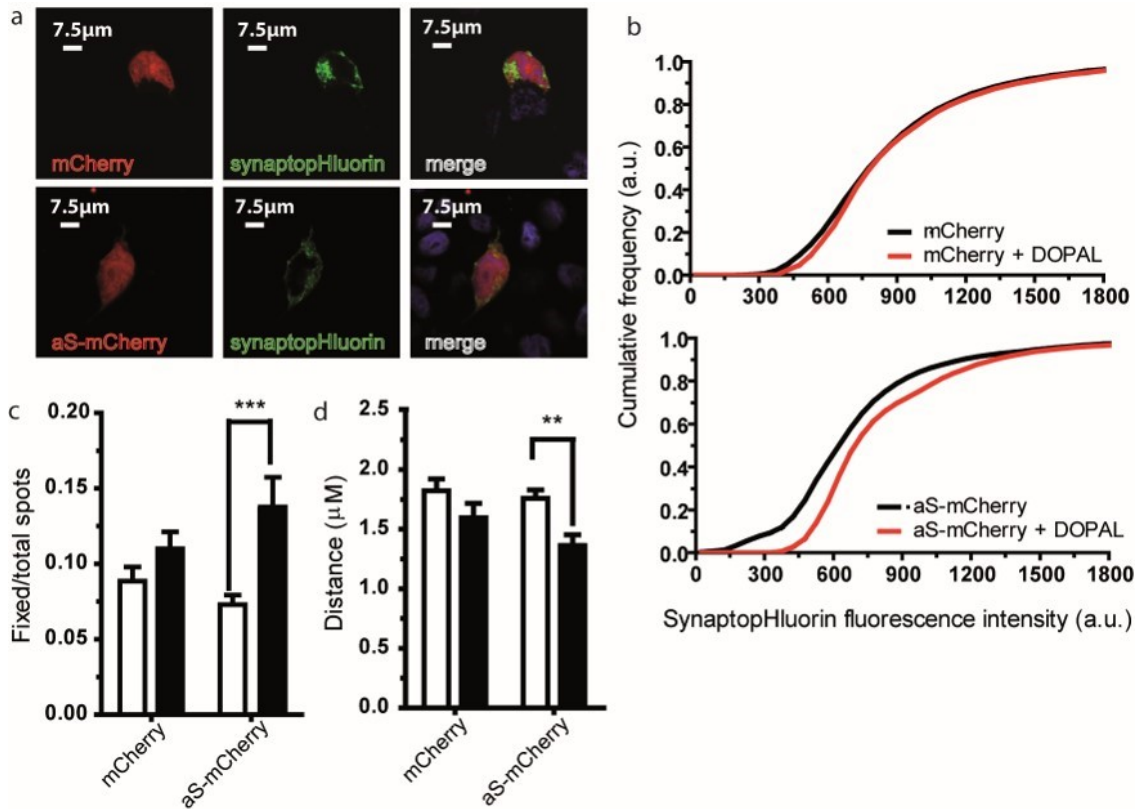
**Figure 52. DOPAL effect on vesicle trafficking in aS overexpressing cells. a.** Confocal images of BE(2)-M17 cells transfected with mCherry or aS-mCherry (red) and synapto-pHluorin (green) and the merge of the two channels. Scale bar is 7.5 μM; **b.** Normalized fluorescence intensity/number of vesicles cumulative graphs for mCherry and aS. Black and red traces refer to control cells and cells treated with DOPAL 100 μM for 24 hours; **c.** Histograms express the ratio between fixed and total vesicles over a certain period of time, i.e. the number of vesicles showing a high fluorescent value for the whole time span of the measure, for mCherry or aS-mCherry overexpressing cells untreated or treated with 100 μM for 24 hours. White and black stand for control cells and cells treated with 100 μM DOPAL for 24 hours; **d.** Average distance covered by vesicles in cells overexpressing mCherry or aS-mCherry at time 0 and after 100 μM DOPAL treatment at 24 hours. White and black stand for control cells and cells treated with 100 μM DOPAL for 24 hours. Bars represent mean ±SEM from n=25-30 cells from at least three independent experiments. Asterisks indicate statistical significance by two-way ANOVA (** p< 0.01 ***p< 0.001).

This result suggests that DOPAL-modified aS or aS-DOPAL oligomers increases vesicle pH, likely due to an efflux of H+, leading to the increased fluorescence intensity [394]. We have, in fact, previously demonstrated that DOPAL-modified aS monomers and oligomers interact with and permeabilise cholesterol containing lipid membranes *in vitro* [106]. Consistently, the number of "basic" vesicles with an increased fluorescent value for the whole time span of the measure (i.e. Fixed/total spots) is increased in the aS overexpressing cells after DOPAL treatment (**Figure 52c**). Interestingly, there was also a significant reduction in the average distance covered by vesicles, i.e. in vesicles mobility, in cells overexpressing aS-mCherry

after the DOPAL treatment compared to the control (**Figure 52d**). No difference is present between mCherry and aS-mCherry overexpressing cells before DOPAL treatment, suggesting that the effect we measured depends on the synergic action of aS and DOPAL, likely through DOPAL-induced modification and oligomerization of aS.

### 3.10 DOPAL impairs vesicle pools in primary neurons

Then, we moved to mice primary cortical neurons that express endogenous aS. We first assessed the formation of aS-DOPAL oligomer also in this cellular model. To this aim, primary neurons at DIV14 were treated overnight with 20 and 50 μM of DOPAL, since 100 μM was toxic. Cell lysates was both analyzed by Western Blot using an antibody against aS (**Figure 53a**) and subjected to the APBA resin (**Figure 53b**).
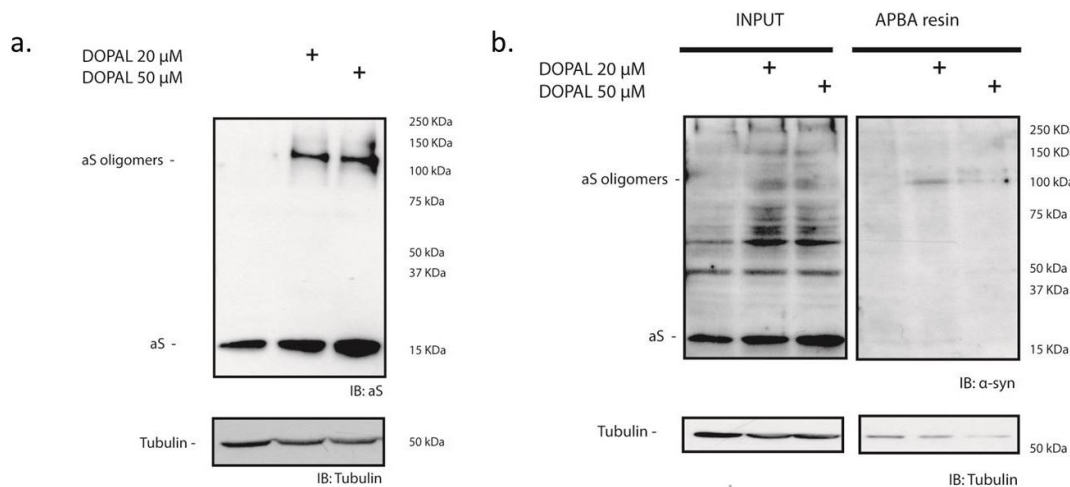


**Figure 53. DOPAL induced aS aggregation in primary cortical neurons.** Primary cortical neurons were treated overnight with 20 μM and 50 μM DOPAL; **a.** Western Blot analysis of cell lysates using antibodies against aS (ab52168) for detect endogenous aS and Tubulin, as loading control reveals SDS-resistant aS oligomers formation upon DOPAL treatment; **b.** ABPA resin pull-down from neuronal lysate of control and treated samples suggested that the accumulated monomeric aS is modified by DOPAL.

As reported in **Figure 53**, DOPAL induced the formation of aS-DOPAL oligomer also in the presence of endogenous neuronal aS.

We then used the same approach reported in **Paragraph 3.7.2** for studying the effect of exogenous administrated DOPAL on synaptic vesicle pools. Mice primary cortical neurons were prepared for TEM imaging and neuronal synapsis of

untreated neurons or treated neurons were imaged (**Figure 54a**).
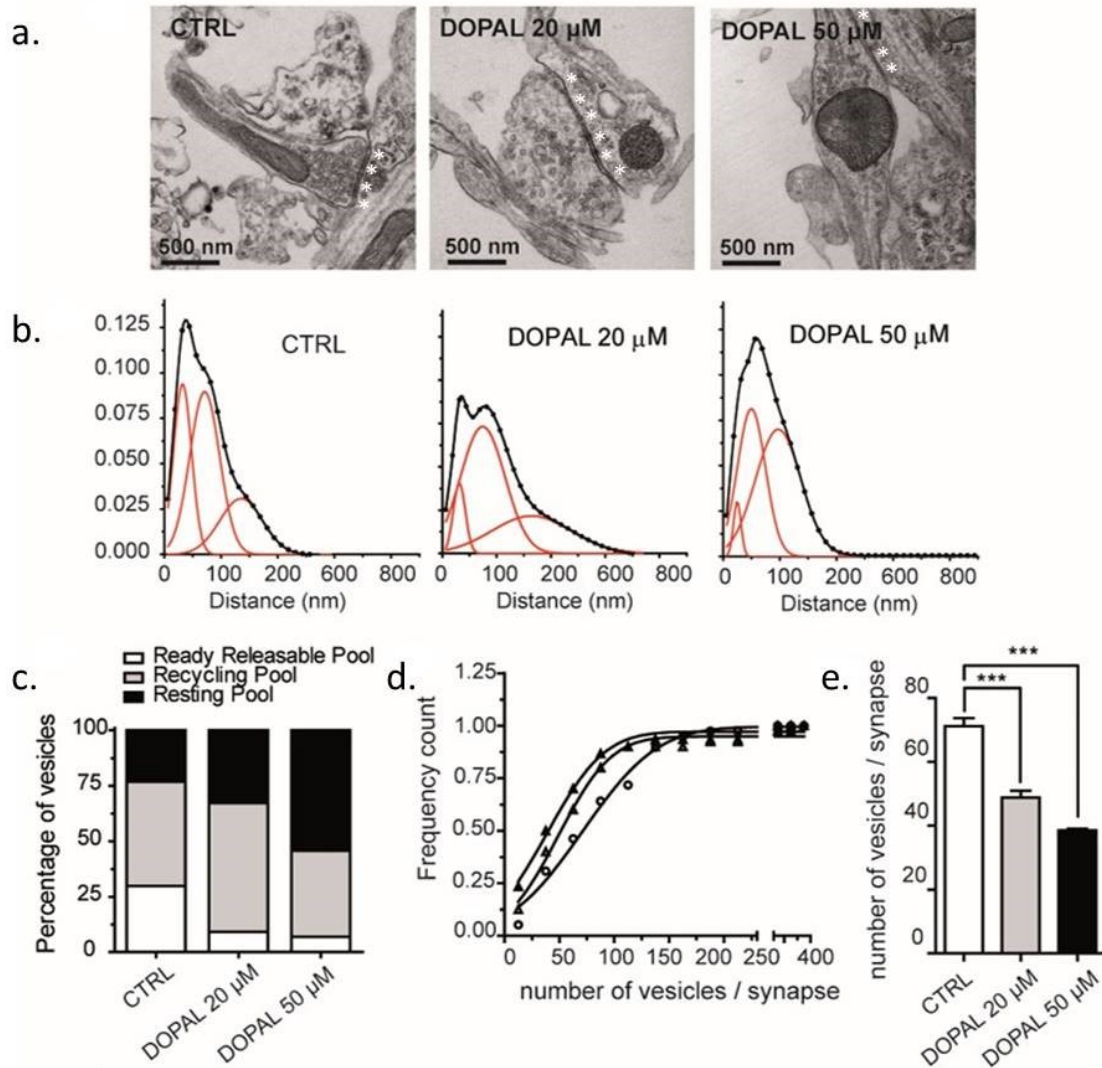


**Figure 54. DOPAL effect on synaptic vesicles in primary mouse neurons. a.** TEM images of mice primary neurons synapses not treated (CTRL) and treated with 20 μM and 50 μM DOPAL. Asterisks indicate the active xone. Scale bar 500 nm; **b.** Frequency distribution of vesicles distance from the active zone of primary neurons in control, treated with 20 μM and 50 μM DOPAL (from left to right). Data were fitted with a three Gaussian function (OriginPro8); **c.** Grouped stack column plot of the percentage of area under curve of the three vesicle populations, representing the percentage of vesicles belonging to the ready-releasable (white), recycling (grey) and resting (black) pools in control neurons and in neurons treated with 20 μM and 50 μM DOPAL; **d.** Cumulative distributions of the number of vesicles per synapse show that the number of vesicles per synapse is higher in controls (full triangle) than in neurons treated with 20 μM and 50 μM DOPAL (empty triangles and empty circles, respectively); **e.** Column graph representing the average inflection point values of the cumulative distribution reported in **d.** of the number of vesicles/synapse showing a significant reduction after 20 μM and 50 μM DOPAL treatment. Bars represent mean ±SEM from n=30-39 synapses from at least three independent experiments. Asterisks indicate statistical significance by two-way ANOVA (***$p < 0.001$).

The relative distributions of the distances between vesicles and the active zone of

the synapses was measured as previously reported by Piccoli and co-workers [364] (**Figure 54b**). As it emerges from **Figure 54c**, DOPAL leads to a reduction in the readily releasable pool of synaptic vesicles, with an increase of the fraction of vesicles belonging to the resting pool. Moreover, the inflection point of the cumulative distribution of the number of vesicles per synapses is about 71±3 for the untreated neurons and drops to 49±2 and 38±2 for the 20 μM and 50 μM DOPAL treated neurons, respectively, and it is decreasing in a [DOPAL]- dependent way (**Figure 54e-f**).

These results suggest that the formed aS-DOPAL oligomers permeabilize the synaptic vesicles and cause protons to leak out and raise the pH value within the vesicles. In conclusion, these observations suggest that aS-DOPAL oligomers preferentially damage the vesicles ready to be released at the synapse, possibly because oligomers formation occurs in the subcellular region where aS is known to participate in the SNARE complex assembly [221]. It should also be mentioned that the chemical modifications of aS by DOPAL, which lead to the formation of oligomers may also hinder a proposed physiological function of aS, i.e. SNARE complex assembly. Therefore, reducing the amount of functional aS at the synapse may affect the number of synaptic vesicles belonging to the different pools [107].

# CHAPTER IV:
# Concluding remarks

This work focuses on α-synucleinopathies, a group of neurodegenerative disorders characterized by the presence of abnormally aggregated aS. Recent evidence suggests that the early site of aS aggregation is synapses, where aS seems to play its physiological role. Moreover, aggregated aS is reported to be secreted by cells, suggesting its potential implication in both disease initiation and progression. Considering the nature of neurodegenerative disorders as well as the defined, step-wise spreading of Lewy body pathology in α-synucleinopathies, the idea of extracellular aS as a potential pathogenic 'prion-like' agent is extremely appealing. Among different mechanisms of aS secretion, we considered the exosomal pathway of relevance in the model of aS propagation for several reasons: (i) aS containing exosomes are released and internalized by immune and neuronal cells; (ii) exosomal encapsulation of aS confers protection against extracellular protein degradation mechanisms, enhancing exosomes probability to play a role in aS toxic species transmission; (iii) these vesicles provide a confined and controlled environment for aS nucleation, which may promote aggregation and lead to toxicity and neurodegeneration; (iv) they have been proposed to be secreted in a spatially and temporally directed manner in neuronal synapses.

On these bases, our hypothesis is that exosomes are involved in both release and transmission of aS toxic species among cells, as an early event in the progression of α-synucleinopathies.

To test this hypothesis, we studied the effects of cell-derived exosomes containing aS aggregated species on neurons and microglia cells. We decided to purify exosomes from aS-EGFP transfected HEK293T cells. Moreover, we focused on the connection between aS aggregation process and dopamine metabolism and exosomes were purified also from aS-EGFP transfected HEK293T cells treated with DOPAL.

DOPAL is a toxic dopamine metabolite, which can modify aS, inducing its aggregation. It is also transmissible to glial cells and enhances intracellular oligomerization of aS, suggesting a possible mechanism for glial cytoplasmic inclusions formation in MSA and in neuroinflammation. In neurons, we demonstrated that DOPAL treatment impacts vesicle trafficking and the synaptic vesicle pools. The formed aS-DOPAL oligomers were proposed to permeabilize the synaptic vesicles and preferentially damage the vesicles ready to be released at the synapse, possibly because oligomers formation occurs in the subcellular region where aS is known to participate in the SNARE complex assembly [221]. However, the role of DOPAL-modified aS has not yet being investigated in disease propagation. Therefore, the purification of aS-DOPAL containing exosomes is of great interest to define an experimental model of exosomes based spreading not only for PD, but possibly for all α-synucleinopathies, characterized by the abnormal aggregation of aS.

The purified vesicles exhibited the typical hallmarks of exosomes and they contained aS and DOPAL-modified aS oligomeric species. The nature of these aS species was further studied by SDS-Page and SEC analysis, revealing the presence of non SDS-resistant aS aggregates in aS containing exosomes. Upon DOPAL modification, this type of oligomers increased and, as attended, it appeared also SDS-resistant high molecular weight aS species. Differences in exosomal aS between the two conditions was further underlined by the evidence that upon DOPAL treatment, aS binds to exosomal membranes and alters vesicle microenvironment, further suggesting a pore formation mechanism ascribable to DOPAL-modified aS oligomers.

Since aS structure seems strictly correlated with is function/dysfunction, an in-depth characterization of exosomal aS was required in order to better understand the effects induced on neurons and microglia.

Our hypothesis, in fact, is that exosomes containing aS aggregated species are secreted in a spatially and temporally regulated manner by neuronal synapses, that are also the primary site of aS induced-toxicity.

On these bases, we have focused our attention on synaptic damage analyzing different factors. First, we have investigated the amount of two proteins, i.e. synaptophysin and PSD-95 as markers of the pre- and post-synapses respectively. Upon incubation with the purified vesicles, only aS containing exosomes induced a reduction of synaptophysin and PSD-95 levels, with a more pronounced effect upon incubation with the DOPAL-modified one. These data suggest that aS containing exosomes are able to diminish the number of synapses, likely altering input between neurons.

To further investigate this hypothesis, we analyzed synaptic architecture, since the structure is strictly connected with function in synapses. We found that aS containing exosomes not only shifts the distribution of distances of synaptic vesicles from the active zone to larger values, but also diminish the number of vesicles, confirming an induced synaptic dysfunction in treated neurons.

Reduction of the synaptic proteins and synaptic impairment were also accompanied by an altered morphology (i.e neurite retraction and reduced neuronal branching) in treated neurons.

However, under our experimental condition, neuronal survival was not impacted upon exosomes treatment. This result is not in line with other works, that reported aS exosomal transfer as a way to induce neurotoxicity [127], suggesting that neuronal death might be exacerbated with increasing incubation time with exosomes. It is also important to mention, that we have not assessed for glial contamination that usually occurs in primary neuronal culture and can hinder neurotoxicity.

These results, however, strongly suggest that exosomes containing aS aggregated species are able to transmit their toxic cargo at least to neuronal synapses. This effect appears more evident in the presence of DOPAL-modified aS, likely due to the increase toxicity of their oligomers. Even if we were not able to clearly detect the presence inside neuronal synapses of exosomal cargos, we propose that they are internalized at these sites, where they exert their harmful effects.

The detailed toxicity mechanism of exosomal-driven aS aggregated species in synapses has not yet been investigated, but starting from recent observation we propose two possibilities. Once internalized at synapses, aS oligomers can act (i) through a pore mechanism formation as suggest by the membrane localization of

DOPAL-modified aS oligomers at membranes and their capacity to alter exosomal environment or/and (ii) seeding neuronal endogenous aS, hindering its physiological function. Regarding the latter hypothesis, aggregates of aS can disrupt its interaction with sybII, compromising SNARE complex formation, vesicle docking and fusion. This results in reduced neurotransmitter release and the redistribution of synaptic proteins, as synaptophysin and PSD-95. Supportively, synaptic deficits are induced by aS overexpression in different *in vitro* [245,353] and *in vivo* models [248,249], and also by ablation of all 3 (α,β,ɣ)-synuclein genes [363].

All these effects may be early events in the propagation of α-synucleinopathies, that lastly lead to neuronal death.

We also investigated another way of impacting neuronal physiology: neuroinflammation induced by microglia activation.

Microglia cells, in fact, upon chronic and excessive aS exposure, are reported to become active and secret toxic substances, including the pro-inflammatory cytokines IL-1β, that might impact neuronal survival. In addition, aS chronic exposure seems to contribute to an impaired microglial phagocytic capacity, leading to aggregation of extracellular aS and further enhancing neurodegeneration.

When we applied exosomes to microglia cells, we confirmed that aS containing exosomes induced an increased release of IL-1 β. However, we did not assess whether this response was mediated by exosomal cargo internalization in primary microglia cells. It would be interesting to investigate this aspect, since different pathways can induce microglia activation, and their identification can pave the way for the development of novel therapeutic strategies.

Moreover, we are also planning to study the effect of all released substances by microglia upon aS containing exosomes incubation on neurons, in order to validate the proposed "vicious circle". aS toxic species secreted in exosomes are transferred to recipient cells (neurons and microglia). In neurons, they mainly impacted synapses, altering synaptic inputs and neuronal plasticity. In microglia they induced the release of substances (i.e. IL-1 β), which in turn are deleterious for neurons.

All the mentioned hypothesized mechanisms imply a toxic gain-of-function of the aS oligomeric species involved in the aggregation pathway. It is likely that the cytotoxicity does not arise from a single mechanism but that several of the proposed mechanisms are involved in the aS propagation mediated by exosomes in α-synucleinopathies. However, our data suggest a trans-synaptic exosomal transfer of aS from cell-to-cell as a key mechanism in the spread of aS aggregates between neurons in the brain and point out synapses as an early site of aS gaining of toxic function. Moreover, being inflammatory status believed to impact neuronal viability, the exosomes secretion pathway may become an interesting therapeutic target to block this vicious circle. This observation is particularly relevant if one consider that microgliosis is an early event, as it occurs in the absence of cell death. Hence, targeting of the immune system or the aS toxic species propagation at synapses can be considered very promising strategies.

Moreover, aS containing exosomes have been detected in different human body fluids and tissue [122,395] and it was recently shown that exosomes isolated from plasma of PD patients contain higher levels of aS when compared to exosomes from control individuals [140]. In the light of all these considerations, aS containing exosomes appeared also as a potential biomarker for the early diagnosis of α-synucleinopathies.

# List of abbreviations

AADC: L-aromatic amino acid decarboxylase

AFM: Atomic Force microscopy

ALDH: aldehyde dehydrogenase

APBA: aminophenylboronic acid

AR: aldose reductase

ARG1: enzymes arginase 1

aS: α-Synuclein

BDNF: brain-derived neurotrophic factor

CNS: central nervous system

COMT: catechol-O-methyl transferase

CSF: cerebrospinal fluid

DA: dopamine

DAMPs: danger-associated molecular patterns

DAT: DA-transporter

DLB: Dementia with Lewy bodies

DOPAC: 3,4-dihydroxyphenylacetic acid

DOPAL: 3,4-dihydroxyphenilacetaldehyde

DOPET: 3,4-dihydroxyphenylethanol

DβH: dopamine-β-hydroxylase

ESCRT: Endosomal Sorting Complexes Required for Transport

EVs: extracellular vesicles

GABA: γ-Aminobutyric acid

GAPDH: Glyceraldehyde 3-phosphate dehydrogenase

GBA: β-glucocerebrosidase

GCIs: glial cytoplasmic inclusions

GRKs: protein-coupled receptor kinases

HEK293T: Human Embryonic Kidney

Hsp70: heat shock protein 70

Hsp90: heat shock protein 90

HSPGs: heparan sulfate proteoglycans

ICAMs: intercellular adhesion molecules

IDE: insulin-degrading enzyme

IL: interleukin

iNOS: inducible nitric oxide synthase

KRS: Kufor-Rakeb syndrome

LAG3: lymphocyte-activation gene 3

LB: Lewy Bodies

LBP: LPS binding protein

L-DOPA: 3,4-dihydroxyphenylalanine

LPS: Lipopolysaccharide

LRRK2: Leucine-rich repeat kinase 2

L-Tyr: aminoacid L-tyrosine

MAO: monoamine oxidase

MBT-SO: S-methyl N-butylthiocarbamate sulfoxide

MPTP: 1-methyl-4-phenyl-1,2,3,6-tetrahydropyridine

MSA: Multiple system atrophy

MSA-C: MSA with cerebellar signs

MSA-P: MSA with parkinsonism

MVBs: multivesicular bodies

NAC: non-Aβ component of plaque

SNARE: soluble N-ethylmaleimide-sensitive fusion protein-attachment protein receptor

NLR: NOD-like receptor

NMT: N-methyltransferase

NO: Nitric oxide

NSAIDs: Nonsteroidal anti-inflammatory drugs

PAMPs: Pathogen-associated molecular patterns

PARP1: Poly (ADP-ribose) polymerase-1

PD: Parkinson's disease

PEI: Polyethylenimine

PK: Proteinase K

PLKs: LRRK2 and Polo-like kinases

PRRs: pattern recognition receptors

PYHIN: HIN domain-containing protein

RBD: REM-sleep behavioural disorder

ROS: reactive oxygen species

RT: room temperature

SDS: Sodium dodecyl sulfate

SNpc: Substantia Nigra pars compacta

STED: stimulated emission depletion

Syb2pHluorin: synaptobrevin2-pHluorin

sybII: synaptobrevin-2

TEM: Transmission Electron Microscopy

TEMs: tetraspanin-enriched domains

TH: tyrosine hydroxylase

TIRF: Total Internal Fluorescence

TLR: Toll-like receptor

TNTs: tunneling nanotubes

VMAT2: vesicular monoamine transporter 2

VPS35: vacuolar sorting protein 35

# References

1       Spillantini, M. G., Crowther, R. A., Jakes, R., Hasegawa, M. & Goedert, M. alpha-Synuclein in filamentous inclusions of Lewy bodies from Parkinson's disease and dementia with lewy bodies. *Proc Natl Acad Sci U S A* **95**, 6469-6473 (1998).

2       Galvin, J. E., Giasson, B., Hurtig, H. I., Lee, V. M. & Trojanowski, J. Q. Neurodegeneration with brain iron accumulation, type 1 is characterized by alpha-, beta-, and gamma-synuclein neuropathology. *Am J Pathol* **157**, 361-368, doi:S0002-9440(10)64548-8 [pii] (2000).

3       McCann, H., Stevens, C. H., Cartwright, H. & Halliday, G. M. alpha-Synucleinopathy phenotypes. *Parkinsonism Relat Disord* **20 Suppl 1**, S62-67, doi:10.1016/S1353-8020(13)70017-8

S1353-8020(13)70017-8 [pii] (2014).

4       Kalia, L. V. & Lang, A. E. Parkinson's disease. *Lancet* **386**, 896-912, doi:10.1016/S0140-6736(14)61393-3 (2015).

5       Dauer, W. & Przedborski, S. Parkinson's disease: Mechanisms and models. *Neuron* **39**, 889-909, doi:Doi 10.1016/S0896-6273(03)00568-3 (2003).

6       Chaudhuri, N. T. P. J. G. L. R. Parkinson's: a syndrome rather than a disease? *J Neural Transm (Vienna)*, doi:10.1007/s00702-016-1667-6 (2016).

7       Gelb, D. J., Oliver, E. & Gilman, S. Diagnostic criteria for Parkinson disease. *Arch Neurol* **56**, 33-39 (1999).

8       Chaudhuri, K. R. & Sauerbier, A. Parkinson disease. Unravelling the nonmotor mysteries of Parkinson disease. *Nat Rev Neurol* **12**, 10-11, doi:10.1038/nrneurol.2015.236

nrneurol.2015.236 [pii] (2016).

9       Berg, D. *et al.* MDS research criteria for prodromal Parkinson's disease. *Movement Disord* **30**, 1600-1609, doi:10.1002/mds.26431 (2015).

10      Postuma, R. B. *et al.* MDS clinical diagnostic criteria for Parkinson's disease. *Movement Disord* **30**, 1591-1599, doi:10.1002/mds.26424 (2015).

11      Lesage, S. *et al.* G51D alpha-synuclein mutation causes a novel parkinsonian-pyramidal syndrome. *Ann Neurol* **73**, 459-471, doi:10.1002/ana.23894 (2013).

12      Hernandez, D. G., Reed, X. & Singleton, A. B. Genetics in Parkinson disease: Mendelian versus non-Mendelian inheritance. *J Neurochem* **139**, 59-74, doi:10.1111/jnc.13593 (2016).

13      Heneka, M. T., Kummer, M. P. & Latz, E. Innate immune activation in neurodegenerative disease. *Nat Rev Immunol* **14**, 463-477, doi:10.1038/nri3705 (2014).

14      Peelaerts, W. & Baekelandt, V.?-Synuclein strains and the variable pathologies of synucleinopathies. *J Neurochem* **139**, 256-274, doi:10.1111/jnc.13595 (2016).

15      Erskine, D. *et al.* Specific patterns of neuronal loss in the pulvinar nucleus in dementia with lewy bodies. *Mov Disord*, doi:10.1002/mds.26887 (2017).

16      Halliday, G. M., Song, Y. J. & Harding, A. J. Striatal beta-amyloid in dementia with Lewy bodies but not Parkinson's disease. *J Neural Transm (Vienna)* **118**, 713-719, doi:10.1007/s00702-011-0641-6 (2011).

17      Mirra, S. S. *et al.* The Consortium to Establish a Registry for Alzheimer's Disease (CERAD). Part II. Standardization of the neuropathologic assessment of Alzheimer's disease. *Neurology* **41**, 479-486 (1991).

18      Schrag, A., Ben-Shlomo, Y. & Quinn, N. P. Prevalence of progressive supranuclear palsy and multiple system atrophy: a cross-sectional study. *Lancet* **354**, 1771-1775, doi:Doi 10.1016/S0140-6736(99)04137-9 (1999).

19      Gilman, S. *et al.* Second consensus statement on the diagnosis of multiple system atrophy. *Neurology* **71**, 670-676, doi:DOI 10.1212/01.wnl.0000324625.00404.15 (2008).

20      Gilman, S. *et al.* Second consensus statement on the diagnosis of multiple system atrophy. *Neurology* **71**, 670-676, doi:10.1212/01.wnl.0000324625.00404.15 71/9/670 [pii] (2008).

21      O'Sullivan, S. S. *et al.* Clinical outcomes of progressive supranuclear palsy and multiple system atrophy. *Brain* **131**, 1362-1372, doi:10.1093/brain/awn065 awn065 [pii] (2008).

22      Hughes, A. J., Colosimo, C., Kleedorfer, B., Daniel, S. E. & Lees, A. J. The dopaminergic response in multiple system atrophy. *J Neurol Neurosurg Psychiatry* **55**, 1009-1013 (1992).

23      Ahmed, Z. *et al.* The neuropathology, pathophysiology and genetics of multiple system atrophy. *Neuropathol Appl Neurobiol* **38**, 4-24, doi:10.1111/j.1365-2990.2011.01234.x (2012).

24      Goldstein, D. S., Sewell, L. & Holmes, C. Association of anosmia with autonomic failure in Parkinson disease. *Neurology* **74**, 245-251 (2010).

25      Boeve, B. F. *et al.* Pathophysiology of REM sleep behaviour disorder and relevance to neurodegenerative disease. *Brain* **130**, 2770-2788, doi:10.1093/brain/awm056 (2007).

26      Puschmann, A., Bhidayasiri, R. & Weiner, W. J. Synucleinopathies from bench to bedside. *Parkinsonism Relat Disord* **18 Suppl 1**, S24-27, doi:10.1016/S1353-8020(11)70010-4 S1353-8020(11)70010-4 [pii] (2012).

27      Breydo, L., Wu, J. W. & Uversky, V. N. Alpha-synuclein misfolding and Parkinson's disease. *Biochim Biophys Acta* **1822**, 261-285, doi:10.1016/j.bbadis.2011.10.002 S0925-4439(11)00225-0 [pii] (2012).

28      Lashuel, H. A., Overk, C. R., Oueslati, A. & Masliah, E. The many faces of alpha-synuclein: from structure and toxicity to therapeutic target. *Nat Rev Neurosci* **14**, 38-48, doi:10.1038/nrn3406 nrn3406 [pii] (2013).

29      Surewicz, W. K., Epand, R. M., Pownall, H. J. & Hui, S. W. Human apolipoprotein A-I forms thermally stable complexes with anionic but not with zwitterionic phospholipids. *J Biol Chem* **261**, 16191-16197 (1986).

30      Pasanen, P. *et al.* Novel alpha-synuclein mutation A53E associated with atypical multiple system atrophy and Parkinson's disease-type pathology. *Neurobiol Aging* **35**, 2180 e2181-2185, doi:10.1016/j.neurobiolaging.2014.03.024 S0197-4580(14)00281-4 [pii] (2014).

31      Appel-Cresswell, S. *et al.* Alpha-synuclein p.H50Q, a novel pathogenic mutation for Parkinson's disease. *Mov Disord* **28**, 811-813, doi:10.1002/mds.25421 (2013).

32      Polymeropoulos, M. H. *et al.* Mutation in the alpha-synuclein gene identified in families with Parkinson's disease. *Science* **276**, 2045-2047 (1997).

33      Kruger, R. *et al.* Ala30Pro mutation in the gene encoding alpha-synuclein in Parkinson's disease. *Nat Genet* **18**, 106-108, doi:10.1038/ng0298-106 (1998).

34      Zarranz, J. J. *et al.* The new mutation, E46K, of alpha-synuclein causes Parkinson and Lewy body dementia. *Ann Neurol* **55**, 164-173, doi:10.1002/ana.10795 (2004).

35      Giasson, B. I., Murray, I. V., Trojanowski, J. Q. & Lee, V. M. A hydrophobic stretch of 12 amino acid residues in the middle of alpha-synuclein is essential for filament assembly. *J Biol Chem* **276**, 2380-2386, doi:10.1074/jbc.M008919200 M008919200 [pii] (2001).

36      Izawa, Y. *et al.* Role of C-terminal negative charges and tyrosine residues in fibril formation of alpha-synuclein. *Brain Behav* **2**, 595-605, doi:10.1002/brb3.86 (2012).

37      Lowe, R., Pountney, D. L., Jensen, P. H., Gai, W. P. & Voelcker, N. H. Calcium(II) selectively induces alpha-synuclein annular oligomers via interaction with the C-terminal domain. *Protein Sci* **13**, 3245-3252, doi:ps.04879704 [pii] 10.1110/ps.04879704 (2004).

38      Souza, J. M., Giasson, B. I., Lee, V. M. & Ischiropoulos, H. Chaperone-like activity of synucleins. *Febs Lett* **474**, 116-119, doi:S0014-5793(00)01563-5 [pii] (2000).

39      Xu, S. L. & Chan, P. Interaction between Neuromelanin and Alpha-Synuclein in Parkinson's Disease. *Biomolecules* **5**, 1122-1142, doi:10.3390/biom5021122 (2015).

40      Weinreb, P. H., Zhen, W. G., Poon, A. W., Conway, K. A. & Lansbury, P. T. NACP, a protein implicated in Alzheimer's disease and learning, is natively unfolded. *Biochemistry-Us* **35**, 13709-13715, doi:Doi 10.1021/Bi961799n (1996).

41      Wang, W. *et al.* A soluble alpha-synuclein construct forms a dynamic tetramer. *Proc Natl Acad Sci U S A* **108**, 17797-17802, doi:10.1073/pnas.1113260108 1113260108 [pii] (2011).

42      Bartels, T., Choi, J. G. & Selkoe, D. J. alpha-Synuclein occurs physiologically as a helically folded tetramer that resists aggregation. *Nature* **477**, 107-U123, doi:10.1038/nature10324 (2011).

43      Smaldone, G. *et al.* Insight into conformational modification of alpha-synuclein in the presence of neuronal whole cells and of their isolated membranes. *Febs Lett* **589**, 798-804, doi:10.1016/j.febslet.2015.02.012 (2015).

44      Burre, J. *et al.* Properties of native brain alpha-synuclein. *Nature* **498**, E4-E6, doi:10.1038/nature12125 (2013).

45      Fauvet, B. *et al.* alpha-Synuclein in central nervous system and from erythrocytes, mammalian cells, and Escherichia coli exists predominantly as disordered monomer. *J Biol Chem* **287**, 15345-15364, doi:10.1074/jbc.M111.318949 M111.318949 [pii] (2012).

46      Binolfi, A., Theillet, F. X. & Selenko, P. Bacterial in-cell NMR of human alpha-synuclein: a disordered monomer by nature? *Biochem Soc T* **40**, 950-U292, doi:10.1042/Bst20120096 (2012).

47      Burre, J., Sharma, M. & Sudhof, T. C. alpha-Synuclein assembles into higher-order multimers upon membrane binding to promote SNARE complex formation. *Proc Natl Acad Sci U S A* **111**, E4274-4283, doi:10.1073/pnas.1416598111 1416598111 [pii] (2014).

48      Luth, E. S., Bartels, T., Dettmer, U., Kim, N. C. & Selkoe, D. J. Purification of alpha-Synuclein from Human Brain Reveals an Instability of Endogenous Multimers as the Protein Approaches Purity. *Biochemistry-Us* **54**, 279-292, doi:10.1021/bi501188a (2015).

49      Burre, J., Sharma, M. & Sudhof, T. C. Definition of a molecular pathway mediating alpha-synuclein neurotoxicity. *J Neurosci* **35**, 5221-5232, doi:10.1523/JNEUROSCI.4650-14.2015 35/13/5221 [pii] (2015).

50      Calo, L., Wegrzynowicz, M., Santivanez-Perez, J. & Grazia Spillantini, M. Synaptic failure and alpha-synuclein. *Mov Disord* **31**, 169-177, doi:10.1002/mds.26479 (2016).

51    Lee, H. J., Choi, C. & Lee, S. J. Membrane-bound alpha-synuclein has a high aggregation propensity and the ability to seed the aggregation of the cytosolic form. *J Biol Chem* **277**, 671-678, doi:10.1074/jbc.M107045200 (2002).

52    Burre, J. The Synaptic Function of alpha-Synuclein. *J Parkinsons Dis* **5**, 699-713, doi:10.3233/JPD-150642

JPD150642 [pii] (2015).

53    Galvagnion, C. *et al.* Lipid vesicles trigger alpha-synuclein aggregation by stimulating primary nucleation. *Nat Chem Biol* **11**, 229-U101, doi:10.1038/Nchembio.1750 (2015).

54    Galvagnion, C. *et al.* Chemical properties of lipids strongly affect the kinetics of the membrane-induced aggregation of alpha-synuclein. *Proc Natl Acad Sci U S A* **113**, 7065-7070, doi:10.1073/pnas.1601899113

1601899113 [pii] (2016).

55    Dedmon, M. M., Lindorff-Larsen, K., Christodoulou, J., Vendruscolo, M. & Dobson, C. M. Mapping long-range interactions in alpha-synuclein using spin-label NMR and ensemble molecular dynamics simulations. *J Am Chem Soc* **127**, 476-477, doi:10.1021/ja044834j (2005).

56    Maltsev, A. S., Ying, J. & Bax, A. Deuterium isotope shifts for backbone (1)H, (1)(5)N and (1)(3)C nuclei in intrinsically disordered protein alpha-synuclein. *J Biomol NMR* **54**, 181-191, doi:10.1007/s10858-012-9666-x (2012).

57    Fusco, G. *et al.* Direct observation of the three regions in alpha-synuclein that determine its membrane-bound behaviour. *Nat Commun* **5**, doi:Artn 3827

10.1038/Ncomms4827 (2014).

58    Uversky, V. N. & Eliezer, D. Biophysics of Parkinson's Disease: Structure and Aggregation of alpha-Synuclein. *Curr Protein Pept Sc* **10**, 483-499 (2009).

59    Snead, D. & Eliezer, D. Alpha-synuclein function and dysfunction on cellular membranes. *Exp Neurobiol* **23**, 292-313, doi:10.5607/en.2014.23.4.292 (2014).

60    Middleton, E. R. & Rhoades, E. Effects of Curvature and Composition on alpha-Synuclein Binding to Lipid Vesicles. *Biophysical Journal* **99**, 2279-2288, doi:10.1016/j.bpj.2010.07.056 (2010).

61    Jo, E., McLaurin, J., Yip, C. M., St George-Hyslop, P. & Fraser, P. E. alpha-Synuclein membrane interactions and lipid specificity. *J Biol Chem* **275**, 34328-34334, doi:10.1074/jbc.M004345200

M004345200 [pii] (2000).

62    Perrin, R. J., Woods, W. S., Clayton, D. F. & George, J. M. Interaction of human alpha-synuclein and Parkinson's disease variants with phospholipids - Structural analysis using site-directed mutagenesis. *J Biol Chem* **275**, 34393-34398, doi:DOI 10.1074/jbc.M004851200 (2000).

63    Kubo, S. *et al.* A combinatorial code for the interaction of alpha-synuclein with membranes. *J Biol Chem* **280**, 31664-31672, doi:10.1074/jbc.M504894200 (2005).

64    Bisaglia, M., Schievano, E., Caporale, A., Peggion, E. & Mammi, S. The 11-mer repeats of human alpha-synuclein in vesicle interactions and lipid composition discrimination: A cooperative role. *Biopolymers* **84**, 310-316, doi:10.1002/hip.20440 (2006).

65    Rhoades, E., Ramlall, T. F., Webb, W. W. & Eliezer, D. Quantification of alpha-synuclein binding to lipid vesicles using fluorescence correlation spectroscopy. *Biophysical Journal* **90**, 4692-4700, doi:10.1529/biophysj.105.079251 (2006).

66    Middleton, E. R. & Rhoades, E. Effects of curvature and composition on alpha-synuclein binding to lipid vesicles. *Biophys J* **99**, 2279-2288, doi:10.1016/j.bpj.2010.07.056

S0006-3495(10)00929-X [pii] (2010).

67    Pranke, I. M. *et al.* alpha-Synuclein and ALPS motifs are membrane curvature sensors whose contrasting chemistry mediates selective vesicle binding. *Journal of Cell Biology* **194**, 88-102, doi:10.1083/jcb.201011118 (2011).

68    Kjaer, L., Giehm, L., Heimburg, T. & Otzen, D. The influence of vesicle size and composition on alpha-synuclein structure and stability. *Biophys J* **96**, 2857-2870, doi:10.1016/j.bpj.2008.12.3940

S0006-3495(09)00412-3 [pii] (2009).

69    Jensen, M. B. *et al.* Membrane curvature sensing by amphipathic helices: a single liposome study using alpha-synuclein and annexin B12. *J Biol Chem* **286**, 42603-42614, doi:10.1074/jbc.M111.271130

M111.271130 [pii] (2011).

70    Cui, H. S., Lyman, E. & Voth, G. A. Mechanism of Membrane Curvature Sensing by Amphipathic Helix Containing Proteins. *Biophysical Journal* **100**, 1271-1279, doi:10.1016/j.bpj.2011.01.036 (2011).

71    Jao, C. C., Hegde, B. G., Chen, J., Haworth, I. S. & Langen, R. Structure of membrane-bound alpha-synuclein from site-directed spin labeling and computational refinement. *Proc Natl Acad Sci U S A* **105**, 19666-19671, doi:10.1073/pnas.0807826105

0807826105 [pii] (2008).

72    Bodner, C. R., Dobson, C. M. & Bax, A. Multiple tight phospholipid-binding modes of alpha-synuclein revealed by solution NMR spectroscopy. *J Mol Biol* **390**, 775-790, doi:10.1016/j.jmb.2009.05.066

S0022-2836(09)00648-2 [pii] (2009).

73    Georgieva, E. R., Ramlall, T. F., Borbat, P. P., Freed, J. H. & Eliezer, D. The lipid-binding domain of wild type and mutant alpha-synuclein: compactness and interconversion between the broken and extended helix forms. *J Biol Chem* **285**, 28261-28274, doi:10.1074/jbc.M110.157214

M110.157214 [pii] (2010).

74    Varkey, J. *et al.* Membrane Curvature Induction and Tubulation Are Common Features of Synucleins and Apolipoproteins. *J Biol Chem* **285**, 32486-32493, doi:10.1074/jbc.M110.139576 (2010).

75    Mizuno, N. *et al.* Remodeling of Lipid Vesicles into Cylindrical Micelles by alpha-Synuclein in an Extended alpha-Helical Conformation. *J Biol Chem* **287**, 29301-29311, doi:10.1074/jbc.M112.365817 (2012).

76    Anderson, J. P. *et al.* Phosphorylation of Ser-129 is the dominant pathological modification of alpha-synuclein in familial and sporadic Lewy body disease. *J Biol Chem* **281**, 29739-29752, doi:10.1074/jbc.M600933200 (2006).

77    Okochi, M. *et al.* Constitutive phosphorylation of the Parkinson's disease associated alpha-synuclein. *J Biol Chem* **275**, 390-397, doi:DOI 10.1074/jbc.275.1.390 (2000).

78    Pronin, A. N., Morris, A. J., Surguchov, A. & Benovic, J. L. Synucleins are a novel class of substrates for G protein-coupled receptor kinases. *J Biol Chem* **275**, 26515-26522, doi:DOI 10.1074/jbc.M003542200 (2000).

79    Ellis, C. E., Schwartzberg, P. L., Grider, T. L., Fink, D. W. & Nussbaum, R. L. alpha-Synuclein is phosphorylated by members of the Src family of protein-tyrosine kinases. *J Biol Chem* **276**, 3879-3884, doi:DOI 10.1074/jbc.M010316200 (2001).

80    Nakamura, T., Yamashita, H., Takahashi, T. & Nakamura, S. Activated Fyn phosphorylates alpha-synuclein at tyrosine residue 125. *Biochem Bioph Res Co* **280**, 1085-1092, doi:10.1006/bbrc.2000.4253 (2001).

81    Giasson, B. I. *et al.* Oxidative damage linked to neurodegeneration by selective alpha-synuclein nitration in synucleinopathy lesions. *Science* **290**, 985-989, doi:DOI 10.1126/science.290.5493.985 (2000).

82    Hasegawa, M. *et al.* Phosphorylated alpha-synuclein is ubiquitinated in alpha-synucleinopathy lesions. *J Biol Chem* **277**, 49071-49076, doi:10.1074/jbc.M208046200 (2002).

83    Dorval, V. & Fraser, P. E. Small ubiquitin-like modifier (SUMO) modification of natively unfolded proteins tau and alpha-synuclein. *J Biol Chem* **281**, 9919-9924, doi:10.1074/jbc.M510127200 (2006).

84    Junn, E., Ronchetti, R. D., Quezado, M. M., Kim, S. Y. & Mouradian, M. M. Tissue transglutaminase-induced aggregation of alpha-synuclein: Implications for Lewy body formation in Parkinson's disease and dementia with Lewy bodies. *P Natl Acad Sci USA* **100**, 2047-2052, doi:10.1073/pnas.0438021100 (2003).

85    Uversky, V. N. *et al.* Methionine oxidation inhibits fibrillation of human alpha-synuclein in vitro. *Febs Lett* **517**, 239-244, doi:S0014579302026388 [pii] (2002).

86    Oueslati, A. Implication of Alpha-Synuclein Phosphorylation at S129 in Synucleinopathies: What Have We Learned in the Last Decade? *J Parkinson Dis* **6**, 39-51, doi:10.3233/Jpd-160779 (2016).

87    Cookson, M. R. The biochemistry of Parkinson's disease. *Annu Rev Biochem* **74**, 29-52, doi:10.1146/annurev.biochem.74.082803.133400 (2005).

88    Rodriguez, J. A. *et al.* Structure of the toxic core of alpha-synuclein from invisible crystals. *Nature* **525**, 486-490, doi:10.1038/nature15368

nature15368 [pii] (2015).

89    Tuttle, M. D. *et al.* Solid-state NMR structure of a pathogenic fibril of full-length human alpha-synuclein. *Nat Struct Mol Biol* **23**, 409-415, doi:10.1038/nsmb.3194

nsmb.3194 [pii] (2016).

90    Villar-Pique, A., Lopes da Fonseca, T. & Outeiro, T. F. Structure, function and toxicity of alpha-synuclein: the Bermuda triangle in synucleinopathies. *J Neurochem* **139 Suppl 1**, 240-255, doi:10.1111/jnc.13249 (2016).

91    Goldstein, D. S., Kopin, I. J. & Sharabi, Y. Catecholamine autotoxicity. Implications for pharmacology and therapeutics of Parkinson disease and related disorders. *Pharmacol Ther* **144**, 268-282, doi:10.1016/j.pharmthera.2014.06.006

S0163-7258(14)00123-5 [pii] (2014).

92    Meiser, J., Weindl, D. & Hiller, K. Complexity of dopamine metabolism. *Cell Commun Signal* **11**, doi:Artn 34

10.1186/1478-811x-11-34 (2013).

93    Marchitti, S. A., Deitrich, R. A. & Vasiliou, V. Neurotoxicity and metabolism of the catecholamine-derived 3,4-dihydroxyphenylacetaldehyde and 3,4-dihydroxyphenylglycolaldehyde: The role of aldehyde dehydrogenase. *Pharmacol Rev* **59**, 125-150, doi:10.1124/pr.59.2.1 (2007).

94    Doorn, J. A., Florang, V. R., Schamp, J. H. & Vanle, B. C. Aldehyde dehydrogenase inhibition generates a reactive dopamine metabolite autotoxic to dopamine neurons. *Parkinsonism Relat Disord* **20 Suppl 1**, S73-75, doi:10.1016/S1353-8020(13)70019-1

S1353-8020(13)70019-1 [pii] (2014).

95    Anderson, D. G., Mariappan, S. V. S., Buettner, G. R. & Doorn, J. A. Oxidation of 3,4-Dihydroxyphenylacetaldehyde, a Toxic Dopaminergic Metabolite, to a Semiquinone Radical and an ortho-Quinone. *J Biol Chem* **286**, 26978-26986, doi:10.1074/jbc.M111.249532 (2011).

96    Goldstein, D. S. *et al.* Determinants of buildup of the toxic dopamine metabolite DOPAL in Parkinson's disease. *J Neurochem* **126**, 591-603, doi:10.1111/jnc.12345 (2013).

97    Rees, J. N., Florang, V. R., Eckert, L. L. & Doorn, J. A. Protein Reactivity of 3,4-Dihydroxyphenylacetaldehyde, a Toxic Dopamine Metabolite, Is Dependent on Both

the Aldehyde and the Catechol. *Chem Res Toxicol* **22**, 1256-1263, doi:10.1021/tx9000557 (2009).

98    Fitzmaurice, A. G., Rhodes, S. L., Cockburn, M., Ritz, B. & Bronstein, J. M. Aldehyde dehydrogenase variation enhances effect of pesticides associated with Parkinson disease. *Neurology* **82**, 419-426, doi:10.1212/Wnl.0000000000000083 (2014).

99    Goldstein, D. S. *et al.* Catechols in post-mortem brain of patients with Parkinson disease. *Eur J Neurol* **18**, 703-710, doi:10.1111/j.1468-1331.2010.03246.x (2011).

100   Liu, G. X. *et al.* Aldehyde dehydrogenase 1 defines and protects a nigrostriatal dopaminergic neuron subpopulation. *Journal of Clinical Investigation* **124**, 3032-3046, doi:10.1172/JCI72176 (2014).

101   Wey, M. C. Y. *et al.* Neurodegeneration and Motor Dysfunction in Mice Lacking Cytosolic and Mitochondrial Aldehyde Dehydrogenases: Implications for Parkinson's Disease. *PLoS One* **7**, doi:ARTN e31522

10.1371/journal.pone.0031522 (2012).

102   Fitzmaurice, A. G. *et al.* Aldehyde dehydrogenase inhibition as a pathogenic mechanism in Parkinson disease. *P Natl Acad Sci USA* **110**, 636-641, doi:10.1073/pnas.1220399110 (2013).

103   Koppaka, V. *et al.* Aldehyde Dehydrogenase Inhibitors: a Comprehensive Review of the Pharmacology, Mechanism of Action, Substrate Specificity, and Clinical Application. *Pharmacol Rev* **64**, 520-539, doi:10.1124/pr.111.005538 (2012).

104   Plotegher, N. & Bubacco, L. Lysines, Achilles' heel in alpha-synuclein conversion to a deadly neuronal endotoxin. *Ageing Res Rev* **26**, 62-71, doi:10.1016/j.arr.2015.12.002 (2016).

105   Burke, W. J. *et al.* Aggregation of alpha-synuclein by DOPAL, the monoamine oxidase metabolite of dopamine. *Acta Neuropathologica* **115**, 193-203, doi:10.1007/s00401-007-0303-9 (2008).

106   Plotegher, N. *et al.* DOPAL derived alpha-synuclein oligomers impair synaptic vesicles physiological function. *Sci Rep* **7**, 40699, doi:10.1038/srep40699

srep40699 [pii] (2017).

107   N. Plotegher, G. B., E. Ferrari, I. Tessari, M. Zanetti, L. Lunelli, E. Greggio, M. Bisaglia, M. Veronesi, S. Girotto, M. Dalla Serra, C. Perego, L. Casella, L. Bubacco. DOPAL derived alpha-synuclein oligomers impair synaptic vesicles physiological function *Sci Rep-Uk* (2016).

108   Follmer, C. *et al.* Oligomerization and Membrane-binding Properties of Covalent Adducts Formed by the Interaction of alpha-Synuclein with the Toxic Dopamine Metabolite 3,4-Dihydroxyphenylacetaldehyde (DOPAL). *J Biol Chem* **290**, 27660-27679, doi:10.1074/jbc.M115.686584

M115.686584 [pii] (2015).

109   Braak, H. *et al.* Staging of brain pathology related to sporadic Parkinson's disease. *Neurobiol Aging* **24**, 197-211, doi:Pii S0197-4580(02)00065-9

Doi 10.1016/S0197-4580(02)00065-9 (2003).

110   Visanji, N. P., Brooks, P. L., Hazrati, L. N. & Lang, A. E. The prion hypothesis in Parkinson's disease: Braak to the future. *Acta Neuropathol Commun* **1**, 2, doi:10.1186/2051-5960-1-2

2051-5960-1-2 [pii] (2013).

111   Brettschneider, J., Del Tredici, K., Lee, V. M. Y. & Trojanowski, J. Q. Spreading of pathology in neurodegenerative diseases: a focus on human studies. *Nature Reviews Neuroscience* **16**, 109-120, doi:10.1038/nrn3887 (2015).

112    da Fonseca, T. L., Villar-Pique, A. & Outeiro, T. F. The Interplay between Alpha-Synuclein Clearance and Spreading. *Biomolecules* **5**, 435-471, doi:10.3390/biom5020435 (2015).

113    Li, J. Y. *et al.* Lewy bodies in grafted neurons in subjects with Parkinson's disease suggest host-to-graft disease propagation. *Nat Med* **14**, 501-503, doi:10.1038/nm1746 nm1746 [pii] (2008).

114    Kordower, J. H., Chu, Y., Hauser, R. A., Freeman, T. B. & Olanow, C. W. Lewy body-like pathology in long-term embryonic nigral transplants in Parkinson's disease. *Nat Med* **14**, 504-506, doi:10.1038/nm1747 nm1747 [pii] (2008).

115    Kordower, J. H., Chu, Y., Hauser, R. A., Olanow, C. W. & Freeman, T. B. Transplanted dopaminergic neurons develop PD pathologic changes: a second case report. *Mov Disord* **23**, 2303-2306, doi:10.1002/mds.22369 (2008).

116    Hansen, C. *et al.* alpha-Synuclein propagates from mouse brain to grafted dopaminergic neurons and seeds aggregation in cultured human cells. *Journal of Clinical Investigation* **121**, 715-725, doi:10.1172/JCI43366 (2011).

117    El-Agnaf, O. M. A. *et al.* alpha-synuclein implicated in Parkinson's disease is present in extracellular biological fluids, including human plasma. *Faseb J* **17**, 1945-+, doi:10.1096/fj.03-0098fje (2003).

118    Abd-Elhadi, S., Basora, M., Vilas, D., Tolosa, E. & Sharon, R. Total alpha-synuclein levels in human blood cells, CSF, and saliva determined by a lipid-ELISA. *Anal Bioanal Chem*, doi:10.1007/s00216-016-9863-7 10.1007/s00216-016-9863-7 [pii] (2016).

119    Vivacqua, G. *et al.* Abnormal Salivary Total and Oligomeric Alpha-Synuclein in Parkinson's Disease. *PLoS One* **11**, doi:ARTN e0151156 10.1371/journal.pone.0151156 (2016).

120    Paleologou, K. E. *et al.* Detection of elevated levels of soluble alpha-synuclein oligomers in post-mortem brain extracts from patients with dementia with Lewy bodies. *Brain* **132**, 1093-1101, doi:10.1093/brain/awn349 awn349 [pii] (2009).

121    Parnetti, L. *et al.* Cerebrospinal fluid lysosomal enzymes and alpha-synuclein in Parkinson's disease. *Mov Disord* **29**, 1019-1027, doi:10.1002/mds.25772 (2014).

122    Cersosimo, M. G. Gastrointestinal Biopsies for the Diagnosis of Alpha-Synuclein Pathology in Parkinson's Disease. *Gastroent Res Pract*, doi:Artn 476041 10.1155/2015/476041 (2015).

123    Xu, L. J. & Pu, J. L. Alpha-Synuclein in Parkinson's Disease: From Pathogenetic Dysfunction to Potential Clinical Application. *Parkinsons Dis-Us*, doi:Artn 1720621 10.1155/2016/1720621 (2016).

124    Costanzo, M. & Zurzolo, C. The cell biology of prion-like spread of protein aggregates: mechanisms and implication in neurodegeneration. *Biochem J* **452**, 1-17, doi:10.1042/BJ20121898 BJ20121898 [pii] (2013).

125    Lee, H. J., Patel, S. & Lee, S. J. Intravesicular localization and exocytosis of alpha-synuclein and its aggregates. *J Neurosci* **25**, 6016-6024, doi:25/25/6016 [pii] 10.1523/JNEUROSCI.0692-05.2005 (2005).

126    Danzer, K. M. *et al.* Exosomal cell-to-cell transmission of alpha synuclein oligomers. *Mol Neurodegener* **7**, 42, doi:10.1186/1750-1326-7-42 #N/A [pii] (2012).

127    Emmanouilidou, E. *et al.* Cell-produced alpha-synuclein is secreted in a calcium-dependent manner by exosomes and impacts neuronal survival. *J Neurosci* **30**, 6838-6851, doi:10.1523/JNEUROSCI.5699-09.2010

30/20/6838 [pii] (2010).

128    Hansen, C. *et al.* alpha-Synuclein propagates from mouse brain to grafted dopaminergic neurons and seeds aggregation in cultured human cells. *J Clin Invest* **121**, 715-725, doi:10.1172/JCI43366

43366 [pii] (2011).

129    Mao, X. *et al.* Pathological alpha-synuclein transmission initiated by binding lymphocyte-activation gene 3. *Science* **353**, doi:aah3374 [pii]

353/6307/aah3374 [pii]

10.1126/science.aah3374 (2016).

130    Freundt, E. C. *et al.* Neuron-to-neuron transmission of alpha-synuclein fibrils through axonal transport. *Annals of Neurology* **72**, 517-524, doi:10.1002/ana.23747 (2012).

131    Jang, A. *et al.* Non-classical exocytosis of alpha-synuclein is sensitive to folding states and promoted under stress conditions. *J Neurochem* **113**, 1263-1274, doi:10.1111/j.1471-4159.2010.06695.x (2010).

132    Masuda-Suzukake, M. *et al.* Pathological alpha-synuclein propagates through neural networks. *Acta Neuropathol Commun* **2**, 88, doi:10.1186/s40478-014-0088-8

s40478-014-0088-8 [pii]

10.1186/PREACCEPT-1296467154135944 (2014).

133    Abounit, S. *et al.* Tunneling nanotubes spread fibrillar alpha-synuclein by intercellular trafficking of lysosomes. *EMBO J* **35**, 2120-2138, doi:embj.201593411 [pii]

10.15252/embj.201593411 (2016).

134    Lee, H. J. *et al.* Dopamine promotes formation and secretion of non-fibrillar alpha-synuclein oligomers. *Exp Mol Med* **43**, 216-222, doi:10.3858/emm.2011.43.4.026 (2011).

135    Emmanouilidou, E. *et al.* GABA transmission via ATP-dependent K+ channels regulates alpha-synuclein secretion in mouse striatum. *Brain* **139**, 871-890, doi:10.1093/brain/awv403

awv403 [pii] (2016).

136    Kondo, K., Obitsu, S. & Teshima, R. alpha-Synuclein aggregation and transmission are enhanced by leucine-rich repeat kinase 2 in human neuroblastoma SH-SY5Y cells. *Biol Pharm Bull* **34**, 1078-1083, doi:JST.JSTAGE/bpb/34.1078 [pii] (2011).

137    Fares, M. B. *et al.* The novel Parkinson's disease linked mutation G51D attenuates in vitro aggregation and membrane binding of alpha-synuclein, and enhances its secretion and nuclear localization in cells. *Hum Mol Genet* **23**, 4491-4509, doi:10.1093/hmg/ddu165 (2014).

138    Khalaf, O. *et al.* The H50Q mutation enhances alpha-synuclein aggregation, secretion, and toxicity. *J Biol Chem* **289**, 21856-21876, doi:10.1074/jbc.M114.553297

M114.553297 [pii] (2014).

139    Villarroya-Beltri, C., Baixauli, F., Gutierrez-Vazquez, C., Sanchez-Madrid, F. & Mittelbrunn, M. Sorting it out: regulation of exosome loading. *Semin Cancer Biol* **28**, 3-13, doi:10.1016/j.semcancer.2014.04.009

S1044-579X(14)00057-1 [pii] (2014).

140    Shi, M. *et al.* Plasma exosomal alpha-synuclein is likely CNS-derived and increased in Parkinson's disease. *Acta Neuropathol* **128**, 639-650, doi:10.1007/s00401-014-1314-y (2014).

141    El Andaloussi, S., Lakhal, S., Mager, I. & Wood, M. J. Exosomes for targeted siRNA delivery across biological barriers. *Adv Drug Deliv Rev* **65**, 391-397, doi:10.1016/j.addr.2012.08.008
S0169-409X(12)00243-8 [pii] (2013).

142    Alvarez-Erviti, L. *et al.* Lysosomal dysfunction increases exosome-mediated alpha-synuclein release and transmission. *Neurobiol Dis* **42**, 360-367, doi:10.1016/j.nbd.2011.01.029 (2011).

143    Colombo, E., Borgiani, B., Verderio, C. & Furlan, R. Microvesicles: novel biomarkers for neurological disorders. *Front Physiol* **3**, doi:Unsp 63
10.3389/Fphys.2012.00063 (2012).

144    Trajkovic, K. Ceramide triggers budding of exosome vesicles into multivesicular endosomes (vol 319, pg 1244, 2008). *Science* **320**, 179-179 (2008).

145    Basso, M. & Bonetto, V. Extracellular Vesicles and a Novel Form of Communication in the Brain. *Front Neurosci-Switz* **10**, doi:Artn 127
10.3389/Fnins.2016.00127 (2016).

146    Escola, J. M. *et al.* Selective enrichment of tetraspan proteins on the internal vesicles of multivesicular endosomes and on exosomes secreted by human B-lymphocytes. *J Biol Chem* **273**, 20121-20127, doi:DOI 10.1074/jbc.273.32.20121 (1998).

147    Yanez-Mo, M., Barreiro, O., Gordon-Alonso, M., Sala-Valdes, M. & Sanchez-Madrid, F. Tetraspanin-enriched microdomains: a functional unit in cell plasma membranes. *Trends in Cell Biology* **19**, 434-446, doi:10.1016/j.tcb.2009.06.004 (2009).

148    Perez-Hernandez, D. *et al.* The Intracellular Interactome of Tetraspanin-enriched Microdomains Reveals Their Function as Sorting Machineries toward Exosomes. *J Biol Chem* **288**, 11649-11661, doi:10.1074/jbc.M112.445304 (2013).

149    Mazurov, D., Barbashova, L. & Filatov, A. Tetraspanin protein CD9 interacts with metalloprotease CD10 and enhances its release via exosomes. *Febs J* **280**, 1200-1213, doi:10.1111/febs.12110 (2013).

150    Kong, S. M. Y. *et al.* Parkinson's disease-linked human PARK9/ATP13A2 maintains zinc homeostasis and promotes alpha-Synuclein externalization via exosomes. *Hum Mol Genet* **23**, 2816-2833, doi:10.1093/hmg/ddu099 (2014).

151    Villarroya-Beltri, C., Baixauli, F., Gutierrez-Vazquez, C., Sanchez-Madrid, F. & Mittelbrunn, M. Sorting it out: Regulation of exosome loading. *Seminars in Cancer Biology* **28**, 3-13, doi:10.1016/j.semcancer.2014.04.009 (2014).

152    Colombo, M., Raposo, G. & Thery, C. Biogenesis, Secretion, and Intercellular Interactions of Exosomes and Other Extracellular Vesicles. *Annu Rev Cell Dev Bi* **30**, 255-289, doi:10.1146/annurev-cellbio-101512-122326 (2014).

153    Binotti, B., Jahn, R. & Chua, J. J. Functions of Rab Proteins at Presynaptic Sites. *Cells* **5**, doi:10.3390/cells5010007
E7 [pii]
cells5010007 [pii] (2016).

154    Savina, A., Fader, C. M., Damiani, M. T. & Colombo, M. I. Rab11 promotes docking and fusion of multivesicular bodies in a calcium-dependent manner. *Traffic* **6**, 131-143, doi:10.1111/j.1600-0854.2004.00257.x (2005).

155    Chutna, O. *et al.* The small GTPase Rab11 co-localizes with alpha-synuclein in intracellular inclusions and modulates its aggregation, secretion and toxicity. *Hum Mol Genet* **23**, 6732-6745, doi:10.1093/hmg/ddu391 (2014).

156    Kelly, E. E., Horgan, C. P., Goud, B. & McCaffrey, M. W. The Rab family of proteins: 25 years on. *Biochem Soc T* **40**, 1337-1347, doi:10.1042/Bst20120203 (2012).

157    Ducharme, N. A., Ham, A. J., Lapierre, L. A. & Goldenring, J. R. Rab11-FIP2 influences multiple components of the endosomal system in polarized MDCK cells. *Cell Logist* **1**, 57-68, doi:10.4161/cl.1.2.15289

2159-2780-1-2-5 [pii] (2011).

158    Hoshino, D. *et al.* Exosome Secretion Is Enhanced by Invadopodia and Drives Invasive Behavior. *Cell Rep* **5**, 1159-1168, doi:10.1016/j.celrep.2013.10.050 (2013).

159    Takata, K. Aquaporin-2 (Aqp2): Its Intracellular Compartment and Trafficking. *Cell Mol Biol* **52**, 34-39, doi:10.1170/T747 (2006).

160    Jahn, R. & Scheller, R. H. SNAREs - engines for membrane fusion. *Nat Rev Mol Cell Bio* **7**, 631-643, doi:10.1038/nrm2002 (2006).

161    Rothman, J. E. & Warren, G. Implications of the Snare Hypothesis for Intracellular Membrane Topology and Dynamics. *Curr Biol* **4**, 220-233, doi:Doi 10.1016/S0960-9822(00)00051-8 (1994).

162    Sollner, T., Bennett, M. K., Whiteheart, S. W., Scheller, R. H. & Rothman, J. E. A Protein Assembly-Disassembly Pathway in-Vitro That May Correspond to Sequential Steps of Synaptic Vesicle Docking, Activation, and Fusion. *Cell* **75**, 409-418, doi:Doi 10.1016/0092-8674(93)90376-2 (1993).

163    Fader, C. M., Sanchez, D. G., Mestre, M. B. & Colombo, M. I. TI-VAMP/VAMP7 and VAMP3/cellubrevin: two v-SNARE proteins involved in specific steps of the autophagy/multivesicular body pathways. *Bba-Mol Cell Res* **1793**, 1901-1916, doi:10.1016/j.bbamcr.2009.09.011 (2009).

164    Liegeois, S., Benedetto, A., Garnier, J. M., Schwab, Y. & Labouesse, M. The V0-ATPase mediates apical secretion of exosomes containing Hedgehog-related proteins in Caenorhabditis elegans. *Journal of Cell Biology* **173**, 949-961, doi:DOI 10.1083/jcb.200511072 (2006).

165    Thery, C. *et al.* Proteomic analysis of dendritic cell-derived exosomes: A secreted subcellular compartment distinct from apoptotic vesicles. *J Immunol* **166**, 7309-7318 (2001).

166    Mathivanan, S., Fahner, C. J., Reid, G. E. & Simpson, R. J. ExoCarta 2012: database of exosomal proteins, RNA and lipids. *Nucleic Acids Res* **40**, D1241-D1244, doi:10.1093/nar/gkr828 (2012).

167    Thery, C. Exosomes: secreted vesicles and intercellular communications. *F1000 Biol Rep* **3**, 15, doi:10.3410/B3-15

15 [pii] (2011).

168    Gupta, A. & Pulliam, L. Exosomes as mediators of neuroinflammation. *J Neuroinflamm* **11**, doi:Artn 68

10.1186/1742-2094-11-68 (2014).

169    Ratajczak, J. *et al.* Embryonic stem cell-derived microvesicles reprogram hematopoietic progenitors: evidence for horizontal transfer of mRNA and protein delivery. *Leukemia* **20**, 847-856, doi:10.1038/sj.leu.2404132 (2006).

170    Valadi, H. *et al.* Exosome-mediated transfer of mRNAs and microRNAs is a novel mechanism of genetic exchange between cells. *Nat Cell Biol* **9**, 654-U672, doi:10.1038/ncb1596 (2007).

171    Azmi, A. S., Bao, B. & Sarkar, F. H. Exosomes in cancer development, metastasis, and drug resistance: a comprehensive review. *Cancer Metast Rev* **32**, 623-642, doi:10.1007/s10555-013-9441-9 (2013).

172    Fruhbeis, C. *et al.* Neurotransmitter-Triggered Transfer of Exosomes Mediates Oligodendrocyte-Neuron Communication. *Plos Biol* **11**, doi:ARTN e1001604

10.1371/journal.pbio.1001604 (2013).

173     Hwang, I., Shen, X. & Sprent, J. Direct stimulation of naive T cells by membrane vesicles from antigen-presenting cells: distinct roles for CD54 and B7 molecules. *Proc Natl Acad Sci U S A* **100**, 6670-6675, doi:10.1073/pnas.1131852100
1131852100 [pii] (2003).

174     Nazarenko, I. Cell Surface Tetraspanin Tspan8 Contributes to Molecular Pathways of Exosome-Induced Endothelial Cell Activation (vol 70, pg 1668, 2010). *Cancer Res* **70**, doi:10.1158/0008-5472.CAN-10-2521 (2010).

175     Hwang, I. *et al.* T cells can use either T cell receptor or CD28 receptors to absorb and internalize cell surface molecules derived from antigen-presenting cells. *J Exp Med* **191**, 1137-1148, doi:DOI 10.1084/jem.191.7.1137 (2000).

176     Miyanishi, M. *et al.* Identification of Tim4 as a phosphatidylserine receptor. *Nature* **450**, 435-439, doi:10.1038/nature06307 (2007).

177     Saunderson, S. C., Dunn, A. C., Crocker, P. R. & McLellan, A. D. CD169 mediates the capture of exosomes in spleen and lymph node. *Blood* **123**, 208-216, doi:10.1182/blood-2013-03-489732 (2014).

178     Barres, C. *et al.* Galectin-5 is bound onto the surface of rat reticulocyte exosomes and modulates vesicle uptake by macrophages. *Blood* **115**, 696-705, doi:10.1182/blood-2009-07-231449 (2010).

179     Christianson, H. C., Svensson, K. J., van Kuppevelt, T. H., Li, J. P. & Belting, M. Cancer cell exosomes depend on cell-surface heparan sulfate proteoglycans for their internalization and functional activity. *P Natl Acad Sci USA* **110**, 17380-17385, doi:10.1073/pnas.1304266110 (2013).

180     Record, M., Carayon, K., Poirot, M. & Silvente-Poirot, S. Exosomes as new vesicular lipid transporters involved in cell-cell communication and various pathophysiologies. *Bba-Mol Cell Biol L* **1841**, 108-120, doi:10.1016/j.bbalip.2013.10.004 (2014).

181     Fitzner, D. *et al.* Selective transfer of exosomes from oligodendrocytes to microglia by macropinocytosis. *J Cell Sci* **124**, 447-458, doi:10.1242/jcs.074088 (2011).

182     Fruhbeis, C. *et al.* Neurotransmitter-triggered transfer of exosomes mediates oligodendrocyte-neuron communication. *Plos Biol* **11**, e1001604, doi:10.1371/journal.pbio.1001604
PBIOLOGY-D-13-01553 [pii] (2013).

183     Nanbo, A., Kawanishi, E., Yoshida, R. & Yoshiyama, H. Exosomes Derived from Epstein-Barr Virus-Infected Cells Are Internalized via Caveola-Dependent Endocytosis and Promote Phenotypic Modulation in Target Cells. *J Virol* **87**, 10334-10347, doi:10.1128/Jvi.01310-13 (2013).

184     Feng, D. *et al.* Cellular Internalization of Exosomes Occurs Through Phagocytosis. *Traffic* **11**, 675-687, doi:10.1111/j.1600-0854.2010.01041.x (2010).

185     Abrami, L. *et al.* Hijacking Multivesicular Bodies Enables Long-Term and Exosome-Mediated Long-Distance Action of Anthrax Toxin. *Cell Rep* **5**, 986-996, doi:10.1016/j.celrep.2013.10.019 (2013).

186     Street, J. M. *et al.* Identification and proteomic profiling of exosomes in human cerebrospinal fluid. *J Transl Med* **10**, doi:Artn 5
10.1186/1479-5876-10-5 (2012).

187     Banigan, M. G. *et al.* Differential Expression of Exosomal microRNAs in Prefrontal Cortices of Schizophrenia and Bipolar Disorder Patients. *PLoS One* **8**, doi:ARTN e48814
10.1371/journal.pone.0048814 (2013).

188     Bakhti, M., Winter, C. & Simons, M. Inhibition of Myelin Membrane Sheath Formation by Oligodendrocyte-derived Exosome-like Vesicles. *J Biol Chem* **286**, 787-796, doi:10.1074/jbc.M110.190009 (2011).

189     Wang, S. W. *et al.* Synapsin I Is an Oligomannose-Carrying Glycoprotein, Acts As an Oligomannose-Binding Lectin, and Promotes Neurite Outgrowth and Neuronal Survival When Released via Glia-Derived Exosomes. *Journal of Neuroscience* **31**, 7275-7290, doi:10.1523/Jneurosci.6476-10.2011 (2011).

190     Antonucci, F. *et al.* Microvesicles released from microglia stimulate synaptic activity via enhanced sphingolipid metabolism. *Embo Journal* **31**, 1231-1240, doi:10.1038/emboj.2011.489 (2012).

191     Taylor, A. R., Robinson, M. B., Gifondorwa, D. J., Tytell, M. & Milligan, C. E. Regulation of heat shock protein 70 release in astrocytes: Role of signaling kinases. *Dev Neurobiol* **67**, 1815-1829, doi:10.1002/dneu.20559 (2007).

192     Tytell, M. Release of heat shock proteins (Hsps) and the effects of extracellular Hsps on neural cells and tissues. *Int J Hyperther* **21**, 445-455, doi:10.1080/02656730500041921 (2005).

193     Lopez-Verrilli, M. A., Picou, F. & Court, F. A. Schwann Cell-Derived Exosomes Enhance Axonal Regeneration in the Peripheral Nervous System. *Glia* **61**, 1795-1806, doi:10.1002/glia.22558 (2013).

194     Stuendl, A. *et al.* Induction of alpha-synuclein aggregate formation by CSF exosomes from patients with Parkinson's disease and dementia with Lewy bodies. *Brain* **139**, 481-494, doi:10.1093/brain/awv346

awv346 [pii] (2016).

195     Cooper, J. M. *et al.* Systemic exosomal siRNA delivery reduced alpha-synuclein aggregates in brains of transgenic mice. *Mov Disord* **29**, 1476-1485, doi:10.1002/mds.25978 (2014).

196     Lee, H. J. *et al.* Direct Transfer of alpha-Synuclein from Neuron to Astroglia Causes Inflammatory Responses in Synucleinopathies. *J Biol Chem* **285**, 9262-9272, doi:10.1074/jbc.M109.081125 (2010).

197     Bliederhaeuser, C. *et al.* Age-dependent defects of alpha-synuclein oligomer uptake in microglia and monocytes. *Acta Neuropathol* **131**, 379-391, doi:10.1007/s00401-015-1504-2

10.1007/s00401-015-1504-2 [pii] (2016).

198     Russo, I., Bubacco, L. & Greggio, E. Exosomes-associated neurodegeneration and progression of Parkinson's disease. *Am J Neurodegener Dis* **1**, 217-225 (2012).

199     Xiong, Y. L. *et al.* GTPase Activity Plays a Key Role in the Pathobiology of LRRK2. *Plos Genet* **6**, doi:ARTN e1000902

10.1371/journal.pgen.1000902 (2010).

200     Alegre-Abarrategui, J. & Wade-Martins, R. Parkinson disease, LRRK2 and the endocytic-autophagic pathway. *Autophagy* **5**, 1208-1210 (2009).

201     Wilhelm, B. G. *et al.* Composition of isolated synaptic boutons reveals the amounts of vesicle trafficking proteins. *Science* **344**, 1023-1028, doi:10.1126/science.1252884

344/6187/1023 [pii] (2014).

202     Withers, G. S., George, J. M., Banker, G. A. & Clayton, D. F. Delayed localization of synelfin (synuclein, NACP) to presynaptic terminals in cultured rat hippocampal neurons. *Dev Brain Res* **99**, 87-94, doi:Doi 10.1016/S0165-3806(96)00210-6 (1997).

203     Zaltieri, M. *et al.* alpha-synuclein and synapsin III cooperatively regulate synaptic function in dopamine neurons. *J Cell Sci* **128**, 2231-2243, doi:10.1242/jcs.157867 (2015).

204     George, J. M., Jin, H., Woods, W. S. & Clayton, D. F. Characterization of a Novel Protein Regulated during the Critical Period for Song Learning in the Zebra Finch. *Neuron* **15**, 361-372, doi:Doi 10.1016/0896-6273(95)90040-3 (1995).

205     Iwai, A. *et al.* The Precursor Protein of Non-a-Beta Component of Alzheimers-Disease Amyloid Is a Presynaptic Protein of the Central-Nervous-System. *Neuron* **14**, 467-475, doi:Doi 10.1016/0896-6273(95)90302-X (1995).

206     Murphy, D. D., Rueter, S. M., Trojanowski, J. Q. & Lee, V. M. Y. Synucleins are developmentally expressed, and alpha-synuclein regulates the size of the presynaptic vesicular pool in primary hippocampal neurons. *Journal of Neuroscience* **20**, 3214-3220 (2000).

207     Burre, J. *et al.* Alpha-synuclein promotes SNARE-complex assembly in vivo and in vitro. *Science* **329**, 1663-1667, doi:10.1126/science.1195227 science.1195227 [pii] (2010).

208     Fortin, D. L. *et al.* Lipid rafts mediate the synaptic localization of alpha-synuclein. *Journal of Neuroscience* **24**, 6715-6723, doi:10.1523/Jneurosci.1594-04.2004 (2004).

209     Totterdell, S., Hanger, D. & Meredith, G. E. The ultrastructural distribution of alpha-synuclein-like protein in normal mouse brain. *Brain Res* **1004**, 61-72, doi:10.1016/j.brainres.2003.10.072 (2004).

210     Petersen, K., Olesen, O. F. & Mikkelsen, J. D. Developmental expression of alpha-synuclein in rat hippocampus and cerebral cortex. *Neuroscience* **91**, 651-659, doi:Doi 10.1016/S0306-4522(98)00596-X (1999).

211     Burre, J., Sharma, M. & Sudhof, T. C. alpha-Synuclein assembles into higher-order multimers upon membrane binding to promote SNARE complex formation. *P Natl Acad Sci USA* **111**, E4274-E4283, doi:10.1073/pnas.1416598111 (2014).

212     Maroteaux, L., Campanelli, J. T. & Scheller, R. H. Synuclein - a Neuron-Specific Protein Localized to the Nucleus and Presynaptic Nerve-Terminal. *Journal of Neuroscience* **8**, 2804-2815 (1988).

213     Fortin, D. L. *et al.* Neural activity controls the synaptic accumulation of alpha-synuclein. *Journal of Neuroscience* **25**, 10913-10921, doi:10.1523/Jneurosci.2922-05.2005 (2005).

214     Fortin, D. L., Nemani, V. M., Nakamura, K. & Edwards, R. H. The Behavior of alpha-Synuclein in Neurons. *Movement Disord* **25**, S21-S26, doi:10.1002/mds.22722 (2010).

215     Lai, Y. *et al.* Nonaggregated alpha-Synuclein Influences SNARE-Dependent Vesicle Docking via Membrane Binding. *Biochemistry-Us* **53**, 3889-3896, doi:10.1021/bi5002536 (2014).

216     Diao, J. J. *et al.* Native alpha-synuclein induces clustering of synaptic-vesicle mimics via binding to phospholipids and synaptobrevin-2/VAMP2. *Elife* **2**, doi:ARTN e00592 10.7554/eLife.00592 (2013).

217     Schoch, S. *et al.* SNARE function analyzed in synaptobrevin/VAMP knockout mice. *Science* **294**, 1117-1122, doi:DOI 10.1126/science.1064335 (2001).

218     Lee, S. J., Jeon, H. & Kandror, K. V. alpha-Synuclein is localized in a subpopulation of rat brain synaptic vesicles. *Acta Neurobiol Exp* **68**, 509-515 (2008).

219     Zaltieri, M. *et al.* alpha-synuclein and synapsin III cooperatively regulate synaptic function in dopamine neurons. *J Cell Sci* **128**, 2231-2243, doi:10.1242/jcs.157867 jcs.157867 [pii] (2015).

220     Cabin, D. E. *et al.* Synaptic vesicle depletion correlates with attenuated synaptic responses to prolonged repetitive stimulation in mice lacking alpha-synuclein. *Journal of Neuroscience* **22**, 8797-8807 (2002).

221     Burre, J. *et al.* alpha-Synuclein Promotes SNARE-Complex Assembly in Vivo and in Vitro. *Science* **329**, 1663-1667, doi:10.1126/science.1195227 (2010).

222     Gordon, S. L. & Cousin, M. A. The Sybtraps: control of synaptobrevin traffic by synaptophysin, alpha-synuclein and AP-180. *Traffic* **15**, 245-254, doi:10.1111/tra.12140 (2014).

223    Spillantini, M. G. *et al.* alpha-synuclein in Lewy bodies. *Nature* **388**, 839-840, doi:Doi 10.1038/42166 (1997).

224    Baba, M. *et al.* Aggregation of alpha-synuclein in Lewy bodies of sporadic Parkinson's disease and dementia with lewy bodies. *Am J Pathol* **152**, 879-884 (1998).

225    Beach, T. G. *et al.* Unified staging system for Lewy body disorders: correlation with nigrostriatal degeneration, cognitive impairment and motor dysfunction. *Acta Neuropathologica* **117**, 613-634, doi:10.1007/s00401-009-0538-8 (2009).

226    Kramer, M. L. & Schulz-Schaeffer, W. J. Presynaptic alpha-synuclein aggregates, not Lewy bodies, cause neurodegeneration in dementia with Lewy bodies. *Journal of Neuroscience* **27**, 1405-1410, doi:10.1523/Jneurosci.4564-06.2007 (2007).

227    Milber, J. M. *et al.* Lewy pathology is not the first sign of degeneration in vulnerable neurons in Parkinson disease. *Neurology* **79**, 2307-2314, doi:10.1212/WNL.0b013e318278fe32 WNL.0b013e318278fe32 [pii] (2012).

228    Winner, B. *et al.* In vivo demonstration that alpha-synuclein oligomers are toxic. *P Natl Acad Sci USA* **108**, 4194-4199, doi:10.1073/pnas.1100976108 (2011).

229    Karpinar, D. P. *et al.* Pre-fibrillar alpha-synuclein variants with impaired beta-structure increase neurotoxicity in Parkinson's disease models. *Embo Journal* **28**, 3256-3268, doi:10.1038/emboj.2009.257 (2009).

230    Hsu, L. J. *et al.* Expression pattern of synucleins (non-Abeta component of Alzheimer's disease amyloid precursor protein/alpha-synuclein) during murine brain development. *J Neurochem* **71**, 338-344 (1998).

231    Burre, J., Sharma, M. & Sudhof, T. C. Systematic Mutagenesis of alpha-Synuclein Reveals Distinct Sequence Requirements for Physiological and Pathological Activities. *Journal of Neuroscience* **32**, 15227-15242, doi:10.1523/Jneurosci.3545-12.2012 (2012).

232    Choi, H. S. *et al.* Phosphorylation of alpha-synuclein is crucial in compensating for proteasomal dysfunction. *Biochem Biophys Res Commun* **424**, 597-603, doi:10.1016/j.bbrc.2012.06.159 S0006-291X(12)01272-7 [pii] (2012).

233    Rockenstein, E. *et al.* Accumulation of oligomer-prone alpha-synuclein exacerbates synaptic and neuronal degeneration in vivo. *Brain* **137**, 1496-1513, doi:10.1093/brain/awu057 awu057 [pii] (2014).

234    Roberts, R. F., Wade-Martins, R. & Alegre-Abarrategui, J. Direct visualization of alpha-synuclein oligomers reveals previously undetected pathology in Parkinson's disease brain. *Brain* **138**, 1642-1657, doi:10.1093/brain/awv040 (2015).

235    Schulz-Schaeffer, W. J. *et al.* The paraffin-embedded tissue blot detects PrP(Sc) early in the incubation time in prion diseases. *Am J Pathol* **156**, 51-56, doi:S0002-9440(10)64705-0 [pii] 10.1016/S0002-9440(10)64705-0 (2000).

236    Tanji, K. *et al.* Proteinase K-resistant alpha-synuclein is deposited in presynapses in human Lewy body disease and A53T alpha-synuclein transgenic mice. *Acta Neuropathologica* **120**, 145-154, doi:10.1007/s00401-010-0676-z (2010).

237    Kopito, R. R. Aggresomes, inclusion bodies and protein aggregation. *Trends in Cell Biology* **10**, 524-530, doi:Doi 10.1016/S0962-8924(00)01852-3 (2000).

238    McNaught, K. S. P., Shashidharan, P., Perl, D. P., Jenner, P. & Olanow, C. W. Aggresome-related biogenesis of Lewy bodies. *Eur J Neurosci* **16**, 2136-2148, doi:10.1046/j.1460-9568.2002.02301.x (2002).

239     Orimo, S. *et al.* Axonal alpha-synuclein (alpha S) aggregates herald centripetal degeneration of cardiac sympathetic nerve in Parkinson's disease (PD). *Movement Disord* **23**, S19-S19 (2008).

240     Klein, J. C. *et al.* Neurotransmitter changes in dementia with Lewy bodies and Parkinson disease dementia in vivo. *Neurology* **74**, 885-892 (2010).

241     Tiraboschi, P. *et al.* Early and widespread cholinergic losses differentiate dementia with Lewy bodies from Alzheimer disease. *Arch Gen Psychiat* **59**, 946-951, doi:DOI 10.1001/archpsyc.59.10.946 (2002).

242     Perry, E. K. *et al.* Neocortical cholinergic activities differentiate Lewy body dementia from classical Alzheimer's disease. *Neuroreport* **5**, 747-749 (1994).

243     Piggott, M. A. *et al.* Striatal dopaminergic markers in dementia with Lewy bodies, Alzheimer's and Parkinson's diseases: rostrocaudal distribution. *Brain* **122**, 1449-1468, doi:DOI 10.1093/brain/122.8.1449 (1999).

244     Hornykiewicz, O. Biochemical aspects of Parkinson's disease. *Neurology* **51**, S2-S9 (1998).

245     Scott, D. A. *et al.* A Pathologic Cascade Leading to Synaptic Dysfunction in alpha-Synuclein-Induced Neurodegeneration. *Journal of Neuroscience* **30**, 8083-8095, doi:10.1523/Jneurosci.1091-10.2010 (2010).

246     Larsen, K. E. *et al.* alpha-synuclein overexpression in PC12 and chromaffin cells impairs catecholamine release by interfering with a late step in exocytosis. *Journal of Neuroscience* **26**, 11915-11922, doi:10.1523/Jneurosci.3821-06.2006 (2006).

247     Lundblad, M., Decressac, M., Mattsson, B. & Bjorklund, A. Impaired neurotransmission caused by overexpression of alpha-synuclein in nigral dopamine neurons. *P Natl Acad Sci USA* **109**, 3213-3219, doi:10.1073/pnas.1200575109 (2012).

248     Gaugler, M. N. *et al.* Nigrostriatal overabundance of alpha-synuclein leads to decreased vesicle density and deficits in dopamine release that correlate with reduced motor activity. *Acta Neuropathologica* **123**, 653-669, doi:10.1007/s00401-012-0963-y (2012).

249     Garcia-Reitbock, P. *et al.* SNARE protein redistribution and synaptic failure in a transgenic mouse model of Parkinson's disease. *Brain* **133**, 2032-2044, doi:10.1093/brain/awq132 (2010).

250     Janezic, S. *et al.* Deficits in dopaminergic transmission precede neuron loss and dysfunction in a new Parkinson model. *P Natl Acad Sci USA* **110**, E4016-E4025, doi:10.1073/pnas.1309143110 (2013).

251     German, D. C., Manaye, K., Smith, W. K., Woodward, D. J. & Saper, C. B. Midbrain dopaminergic cell loss in Parkinson's disease: computer visualization. *Ann Neurol* **26**, 507-514, doi:10.1002/ana.410260403 (1989).

252     Kish, S. J., Shannak, K. & Hornykiewicz, O. Uneven pattern of dopamine loss in the striatum of patients with idiopathic Parkinson's disease. Pathophysiologic and clinical implications. *N Engl J Med* **318**, 876-880, doi:10.1056/NEJM198804073181402 (1988).

253     Nikolaus, S., Antke, C. & Muller, H. W. In vivo imaging of synaptic function in the central nervous system I. Movement disorders and dementia. *Behav Brain Res* **204**, 1-31, doi:10.1016/j.bbr.2009.06.008 (2009).

254     Volpicelli-Daley, L. A. *et al.* Exogenous alpha-synuclein fibrils induce Lewy body pathology leading to synaptic dysfunction and neuron death. *Neuron* **72**, 57-71, doi:10.1016/j.neuron.2011.08.033
S0896-6273(11)00844-0 [pii] (2011).

255     Liu, B. Modulation of microglial pro-inflammatory and neurotoxic activity for the treatment of Parkinson's disease. *Aaps J* **8**, E606-E621, doi:Doi 10.1208/Aapsj080369 (2006).

256    McGeer, P. L., Itagaki, S., Boyes, B. E. & McGeer, E. G. Reactive microglia are positive for HLA-DR in the substantia nigra of Parkinson's and Alzheimer's disease brains. *Neurology* **38**, 1285-1291 (1988).

257    Blandini, F. Neural and Immune Mechanisms in the Pathogenesis of Parkinson's Disease. *J Neuroimmune Pharm* **8**, 189-201, doi:10.1007/s11481-013-9435-y (2013).

258    Vilhardt, F. Microglia: phagocyte and glia cell. *Int J Biochem Cell B* **37**, 17-21, doi:10.1016/j.biocel.2004.06.010 (2005).

259    Hirsch, E. C. & Hunot, S. Neuroinflammation in Parkinson's disease: a target for neuroprotection? *Lancet Neurol* **8**, 382-397 (2009).

260    Rayaprolu, S. *et al.* TREM2 in neurodegeneration: evidence for association of the p.R47H variant with frontotemporal dementia and Parkinson's disease. *Molecular Neurodegeneration* **8**, doi:Artn 19

10.1186/1750-1326-8-19 (2013).

261    Sun, C. C. *et al.* HLA-DRB1 Alleles Are Associated with the Susceptibility to Sporadic Parkinson's Disease in Chinese Han Population. *PLoS One* **7**, doi:ARTN e48594

10.1371/journal.pone.0048594 (2012).

262    Noelker, C. *et al.* Toll like receptor 4 mediates cell death in a mouse MPTP model of Parkinson disease. *Sci Rep-Uk* **3**, doi:Artn 1393

10.1038/Srep01393 (2013).

263    Rees, K. *et al.* Non-steroidal anti-inflammatory drugs as disease-modifying agents for Parkinson's disease: evidence from observational studies. *Cochrane Db Syst Rev*, doi:Artn Cd008454

10.1002/14651858.Cd008454.Pub2 (2011).

264    Aloisi, F. Immune function of microglia. *Glia* **36**, 165-179, doi:Doi 10.1002/Glia.1106 (2001).

265    Kreutzberg, G. W. Microglia: A sensor for pathological events in the CNS. *Trends Neurosci* **19**, 312-318, doi:Doi 10.1016/0166-2236(96)10049-7 (1996).

266    Kim, Y. S. & Joh, T. H. Microglia, major player in the brain inflammation: their roles in the pathogenesis of Parkinson's disease. *Exp Mol Med* **38**, 333-347 (2006).

267    Lawson, L. J., Perry, V. H., Dri, P. & Gordon, S. Heterogeneity in the Distribution and Morphology of Microglia in the Normal Adult-Mouse Brain. *Neuroscience* **39**, 151-170, doi:Doi 10.1016/0306-4522(90)90229-W (1990).

268    Parkhurst, C. N. *et al.* Microglia Promote Learning-Dependent Synapse Formation through Brain-Derived Neurotrophic Factor. *Cell* **155**, 1596-1609, doi:10.1016/j.cell.2013.11.030 (2013).

269    Wake, H., Moorhouse, A. J., Jinno, S., Kohsaka, S. & Nabekura, J. Resting Microglia Directly Monitor the Functional State of Synapses In Vivo and Determine the Fate of Ischemic Terminals. *Journal of Neuroscience* **29**, 3974-3980, doi:10.1523/Jneurosci.4363-08.2009 (2009).

270    Paolicelli, R. C. *et al.* Synaptic Pruning by Microglia Is Necessary for Normal Brain Development. *Science* **333**, 1456-1458, doi:10.1126/science.1202529 (2011).

271    Schafer, D. P. *et al.* Microglia Sculpt Postnatal Neural Circuits in an Activity and Complement-Dependent Manner. *Neuron* **74**, 691-705, doi:10.1016/j.neuron.2012.03.026 (2012).

272    Latz, E., Xiao, T. S. & Stutz, A. Activation and regulation of the inflammasomes. *Nat Rev Immunol* **13**, 397-411, doi:10.1038/nri3452 (2013).

273    Strowig, T., Henao-Mejia, J., Elinav, E. & Flavell, R. Inflammasomes in health and disease. *Nature* **481**, 278-286, doi:10.1038/nature10759 (2012).

274    Guo, H. T., Callaway, J. B. & Ting, J. P. Y. Inflammasomes: mechanism of action, role in disease, and therapeutics. *Nature Medicine* **21**, 677-687, doi:10.1038/nm.3893 (2015).

275     Monje, M. L., Toda, H. & Palmer, T. D. Inflammatory blockade restores adult hippocampal neurogenesis. *Science* **302**, 1760-1765, doi:DOI 10.1126/science.1088417 (2003).

276     Nagatsu, T. & Sawada, M. Inflammatory process in Parkinson's disease: Role for cytokines. *Curr Pharm Design* **11**, 999-1016, doi:Doi 10.2174/1381612053381620 (2005).

277     Alirezaei, M., Kiosses, W. B., Flynn, C. T., Brady, N. R. & Fox, H. S. Disruption of Neuronal Autophagy by Infected Microglia Results in Neurodegeneration. *PLoS One* **3**, doi:ARTN e2906

10.1371/journal.pone.0002906 (2008).

278     Koenigsknecht-Talboo, J. & Landreth, G. E. Microglial phagocytosis induced by fibrillar beta-amyloid and IgGs are differentially regulated by proinflammatory cytokines. *J Neurosci* **25**, 8240-8249, doi:25/36/8240 [pii]

10.1523/JNEUROSCI.1808-05.2005 (2005).

279     Dentener, M. A., Vonasmuth, E. J. U., Francot, G. J. M., Marra, M. N. & Buurman, W. A. Antagonistic Effects of Lipopolysaccharide-Binding Protein and Bactericidal Permeability-Increasing Protein on Lipopolysaccharide-Induced Cytokine Release by Mononuclear Phagocytes - Competition for Binding to Lipopolysaccharide. *J Immunol* **151**, 4258-4265 (1993).

280     Medvedev, A. E., Kopydlowski, K. M. & Vogel, S. N. Inhibition of lipopolysaccharide-induced signal transduction in endotoxin-tolerized mouse macrophages: Dysregulation of cytokine, chemokine, and Toll-like receptor 2 and 4 gene expression. *J Immunol* **164**, 5564-5574 (2000).

281     Raetz, C. R. H. *et al.* Gram-Negative Endotoxin - an Extraordinary Lipid with Profound Effects on Eukaryotic Signal Transduction. *Faseb J* **5**, 2652-2660 (1991).

282     Sanlioglu, S. *et al.* Lipopolysaccharide induces Rac1-dependent reactive oxygen species formation and coordinates tumor necrosis factor-alpha secretion through IKK regulation of NF-kappa B. *J Biol Chem* **276**, 30188-30198, doi:DOI 10.1074/jbc.M102061200 (2001).

283     Lehnardt, S. *et al.* Activation of innate immunity in the CNS triggers neurodegeneration through a Toll-like receptor 4-dependent pathway. *P Natl Acad Sci USA* **100**, 8514-8519, doi:10.1073/pnas.1432609100 (2003).

284     Liu, B. *et al.* Role of nitric oxide in inflammation-mediated neurodegeneration. *Ann Ny Acad Sci* **962**, 318-331 (2002).

285     Lee, H. J., Suk, J. E., Bae, E. J. & Lee, S. J. Clearance and deposition of extracellular alpha-synuclein aggregates in microglia. *Biochem Bioph Res Co* **372**, 423-428, doi:10.1016/j.bbrc.2008.05.045 (2008).

286     Park, J. Y., Paik, S. R., Jou, I. & Park, S. M. Microglial phagocytosis is enhanced by monomeric alpha-synuclein, not aggregated alpha-synuclein: Implications for Parkinson's disease. *Glia* **56**, 1215-1223, doi:10.1002/glia.20691 (2008).

287     Klegeris, A. *et al.* alpha-Synuclein activates stress signaling protein kinases in THP-1 cells and microglia. *Neurobiol Aging* **29**, 739-752, doi:10.1016/j.neurobiolaging.2006.11.013 (2008).

288     Zhang, W. *et al.* Aggregated alpha-synuclein activates microglia: a process leading to disease progression in Parkinson's disease. *Faseb J* **19**, 533-542, doi:19/6/533 [pii]

10.1096/fj.04-2751com (2005).

289     Alvarez-Erviti, L., Couch, Y., Richardson, J., Cooper, J. M. & Wood, M. J. A. Alpha-synuclein release by neurons activates the inflammatory response in a microglial cell line. *Neurosci Res* **69**, 337-342, doi:10.1016/j.neures.2010.12.020 (2011).

290     Kim, C. *et al.* beta1-integrin-dependent migration of microglia in response to neuron-released alpha-synuclein. *Exp Mol Med* **46**, e91, doi:10.1038/emm.2014.6 emm20146 [pii] (2014).

291     Kim, C., Lee, H. J., Masliah, E. & Lee, S. J. Non-cell-autonomous Neurotoxicity of alpha-synuclein Through Microglial Toll-like Receptor 2. *Exp Neurobiol* **25**, 113-119, doi:10.5607/en.2016.25.3.113 (2016).

292     Kim, C. *et al.* Neuron-released oligomeric alpha-synuclein is an endogenous agonist of TLR2 for paracrine activation of microglia. *Nat Commun* **4**, doi:Artn 1562 10.1038/Ncomms2534 (2013).

293     Fellner, L. *et al.* Toll-like receptor 4 is required for alpha-synuclein dependent activation of microglia and astroglia. *Glia* **61**, 349-360, doi:10.1002/glia.22437 (2013).

294     Stefanova, N. *et al.* Toll-like receptor 4 promotes alpha-synuclein clearance and survival of nigral dopaminergic neurons. *Am J Pathol* **179**, 954-963, doi:10.1016/j.ajpath.2011.04.013 S0002-9440(11)00417-2 [pii] (2011).

295     Bennett, N. K. *et al.* Polymer brain-nanotherapeutics for multipronged inhibition of microglial alpha-synuclein aggregation, activation, and neurotoxicity. *Biomaterials* **111**, 179-189, doi:S0142-9612(16)30537-3 [pii] 10.1016/j.biomaterials.2016.10.001 (2016).

296     Gustot, A. *et al.* Amyloid fibrils are the molecular trigger of inflammation in Parkinson's disease. *Biochemical Journal* **471**, 323-333, doi:10.1042/Bj20150617 (2015).

297     Hoang, T. Q., Rampon, C., Freyssinet, J. M., Vriz, S. & Kerbiriou-Nabias, D. A method to assess the migration properties of cell-derived microparticles within a living tissue. *Bba-Gen Subjects* **1810**, 863-866, doi:10.1016/j.bbagen.2011.05.003 (2011).

298     Ferreira, T. A., Lo Iacono, L. & Gross, C. T. Serotonin receptor 1A modulates actin dynamics and restricts dendritic growth in hippocampal neurons. *Eur J Neurosci* **32**, 18-26, doi:10.1111/j.1460-9568.2010.07283.x (2010).

299     Nikonenko, A. G. & Skibo, G. G. Technique to quantify local clustering of synaptic vesicles using single section data. *Microsc Res Techniq* **65**, 287-291, doi:10.1002/jemt.20134 (2004).

300     Bianco, F. *et al.* Acid sphingomyelinase activity triggers microparticle release from glial cells. *EMBO J* **28**, 1043-1054, doi:10.1038/emboj.2009.45 emboj200945 [pii] (2009).

301     Faure, J. *et al.* Exosomes are released by cultured cortical neurones. *Mol Cell Neurosci* **31**, 642-648, doi:S1044-7431(05)00302-7 [pii] 10.1016/j.mcn.2005.12.003 (2006).

302     Hedlund, M., Nagaeva, O., Kargl, D., Baranov, V. & Mincheva-Nilsson, L. Thermal- and Oxidative Stress Causes Enhanced Release of NKG2D Ligand-Bearing Immunosuppressive Exosomes in Leukemia/Lymphoma T and B Cells. *PLoS One* **6**, doi:ARTN e16899 10.1371/journal.pone.0016899 (2011).

303     Montecalvo, A. *et al.* Mechanism of transfer of functional microRNAs between mouse dendritic cells via exosomes. *Blood* **119**, 756-766, doi:10.1182/blood-2011-02-338004 (2012).

304     Chivet, M., Hemming, F., Pernet-Gallay, K., Fraboulet, S. & Sadoul, R. Emerging role of neuronal exosomes in the central nervous system. *Front Physiol* **3**, 145, doi:10.3389/fphys.2012.00145 (2012).

305     Thery, C., Amigorena, S., Raposo, G. & Clayton, A. Isolation and characterization of exosomes from cell culture supernatants and biological fluids. *Curr Protoc Cell Biol* **Chapter 3**, Unit 3 22, doi:10.1002/0471143030.cb0322s30 (2006).

306     Dalton, A. C. & Barton, W. A. Over-expression of secreted proteins from mammalian cell lines. *Protein Sci* **23**, 517-525, doi:10.1002/pro.2439 (2014).

307     Tang, Z. *et al.* mTor mediates tau localization and secretion: Implication for Alzheimer's disease. *Bba-Mol Cell Res* **1853**, 1646-1657, doi:10.1016/j.bbamcr.2015.03.003 (2015).

308     Filograna, R. *et al.* Analysis of the Catecholaminergic Phenotype in Human SH-SY5Y and BE(2)-M17 Neuroblastoma Cell Lines upon Differentiation. *PLoS One* **10**, doi:ARTN e0136769

10.1371/journal.pone.0136769 (2015).

309     Bliederhaeuser, C. *et al.* Age-dependent defects of alpha-synuclein oligomer uptake in microglia and monocytes. *Acta Neuropathologica* **131**, 379-391, doi:10.1007/s00401-015-1504-2 (2016).

310     Dedkova, E. N., Sigova, A. A. & Zinchenko, V. P. Mechanism of action of calcium ionophores on intact cells: ionophore-resistant cells. *Membr Cell Biol* **13**, 357-368 (2000).

311     Miyake, H., Hara, I., Arakawa, S. & Kamidono, S. Stress protein GRP78 prevents apoptosis induced by calcium ionophore, ionomycin, but not by glycosylation inhibitor, tunicamycin, in human prostate cancer cells. *J Cell Biochem* **77**, 396-408, doi:10.1002/(SICI)1097-4644(20000601)77:3<396::AID-JCB5>3.0.CO;2-5 [pii] (2000).

312     Nakamura, N. *et al.* Characterization of a cis-Golgi matrix protein, GM130. *J Cell Biol* **131**, 1715-1726 (1995).

313     Schuel, H., Tipton, S. R. & Anderson, N. G. Studies on Isolated Cell Components. Xvii. The Distribution of Cytochrome Oxidase Activity in Rat Liver Brei Fractionated in the Zonal Ultracentrifuge. *J Cell Biol* **22**, 317-326 (1964).

314     Chernyshev, V. S. *et al.* Size and shape characterization of hydrated and desiccated exosomes. *Anal Bioanal Chem* **407**, 3285-3301, doi:10.1007/s00216-015-8535-3 (2015).

315     Khan, M. B. *et al.* Nef exosomes isolated from the plasma of individuals with HIV-associated dementia (HAD) can induce Abeta(1-42) secretion in SH-SY5Y neural cells. *J Neurovirol* **22**, 179-190, doi:10.1007/s13365-015-0383-6

10.1007/s13365-015-0383-6 [pii] (2016).

316     Bendor, J. T., Logan, T. P. & Edwards, R. H. The function of alpha-synuclein. *Neuron* **79**, 1044-1066, doi:10.1016/j.neuron.2013.09.004

S0896-6273(13)00802-7 [pii] (2013).

317     Komatsu, T., Arashiki, N., Otsuka, Y., Sato, K. & Inaba, M. Extrusion of Na,K-ATPase and transferrin receptor with lipid raft-associated proteins in different populations of exosomes during reticulocyte maturation in dogs. *Jpn J Vet Res* **58**, 17-27 (2010).

318     Burke, W. J. *et al.* Aggregation of alpha-synuclein by DOPAL, the monoamine oxidase metabolite of dopamine. *Acta Neuropathol* **115**, 193-203, doi:10.1007/s00401-007-0303-9 (2008).

319     Jinsmaa, Y., Sullivan, P., Sharabi, Y. & Goldstein, D. S. DOPAL is transmissible to and oligomerizes alpha-synuclein in human glial cells. *Auton Neurosci-Basic* **194**, 46-51, doi:10.1016/j.autneu.2015.12.008 (2016).

320     Jinsmaa, Y. *et al.* Divalent metal ions enhance DOPAL-induced oligomerization of alpha-synuclein. *Neuroscience Letters* **569**, 27-32, doi:10.1016/j.neulet.2014.03.016 (2014).

321     Vermeer, L. M. M., Florang, V. R. & Doorn, J. A. Catechol and aldehyde moieties of 3,4-dihydroxyphenylacetaldehyde contribute to tyrosine hydroxylase inhibition and neurotoxicity. *Brain Res* **1474**, 100-109, doi:10.1016/j.brainres.2012.07.048 (2012).

322    Liu, G. *et al.* Aldehyde dehydrogenase 1 defines and protects a nigrostriatal dopaminergic neuron subpopulation. *J Clin Invest* **124**, 3032-3046, doi:10.1172/JCI72176

72176 [pii] (2014).

323    Guerrero, E., Vasudevaraju, P., Hegde, M. L., Britton, G. B. & Rao, K. S. Recent advances in alpha-synuclein functions, advanced glycation, and toxicity: implications for Parkinson's disease. *Mol Neurobiol* **47**, 525-536, doi:10.1007/s12035-012-8328-z (2013).

324    Frank, L. A. *et al.* Hyperglycaemic conditions perturb mouse oocyte in vitro developmental competence via beta-O-linked glycosylation of Heat shock protein 90. *Hum Reprod* **29**, 1292-1303, doi:10.1093/humrep/deu066 (2014).

325    Kreger, B. T., Johansen, E. R., Cerione, R. A. & Antonyak, M. A. The Enrichment of Survivin in Exosomes from Breast Cancer Cells Treated with Paclitaxel Promotes Cell Survival and Chemoresistance. *Cancers (Basel)* **8**, doi:E111 [pii]

cancers8120111 [pii]

10.3390/cancers8120111 (2016).

326    Barth, H. G., Boyes, B. E. & Jackson, C. Size-Exclusion Chromatography. *Anal Chem* **66**, R595-R620 (1994).

327    McNulty, B. C. *et al.* Temperature-induced reversible conformational change in the first 100 residues of alpha-synuclein. *Protein Sci* **15**, 602-608, doi:ps.051867106 [pii]

10.1110/ps.051867106 (2006).

328    Taylor, S. C., Berkelman, T., Yadav, G. & Hammond, M. A Defined Methodology for Reliable Quantification of Western Blot Data. *Mol Biotechnol* **55**, 217-226, doi:10.1007/s12033-013-9672-6 (2013).

329    Anandhan, A. *et al.* Overexpression of alpha-synuclein at non-toxic levels increases dopaminergic cell death induced by copper exposure via modulation of protein degradation pathways. *Neurobiol Dis* **81**, 76-92, doi:10.1016/j.nbd.2014.11.018 (2015).

330    Jiang, P. Z., Gan, M., Lin, W. L. & Yen, S. H. C. Nutrient deprivation induces alpha-synuclein aggregation through endoplasmic reticulum stress response and SREBP2 pathway. *Front Aging Neurosci* **6**, doi:Artn 268

10.3389/Fnagi.2014.00268 (2014).

331    Deng, H. & Yuan, L. M. Genetic variants and animal models in SNCA and Parkinson disease. *Ageing Res Rev* **15**, 161-176, doi:10.1016/j.arr.2014.04.002 (2014).

332    Abels, E. R. & Breakefield, X. O. Introduction to Extracellular Vesicles: Biogenesis, RNA Cargo Selection, Content, Release, and Uptake. *Cell Mol Neurobiol* **36**, 301-312, doi:10.1007/s10571-016-0366-z (2016).

333    Andreasen, M., Lorenzen, N. & Otzen, D. Interactions between misfolded protein oligomers and membranes: A central topic in neurodegenerative diseases? *Bba-Biomembranes* **1848**, 1897-1907, doi:10.1016/j.bbamem.2015.01.018 (2015).

334    Chacko, J. V., Zanacchi, F. C. & Diaspro, A. Probing Cytoskeletal Structures by Coupling Optical Superresolution and AFM Techniques for a Correlative Approach. *Cytoskeleton* **70**, 729-740, doi:10.1002/cm.21139 (2013).

335    Yilmaz, N. & Kobayashi, T. Assemblies of pore-forming toxins visualized by atomic force microscopy. *Bba-Biomembranes* **1858**, 500-511, doi:10.1016/j.bbamem.2015.11.005 (2016).

336    Graner, M. W. *et al.* Proteomic and immunologic analyses of brain tumor exosomes. *Faseb J* **23**, 1541-1557, doi:10.1096/fj.08-122184 (2009).

337    Silverman, J. M. *et al.* Disease Mechanisms in ALS: Misfolded SOD1 Transferred Through Exosome-Dependent and Exosome-Independent Pathways. *Cell Mol Neurobiol* **36**, 377-381, doi:10.1007/s10571-015-0294-3 (2016).

338    Kruger, S. *et al.* Molecular characterization of exosome-like vesicles from breast cancer cells. *Bmc Cancer* **14**, doi:Artn 44
10.1186/1471-2407-14-44 (2014).

339    Cheng, X., Shen, D., Samie, M. & Xu, H. Mucolipins: Intracellular TRPML1-3 channels. *Febs Lett* **584**, 2013-2021, doi:10.1016/j.febslet.2009.12.056
S0014-5793(10)00028-1 [pii] (2010).

340    Xiong, J. & Zhu, M. X. Regulation of lysosomal ion homeostasis by channels and transporters. *Sci China Life Sci* **59**, 777-791, doi:10.1007/s11427-016-5090-x
10.1007/s11427-016-5090-x [pii] (2016).

341    Papanikolaou, G. & Pantopoulos, K. Iron metabolism and toxicity. *Toxicol Appl Pharm* **202**, 199-211, doi:10.1016/j.taap.2004.06.021 (2005).

342    Fruhbeis, C., Frohlich, D. & Kramer-Albers, E. M. Emerging roles of exosomes in neuron-glia communication. *Front Physiol* **3**, doi:Unsp 119
10.3389/Fphys.2012.00119 (2012).

343    Ximerakis, M. *et al.* Resistance of naturally secreted alpha-synuclein to proteolysis. *Faseb J* **28**, 3146-3158, doi:10.1096/fj.13-245852 (2014).

344    Grey, M. *et al.* Acceleration of alpha-Synuclein Aggregation by Exosomes. *J Biol Chem* **290**, 2969-2982, doi:10.1074/jbc.M114.585703 (2015).

345    Shi, M. *et al.* Plasma exosomal alpha-synuclein is likely CNS-derived and increased in Parkinson's disease. *Acta Neuropathologica* **128**, 639-650, doi:10.1007/s00401-014-1314-y (2014).

346    Mittelbrunn, M., Vicente-Manzanares, M. & Sanchez-Madrid, F. Organizing Polarized Delivery of Exosomes at Synapses. *Traffic* **16**, 327-337, doi:10.1111/tra.12258 (2015).

347    Korkut, C. *et al.* Trans-Synaptic Transmission of Vesicular Wnt Signals through Evi/Wntless. *Cell* **139**, 393-404, doi:10.1016/j.cell.2009.07.051 (2009).

348    Koles, K. *et al.* Mechanism of Evenness Interrupted (Evi)-Exosome Release at Synaptic Boutons. *J Biol Chem* **287**, 16820-16834, doi:10.1074/jbc.M112.342667 (2012).

349    Lachenal, G. *et al.* Release of exosomes from differentiated neurons and its regulation by synaptic glutamatergic activity. *Mol Cell Neurosci* **46**, 409-418, doi:10.1016/j.mcn.2010.11.004
S1044-7431(10)00255-1 [pii] (2011).

350    Faure, J. *et al.* Exosomes are released by cultured cortical neurones. *Molecular and Cellular Neuroscience* **31**, 642-648, doi:10.1016/j.mcn.2005.12.003 (2006).

351    Kolos, Y. A., Grigoriyev, I. P. & Korzhevskyi, D. E. [A synaptic marker synaptophysin]. *Morfologiia* **147**, 78-82 (2015).

352    Ostapchenko, V. G. *et al.* The Transient Receptor Potential Melastatin 2 (TRPM2) Channel Contributes to beta-Amyloid Oligomer-Related Neurotoxicity and Memory Impairment. *J Neurosci* **35**, 15157-15169, doi:10.1523/JNEUROSCI.4081-14.2015
35/45/15157 [pii] (2015).

353    Koch, J. C. *et al.* Alpha-Synuclein affects neurite morphology, autophagy, vesicle transport and axonal degeneration in CNS neurons. *Cell Death & Disease* **6**, doi:Artn E1811
10.1038/Cddis.2015.169 (2015).

354    Gong, Y. & Lippa, C. F. Review: disruption of the postsynaptic density in Alzheimer's disease and other neurodegenerative dementias. *Am J Alzheimers Dis Other Demen* **25**, 547-555, doi:10.1177/1533317510382893
1533317510382893 [pii] (2010).

355    Tomiyama, T. *et al.* A mouse model of amyloid beta oligomers: their contribution to synaptic alteration, abnormal tau phosphorylation, glial activation, and neuronal loss in vivo. *J Neurosci* **30**, 4845-4856, doi:10.1523/JNEUROSCI.5825-09.2010

30/14/4845 [pii] (2010).

356     Mao, L. M. & Wang, J. Q. Synaptically Localized Mitogen-Activated Protein Kinases: Local Substrates and Regulation. *Mol Neurobiol* **53**, 6309-6315, doi:10.1007/s12035-015-9535-1

10.1007/s12035-015-9535-1 [pii] (2016).

357     Segal, M. Dendritic spines and long-term plasticity. *Nature Reviews Neuroscience* **6**, 277-284, doi:10.1038/nrn1649 (2005).

358     Love, S. *et al.* Premorbid effects of APOE on synaptic proteins in human temporal neocortex. *Neurobiol Aging* **27**, 797-803, doi:10.1016/j.neurobiolaging.2005.04.008 (2006).

359     Leuba, G. *et al.* Differential changes in synaptic proteins in the Alzheimer frontal cortex with marked increase in PSD-95 postsynaptic protein. *J Alzheimers Dis* **15**, 139-151 (2008).

360     Nyffeler, M., Zhang, W. N., Feldon, J. & Knuesel, I. Differential expression of PSD proteins in age-related spatial learning impairments. *Neurobiol Aging* **28**, 143-155, doi:10.1016/j.neurobiolaging.2005.11.003 (2007).

361     Whitfield, D. R. *et al.* Assessment of ZnT3 and PSD95 protein levels in Lewy body dementias and Alzheimer's disease: association with cognitive impairment. *Neurobiol Aging* **35**, 2836-2844, doi:10.1016/j.neurobiolaging.2014.06.015 (2014).

362     Goetzl, E. J. *et al.* Decreased synaptic proteins in neuronal exosomes of frontotemporal dementia and Alzheimer's disease. *Faseb J* **30**, 4141-4148, doi:fj.201600816R [pii]

10.1096/fj.201600816R (2016).

363     Vargas, K. J. *et al.* Synucleins Have Multiple Effects on Presynaptic Architecture. *Cell Rep* **18**, 161-173, doi:S2211-1247(16)31713-2 [pii]

10.1016/j.celrep.2016.12.023 (2017).

364     Piccoli, G. *et al.* LRRK2 Controls Synaptic Vesicle Storage and Mobilization within the Recycling Pool. *Journal of Neuroscience* **31**, 2225-2237, doi:10.1523/Jneurosci.3730-10.2011 (2011).

365     Zagrebelsky, M. *et al.* The p75 neurotrophin receptor negatively modulates dendrite complexity and spine density in hippocampal neurons. *Journal of Neuroscience* **25**, 9989-9999, doi:10.1523/Jneurosci.2492-05.2005 (2005).

366     Gutierrez, H. & Davies, A. M. A fast and accurate procedure for deriving the Sholl profile in quantitative studies of neuronal morphology. *J Neurosci Meth* **163**, 24-30, doi:10.1016/j.jneumeth.2007.02.002 (2007).

367     Sholl, D. A. Dendritic organization in the neurons of the visual and motor cortices of the cat. *J Anat* **87**, 387-406 (1953).

368     Melachroinou, K. *et al.* Deregulation of calcium homeostasis mediates secreted alpha-synuclein-induced neurotoxicity. *Neurobiol Aging* **34**, 2853-2865, doi:10.1016/j.neurobiolaging.2013.06.006

S0197-4580(13)00261-3 [pii] (2013).

369     Kerr, J. F., Wyllie, A. H. & Currie, A. R. Apoptosis: a basic biological phenomenon with wide-ranging implications in tissue kinetics. *Br J Cancer* **26**, 239-257 (1972).

370     Tait, S. W. & Green, D. R. Mitochondria and cell death: outer membrane permeabilization and beyond. *Nat Rev Mol Cell Biol* **11**, 621-632, doi:10.1038/nrm2952

nrm2952 [pii] (2010).

371     Polverino, A. J. & Patterson, S. D. Selective activation of caspases during apoptotic induction in HL-60 cells. *J Biol Chem* **272**, 7013-7021 (1997).

372     Soldani, C. *et al.* Poly(ADP-ribose) polymerase cleavage during apoptosis: When and where? *Exp Cell Res* **269**, 193-201, doi:10.1006/excr.2001.5293 (2001).

150

373    D'Amours, D., Sallmann, F. R., Dixit, V. M. & Poirier, G. G. Gain-of-function of poly(ADP-ribose) polymerase-1 upon cleavage by apoptotic proteases: implications for apoptosis. *J Cell Sci* **114**, 3771-3778 (2001).

374    Eguchi, Y., Shimizu, S. & Tsujimoto, Y. Intracellular ATP levels determine cell death fate by apoptosis or necrosis. *Cancer Res* **57**, 1835-1840 (1997).

375    Herceg, Z. & Wang, Z. Q. Failure of poly(ADP-ribose) polymerase cleavage by caspases leads to induction of necrosis and enhanced apoptosis. *Mol Cell Biol* **19**, 5124-5133 (1999).

376    Rahimian, P. & He, J. J. Exosome-associated release, uptake, and neurotoxicity of HIV-1 Tat protein. *J Neurovirol*, doi:10.1007/s13365-016-0451-6

10.1007/s13365-016-0451-6 [pii] (2016).

377    Lee, H. J. *et al.* Assembly-dependent endocytosis and clearance of extracellular alpha-synuclein. *Int J Biochem Cell B* **40**, 1835-1849, doi:10.1016/j.biocel.2008.01.017 (2008).

378    Eikelenboom, P. *et al.* The significance of neuroinflammation in understanding Alzheimer's disease. *J Neural Transm* **113**, 1685-1695, doi:10.1007/s00702-006-0575-6 (2006).

379    Hensley, K. *et al.* Primary glia expressing the G93A-SOD1 mutation present a neuroinflammatory phenotype and provide a cellular system for studies of glial inflammation. *J Neuroinflamm* **3**, doi:Artn 2

10.1186/1742-2094-3-2 (2006).

380    Rojanathammanee, L., Murphy, E. J. & Combs, C. K. Expression of mutant alpha-synuclein modulates microglial phenotype in vitro. *J Neuroinflamm* **8**, doi:Artn 44

10.1186/1742-2094-8-44 (2011).

381    Hoffmann, A. *et al.* Alpha-synuclein activates BV2 microglia dependent on its aggregation state. *Biochem Biophys Res Commun*, doi:S0006-291X(16)31576-5 [pii]

10.1016/j.bbrc.2016.09.109 (2016).

382    Croisier, E. & Graeber, M. B. Glial degeneration and reactive gliosis in alpha-synucleinopathies: the emerging concept of primary gliodegeneration. *Acta Neuropathol* **112**, 517-530, doi:10.1007/s00401-006-0119-z (2006).

383    Salvesen, L. *et al.* Changes in total cell numbers of the basal ganglia in patients with multiple system atrophy A - stereological study. *Neurobiol Dis* **74**, 104-113, doi:10.1016/j.nbd.2014.11.008 (2015).

384    Horvath, R. J., Nutile-McMenemy, N., Alkaitis, M. S. & DeLeo, J. A. Differential migration, LPS-induced cytokine, chemokine, and NO expression in immortalized BV-2 and HAPI cell lines and primary microglial cultures. *J Neurochem* **107**, 557-569, doi:10.1111/j.1471-4159.2008.05633.x (2008).

385    Henn, A. *et al.* The Suitability of BV2 Cells as Alternative Model System for Primary Microglia Cultures or for Animal Experiments Examining Brain Inflammation. *Altex-Altern Tierexp* **26**, 83-94 (2009).

386    Muralidharan, S. & Mandrekar, P. Cellular stress response and innate immune signaling: integrating pathways in host defense and inflammation. *J Leukocyte Biol* **94**, 1167-1184, doi:10.1189/jlb.0313153 (2013).

387    Fennrich, S. *et al.* More than 70 years of pyrogen detection: Current state and future perspectives. *Altern Lab Anim* **44**, 239-253 (2016).

388    Rannikko, E. H., Weber, S. S. & Kahle, P. J. Exogenous alpha-synuclein induces toll-like receptor 4 dependent inflammatory responses in astrocytes. *BMC Neurosci* **16**, 57, doi:10.1186/s12868-015-0192-0

10.1186/s12868-015-0192-0 [pii] (2015).

389    Streit, W. J., Graeber, M. B. & Kreutzberg, G. W. Functional plasticity of microglia: a review. *Glia* **1**, 301-307, doi:10.1002/glia.440010502 (1988).

390     Dutta, G., Zhang, P. & Liu, B. The lipopolysaccharide Parkinson's disease animal model: mechanistic studies and drug discovery. *Fundam Clin Pharmacol* **22**, 453-464, doi:10.1111/j.1472-8206.2008.00616.x
FCP616 [pii] (2008).
391     Sanchez-Guajardo, V., Tentillier, N. & Romero-Ramos, M. THE RELATION BETWEEN alpha-SYNUCLEIN AND MICROGLIA IN PARKINSON'S DISEASE: RECENT DEVELOPMENTS. *Neuroscience* **302**, 47-58, doi:10.1016/j.neuroscience.2015.02.008 (2015).
392     Mattheyses, A. L., Simon, S. M. & Rappoport, J. Z. Imaging with total internal reflection fluorescence microscopy for the cell biologist. *J Cell Sci* **123**, 3621-3628, doi:10.1242/jcs.056218 (2010).
393     Daniele, F., Di Cairano, E. S., Moretti, S., Piccoli, G. & Perego, C. TIRFM and pH-sensitive GFP-probes to evaluate neurotransmitter vesicle dynamics in SH-SY5Y neuroblastoma cells: cell imaging and data analysis. *J Vis Exp*, doi:10.3791/52267 (2015).
394     Kavalali, E. T. & Jorgensen, E. M. Visualizing presynaptic function. *Nat Neurosci* **17**, 10-16, doi:10.1038/nn.3578 (2014).
395     Properzi, F., Logozzi, M. & Fais, S. Exosomes: the future of biomarkers in medicine. *Biomark Med* **7**, 769-778, doi:10.2217/bmm.13.63 (2013).